NOVEL MULTIMODAL APPROACHES IN NON-INVASIVE BRAIN STIMULATION

EDITED BY: Nivethida Thirugnanasambandam, Florian H. Kasten and Kaviraja Udupa

PUBLISHED IN: Frontiers in Human Neuroscience

frontiers Research Topics

frontiers

ISSN 1664-8714
ISBN 978-2-88974-022-2
DOI 10.3389/978-2-88974-022-2

About Frontiers

Frontiers is more than just an open-access publisher of scholarly articles: it is a pioneering approach to the world of academia, radically improving the way scholarly research is managed. The grand vision of Frontiers is a world where all people have an equal opportunity to seek, share and generate knowledge. Frontiers provides immediate and permanent online open access to all its publications, but this alone is not enough to realize our grand goals.

Frontiers Journal Series

The Frontiers Journal Series is a multi-tier and interdisciplinary set of open-access, online journals, promising a paradigm shift from the current review, selection and dissemination processes in academic publishing. All Frontiers journals are driven by researchers for researchers; therefore, they constitute a service to the scholarly community. At the same time, the Frontiers Journal Series operates on a revolutionary invention, the tiered publishing system, initially addressing specific communities of scholars, and gradually climbing up to broader public understanding, thus serving the interests of the lay society, too.

Dedication to Quality

Each Frontiers article is a landmark of the highest quality, thanks to genuinely collaborative interactions between authors and review editors, who include some of the world's best academicians. Research must be certified by peers before entering a stream of knowledge that may eventually reach the public - and shape society; therefore, Frontiers only applies the most rigorous and unbiased reviews.
Frontiers revolutionizes research publishing by freely delivering the most outstanding research, evaluated with no bias from both the academic and social point of view. By applying the most advanced information technologies, Frontiers is catapulting scholarly publishing into a new generation.

What are Frontiers Research Topics?

Frontiers Research Topics are very popular trademarks of the Frontiers Journals Series: they are collections of at least ten articles, all centered on a particular subject. With their unique mix of varied contributions from Original Research to Review Articles, Frontiers Research Topics unify the most influential researchers, the latest key findings and historical advances in a hot research area! Find out more on how to host your own Frontiers Research Topic or contribute to one as an author by contacting the Frontiers Editorial Office: frontiersin.org/about/contact

NOVEL MULTIMODAL APPROACHES IN NON-INVASIVE BRAIN STIMULATION

Topic Editors:
Nivethida Thirugnanasambandam, National Brain Research Centre (NBRC), India
Florian H. Kasten, University of Oldenburg, Germany
Kaviraja Udupa, Department of Neurophysiology, National Institute of Mental Health and Neurosciences, India

Citation: Thirugnanasambandam, N., Kasten, F. H., Udupa, K., eds. (2021). Novel Multimodal Approaches in Non-Invasive Brain Stimulation. Lausanne: Frontiers Media SA. doi: 10.3389/978-2-88974-022-2

Table of Contents

frontiers in Human Neuroscience

EDITORIAL
published: 19 November 2021
doi: 10.3389/fnhum.2021.784637

Editorial: Novel Multimodal Approaches in Non-invasive Brain Stimulation

Nivethida Thirugnanasambandam[1]*, *Florian H. Kasten*[2] and *Kaviraja Udupa*[3]

[1] Human Motor Neurophysiology and Neuromodulation Lab, National Brain Research Centre (NBRC), Manesar, India, [2] Experimental Psychology Lab, Department of Psychology, European Medical School, Cluster of Excellence "Hearing4All", Carl von Ossietzky University, Oldenburg, Germany, [3] Department of Neurophysiology, National Institute of Mental Health and Neurosciences (NIMHANS), Bengaluru, India

Keywords: brain stimulation, multimodal, tACS-EEG, repetitive transcranial magnetic stimulation (rTMS), transcranial electrical stimulation (tES)

Editorial on the Research Topic

Novel Multimodal Approaches in Non-invasive Brain Stimulation

Over the last two decades, the number of techniques that fall into the realm of non-invasive brain stimulation (NIBS) has increased due to their immense potential in the diagnosis and treatment of neuropsychiatric diseases. Further, researchers have successfully integrated some of these techniques with neurophysiological/neuroimaging methods with the aim of enriching our understanding of brain function and of mechanisms underlying the effects of stimulation on the brain. However, such a multimodal approach is not without challenges and pitfalls. This Research Topic brings together original articles, reviews and a perspective article showcasing advances in multimodal NIBS approaches for studying physiological and pathological states of the brain.

All original research articles were based on work done using low intensity transcranial electrical stimulation (tES). The first one is an elaborate study by Karabanov et al. that used fMRI to probe the after-effects of transcranial direct current stimulation (tDCS) on motor cortical excitability, visuomotor task performance and task-related neural activity. The study revealed inconsistent group effect on primary outcome measures owing to high response variability. However, the authors report significant changes in the supplementary motor area, upstream from the primary motor cortex. Their findings warrant a more detailed data-driven approach for analyzing brain stimulation data. The four research articles on combination of transcranial alternating current stimulation (tACS) and EEG show the strong interest on this topic. On the one hand, Zarubin et al. and Stecher et al. have clearly demonstrated the inconsistencies observed in closed loop tACS-EEG studies which could probably be due to the subthreshold stimulation intensity of tACS being too low to bring about a consistent effect and/or alternative mechanisms other than entrainment that may underlie the effects of tACS. While Zarubin et al. showed that modulation of intrinsic oscillations by tACS is independent of the phase relationship between the signals, Stecher et al., demonstrated that matching the frequency of the tACS signal to that of the intrinsic neural signal using the closed-loop setup did not modulate behavior, rather the fixed-frequency tACS did. These results necessitate further research on the mechanisms of NIBS effects and factors that impact behavioral and neurophysiological modulation. On the other hand, two studies aimed to address the technical challenges in data acquisition and analysis using tACS-EEG—Vosskuhl et al. tested the feasibility of applying signal-space-projection to reduce tACS-induced artifacts in the EEG and compared its performance to other approaches such as sine and template subtraction. Holzmann et al. describe the

OPEN ACCESS

Edited and reviewed by:
Sandra Carvalho, University of Aveiro, Portugal

***Correspondence:**
Nivethida Thirugnanasambandam
dr.nivethida@gmail.com

Specialty section:
This article was submitted to Brain Imaging and Stimulation, a section of the journal Frontiers in Human Neuroscience

Received: *28 September 2021*
Accepted: *28 October 2021*
Published: *19 November 2021*

Citation:
Thirugnanasambandam N, Kasten FH and Udupa K (2021) Editorial: Novel Multimodal Approaches in Non-invasive Brain Stimulation. Front. Hum. Neurosci. 15:784637. doi: 10.3389/fnhum.2021.784637

removal of tACS artifacts with a special emphasis on non-linear amplitude modulations of the artifact, which occur due to physiological processes in the body such as heartbeat or respiration, using a multi-step artifact removal procedure, which they assess using a novel demonstrator setup, that allows to simulate these non-linear dynamics.

Besides original studies, the Research Topic features four review articles discussing general theoretical considerations in the combination of NIBS and neuroimaging as well as their application in clinical settings. The article by Hobot et al. is timely and discusses the limitations of making causal inferences in repetitive transcranial magnetic stimulation (rTMS) research. The authors have critically evaluated literature for studies that have inappropriately used TMS methods to answer causality-related questions and have emphasized on the importance of designing experiments carefully to draw such inferences. In addition, three review articles extensively cover the clinical and research implications of multimodal NIBS in specific pathological states namely schizophrenia, movement disorders and depression. While Shukla and Thirugnanasambandam showcase the untapped potential of multimodal NIBS in understanding the pathophysiology of movement disorders and call for multidisciplinary collaborations for better progress in the field, Baliga and Mehta have focused on the numerous studies that shed light on the pathophysiological mechanisms and scope for personalized treatment in schizophrenia by combining TMS with functional magnetic resonance imaging (fMRI). Finally, Sinha et al. have presented a systematic review and coordinate-based meta-analysis of the effects of electroconvulsive therapy (ECT) on the resting state functional connectivity in depression.

A major highlight under this Research Topic is the perspective article in which Ruhnau and Zaehle propose a novel combination of transcranial auricular vagus nerve stimulation (taVNS) and ear-EEG in a closed loop fashion that could have the potential to modulate attention. The authors have discussed how ear-EEG, a relatively novel form of mobile EEG technique, can reliably record alpha activity from the parietal and temporal brain regions, and when fed in to stimulate the vagus nerve non-invasively in a closed loop manner could modulate attention.

Overall, this Research Topic nicely portrays the spectrum of research undertaken using multimodal NIBS spanning from pathophysiology to clinical applications and from technical advances to behavioral impact. We can conclude that there is a unanimous agreement among the scientific community on the enormous potential of multimodal NIBS approaches to largely improve our understanding of brain function. However, currently there are several limitations that need to be addressed, especially to obtain more consistent and reproducible responses. Although we have made great progress over the past decade in exploring the vast prospects of multimodal NIBS, a more collaborative and multi-disciplinary approach will be necessary to confront technical challenges and optimize protocols for clinical and research applications. The collection of articles in this Research Topic have portrayed this convincingly.

AUTHOR CONTRIBUTIONS

All authors listed have made a substantial, direct, and intellectual contribution to the work and approved it for publication.

Conflict of Interest: The authors declare that the research was conducted in the absence of any commercial or financial relationships that could be construed as a potential conflict of interest.

Publisher's Note: All claims expressed in this article are solely those of the authors and do not necessarily represent those of their affiliated organizations, or those of the publisher, the editors and the reviewers. Any product that may be evaluated in this article, or claim that may be made by its manufacturer, is not guaranteed or endorsed by the publisher.

frontiers in Human Neuroscience

ORIGINAL RESEARCH
published: 04 September 2020
doi: 10.3389/fnhum.2020.00366

Transient Amplitude Modulation of Alpha-Band Oscillations by Short-Time Intermittent Closed-Loop tACS

Georgy Zarubin[1,2*†], *Christopher Gundlach*[2,3*†], *Vadim Nikulin*[2,4], *Arno Villringer*[2,5,6,7] *and Martin Bogdan*[1]

[1]*Technical Informatics Department, Leipzig University, Leipzig, Germany,* [2]*Department of Neurology, Max Planck Institute for Human Cognitive and Brain Sciences, Leipzig, Germany,* [3]*Institute of Psychology, University of Leipzig, Leipzig, Germany,* [4]*Centre for Cognition and Decision Making, Institute for Cognitive Neuroscience, National Research University Higher School of Economics, Moscow, Russia,* [5]*Neurophysics Group, Department of Neurology, Campus Benjamin Franklin, Charité Universitätsmedizin Berlin, Berlin, Germany,* [6]*Department of Cognitive Neurology, University Hospital Leipzig, Leipzig, Germany,* [7]*Mind Brain Body Institute at the Berlin School of Mind and Brain, Humboldt-Universität zu Berlin, Berlin, Germany*

OPEN ACCESS

Edited by:
Nivethida Thirugnanasambandam, National Brain Research Centre (NBRC), India

Reviewed by:
Pekcan Ungan, Koç University, Turkey
Reza Kazemi, Atieh Clinical Neuroscience Center, Iran

***Correspondence:**
Georgy Zarubin
zarubin@cbs.mpg.de
Christopher Gundlach
gundlach@cbs.mpg.de

†These authors share first authorship

Specialty section:
This article was submitted to Brain Imaging and Stimulation, a section of the journal Frontiers in Human Neuroscience

Received: *22 January 2020*
Accepted: *10 August 2020*
Published: *04 September 2020*

Citation:
Zarubin G, Gundlach C, Nikulin V, Villringer A and Bogdan M (2020) Transient Amplitude Modulation of Alpha-Band Oscillations by Short-Time Intermittent Closed-Loop tACS. Front. Hum. Neurosci. 14:366. doi: 10.3389/fnhum.2020.00366

Non-invasive brain stimulation (NIBS) techniques such as transcranial alternating current stimulation (tACS) have recently become extensively utilized due to their potential to modulate ongoing neuronal oscillatory activity and consequently to induce cortical plasticity relevant for various cognitive functions. However, the neurophysiological basis for stimulation effects as well as their inter-individual differences is not yet understood. In the present study, we used a closed-loop electroencephalography-tACS (EEG-tACS) protocol to examine the modulation of alpha oscillations generated in occipito-parietal areas. In particular, we investigated the effects of a repeated short-time intermittent stimulation protocol (1 s in every trial) applied over the visual cortex (Cz and Oz) and adjusted according to the phase and frequency of visual alpha oscillations on the amplitude of these oscillations. Based on previous findings, we expected higher increases in alpha amplitudes for tACS applied in-phase with ongoing oscillations as compared to an application in anti-phase and this modulation to be present in low-alpha amplitude states of the visual system (eyes opened, EO) but not high (eyes closed, EC). Contrary to our expectations, we found a transient suppression of alpha power in inter-individually derived spatially specific parieto-occipital components obtained *via* the estimation of spatial filters by using the common spatial patterns approach. The amplitude modulation was independent of the phase relationship between the tACS signal and alpha oscillations, and the state of the visual system manipulated *via* closed- and open-eye conditions. It was also absent in conventionally analyzed single-channel and multi-channel data from an average parieto-occipital region. The fact that the tACS modulation of oscillations was phase-independent suggests that mechanisms driving the effects of tACS may not be explained by entrainment alone, but rather require neuroplastic changes or transient disruption of neural oscillations. Our study also supports the notion that the response to tACS is subject-specific, where the modulatory effects are shaped by the interplay between the stimulation and different

alpha generators. This favors stimulation protocols as well as analysis regimes exploiting inter-individual differences, such as spatial filters to reveal otherwise hidden stimulation effects and, thereby, comprehensively induce and study the effects and underlying mechanisms of tACS.

Keywords: tACS, closed-loop, alpha, EEG, stimulation, neural oscillations

INTRODUCTION

Non-invasive brain stimulation (NIBS) technology has gained increasing attention in the last few years from the scientific community (Bergmann et al., 2016; Antal et al., 2017; Thut et al., 2017; Vosskuhl et al., 2018), clinical (Palm et al., 2014; Yavari et al., 2017), sports (Edwards et al., 2017; Angius et al., 2018), military (Nelson et al., 2016), and other fields. One of the reasons for this growing interest is the successful modulation of cognitive, motor, and perceptual functions in numerous studies in different domains such as motor function (Feurra et al., 2011a; Brittain et al., 2013; Angius et al., 2018), visual (Zaehle et al., 2010; Helfrich et al., 2014), auditory (Riecke et al., 2015), somatosensory (Feurra et al., 2011b; Gundlach et al., 2016, 2017), or linguistic processing (Riecke et al., 2018; Wilsch et al., 2018) and for higher cognitive functions such as decision making, creativity, or self-aware dreaming (Sela et al., 2012; Voss et al., 2014; Lustenberger et al., 2015). Another reason is the widespread availability of various experimental, clinical protocols, and instructions (Bergmann et al., 2016; Antal et al., 2017; Tavakoli and Yun, 2017). Also, NIBS is generally a safe and well-tolerated form of brain stimulation with a comparatively simple set up. Transcranial alternating current stimulation (tACS) also has broad applications due to its ability to modulate ongoing neural oscillatory activity flexibly by precisely tuning stimulation parameters (such as frequency, phase, amplitude, or a combination of these) to each individual or each experimental session (Herrmann et al., 2013; Reato et al., 2013).

The advantages of tACS may be exploited even further in case of an adaptive or closed-loop approach, when stimulation parameters are tuned online during the experiment in a particular determined manner (Karabanov et al., 2016; Zrenner et al., 2016). In such a framework, brain responses to the stimulation, usually obtained from electroencephalography (EEG) or magnetoencephalography (MEG) data, serves as feedback and are used for the modification of control parameters. Significant efforts in recent research have been devoted to the establishment and application of closed-loop tACS-EEG/MEG models (Bergmann et al., 2016; Thut et al., 2017). However, despite an increasing number of proposed models, the field of adaptive tACS still lacks experimentally validated solutions. This can be explained by the complexity of the task: implementation and utilization of closed-loop tACS have various technical challenges and fundamental questions, which narrow and delay the development of this field.

First of all, despite numerous studies, the exact neural mechanisms of the effects of tACS are still not well understood. Animal, as well as human and computational modeling studies, suggest that weak alternating electric fields modulate spiking patterns of neurons utilizing neural entrainment (Deans et al., 2007; Fröhlich and McCormick, 2010; Ozen et al., 2010; Helfrich et al., 2014) or induction of spike-timing plasticity (Zaehle et al., 2010; Polanía et al., 2012; Vossen et al., 2015; Sliva et al., 2018). As suggested by resonance theory, these effects should be highly frequency-dependent and observable online during stimulation (Hutcheon and Yarom, 2000). In line with this, various studies have reported online effects of tACS on behavior (Kanai et al., 2010; Strüber et al., 2013; Vosskuhl et al., 2015; Gundlach et al., 2016) as well as markers of neural activity in the EEG, MEG or fMRI (Cabral-Calderin et al., 2015; Neuling et al., 2015; Witkowski et al., 2016). However, it has recently been shown (Asamoah et al., 2019) that effects of tACS on the motor system are, at least, partly related to transcutaneous stimulation of peripheral nerves in the skin beyond transcranial stimulation of cortical neurons (however, see Kasten et al., 2019; Krause et al., 2019; Vieira et al., 2019). Additionally, as suggested in some studies, processes leading to online effects of tACS and those leading to offline effects that sustain (or even manifest) after stimulation may rely on different neural mechanisms (Reato et al., 2010; Strüber et al., 2015). In a recent review article on the immediate effects of tACS (Liu et al., 2018), five possible neural mechanisms were suggested: "stochastic resonance, rhythm resonance, temporal biasing of neuronal spikes, entrainment of network patterns, and imposed patterns." Importantly, how these mechanisms contribute to observed effects specifically and how they interact or compensate each other is largely unknown. Examining stimulation mechanisms, therefore, remains an open question.

Second, one of the biggest challenges with tACS and NIBS, in general, is high inter- and intra-individual variability of effects (Ziemann and Siebner, 2015). As mentioned by Guerra et al. (2017), this variability can be due to different factors, including physiological (variability of brain morphology, endogenous states, and different responses to stimulation), technical (particular setup and parameters of stimulation), and also statistical differences (numbers of participants and trials per groups and conditions). Tailoring stimulation protocols to individual factors may help to address (some) aspects of this variability.

Third, while behavioral effects for short-interval trial-by-trial alternated tACS points towards a fast onset of stimulation effects in the range of seconds (see Joundi et al., 2012), temporal dynamics of stimulation effects are largely unknown. The analysis of online stimulation effects is additionally impeded by tACS-induced artifacts in EEG data for instance that exceed the measured neural signals by several orders of magnitude. While some solutions to this challenge have been proposed

(Witkowski et al., 2016; Noury and Siegel, 2017; Kasten et al., 2018; Kohli and Casson, 2019), the estimation of temporal dynamics of tACS-effects largely relies on probing lower temporal boundaries. Previous studies using conventional tACS (Vossen et al., 2015), found that intermittent tACS in the alpha range, applied over the visual cortex with trains of 8 s, but not 3 s, led to a modulation of visual alpha amplitude. Strüber et al. (2015) also applied tACS intermittently with 1 s intervals but found no significant after-effects. Given that a likely neural mechanism for tACS effects relies on the entrainment of ongoing neural oscillations by tACS, the relation between parameters such as phase, amplitude, and frequency of the targeted neural oscillations and applied tACS signal should modulate the effects of tACS, even more so for short stimulation intervals. By probing the coupling between tACS and alpha-band oscillations tACS effective may be rendered effective, even for low stimulation durations previously found ineffective. This would allow elucidating potential stimulation mechanisms as well as lower temporal boundaries of tACS effects.

In this work, we present the results of a study using a previously used closed-loop EEG-tACS protocol (Zarubin et al., 2018) by which the stimulation signal was phase coupled with ongoing alpha oscillations. In particular, we investigated the effects of repeated short durations of tACS (1 s) applied over the visual cortex on alpha amplitude when tACS signals and ongoing alpha visual alpha oscillations were phase-synchronized (in-phase) or in opposite phase (anti-phase) and in different states, when alpha levels were high in amplitude (eyes closed, EC) or low (eyes opened, EO). We specifically expect higher pre-to post-stimulation increases in alpha amplitudes for tACS applied in-phase as compared to an application in anti-phase and this modulation to be present in low-alpha amplitude states of the visual system (EO), but not high (EC). A dependency of stimulation effects on the phase of the tACS signal would also point towards online entrainment of visual alpha oscillations by tACS as a candidate mechanism for tACS effects. In addition to tailoring tACS to each subject's alpha frequency and phase, we also adapted the analysis regime to acknowledge inter-individual differences in the spatial pattern of stimulation effects. Specifically, we studied potential modulations of neural oscillations conventionally, using single-channel and multi-channel data, from the parietal-occipital region and contrasted it with data individually derived *via* the application of spatial filters with the common spatial patterns approach (Blankertz et al., 2008). We expected pre- to post-stimulation changes in alpha-band activity to be more pronounced for individual spatial patterns.

MATERIALS AND METHODS

Participants

Twenty healthy adults (nine females, mean age 28.4 ± 3.2 years) took part in this experiment and received monetary compensation for their participation. None of the participants had a history of psychiatric or neurological diseases and none were on any current medication affecting the central nervous system. Participants were informed about all aspects of the study and gave their written informed consent before the experiment. The study protocol was approved by the local ethics committee ("Modulation neuronaler Oszillationen mittels transkranieller Wechselstromstimulation und ihr Effekt auf die somatosensorische Wahrnehmung," 12.08.2014, Reference number: 218-14-14072014). None of the participants have claimed that the feeling of stimulation was unpleasant, and none of them have experienced phosphenes.

Experimental Procedure

Each experimental session consisted of a preparation and information part, as well as the actual stimulation and EEG recording. During the preparation and information part, participants were introduced to the aim, set-up, and procedure of the study as well as the technical background of the stimulation. Individual contraindications for tACS were checked and the consent form was given, explained, and signed. tACS electrodes as well as EEG electrodes were then set up. Participants were subsequently instructed to sit relaxed, avoid movements, and later to keep their eyes opened or closed cued block-wise. The experiment included one session, which was completed by all participants. In the beginning, four 1-min resting-state EEG data (two EC, two EO, one after another) were collected to determine individual alpha frequencies (IAFs) by contrasting peaks in fast Fourier transform (FFT) spectra between EC and EO states at channel POz. Approximately five short stimulation sequences were then applied to test the correct functioning of closed-loop model units. Thereafter, 10 blocks (in an alternating sequence of EO and EC instruction) of 50 tACS-trials were executed consecutively with short breaks between each block. Each trial consisted of a 1 s pre-stimulation interval, 1 s of stimulation (with phase adjusted by prediction from pre-stimulation), a 1 s post-stimulation interval, and an inter-trial interval (ITI) (**Figure 1C**). The random ITI was in the range of 333–666 ms with a mean value of 500 ms. Every block consisted of 25 in-phase and 25 anti-phase stimulation trials in randomly shuffled order (**Figure 1B**). The total time for each block was 3 min, resulting in a total time of approximately 45 min for all 10 blocks with breaks between and a total stimulation time of 8 min, 20 s. This allowed us to examine changes in alpha-band activity based on the overall amplitude of alpha-band power/brain state (factor STATE: EO vs. EC) and the phase-relationship between ongoing alpha-band activity and the applied tACS signal (factor STIMULATION: in-phase vs. anti-phase).

Electrical Stimulation

tACS electrodes (two conductive rubber 4 × 4 cm) were attached over standardized Cz and Oz channel locations (Jasper, 1958; Herwig et al., 2003) underneath the EEG recording cap and the sinusoidal alternating current was applied at IAF (calculated according to the procedure described above) using a battery-driven stimulator (DC-Stimulator Plus, NeuroConn, Ilmenau, Germany). Stimulation electrode positions were selected based on previous studies, in which modulations of visual alpha oscillations by tACS were reported (Neuling et al., 2013; Helfrich et al., 2014; Ruhnau et al., 2016). Impedances were kept below 10 kΩ with Ten20 conductive paste (Weaver and Company,

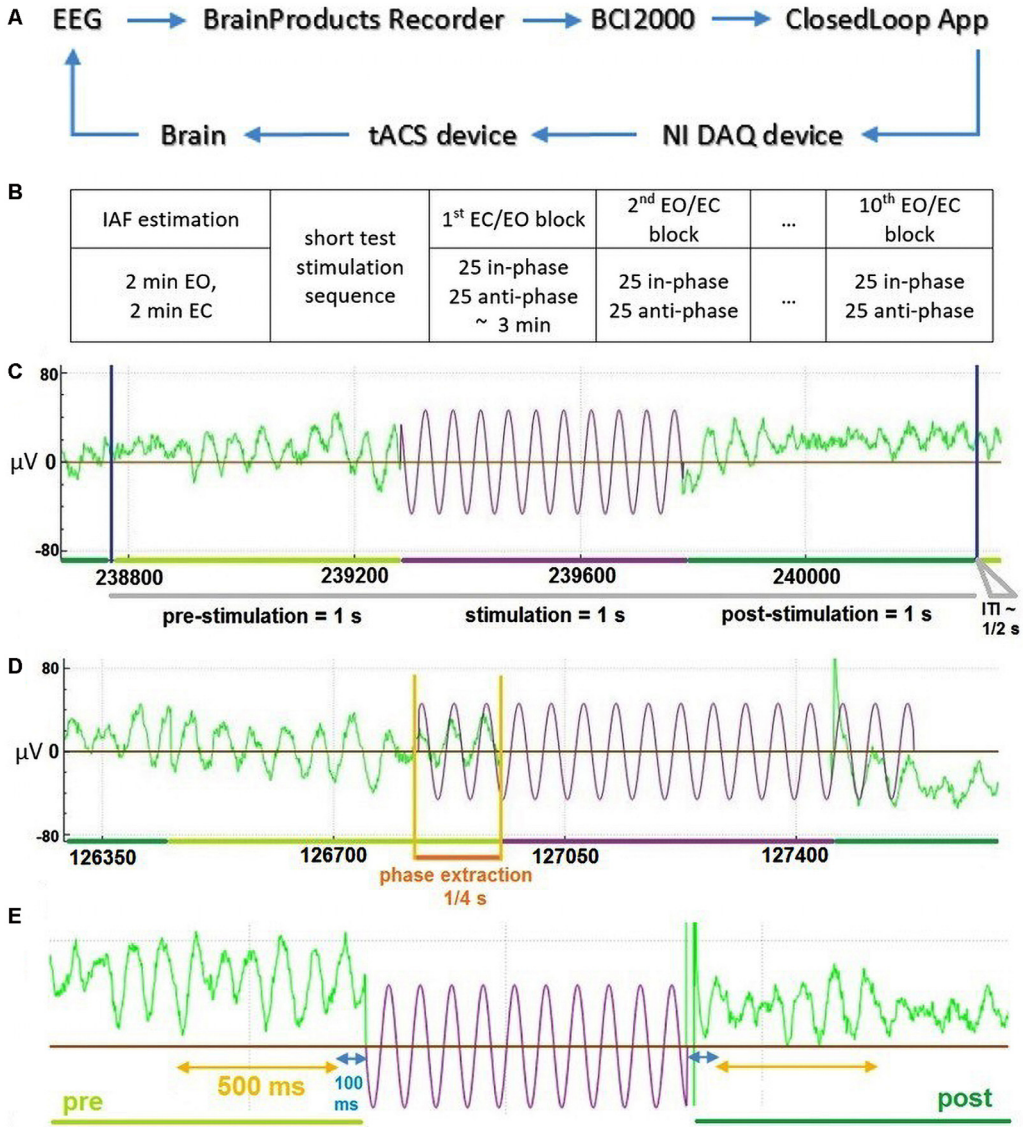

FIGURE 1 | General description of the Closed-Loop model and the temporal structure of the data. **(A)** The general model scheme of the Closed-Loop setup. **(B)** Outline of experimental procedure. **(C)** An exemplary temporal trial structure with data in green representing recorded electroencephalography (EEG) data and data in violet depicting stimulation signal. **(D)** Illustration of the stimulation signal estimation based on an extraction interval of 0.25 s for an exemplary "in-phase" stimulation trial. **(E)** Temporal scheme of EEG data (green) used for the analysis of stimulation effects due to tACS (in violet—schematic representation of stimulation wave). Interval in blue represents 100 ms data interval excluded to reduced stimulation artifacts and potential edge filtering effect.

Aurora, CO, USA). tACS at IAF was applied with an intensity of 1 mA (peak-to-peak) for all subjects. The stimulation signal for every trial was initially determined in a closed-loop application (custom made, C++), then generated through NI DAQ card (USB 6343, National Instruments, TX, USA) and transmitted to the DC-Stimulator Plus "remote input" port.

EEG Recording

EEG data were recorded using Brain Products amplifier BrainAmp MRplus (Brain Products GmbH, Gilching, Germany) with 31 Ag-AgCl electrodes mounted in a passive EEG EasyCap using a standard 10-20 system layout without Oz and Cz electrodes, with reference and ground electrode positioned at FCz and AFz and applying a sampling rate of 500 Hz. The low sampling rate was used to reduce data transfer delays through components of the model, and during recording, the data was streamed from BrainVision Recorder through its RDA client to BCI2000 (open-source software, SchalkLab), which then transmitted it to the Closed-Loop application for analysis and optimal phase prediction.

Closed-Loop Model

We used a closed-loop implementation based on a model described earlier (see **Figure 1A** and Zarubin et al., 2018) to apply

tACS stimulation either in-phase or in anti-phase (phase-shifted by 180°) of ongoing visual alpha-band activity. In brief EEG signals were extracted online. For each stimulation interval, the phase of 250 ms of previous visual alpha-band activity recorded at electrode POz was estimated *via* its the Hilbert-transform. Depending on the experimental condition a stimulation signal of length 1 s was generated that was either in-phase with the previous 250 ms of data or in the opposite phase (see **Figure 1D**). This signal was then sent to the stimulator and applied as tACS either in or in the opposite phase. Any transduction delays were accounted for (please refer to **Supplementary Materials** for a detailed explanation).

Data Analysis

Analysis of Alpha Power

The main focus of the analysis was to examine a potential modulation of alpha-band activity by tACS depending on: (1) the state (EO vs. EC); and on (2) the phase relationship of the applied tACS signal and ongoing visual alpha-band activity (in phase vs. opposite phase).

The 1 s long pre- and post-stimulation data intervals for each stimulation interval were extracted and bandpass-filtered with a 5–40 Hz 4th order Butterworth zero-phase filter, to reduce the impact of unspecific high-and low-frequency noise in our data. Pre-stimulation and post-stimulation alpha-band power were extracted from 500 ms before and 500 ms after each tACS interval (see **Figure 1E**; Note: we omitted the first 100 ms from the beginning of the post-stimulation interval, and the last 100 ms from the end of pre-stimulation to avoid any influence of the filtering edge effects and possible stimulation artifacts). For these windows, power values were then calculated *via* FFT of the detrended EEG data (zero-padding up to 512 samples). Afterward, individual alpha power values were calculated by averaging power values in the range of IAF − 1 Hz to IAF + 1 Hz (IAF was determined in the pre-experimental resting-state EEG measurement, as described above) for pre- and post-stimulation time windows and averaging across trials of each condition. Alpha-power values were extracted conventionally from a single parieto-occipital channel (POz; closest to stimulation electrode) and a parietal-occipital cluster (POC-region: P3, PO3, PO7, O1, POz, O2, PO8, PO4, P4). Also, we used a novel analysis approach tailored to account for inter-individual differences in signal representations by extracting alpha-signals, not from single channels but spatial filters weighing all electrodes to maximize signal representation (see **Supplementary Materials** for a detailed description). In brief, for each subject we calculated Common Spatial Patterns (first introduced by Blankertz et al., 2008), that either maximized pre- over post-stimulation alpha-power CSP(pre) or post-over pre-stimulation alpha-power CSP(post) for each trial with a cross-validation regime using all but the current trial for the calculation thereby avoiding overfitting of the data. Signals from these individual spatial filters were then used to calculate pre- and post-stimulation alpha power values for all experimental conditions as described above. Modulations of alpha power were tested with a repeated-measures ANOVA ($ANOVA_{RM}$) comprising the factors TIME (pre- vs. post-stimulation), STATE (EO vs. EC) and STIMULATION (in-phase vs. anti-phase) separately for all signal sources: POz data, POC data, CSP(pre) data, and CSP(post) data.

Analysis of Average Power Spectra

To investigate the frequency specificity of alpha-power modulations, we computed and analyzed the FFT-derived power spectra separately for all experimental conditions, both time windows, and all signal sources. We additionally extracted the pre-experimental power spectra as the grand-mean FFT-spectra derived from 1 s long data segments for the EO and EC blocks of the resting-state measurement recorded from POz.

Analysis of Alpha Power Modulations Across the Time Course of the Experiment

In an exploratory *post hoc* analysis, we investigated whether the alpha power decreases found for the CSP(pre) data (see "Results" section) change across the time course of the experiment as responsiveness to the stimulation may change. For this purpose, pre-to post-stimulation power modulations in percent were calculated for each trial and averaged separately for each experimental block and condition. In an $ANOVA_{RM}$ the factors BLOCK, STATE, and STIMULATION were then tested.

Analysis of Alpha Power Modulations Separately for Different Post-stimulation Time Windows

In a second *post hoc* analysis we wanted to investigate the time scale of post-stimulation alpha power decreases. For this purpose, we examined the temporal evolution of the decrease by comparing alpha power of a pre-stimulation time window [(−600 to −100) ms] to four different 500-ms long, overlapping, post-stimulation time windows [(100–600) ms, (200–700) ms, (300–800) ms, and (400–900) ms in relation to the onset of stimulation]. Pre-to-post modulations of alpha power values for the CSP(pre) data were modeled with an $ANOVA_{RM}$ comprising the factors TIMEBIN, STATE, and STIMULATION.

Results for $ANOVA_{RM}$ models were corrected for multiple comparisons using Bonferroni correction, when necessary. In the case of a violation of the homoscedasticity, degrees of freedom were corrected based on the Greenhouse–Geisser correction. Statistical analysis was performed in R (R Core Team, 2016), using the package afex (Singmann et al., 2018) running in R Studio (RStudio Team, 2015). Generalized Eta Squared (Bakeman, 2005) and Cohen's d (Lakens, 2013) served as estimates of effect sizes. *Post hoc* contrasts and marginal means (Searle et al., 1980) were calculated *via* the emmeans package.

RESULTS

Alpha Power Is Modulated by tACS in Individual Spatial Components

The main focus of the experiment was to analyze a potential modulation of visual alpha-band activity by the application of tACS either applied in- or anti-phase with ongoing visual alpha-band activity. As visible in **Figures 2A,B**, pre- and post-stimulation values only differ for power values derived from the CSP(pre) data. This difference is substantiated by the main effect for the factor time (p = 0.002; see **Table 1**): across

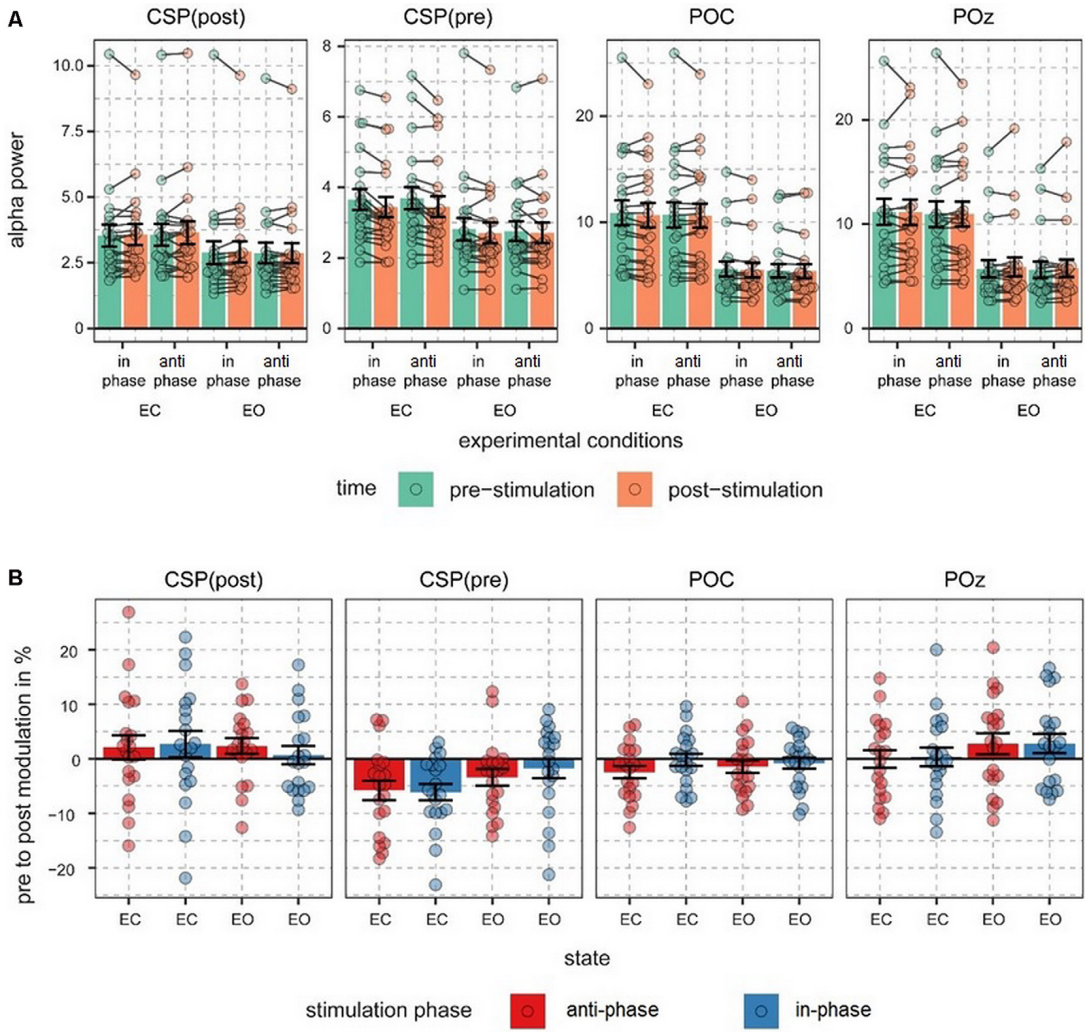

FIGURE 2 | Alpha power values and pre- to post-stimulation modulations of alpha power. **(A)** Fast Fourier transform (FFT)-derived power values were calculated for a 500-ms long pre- and post-stimulation time window separately for all experimental conditions and signal sources. Note different scales. Connected dots represent single subjects' pre- to post- alpha power changes. **(B)** Pre- to post-stimulation modulations in % are shown for all signals and conditions. Dots represent single-subject data and error bars represent standard error of the mean.

experimental conditions pre-stimulation power values are larger [M = 3.23; CI = (2.48, 3.67)] than post-stimulation power values [M = 3.08; CI = (2.64, 3.82)]. Additionally, there is a trend for an interaction of factors TIME × STATE (p = 0.058), with larger pre- to post-stimulation decreases when eyes are closed (M = −0.23; SE = 0.047) as compared to EO (M = −0.076; SE = 0.047). As revealed by the main effects STATE, for all signals (ps < 0.001; see **Table 1**) alpha power values are always larger when eyes are closed as compared to when they are open.

Alpha power values (conventionally) derived from the single electrode POz as well as the parieto-occipital cluster (POC), in contrast, are also modulated by the factor STATE (i.e., higher when eyes are closed as compared to EO; p <0.001), but are not significantly modulated by tACS or any interaction between the experimental factors (all ps > 0.292; see **Table 1**). For these channels single-subject signal dynamics vary substantially between subjects (largest between-subject variation when eyes are closed: average std = 6.806, mean = 11.25; for EO: average std = 3.817, mean = 5.742) with no clear changes between pre- and post-stimulation on the group level (see **Figure 3**).

Overall only for individual spatial components (see **Supplementary Materials** for individual and average topographical distributions of the weights), accounting for differences in the topographical distribution of modulated visual alpha-band activity, a decrease of visual alpha power was measurable, independent of the phase relationship between tACS and ongoing alpha-band activity.

Modulation of Power of Neural Oscillations Is Specific to the Alpha Range

Mean spectra averaged across all trials for different conditions, stimulation relations, with data from POz,

TABLE 1 | $ANOVA_{RM}$ table representing the results of the analysis of FFT-derived power values separately for all signals.

signal	Factor	*df*	*F*	*p*	η^2_G
CSP(post)	TIME	(1,19)	0.524	>0.999	<0.001
	*STATE***	**(1,19)**	**39.322**	**<0.001**	**0.037**
	STIMULATION	(1,19)	0.111	>0.999	<0.001
	TIME × STATE	(1,19)	0.647	>0.999	<0.001
	TIME × STIMULATION	(1,19)	0.025	>0.999	<0.001
	STATE × STIMULATION	(1,19)	1.636	0.8651	<0.001
	TIME × STATE × STIMULATION	(1,19)	0.709	>0.999	<0.001
CSP(pre)	*TIME***	**(1,19)**	**17.14**	**0.0022**	**0.004**
	*STATE****	**(1,19)**	**26.6**	**<0.001**	**0.09**
	STIMULATION	(1,19)	0	>0.999	<0.001
	TIME × STATE	(1,19)	7.246	0.0578	0.001
	TIME × STIMULATION	(1,19)	0.224	>0.999	<0.001
	STATE × STIMULATION	(1,19)	1.114	>0.999	<0.001
	TIME × STATE × STIMULATION	(1,19)	0.712	>0.999	<0.001
POC	TIME	(1,19)	3.684	0.797	0.002
	*STATE****	**(1,19)**	**20.38**	**<0.001**	**0.12**
	STIMULATION	(1,19)	1.53	0.4588	0.001
	TIME × STATE	(1,19)	1.725	>0.999	<0.001
	TIME × STIMULATION	(1,19)	1.544	0.876	0.001
	STATE × STIMULATION	(1,19)	0.432	>0.999	<0.001
	TIME × STATE × STIMULATION	(1,19)	0.36	>0.999	<0.001
POz	TIME	(1,19)	1.3	>0.999	<0.001
	*STATE****	**(1,19)**	**43.192**	**<0.001**	**0.253**
	STIMULATION	(1,19)	3.923	0.2492	<0.001
	TIME × STATE	(1,19)	0.347	>0.999	<0.001
	TIME × STIMULATION	(1,19)	0.015	>0.999	<0.001
	STATE × STIMULATION	(1,19)	0.226	>0.999	<0.001
	TIME × STATE × STIMULATION	(1,19)	0.166	>0.999	<0.001

*Significant effects are marked by asterisks and bold text. ***p <0.001, **p < 0.01. p-Values are Bonferroni corrected for the four $ANOVA_{RM}$ models.*

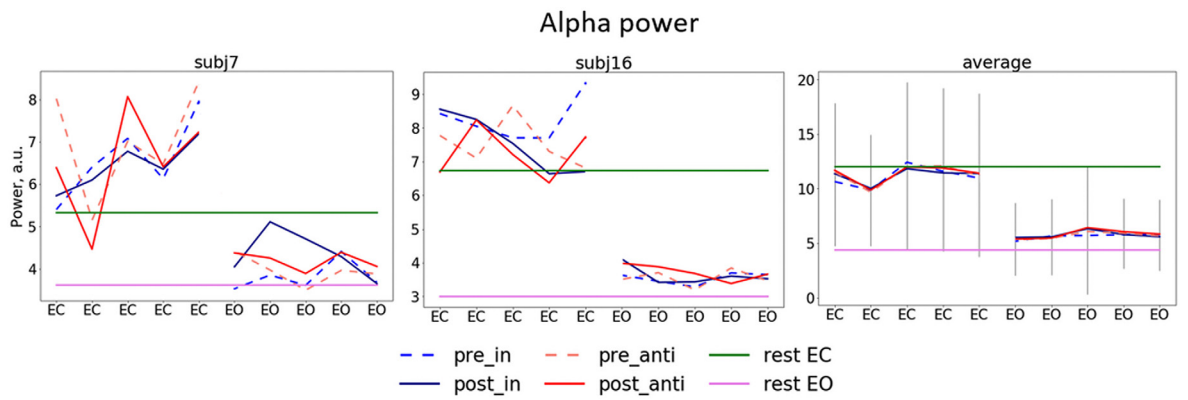

FIGURE 3 | Dynamics of alpha power separate for stimulation blocks. Mean pre/post-stimulation values for in-phase and anti-phase relation (pre_in, post_in, pre_anti, post_anti) for exemplary subjects (the left and the center plots) and the group average (the right plot) first five blocks (eyes closed, EC) correspond to blocks in which participants had their EC and second five blocks eyes open (EO), green and pink horizontal lines represent alpha power for EC and EO in resting state, gray lines represent average standard deviation.

both CSP components, POC, as well as relations of post- to pre-stimulation are shown in **Figure 4**. The analysis of the spectra revealed visible differences between pre- and post-stimulation time for signals extracted from both CSP components (**Figure 4A**) for when participants had their eyes closed as well as open. As visible in **Figure 4B**, these differences have their maxima in the alpha range without prominent changes to frequencies other than in a range near individual alpha bands.

Modulations of Alpha Power Do Not Change Across the Time Course of the Experiment

In an exploratory *post hoc* analysis, we investigated whether the modulation of CSP(pre)-derived alpha power values by tACS changed across the experimental blocks. As visible in **Figure 5**, there was no systematic change of pre- to post alpha-power modulations across the time course of the experiment.

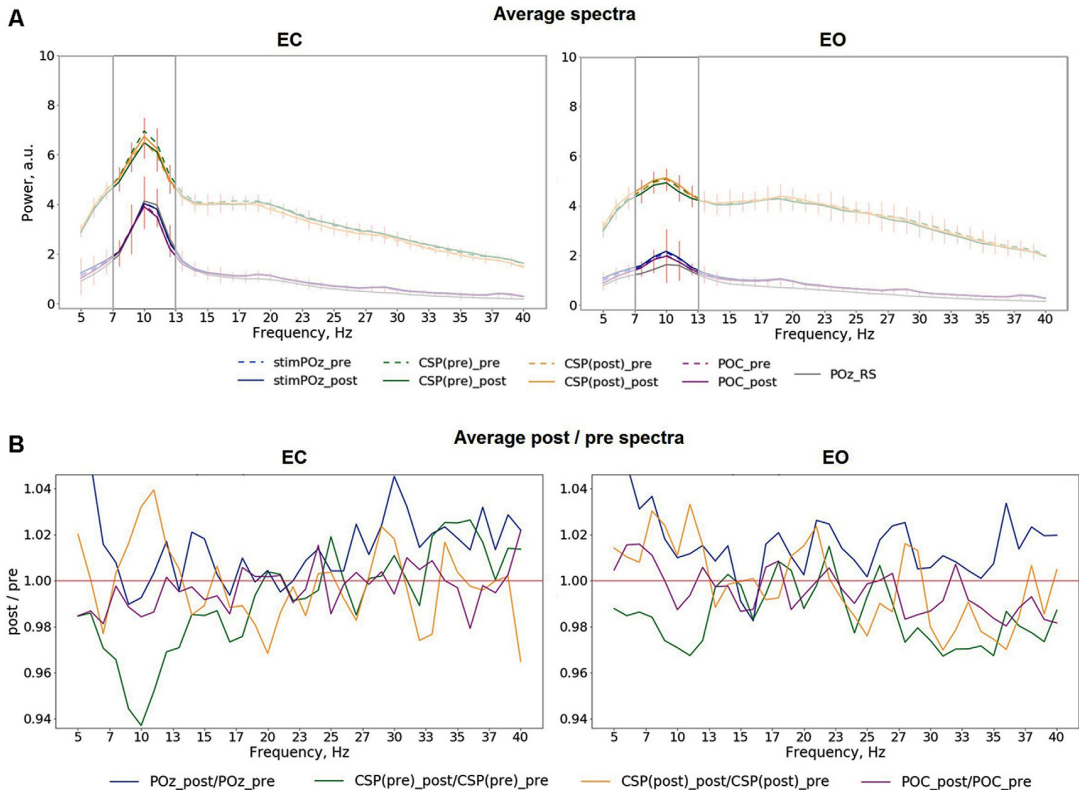

FIGURE 4 | (A) Average pre- and post-stimulation spectra for different eye conditions, including both in- and anti-phase trials: EC (left), EO (right), red vertical lines represent the standard deviation of the average difference between pre- and post-stimulation. **(B)** Average relation of post-/pre-stimulation spectra.

Consequently, modeling CSP(pre)-derived pre- to post power modulations with an $ANOVA_{RM}$ model revealed the factor BLOCK to be insignificant (see **Table 2**). Therefore, overall pre-to post-stimulation modulations of alpha power seemed to be stable across the experiment. Pre- to post-stimulation decreases were, however, dependent on the state, as revealed by the main effect for the factor STATE ($p = 0.031$) and was larger when eyes were closed [$M = -5.786$; CI = $(-8.756, -2.816)$] as compared to eyes open [$M = -1.829$; CI = $(-4.8, 1.141)$].

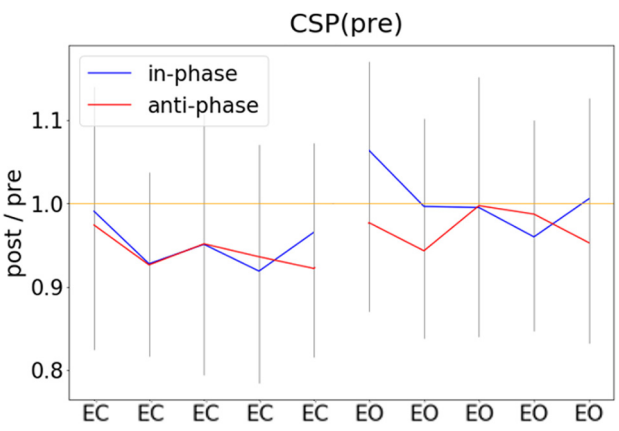

FIGURE 5 | Pre- to post-stimulation power modulations computed separately for experimental blocks. Pre- and post-stimulation ratios of FFT-derived power values were calculated for a 500-ms long pre- and post-stimulation time window separately for all experimental conditions and experimental blocks, gray lines represent standard deviation.

Modulation of Alpha Power Is Transient

We investigated the time scale of post-stimulation alpha power decreases by additionally modeling the effects of pre- to post-stimulation power modulations separately for different overlapping post-cue time windows. The analysis revealed the factor TIMEBIN to be significant ($p = 0.018$; see **Table 3**). *Post hoc* linear contrasts revealed pre- to post-stimulation decreases to be modeled best by a linear decrease ($t_{(57)} = 3.497$; $p = 0.001$). Overall, independent of the experimental condition (i.e., EO vs. EC; stimulation in- vs. anti-phase) the pre-to post-stimulation decreases are largest right after the stimulation and then decay across subsequent time windows (see **Figure 6**).

DISCUSSION

Our study aimed to investigate the effects of tACS applied bilaterally over the visual cortex, tuned to neural alpha oscillations with a closed-loop EEG-tACS setup on visual alpha oscillations. Specifically, we have studied stimulation effects of tACS applied either in-phase or anti-phase with

TABLE 2 | $ANOVA_{RM}$ table representing results of the analysis of FFT-derived pre-to post-stimulation power modulation for the CSP(pre) data for time-course analysis of the stimulation effects across the experiment.

Factor	*df*	*F*	*p*	η^2_G
STATE*	**(1,17)**	**5.563**	**0.0306**	**0.022**
STIMULATION	(1,17)	0.684	0.4196	0.002
BLOCK	(3.13, 53.2)	2.009	0.1213	0.021
STATE × STIMULATION	(1,17)	0.279	0.604	0.001
STATE × BLOCK	(3.33, 56.6)	0.289	0.8522	0.003
STIMULATION × BLOCK	(3.58, 60.9)	0.43	0.766	0.004
STATE × STIMULATION × BLOCK	(3.22, 54.7)	1.571	0.2043	0.017

*Significant effects are marked by asterisks and bold text. *p < 0.05.*

TABLE 3 | $ANOVA_{RM}$ table representing results of the analysis of FFT-derived pre-to post-stimulation power modulation for the CSP(pre) data for analyzing the time scale of the stimulation effects.

Factor	*df*	*F*	*p*	η^2_G
STATE	(1,19)	3.201	0.0895	0.037
STIMULATION	(1,19)	0.58	0.4557	0.004
*TIME BIN**	**(1.95, 37)**	**4.537**	**0.018**	**0.006**
STATE × STIMULATION	(1,19)	0.76	0.3941	0.007
STATE × TIME BIN	(1.34, 25.4)	1.303	0.2772	0.002
STIMULATION × BLOCK	(1.41, 26.9)	0.055	0.8926	<0.001
STATE × STIMULATION × BLOCK	(1.8, 34.2)	0.141	0.8487	<0.001

*Significant effects are marked by asterisks and bold text. *p < 0.05.*

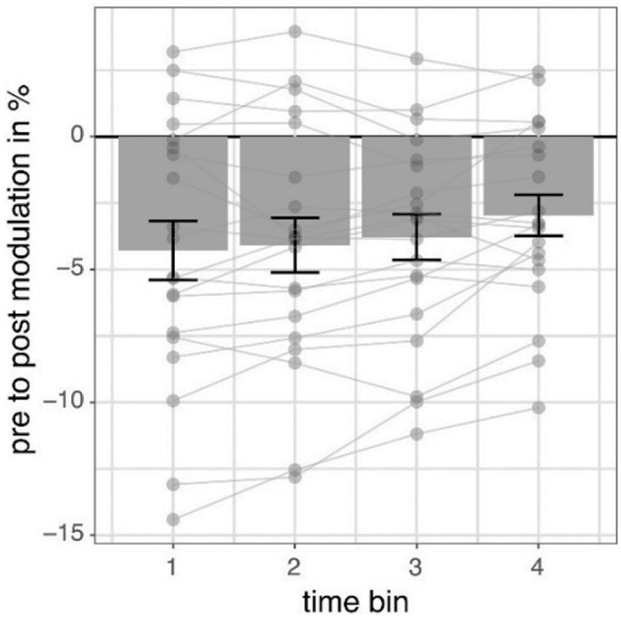

FIGURE 6 | Pre- to post-stimulation power modulations separately for different time windows. The data represents pre- to post-stimulation modulations of alpha power from a 500-ms long pre-stimulation time window to four different 500-ms long overlapping post-stimulation time windows averaged for all experimental conditions in percent. Post-stimulation time bins are made up by data from the following time windows: (100; 600) ms, (200; 700) ms, (300; 800) ms, (400; 900) ms concerning the onset of the stimulation and always compared to the same pre-stimulation time window (−600; −100) ms. Error bars represent standard error of the mean and dots represent single subjects.

ongoing alpha oscillations during periods of a high-amplitude vs. low-amplitude alpha oscillations on the amplitude of alpha oscillations.

Overall, we found a decrease in alpha amplitude immediately after tACS when accounting for individual spatially specific alpha components with a cross-validation procedure. While these changes had an overall topographical center of gravity in occipital regions, they were individually specific and effects were not observable when data was extracted from a single occipital electrode or a general occipital electrode cluster as in a conventional analysis approach. Although the decreases in amplitude found for a 500-ms long time window seem to be only transient and attenuate across the range of 400 ms, they were constant across the time course of the experiment.

In contrast to previous studies, we found a decrease of alpha amplitude as a response to tACS. Zaehle et al. (2010) previously reported an increase of alpha amplitude after 10 min of tACS applied over occipital areas at the individual alpha frequency. Similarly, in various subsequently published studies the application of alpha tACS over visual areas in the range of minutes led to an increase in alpha amplitude (Neuling et al., 2013; Helfrich et al., 2014; Kasten et al., 2016). While these studies differ in their overall stimulation duration, some studies used intermittent short stimulation protocols closer to the design in our study. Strüber et al. (2015) used an experimental protocol similar to ours by intermittently applying 1-s long stimulation trials using conventional tACS. They found no evidence of a modulation of alpha power by tACS. However, they analyzed data only from a single channel (POz) and a longer time interval (1 s). Our data revealed significant stimulation effects to be present only in individual spatial components, but absent at POz and to be transient as they decreased within 400 ms after the end of stimulation. Vossen et al. (2015) applied longer stimulation durations with a different stimulation electrode montage (bilaterally over PO7/PO9 and PO8/PO10) and found that only 8-s intermittent stimulation, but not 3 s, led to pronounced alpha amplitude increases. In another study, Sliva et al. (2018) applied intermittent non-adaptive stimulation of a 6-s duration to investigate the influence of tACS on somatosensory perception and found that such stimulation was not sufficient to induce significant causal effects on EEG-measured alpha oscillations.

Because stimulation protocols with longer stimulation durations seem to lead to an increase in alpha amplitude and studies employing trains of stimulation with a duration of 3 s or less either found no evidence for a stimulation effect or a decrease in amplitude, as we did here, it is tempting to speculate about the parameters that shape the stimulation effect. If decreases and increases in amplitude represent two extreme cases, is there a stimulation duration that represents a transition from one to another? What additional factors may contribute to shaping the stimulation effects? Recent studies suggest that the brain state plays a crucial role: when eyes were closed or the room was not illuminated, alpha tACS did not lead to an increase in the amplitude, suggesting that tACS may not modulate the amplitude of oscillations that are already in a high amplitude state (Neuling et al., 2013; Ruhnau et al., 2016). An additional

factor may be related to the electrode positioning. When in anti-phase and inter-hemispherically stimulating two coupled mu-alpha generators in the somatosensory system, we previously found a decrease of mu-alpha amplitude after a 5-min tACS application (Gundlach et al., 2017). This decrease was also found for inter-hemispheric tACS targeting theta oscillations (Garside et al., 2015). In a computational study, simulating stimulation after-effects in neural networks with nodes coupled with a time delay in-phasic stimulation led to amplitude increases, while anti-phasic stimulation led to no increases in oscillatory activity (Kutchko and Fröhlich, 2013). Therefore, further studies parametrically manipulating different factors such as duration and electrodeposition are required to map the effects of tACS more completely.

We found stimulation related decreases in the amplitude to be independent of the phase relationship between ongoing alpha oscillations and the tACS signal. Both in-phase, as well as anti-phase stimulation (i.e., stimulation phase being identical to the phase of ongoing alpha oscillation measured over POz vs. shifted by 180 degrees and thereby reversed in polarity), disrupted ongoing alpha oscillations. This finding is difficult to reconcile with a stimulation effect mediated by entrainment. While in animal studies online effects were found to be directly related to entrainment of ongoing neural activity by the applied electric oscillation (Fröhlich and McCormick, 2010; Ozen et al., 2010; Reato et al., 2010), in human studies investigating post-stimulation modulations of oscillations it was proposed that these offline effects may stem from LTP/LTD related effects (Zaehle et al., 2010; Vossen et al., 2015; Vosskuhl et al., 2018). Like others, we previously reported on tACS driven decreases in the amplitude of ongoing oscillations (Garside et al., 2015; Gundlach et al., 2017). While stimulation locations and protocols differed in these studies, the findings common to them and reported here showed, that amplitude decreases even beyond the stimulation period cannot be caused and explained by mere entrainment of ongoing oscillations by tACS on its own. Thus, it seems to be the case that offline effects are caused by neurophysiological mechanisms different from entrainment. Interestingly, similar to the effects found in the animal studies described above, the online effects of tACS measured in humans during the stimulation are consistent with the entrainment of neural activity by tACS. For instance, behavioral modulations depend on the stimulation frequency (Joundi et al., 2012; Santarnecchi et al., 2013) and phase of the tACS signal (Neuling et al., 2012; Gundlach et al., 2016). In the same vein in recent work by Fiene et al. (2020), it was shown that the interaction between ongoing stimulus processing and tACS was dependent on their phase relationship. The authors measured SSVEP amplitudes driven by a visual flicker after a period of tACS applied over visual areas with the same frequency as the flicker. Crucially they varied the phase relationship between tACS and flicker and found that the SSVEP amplitude varied accordingly. These findings show an interaction between stimulus processing and tACS modulated neural activity pointing towards a mechanism of entrainment of ongoing neural activity by tACS that affects stimulus processing even after the termination of the stimulation. It would be of great interest to see whether these effects would hold for other stimulation frequencies and could thus be related to the modulation of ongoing neural activity or whether these effects may arise from a mere phasic modulation of excitability. Overall, previous studies suggest that tACS effects may be caused by two different and potentially distinct mechanisms (see Heise et al., 2019): tACS may lead to online entrainment of ongoing oscillations and additional changes in neural plasticity responsible for stimulation outlasting offline effects. While Kar and Krekelberg (2014) found tACS-induced changes in neural adaptation to be potentially closely linked to changes in neural plasticity, the functional underpinnings of such effects as well as the relationship between online entrainment and offline neural plasticity remain unknown.

Interestingly, the stimulation effects in our study seem to be only transient, as they decreased after the end of the stimulation and were not different across the time course of the experiment (i.e., there was no evidence for an increased or decreased responsiveness to the stimulation). Effects related to neuroplastic changes seem to depend on the stimulation duration. For instance, neural excitability is longer modulated the longer tDCS was applied (Nitsche et al., 2003), and after-effects of tACS on behavior increased across the time course of the experiment (Heise et al., 2019). A tentative and an alternative interpretation of our findings showing the stimulation effect to be independent of the time in the experiment could be that the application of short stimulation periods in our experiment did not lead to plastic modulation of alpha generators, but instead briefly disturbed ongoing oscillations. Because alpha rhythm seems to fluctuate between different states of activity level (Freyer et al., 2009, 2011), the transient decrease in amplitude after the application of tACS may index a brief shift of alpha activity towards a lower activity level by tACS. However, when assuming online entrainment of alpha activity by tACS, it is puzzling that both in- and anti-phase stimulation lead to a similar effect of amplitude attenuation. Specifically, one would hypothesize a synchronous application (no phase difference and the same polarity) not to disrupt the specific oscillation, while an asynchronous application would be more likely to be disruptive. We extensively tested our setup and phase extraction as well as forecast algorithms to ensure that the relation of the stimulation phase and phase of ongoing alpha oscillations was captured correctly (see Zarubin et al., 2018). While small deviations in the phase relation may arise from the phase estimation, forecast process, and underlying assumptions of stationarity, the overall phase relation is thus estimated accurately. If in- and anti-phase stimulation are indeed different in their phase relationship, why would they lead to a similar effect, namely the decrease in alpha amplitude? Several recent studies have suggested that alpha oscillations measured on a macroscale-level are the product of different alpha generators with different spatial, laminar, or functional profiles rather than being produced by a single generator (Bollimunta et al., 2008; Haegens et al., 2015; Keitel and Gross, 2016; Scheeringa et al., 2016; Barzegaran et al., 2017; Benwell et al., 2019; Schaworonkow and Nikulin, 2019). The potential interaction, coupling, and interdependence of different alpha generators are, however, vastly unknown.

There is some evidence that different alpha generators may be antagonistically coupled, for instance, seen in the relationship of visual alpha and sensorimotor mu-alpha (Gerloff et al., 1998; Neuper and Pfurtscheller, 2001) or the focal down- and surround up-regulation of alpha generators in the somatomotor system (Suffcynski et al., 1999) or the different alpha profiles in different layers of intracortical measurements (Bollimunta et al., 2008, 2011). If different alpha generators were indeed negatively coupled, the up-modulation in one (i.e., by NIBS) could lead to a down-modulation of the other. The single trial, cross-validated CSP filtering procedure extracts components and maximizes a stimulation-induced change in alpha power, facilitating the revelation of a spatially distinct alpha component that shows a decrease in power. Crucially this decrease captured in different components may be caused by different underlying mechanisms: it may capture an antagonistic decrease during in-phase tACS up-modulation, a decrease due to a potentially disturbing effect of anti-phase tACS or a homeostatic rebound after an up-regulation during tACS as a (meta)-plastic effect (Abraham, 2008; Gundlach et al., 2017). Our optimization algorithm (CSP) indicated consistently a decrease in the amplitude of alpha oscillations, regardless of the relationship between the phase of tACS and the phase of the ongoing alpha oscillations. This finding may thus suggest that the effect of any briefly applied tACS for occipital alpha generators, be it in- or anti-phase may be rather disruptive in its nature.

To our knowledge, we are the first to utilize CSP filtering for the analysis of tACS effects and thus to obtain neural activity selectively tuned to show a decrease or an increase of alpha oscillations following tACS. Although CSP is mainly applied in BCI paradigms to differentiate particular activation patterns, which usually correspond to different anatomical regions (e.g., left or right motor imaginary corresponding to the activation of the right or left motor cortex), this method also can be useful for discriminating between activity in the same spatial region, which was previously shown for alpha oscillations with standard and deviant visual stimuli (Tugin et al., 2016). In our study, CSP was used to provide spatial filters maximally discriminating activity between the periods with and without stimulation. This in turn allowed the contribution of stimulation-related neural changes to be maximized while attenuating irrelevant neural activity typically masking effects of stimulation in the sensor space. As previously mentioned, tACS always affects a broad region of neural populations, and thus studying its influence based only on data from a single or few channels is only an approximate simplification. Such approaches lead to a significant reduction of the observation space, the omission of region-specific dynamics, and raises the impact of noise and volume conduction in the data. Therefore, to perform a deeper, more comprehensive, and more extensive investigation of the respective research question, CSP and other spatial filtering methods should be considered for the analysis of tACS effects and brain stimulation effects in general. Importantly, the modulatory effects of tACS were primarily limited to the occipito-parietal regions—areas targeted with tACS in our study. Such spatial distribution of the observed effects challenges the possibility that the effects of tACS might have been due to the stimulation of the scalp (Vöröslakos et al., 2018; Asamoah et al., 2019). In this case, we would expect attenuation of alpha/mu oscillations over the sensorimotor areas, which was not the case here. Even though recent work strongly favors the direct modulation of neural activity by tACS (Kasten et al., 2019; Krause et al., 2019; Negahbani et al., 2019; Vieira et al., 2019) the contribution of various sources such as peripheral or retinal stimulation is currently controversially discussed. Given the here found phase-independent stimulation effects, we cannot rule out a potential contribution of general stimulation effects. Future work will have to disentangle the contribution of different mechanisms to overall effects.

One limitation of our study is that our design may be suboptimal in promoting plastic changes in neural activity developing during the time of the stimulation. Using a purely event-related design, the stimulation phase varied randomly between in-phase and anti-phase with ongoing alpha oscillations. If tACS were able to lead to online entrainment of ongoing neural oscillations as a potential prerequisite for offline effects, one could hypothesize that this effect would be more pronounced when the same phase-orientation ("in" or "anti") were utilized over the whole duration of the stimulation block or experiment (Deans et al., 2007; Fröhlich and McCormick, 2010; Ozen et al., 2010; Helfrich et al., 2014). Varying the phase relationship across trials might have interfered with an effect that relies on accumulating over time and may have masked the potential effects of tACS.

Another limitation concerns the sampling of the phase space phase to evaluate a potential relationship between mu-alpha-band activity and applied tACS. While we varied signals to examine the two most-extreme relationships (in phases vs. in opposite phase) and focused our phase extraction-, stimulation- and analysis-regimes to capture and modulate parieto-occipital alpha-generators, this may not capture the richness of the underlying dynamics that may stem from an interplay of thalamic and multiple cortical alpha generators (Bollimunta et al., 2008; Meij et al., 2016). Given the cost of extensively sampling the whole parameter space, promising new approaches like Bayesian sampling (Lorenz et al., 2019), may help to draw a more complete picture of underlying dynamics. These approaches may also help to elucidate the impact of different stimulation parameters like the amplitude of the applied tACS current which varies between studies (for an overview see Strüber et al., 2015; Veniero et al., 2015) and may likely affect stimulation outcomes. While we used a stimulation intensity that is comparable to previous studies (Helfrich et al., 2014; Strüber et al., 2015; Gundlach et al., 2016, 2017), we cannot rule out that phase-dependent stimulation effects may potentially be measurable for higher stimulation intensities.

Closed-loop tACS and, in general, adaptive NIBS in comparison to conventional stimulation protocols have several advantages, which could be potentially beneficial for the whole brain stimulation research field and transform it into a more reliable and clinically applicable approach. As mentioned by Zrenner et al. (2016), these advantages include: personalized neuromodulation to decrease inter-individual variability of effects, analysis of network reorganization dynamics, such as

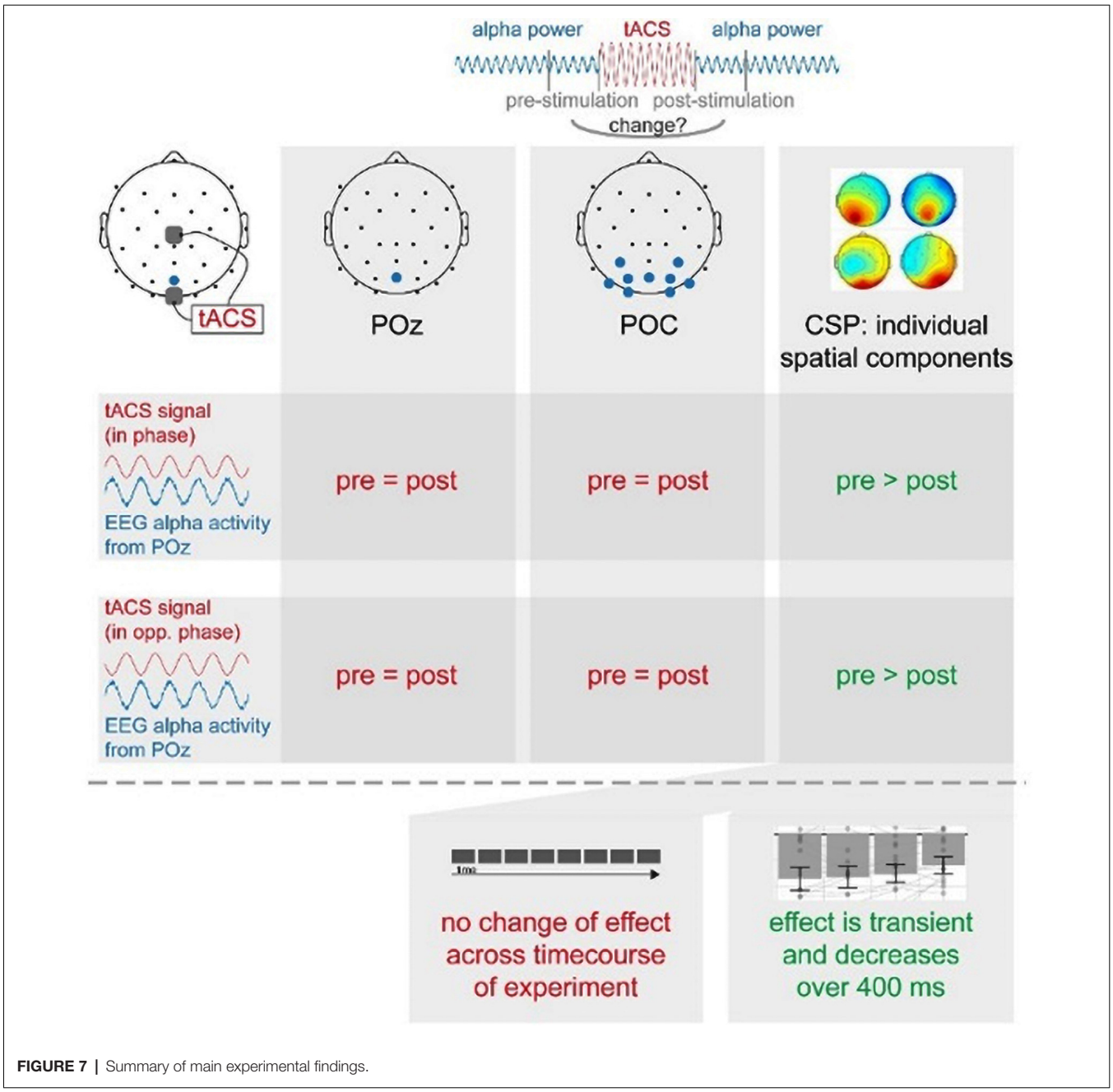

FIGURE 7 | Summary of main experimental findings.

during stroke, for instance, to aid rehabilitation and target as well as specifically modify potentially different plasticity patterns. One of the main challenges impeding the development of closed-loop tACS, however, is the fact that the analysis of online effects during stimulation is compromised by massive stimulation-induced artifacts. In principle, the signal to be analyzed and modulated (e.g., a signature of alpha oscillations measured in the EEG) is overwritten by the tACS signal, which is several magnitudes larger but covers the same spatial and temporal space. Thus, substantial efforts in recent studies have been directed to the development of artifact elimination methods using different techniques and experimental protocols (Witkowski et al., 2016; Noury and Siegel, 2017; Kasten et al., 2018; Kohli and Casson, 2019). However, intermittent stimulation allows one to follow another approach while still based on adaptive principles. By studying the immediate after-effects in intervals between periods of stimulation without artifacts, such studies may contribute towards exploring related online effects and enhance the understanding of tACS effects and mechanisms in general. One prominent recent study with phase-locked closed-loop stimulation was presented by Mansouri et al. (2018). By using intermittent stimulation with very short (5 ms) square-wave pulses and an artifact removal procedure using a spline interpolation (Waddell et al., 2009), they were able to

extract the artifact-free EEG signal and thus control for the actual phase locking of delivered stimulation and ongoing oscillation in alpha and theta bands. Such approaches may help to elucidate the role of adaptive NIBS on brain activity and ultimately the role of brain activity on cognition, perception, and behavior in general.

In summary (see **Figure 7**), we found that short-time intermittent tACS applied over occipital regions (Cz and Oz), as used in previous studies, induces a transient suppression of occipital alpha generators, leading to a decrease in alpha power in spatially specific components centered over a parieto-occipital region. This effect was independent of the phase relationship between the tACS signal and alpha oscillations. This suggests to us that these offline effects of short-timed intermittent tACS are not explainable by entrainment alone but rather require neuroplastic changes or a transient disruption of neural oscillations. These effects were only visible in individual spatial alpha components, but not in a broad occipital cluster or pre-selected electrode. Our study thus supports the notion that the response to tACS differs inter-individually and that even intra-individual effects are shaped by the interplay between different alpha generators. This favors stimulation protocols as well as analysis regimes exploiting inter-individual differences to more efficiently induce as well as more reliably reveal otherwise hidden stimulation effects and thereby comprehensively study the effects and the underlying mechanisms of tACS.

DATA AVAILABILITY STATEMENT

The datasets generated for this study are available on request to the corresponding author.

ETHICS STATEMENT

The studies involving human participants were reviewed and approved by the Ethical Committee at the Medical Faculty, Leipzig University, under the protocol "Modulation neuronaler Oszillationen mittels transkranieller Wechselstromstimulation und ihr Effekt auf die somatosensorische Wahrnehmung," 12.08.2014, Reference number: 218-14-14072014. The patients/participants provided their written informed consent to participate in this study.

AUTHOR CONTRIBUTIONS

GZ, CG, AV, and MB: conceptualization. GZ and CG: data curation. GZ, CG, and VN: formal analysis. AV and MB: funding acquisition. GZ, CG, and VN: investigation. GZ, CG, VN, and MB: methodology. GZ and CG: project administration, visualization, and writing—original draft. MB and AV: resources. GZ, CG, VN, and MB: software. VN, AV, MB, and CG: supervision. GZ, CG, and VN: validation. GZ, CG, VN, AV, and MB: writing—review and editing.

FUNDING

This work was supported by the funding of the Max Planck Society (Max-Planck-Institut für Kognitions- und Neurowissenschaften), Leipzig University and IMPRS NeuroCom Ph.D. program. VN was supported in part by the HSE Basic Research Program and the Russian Academic Excellence Project "5-100."

ACKNOWLEDGMENTS

We thank Sylvia Stasch for her help during the recruitment and data recording phase.

SUPPLEMENTARY MATERIAL

The Supplementary Material for this article can be found online at: https://www.frontiersin.org/articles/10.3389/fnhum.2020.00366/full#supplementary-material.

REFERENCES

Abraham, W. C. (2008). Metaplasticity: tuning synapses and networks for plasticity. *Nat. Rev. Neurosci.* 9, 387–387. doi: 10.1038/nrn2356

Angius, L., Mauger, A., Hopker, J., Pascual-Leone, A., Santarnecchi, E., and Marcora, S. (2018). Bilateral extracephalic transcranial direct current stimulation improves endurance performance in healthy individuals. *Brain Stimul.* 11, 108–117. doi: 10.1016/j.brs.2017.09.017

Antal, A., Alekseichuk, I., Bikson, M., Brockmöller, J., Brunoni, A., Chen, R., et al. (2017). Low intensity transcranial electric stimulation: safety, ethical, legal regulatory and application guidelines. *Clin. Neurophysiol.* 128, 1774–1809. doi: 10.1016/j.clinph.2017.06.001

Asamoah, B., Khatoun, A., and Mc Laughlin, M. (2019). tACS motor system effects can be caused by transcutaneous stimulation of peripheral nerves. *Nat. Commun.* 10:266. doi: 10.1038/s41467-018-08183-w

Bakeman, R. (2005). Recommended effect size statistics for repeated measures designs. *Behav. Res. Methods* 37, 379–384. doi: 10.3758/bf03192707

Barzegaran, E., Vildavski, V., and Knyazeva, M. (2017). Fine structure of posterior α rhythm in human EEG: frequency components, their cortical sources, and temporal behavior. *Sci. Rep.* 7:8249. doi: 10.1038/s41598-017-08421-z

Benwell, C., London, R., Tagliabue, C., Veniero, D., Gross, J., Keitel, C., et al. (2019). Frequency and power of human α oscillations drift systematically with time-on-task. *NeuroImage* 192, 101–114. doi: 10.1016/j.neuroimage.2019.02.067

Bergmann, T., Karabanov, A., Hartwigsen, G., Thielscher, A., and Siebner, H. (2016). Combining non-invasive transcranial brain stimulation with neuroimaging and electrophysiology: current approaches and future perspectives. *NeuroImage* 140, 4–19. doi: 10.1016/j.neuroimage.2016.02.012

Blankertz, B., Tomioka, R., Lemm, S., Kawanabe, M., and Muller, K. (2008). Optimizing spatial filters for robust EEG single-trial analysis. *IEEE Signal Process. Magaz.* 25, 41–56. doi: 10.1109/MSP.2008.4408441

Bollimunta, A., Chen, Y., Schroeder, C. E., and Ding, M. (2008). Neuronal mechanisms of cortical α oscillations in awake-behaving macaques. *J. Neurosci.* 28, 9976–9988. doi: 10.1523/jneurosci.2699-08.2008

Bollimunta, A., Mo, J., Schroeder, C., and Ding, M. (2011). Neuronal mechanisms and attentional modulation of corticothalamic α oscillations. *J. Neurosci.* 31, 4935–4943. doi: 10.1523/jneurosci.5580-10.2011

Brittain, J., Probert-Smith, P., Aziz, T., and Brown, P. (2013). Tremor suppression by rhythmic transcranial current stimulation. *Curr. Biol.* 23, 436–440. doi: 10.1016/j.cub.2013.01.068

Cabral-Calderin, Y., Anne Weinrich, C., Schmidt-Samoa, C., Poland, E., Dechent, P., Bähr, M., et al. (2015). Transcranial alternating current stimulation affects the BOLD signal in a frequency and task-dependent manner. *Hum. Brain Mapp.* 37, 94–121. doi: 10.1002/hbm.23016

Deans, J., Powell, A., and Jefferys, J. (2007). Sensitivity of coherent oscillations in rat hippocampus to AC electric fields. *J. Physiol.* 583, 555–565. doi: 10.1113/jphysiol.2007.137711

Edwards, D., Cortes, M., Wortman-Jutt, S., Putrino, D., Bikson, M., Thickbroom, G., et al. (2017). Transcranial direct current stimulation and sports performance. *Front. Hum. Neurosci.* 11:243. doi: 10.3389/fnhum.2017.00243

Feurra, M., Bianco, G., Santarnecchi, E., Del Testa, M., Rossi, A., and Rossi, S. (2011a). Frequency-dependent tuning of the human motor system induced by transcranial oscillatory potentials. *J. Neurosci.* 31, 12165–12170. doi: 10.1523/JNEUROSCI.0978-11.2011

Feurra, M., Paulus, W., Walsh, V., and Kanai, R. (2011b). Frequency specific modulation of human somatosensory cortex. *Front. Psychol.* 2:13. doi: 10.3389/fpsyg.2011.00013

Fiene, M., Schwab, B. C., Misselhorn, J., Herrmann, C. S., Schneider, T. R., and Engel, A. K.. (2020). Phase-specific manipulation of rhythmic brain activity by transcranial alternating current stimulation. *Brain Stimulation* 13, 1254–1262. doi: 10.1016/j.brs.2020.06.008

Freyer, F., Aquino, K., Robinson, P., Ritter, P., and Breakspear, M. (2009). Bistability and non-gaussian fluctuations in spontaneous cortical activity. *J. Neurosci.* 29, 8512–8524. doi: 10.1523/jneurosci.0754-09.2009

Freyer, F., Roberts, J., Becker, R., Robinson, P., Ritter, P., and Breakspear, M. (2011). Biophysical mechanisms of multistability in resting-state cortical rhythms. *J. Neurosci.* 31, 6353–6361. doi: 10.1523/jneurosci.6693-10.2011

Fröhlich, F., and McCormick, D. (2010). Endogenous electric fields may guide neocortical network activity. *Neuron* 67, 129–143. doi: 10.1016/j.neuron.2010.06.005

Garside, P., Arizpe, J., Lau, C., Goh, C., and Walsh, V. (2015). Cross-hemispheric alternating current stimulation during a nap disrupts slow wave activity and associated memory consolidation. *Brain Stimul.* 8, 520–527. doi: 10.1016/j.brs.2014.12.010

Gerloff, C., Richard, J., Hadley, J., Schulman, A. E., Honda, M., and Hallett, M. (1998). Functional coupling and regional activation of human cortical motor areas during simple, internally paced and externally paced finger movements. *Brain* 121, 1513–1531. doi: 10.1093/brain/121.8.1513

Guerra, A., López-Alonso, V., Cheeran, B., and Suppa, A. (2017). Solutions for managing variability in non-invasive brain stimulation studies. *Neurosci. Lett.* 30:133332. doi: 10.1016/j.neulet.2017.12.060

Gundlach, C., Müller, M., Nierhaus, T., Villringer, A., and Sehm, B. (2016). Phasic modulation of human somatosensory perception by transcranially applied oscillating currents. *Brain Stimul.* 9, 712–719. doi: 10.1016/j.brs.2016.04.014

Gundlach, C., Müller, M., Nierhaus, T., Villringer, A., and Sehm, B. (2017). Modulation of somatosensory α rhythm by transcranial alternating current stimulation at mu-frequency. *Front. Hum. Neurosci.* 11:432. doi: 10.3389/fnhum.2017.00432

Haegens, S., Barczak, A., Musacchia, G., Lipton, M., Mehta, A., Lakatos, P., et al. (2015). Laminar profile and physiology of the α rhythm in primary visual, auditory, and somatosensory regions of neocortex. *J. Neurosci.* 35, 14341–14352. doi: 10.1523/JNEUROSCI.0600-15.2015

Heise, K., Monteiro, T., Leunissen, I., Mantini, D., and Swinnen, S. (2019). Distinct online and offline effects of α and β transcranial alternating current stimulation (tACS) on continuous bimanual performance and task-set switching. *Sci. Rep.* 9:3144. doi: 10.1038/s41598-019-39900-0

Helfrich, R., Schneider, T., Rach, S., Trautmann-Lengsfeld, S., Engel, A., and Herrmann, C. (2014). Entrainment of brain oscillations by transcranial alternating current stimulation. *Curr. Biol.* 24, 333–339. doi: 10.1016/j.cub.2013.12.041

Herrmann, C., Rach, S., Neuling, T., and Strüber, D. (2013). Transcranial alternating current stimulation: a review of the underlying mechanisms and modulation of cognitive processes. *Front. Hum. Neurosci.* 7:279. doi: 10.3389/fnhum.2013.00279

Herwig, U., Satrapi, P., and Schönfeldt-Lecuona, C. (2003). Using the international 10-20 EEG system for positioning of transcranial magnetic stimulation. *Brain Topogr.* 16, 95–99. doi: 10.1023/b:brat.0000006333.93597.9d

Hutcheon, B., and Yarom, Y. (2000). Resonance, oscillation and the intrinsic frequency preferences of neurons. *Trends Neurosci.* 23, 216–222. doi: 10.1016/s0166-2236(00)01547-2

Jasper, H. (1958). Report of the committee on methods of clinical examination in electroencephalography. *Electroencephalogr. Clin. Neurophysiol.* 10, 370–375. doi: 10.1016/0013-4694(58)90053-1

Joundi, R., Jenkinson, N., Brittain, J., Aziz, T., and Brown, P. (2012). Driving oscillatory activity in the human cortex enhances motor performance. *Curr. Biol.* 22, 403–407. doi: 10.1016/j.cub.2012.01.024

Kanai, R., Paulus, W., and Walsh, V. (2010). Transcranial alternating current stimulation (tACS) modulates cortical excitability as assessed by TMS-induced phosphene thresholds. *Clin. Neurophysiol.* 121, 1551–1554. doi: 10.1016/j.clinph.2010.03.022

Kar, K., and Krekelberg, B. (2014). Transcranial alternating current stimulation attenuates visual motion adaptation. *J. Neurosci.* 34, 7334–7340. doi: 10.1523/jneurosci.5248-13.2014

Karabanov, A., Thielscher, A., and Siebner, H. (2016). Transcranial brain stimulation: closing the loop between brain and stimulation. *Curr. Opin. Neurol.* 29, 397–404. doi: 10.1097/wco.0000000000000342

Kasten, F. H., Duecker, K., Maack, M. C., Meiser, A., and Herrmann, C. S. (2019). Integrating electric field modeling and neuroimaging to explain inter-individual variability of tACS effects. *Nat. Commun.* 10:5427. doi: 10.1038/s41467-019-13417-6

Kasten, F., Dowsett, J., and Herrmann, C. (2016). Sustained aftereffect of α-tACS lasts up to 70 min after stimulation. *Front. Hum. Neurosci.* 10:245. doi: 10.3389/fnhum.2016.00245

Kasten, F., Negahbani, E., Fröhlich, F., and Herrmann, C. (2018). Non-linear transfer characteristics of stimulation and recording hardware account for spurious low-frequency artifacts during amplitude modulated transcranial alternating current stimulation (AM-tACS). *NeuroImage* 179, 134–143. doi: 10.1016/j.neuroimage.2018.05.068

Keitel, A., and Gross, J. (2016). Individual human brain areas can be identified from their characteristic spectral activation fingerprints. *PLoS Biol.* 14:e1002498. doi: 10.1371/journal.pbio.1002498

Kohli, S., and Casson, A. (2019). Removal of gross artifacts of transcranial alternating current stimulation in simultaneous EEG monitoring. *Sensors* 19:190. doi: 10.3390/s19010190

Krause, M., Vieira, P., Csorba, B., Pilly, P., and Pack, C. (2019). Transcranial alternating current stimulation entrains single-neuron activity in the primate brain. *Proc. Natl. Acad. Sci. U S A* 116, 5747–5755. doi: 10.1073/pnas.1815958116

Kutchko, K., and Fröhlich, F. (2013). Emergence of metastable state dynamics in interconnected cortical networks with propagation delays. *PLoS Computat. Biol.* 9:e1003304. doi: 10.1371/journal.pcbi.1003304

Lakens, D. (2013). Calculating and reporting effect sizes to facilitate cumulative science: a practical primer for *t*-tests and ANOVAs. *Front. Psychol.* 4:863. doi: 10.3389/fpsyg.2013.00863

Liu, A., Vöröslakos, M., Kronberg, G., Henin, S., Krause, M., Huang, Y., et al. (2018). Immediate neurophysiological effects of transcranial electrical stimulation. *Nat. Commun.* 9:5092. doi: 10.1016/j.brs.2017.01.163

Lorenz, R., Simmons, L. E., Monti, R. P., Arthur, J. L., Limal, S., Laakso, I., et al. (2019). Efficiently searching through large tACS parameter spaces using closed-loop Bayesian optimization. *Brain Stimul.* 12, 1484–1489. doi: 10.1016/j.brs.2019.07.003

Lustenberger, C., Boyle, M., Foulser, A., Mellin, J., and Fröhlich, F. (2015). Functional role of frontal α oscillations in creativity. *Cortex* 67, 74–82. doi: 10.1016/j.cortex.2015.03.012

Mansouri, F., Fettes, P., Schulze, L., Giacobbe, P., Zariffa, J., and Downar, J. (2018). A real-time phase-locking system for non-invasive brain stimulation. *Front. Neurosci.* 12:877. doi: 10.3389/fnins.2018.00877

Meij, R. V. D., Ede, F. V., and Maris, E. (2016). Rhythmic components in extracranial brain signals reveal multifaceted task modulation of overlapping neuronal activity. *PLoS One* 11:e0154881. doi: 10.1371/journal.pone.0154881

Negahbani, E., Stitt, I. M., Davey, M., Doan, T. T., Dannhauer, M., Hoover, A. C., et al. (2019). Transcranial alternating current stimulation (tACS) entrains alpha oscillations by preferential phase synchronization of fast-spiking cortical neurons to stimulation waveform. *bioRxiv* [Preprint]. doi: 10.1101/563163

Nelson, J., McKinley, R., Phillips, C., McIntire, L., Goodyear, C., Kreiner, A., et al. (2016). The effects of transcranial direct current stimulation (tDCS)

on multitasking throughput capacity. *Front. Hum. Neurosci.* 10:589. doi: 10.3389/fnhum.2016.00589

Neuling, T., Rach, S., and Herrmann, C. (2013). Orchestrating neuronal networks: sustained after-effects of transcranial alternating current stimulation depend upon brain states. *Front. Hum. Neurosci.* 7:161. doi: 10.3389/fnhum.2013.00161

Neuling, T., Rach, S., Wagner, S., Wolters, C., and Herrmann, C. (2012). Good vibrations: oscillatory phase shapes perception. *NeuroImage* 63, 771–778. doi: 10.1016/j.neuroimage.2012.07.024

Neuling, T., Ruhnau, P., Fuscà, M., Demarchi, G., Herrmann, C., and Weisz, N. (2015). Friends, not foes: magnetoencephalography as a tool to uncover brain dynamics during transcranial alternating current stimulation. *NeuroImage* 118, 406–413. doi: 10.1016/j.neuroimage.2015.06.026

Neuper, C., and Pfurtscheller, G. (2001). Event-related dynamics of cortical rhythms: frequency-specific features and functional correlates. *Int. J. Psychophysiol.* 43, 41–58. doi: 10.1016/s0167-8760(01)00178-7

Nitsche, M. A., Nitsche, M. S., Klein, C. C., Tergau, F., Rothwell, J. C., and Paulus, W. (2003). Level of action of cathodal DC polarisation induced inhibition of the human motor cortex. *Clin. Neurophysiol.* 114, 600–604. doi: 10.1016/s1388-2457(02)00412-1

Noury, N., and Siegel, M. (2017). Phase properties of transcranial electrical stimulation artifacts in electrophysiological recordings. *NeuroImage* 158, 406–416. doi: 10.1016/j.neuroimage.2017.07.010

Ozen, S., Sirota, A., Belluscio, M., Anastassiou, C., Stark, E., Koch, C., et al. (2010). Transcranial electric stimulation entrains cortical neuronal populations in rats. *J. Neurosci.* 30, 11476–11485. doi: 10.1523/jneurosci.5252-09.2010

Palm, U., Ayache, S., Padberg, F., and Lefaucheur, J. (2014). Non-invasive brain stimulation therapy in multiple sclerosis: a review of tDCS, rTMS and ECT results. *Brain Stimul.* 7, 849–854. doi: 10.1016/j.brs.2014.09.014

Polanía, R., Nitsche, M., Korman, C., Batsikadze, G., and Paulus, W. (2012). The importance of timing in segregated theta phase-coupling for cognitive performance. *Curr. Biol.* 22, 1314–1318. doi: 10.1016/j.cub.2012.05.021

R Core Team. (2016). R: A Language and Environment for Statistical Computing. Vienna, Austria: R Foundation for Statistical Computing. Available online at: https://www.R-project.org/.

RStudio Team. (2015). RStudio: Integrated Development for R. Boston, MA: RStudio, Inc. Available online at: http://www.rstudio.com/.

Reato, D., Rahman, A., Bikson, M., and Parra, L. (2010). Low-intensity electrical stimulation affects network dynamics by modulating population rate and spike timing. *J. Neurosci.* 30, 15067–15079. doi: 10.1523/jneurosci.2059-10.2010

Reato, D., Rahman, A., Bikson, M., and Parra, L. (2013). Effects of weak transcranial alternating current stimulation on brain activity—a review of known mechanisms from animal studies. *Front. Hum. Neurosci.* 7:687. doi: 10.3389/fnhum.2013.00687

Riecke, L., Formisano, E., Herrmann, C., and Sack, A. (2015). 4-Hz transcranial alternating current stimulation phase modulates hearing. *Brain Stimul.* 8, 777–783. doi: 10.1016/j.brs.2015.04.004

Riecke, L., Formisano, E., Sorger, B., Başkent, D., and Gaudrain, E. (2018). Neural entrainment to speech modulates speech intelligibility. *Curr. Biol.* 28, 161.e5–169.e5. doi: 10.1016/j.cub.2017.11.033

Ruhnau, P., Neuling, T., Fuscá, M., Herrmann, C., Demarchi, G., and Weisz, N. (2016). Eyes wide shut: transcranial alternating current stimulation drives α rhythm in a state dependent manner. *Sci. Rep.* 6:27138. doi: 10.1038/srep27138

Santarnecchi, E., Polizzotto, N., Godone, M., Giovannelli, F., Feurra, M., Matzen, L., et al. (2013). Frequency-dependent enhancement of fluid intelligence induced by transcranial oscillatory potentials. *Curr. Biol.* 23, 1449–1453. doi: 10.1016/j.cub.2013.06.022

Schaworonkow, N., and Nikulin, V. (2019). Spatial neuronal synchronization and the waveform of oscillations: implications for EEG and MEG. *PLoS Comput. Biol.* 15:e1007055. doi: 10.1371/journal.pcbi.1007055

Scheeringa, R., Koopmans, P., van Mourik, T., Jensen, O., and Norris, D. (2016). The relationship between oscillatory EEG activity and the laminar-specific BOLD signal. *Proc. Natl. Acad. Sci. U S A* 113, 6761–6766. doi: 10.1073/pnas.1522577113

Searle, S., Speed, F., and Milliken, G. (1980). Population marginal means in the linear model: an alternative to least squares means. *Am. Statist.* 34:216. doi: 10.2307/2684063

Sela, T., Kilim, A., and Lavidor, M. (2012). Transcranial alternating current stimulation increases risk-taking behavior in the balloon analog risk task. *Front. Neurosci.* 6:22. doi: 10.3389/fnins.2012.00022

Singmann, H., Bolker, B., Westfall, J., and Aust, F. (2018). *afex: Analysis of Factorial Experiments.* Available online at: https://CRAN.R-project.org/package=afex. Accessed November 2019.

Sliva, D., Black, C., Bowary, P., Agrawal, U., Santoyo, J., Philip, N., et al. (2018). A prospective study of the impact of transcranial alternating current stimulation on EEG correlates of somatosensory perception. *Front. Psychol.* 9:2117. doi: 10.3389/fpsyg.2018.02117

Strüber, D., Rach, S., Neuling, T., and Herrmann, C. (2015). On the possible role of stimulation duration for after-effects of transcranial alternating current stimulation. *Front. Cell. Neurosci.* 9:311. doi: 10.3389/fnsys.2015.00148

Strüber, D., Rach, S., Trautmann-Lengsfeld, S., Engel, A., and Herrmann, C. (2013). Antiphasic 40 Hz oscillatory current stimulation affects bistable motion perception. *Brain Topogr.* 27, 158–171. doi: 10.1007/s10548-013-0294-x

Suffcynski, P., Pijn, P. J. M., Pfurtscheller, G., and Lopes da Silva, F. H. (1999). "Event-related dynamics of α band rhythms: a neuronal network model of focal ERD/surround ERS," in *Event-Related Desynchronization. Handbook of Electroencephalography and Clinical Neurophysiology*, 6th Edn, (Amsterdam: Elsevier), 67–85.

Tavakoli, A., and Yun, K. (2017). Transcranial alternating current stimulation (tACS) mechanisms and protocols. *Front. Cell. Neurosci.* 11:214. doi: 10.3389/fncel.2017.00214

Thut, G., Bergmann, T., Fröhlich, F., Soekadar, S., Brittain, J., Valero-Cabré, A., et al. (2017). Guiding transcranial brain stimulation by EEG/MEG to interact with ongoing brain activity and associated functions: a position paper. *Clin. Neurophysiol.* 128, 843–857. doi: 10.1016/j.clinph.2017.01.003

Tugin, S., Hernandez-Pavon, J., Ilmoniemi, R., and Nikulin, V. (2016). Visual deviant stimuli produce mismatch responses in the amplitude dynamics of neuronal oscillations. *NeuroImage* 142, 645–655. doi: 10.1016/j.neuroimage.2016.07.024

Veniero, D., Vossen, A., Gross, J., and Thut, G. (2015). Lasting EEG/MEG aftereffects of rhythmic transcranial brain stimulation: level of control over oscillatory network activity. *Front. Cell. Neurosci.* 9:477. doi: 10.3389/fncel.2015.00477

Vieira, P., Krause, M., and Pack, C. (2019). tACS entrains neural activity while somatosensory input is blocked. *bioRxiv* [Preprint]. doi: 10.1101/691022

Vöröslakos, M., Takeuchi, Y., Brinyiczki, K., Zombori, T., Oliva, A., Fernández-Ruiz, A., et al. (2018). Direct effects of transcranial electric stimulation on brain circuits in rats and humans. *Nat. Commun.* 9:483. doi: 10.1038/s41467-018-02928-3

Voss, U., Holzmann, R., Hobson, A., Paulus, W., Koppehele-Gossel, J., Klimke, A., et al. (2014). Induction of self awareness in dreams through frontal low current stimulation of γ activity. *Nat. Neurosci.* 17, 810–812. doi: 10.1038/nn.3719

Vossen, A., Gross, J., and Thut, G. (2015). α power increase after transcranial alternating current stimulation at α frequency (α-tACS) reflects plastic changes rather than entrainment. *Brain Stimul.* 8, 499–508. doi: 10.1016/j.brs.2014.12.004

Vosskuhl, J., Huster, R., and Herrmann, C. (2015). Increase in short-term memory capacity induced by down-regulating individual theta frequency *via* transcranial alternating current stimulation. *Front. Hum. Neurosci.* 9:257. doi: 10.3389/fnhum.2015.00257

Vosskuhl, J., Strüber, D., and Herrmann, C. (2018). Non-invasive brain stimulation: a paradigm shift in understanding brain oscillations. *Front. Hum. Neurosci.* 12:211. doi: 10.3389/fnhum.2018.00211

Waddell, C., Pratt, J., Porr, B., and Ewing, S. (2009). " Deep brain stimulation artifact removal through under-sampling and cubic-spline interpolation", in *2nd International Congress on Image and Signal Processing*, (Tianjin, China: IEEE) 1–5. doi: 10.1109/CISP.2009.5301199

Wilsch, A., Neuling, T., Obleser, J., and Herrmann, C. (2018). Transcranial alternating current stimulation with speech envelopes modulates speech comprehension. *NeuroImage* 172, 766–774. doi: 10.1016/j.neuroimage.2018.01.038

Witkowski, M., Garcia-Cossio, E., Chander, B., Braun, C., Birbaumer, N., Robinson, S., et al. (2016). Mapping entrained brain oscillations during

transcranial alternating current stimulation (tACS). *NeuroImage* 140, 89–98. doi: 10.1016/j.neuroimage.2015.10.024

Yavari, F., Nitsche, M., and Ekhtiari, H. (2017). Transcranial electric stimulation for precision medicine: a spatiomechanistic framework. *Front. Hum. Neurosci.* 11:159. doi: 10.3389/fnhum.2017.00159

Zaehle, T., Rach, S., and Herrmann, C. (2010). Transcranial alternating current stimulation enhances individual α activity in human EEG. *PLoS One* 5:e13766. doi: 10.1371/journal.pone.0013766

Zarubin, G., Gundlach, C., Nikulin, V., and Bogdan, M. (2018). "Real-time phase detection for EEG-based tACS closed-loop system", in *Proceedings of the 6th International Congress on Neurotechnology, Electronics and Informatics*, (Seville, Spain: SciTePress), 13–20. doi: 10.5220/0006927300130020

Ziemann, U., and Siebner, H. (2015). Inter-subject and inter-session variability of plasticity induction by non-invasive brain stimulation: boon or bane? *Brain Stimul.* 8, 662–663. doi: 10.1016/j.brs.2015.01.409

Zrenner, C., Belardinelli, P., Müller-Dahlhaus, F., and Ziemann, U. (2016). Closed-loop neuroscience and non-invasive brain stimulation: a tale of two loops. *Front. Cell. Neurosci.* 10:92. doi: 10.3389/fncel.2016.00092

Conflict of Interest: The authors declare that the research was conducted in the absence of any commercial or financial relationships that could be construed as a potential conflict of interest.

frontiers in Human Neuroscience

ORIGINAL RESEARCH
published: 18 December 2020
doi: 10.3389/fnhum.2020.536070

Signal-Space Projection Suppresses the tACS Artifact in EEG Recordings

Johannes Vosskuhl[1†], Tuomas P. Mutanen[2†], Toralf Neuling[3,4], Risto J. Ilmoniemi[2] and Christoph S. Herrmann[1,5]*

[1] Experimental Psychology Lab, Cluster of Excellence "Hearing4all", European Medical School, University of Oldenburg, Oldenburg, Germany, [2] Department of Neuroscience and Biomedical Engineering, Aalto University School of Science, Espoo, Finland, [3] Physiological Psychology Lab, University of Salzburg, Salzburg, Austria, [4] Center for Mind/Brain Sciences, University of Trento, Trento, Italy, [5] Research Center Neurosensory Science, University of Oldenburg, Oldenburg, Germany

OPEN ACCESS

Edited by:
Nivethida Thirugnanasambandam, National Brain Research Centre (NBRC), India

Reviewed by:
Philipp Ruhnau, University Hospital Magdeburg, Germany
Ivan Alekseichuk, University of Minnesota Twin Cities, United States
Alexander James Casson, The University of Manchester, United Kingdom

***Correspondence:**
Christoph S. Herrmann
christoph.herrmann@uni-oldenburg.de

[†] These authors have contributed equally to this work

Specialty section:
This article was submitted to Brain Imaging and Stimulation, a section of the journal Frontiers in Human Neuroscience

Received: 18 February 2020
Accepted: 09 November 2020
Published: 18 December 2020

Citation:
Vosskuhl J, Mutanen TP, Neuling T, Ilmoniemi RJ and Herrmann CS (2020) Signal-Space Projection Suppresses the tACS Artifact in EEG Recordings. Front. Hum. Neurosci. 14:536070. doi: 10.3389/fnhum.2020.536070

Background: To probe the functional role of brain oscillations, transcranial alternating current stimulation (tACS) has proven to be a useful neuroscientific tool. Because of the excessive tACS-caused artifact at the stimulation frequency in electroencephalography (EEG) signals, tACS + EEG studies have been mostly limited to compare brain activity between recordings before and after concurrent tACS. Critically, attempts to suppress the artifact in the data cannot assure that the entire artifact is removed while brain activity is preserved. The current study aims to evaluate the feasibility of specific artifact correction techniques to clean tACS-contaminated EEG data.

New Method: In the first experiment, we used a phantom head to have full control over the signal to be analyzed. Driving pre-recorded human brain-oscillation signals through a dipolar current source within the phantom, we simultaneously applied tACS and compared the performance of different artifact-correction techniques: sine subtraction, template subtraction, and signal-space projection (SSP). In the second experiment, we combined tACS and EEG on one human subject to demonstrate the best-performing data-correction approach in a proof of principle.

Results: The tACS artifact was highly attenuated by SSP in the phantom and the human EEG; thus, we were able to recover the amplitude and phase of the oscillatory activity. In the human experiment, event-related desynchronization could be restored after correcting the artifact.

Comparison With Existing Methods: The best results were achieved with SSP, which outperformed sine subtraction and template subtraction.

Conclusion: Our results demonstrate the feasibility of SSP by applying it to a phantom measurement with pre-recorded signal and one human tACS + EEG dataset. For a full validation of SSP, more data are needed.

Keywords: EEG, artifact, phantom head, signal-space projection, tACS (transcranial alternating current stimulation)

INTRODUCTION

The goal of transcranial alternating current stimulation (tACS) is often the modulation of oscillatory brain activity and the concurrent demonstration of behavioral consequences of the intervention (Herrmann et al., 2013). Thus far, most studies combining tACS with electroencephalography (EEG) have demonstrated effects on oscillatory brain activity only by comparing the EEG before and after tACS (Zaehle et al., 2010; Vossen et al., 2015; Kasten and Herrmann, 2017), because EEG data recorded during stimulation are contaminated by an immense tACS-generated artifact at the stimulation frequency which exceeds the range of physiological EEG signals by several orders of magnitude. As a first indicator for the successful manipulation of brain oscillations, behavioral effects found during application of tACS have been interpreted (Neuling et al., 2012; Polanía et al., 2012; Cecere et al., 2015), sometimes together with aftereffects of the stimulation (Neuling et al., 2012). Additionally, it is possible to analyze the EEG spectrum outside the tACS frequency, simply by applying adequate bandpass filters to the stimulated frequency band. It is particularly important, however, to measure the neuronal activity at the stimulation frequency, because the changes at the stimulated frequency are expected during successful entrainment (Thut et al., 2011; Kasten et al., 2018). At present, the neuronal activity directly at the stimulated frequency is technically not measurable because it is masked by an excessive electrical artifact. In this study, we aim at recovering physiological signals from EEG data at the frequency of stimulation, while the stimulation has been active.

Correction of the tACS artifact in EEG recordings is more challenging as it is the case for magnetoencephalography (MEG). Due to the high spatial sampling, MEG studies on concurrent tACS online effects rely on the application of spatial filtering (a.k.a. beamforming) to deal with the artifact (Neuling et al., 2015; Kasten et al., 2018; Herring et al., 2019). These spatial filters achieve a strong, yet imperfect attenuation of the tACS induced electromagnetic that required additional correction, e.g., by contrasting two conditions with similar extent of the residual artifacts (Kasten et al., 2018; Herring et al., 2019). These residuals likely originate from non-linear modulations of the tACS artifact elicited by physiological processes in the human body (Noury et al., 2016; Noury and Siegel, 2018), which also have to be taken into account in EEG recordings. The issue of tACS artifact correction in MEG data is discussed elsewhere (Neuling et al., 2015; Noury et al., 2016; Neuling et al., 2017; Noury and Siegel, 2018; Kasten and Herrmann, 2019) and will not be further addressed in this article.

Even though MEG might be better suited to analyze concurrent neurophysiology during tACS, EEG is a lot more common as a research method and thus it is desirable to have a method to suppress the artifact in EEG as well. Only a few studies so far have approached this issue (Helfrich et al., 2014; Voss et al., 2014; Dowsett and Herrmann, 2016; Kohli and Casson, 2019). While they represent milestones in tACS research, these studies also disclose a fundamental question: How can one assure that the brain responses of interest are not removed and that no residual artifact remains? To answer this question, it would be necessary to evaluate the performance of the artifact-correction procedure; however, this cannot be easily achieved when the brain activity to be recovered is virtually unknown. To tackle this issue, we conducted two experiments. First, we used a phantom to have full control over the "brain" signal and the "tACS" signal. Using pre-recorded human EEG as the source-current waveform in the phantom, we simultaneously applied tACS and compared different artifact-correction techniques. Second, the obtained results were used to demonstrate the feasibility of the artifact-correction performance in a human tACS+EEG experiment.

EXPERIMENT 1: PHANTOM STUDY

Material and Methods

Terminology

Although we used a phantom head in the first experiment, we will use terminology that has been established in human experiments in order to promote readability. For example, we will use "EEG" to refer to the recorded signal and "tACS" to refer to the application of sine-wave current to the phantom head's outer layer ("scalp").

Experimental Setup

The experimental setup is depicted in **Figure 1A**. We used Matlab 2012b (The MathWorks Inc., Natick, MA, United States) on a laptop to control the delivery of pre-recorded EEG and the tACS signal to a digital-to-analog converter (USB-6229 BNC, National Instruments, Austin, TX, United States). From here, the EEG signal was driven through a dipole source located inside a phantom head. The tACS signal was first sent to a battery-operated stimulator system (DC stimulator plus, Eldith, Neuroconn, Ilmenau, Germany) before being applied to the phantom head. We used a system here that we have regularly used in experiments on human participants from our lab (e.g., Neuling et al., 2015; Vosskuhl et al., 2016) and which is widely used throughout tACS-literature. For comparability, we also used the same machinery in experiment 2 of this study. The EEG that was recorded from the phantom head was stored for offline analysis.

Phantom Head

Our goal was to construct a phantom that captures crucial aspects of a human head receiving tACS: First, an artificial neural current source, second, a possibility to apply tACS to the surface of the phantom, and third, recording the combined signals. Furthermore, the phantom should possess the fundamental conductive properties of a human head: Most of the external current (tACS) is transmitted through the well-conducting skin, whereas the skull is a poor conductor of electricity. Likewise, most of the internal neuronally-driven ohmic currents remain inside the skull. Therefore, we built a spherical three-compartment phantom head with a dipolar current source inside the innermost space, as well as stimulation electrodes and recording electrodes on the outermost layer (**Figures 1B–D**). The phantom head was filled with a fluid whose conductivity roughly matched that of human brain and scalp (0.57 S/m). The skull was realized as a porous spherical shell between the scalp and the brain with

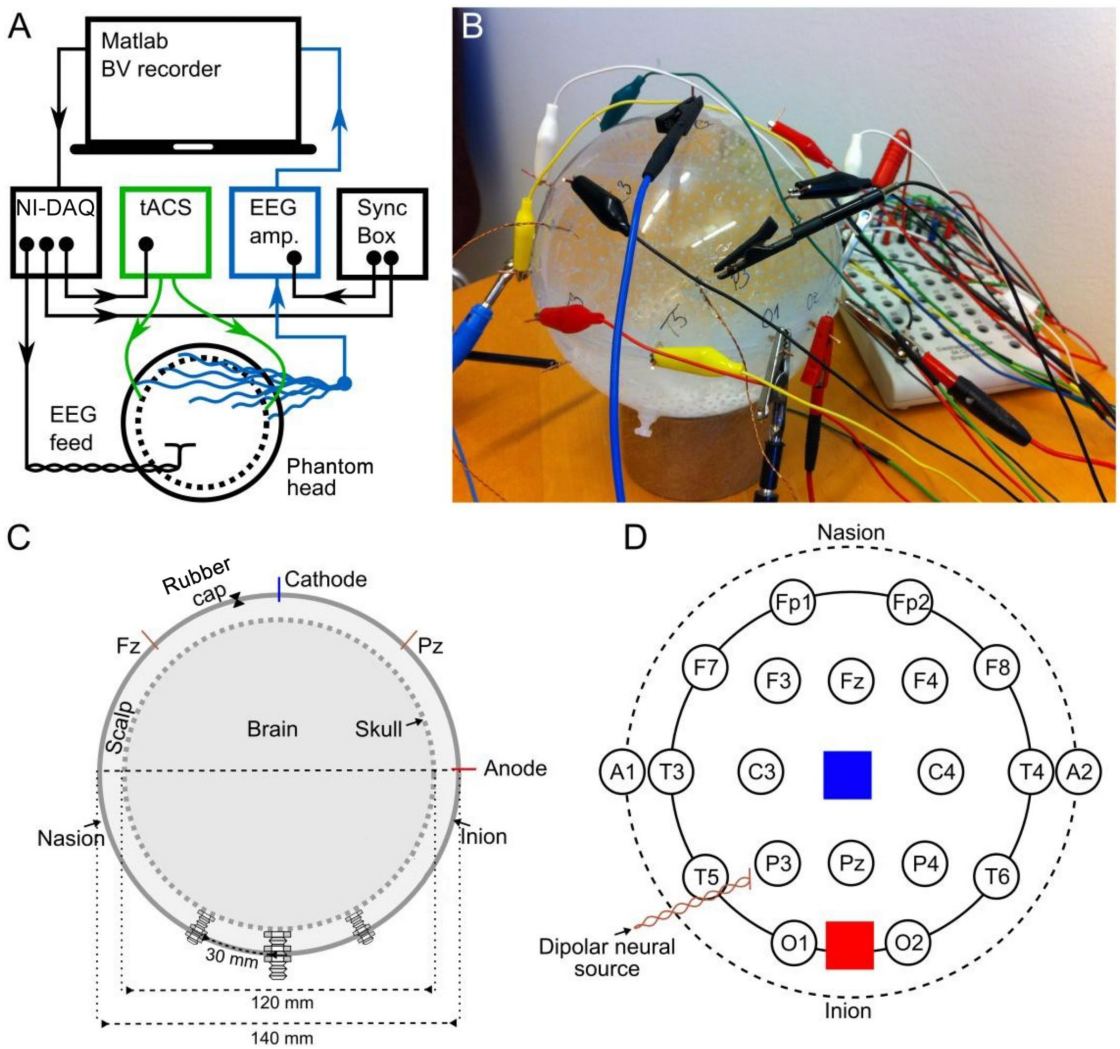

FIGURE 1 | Experimental set-up and the structure of the phantom. **(A)** Schematic illustration of the hardware setup as well as the signal delivery and recording (BV recorder: Brain Vision EEG recording software; NI-DAQ: National Instruments digital-to-analog converter). Arrowheads indicate the direction of information flow. **(B)** Photo of the phantom head. **(C)** Cross section of the phantom head along the midline. The dashed inner circle shows the inner porous spherical shell (skull), and the outer circle shows the outer spherical shell confining the scalp. Both the inner and outer shells were 2 mm thick. **(D)** Stereographic projection of the phantom from above, depicting locations of EEG (circles) and tACS electrodes (blue and red squares), and the dipolar source.

a conductivity of 0.019 S/m (conductivity values adapted from Gonçalves et al., 2003; Lai et al., 2005). A detailed description of the construction of the phantom head can be found in the Supplementary Section "Phantom Head Construction."

EEG

We delivered to the dipolar source of the phantom a signal waveform that resembles human EEG. We used 60 s of human resting-state EEG previously recorded from a human participant (male, 24 years, right-handed) with his eyes closed over the occipital cortex at electrode position O2 (Reference: nose) of the international 10–20 EEG system at 1 kHz sampling frequency using the Brain Vision Recorder with a BrainAmp DC amplifier system (Brain Products, Munich, Germany). After up-sampling the signal to 100 kHz and high-pass filtering at 1 Hz, the signal was delivered to a dipole inside the phantom head and recorded from 18 electrodes (**Figure 1D**) with 5 kHz sampling frequency. We call this signal the "phantom EEG." The recordings were amplified in the range of ±3.2768 mV at a resolution of 0.1 μV (16 bits) using the Brain Vision Recorder and BrainAmp MR amplifier with an online notch filter (50 Hz). The ground electrode was at location A1, the reference at a point comparable to the tip of the nose. The amplitude of the EEG signal driven through the dipole inside the phantom head was adjusted so that the amplitude of the resulting phantom EEG matched that of the pre-recorded human EEG (0.1–2.3 μV). To guarantee a perfect temporal alignment of the measured EEG at the phantom, the neural current source was synchronized with the tACS and the playback EEG via the BrainVision Syncbox (Brain Products, Munich, Germany;

Figure 1A). The EEG data were digitally stored for further offline analysis.

Transcranial Alternating Current Stimulation (tACS)

We generated a digital 10-Hz sine wave at a temporal resolution of 100 kHz and output it via a digital-to-analog converter to the tACS electrodes of the phantom at electrode positions that were similar to Cz and Oz (**Figure 1D**, **Figure 2A**). The amplitude of the tACS signal was adjusted to avoid clipping, which would make the recovery of the EEG signal impossible. The largest tACS intensity that we could drive to the phantom without causing any clipping in the EEG channels was 150 μA, resulting in a maximum voltage between 30.5 and 1197.0 μV across the channels. We used two different tACS current intensities: 50 and 150 μA. The EEG amplitudes of the artifact depended linearly on the tACS current amplitude (50 μA: 10.2–399.3 μV) and were strongest in channels close to the tACS electrodes (**Figure 2B**, top row).

Artifact Correction

To evaluate the performance of different artifact-correction techniques, we first recorded the phantom head EEG resulting from the dipole current alone; this served as the baseline condition. Then, we applied tACS to the phantom while the dipolar source was active. Subsequently, we compared the performance of different artifact-rejection techniques [sine fitting, template subtraction, and signal-space projection (SSP)] in recovering the baseline signal from the data contaminated with the tACS artifact. Spectra of the uncorrected data, recorded from the phantom can be seen in **Figure 2D**.

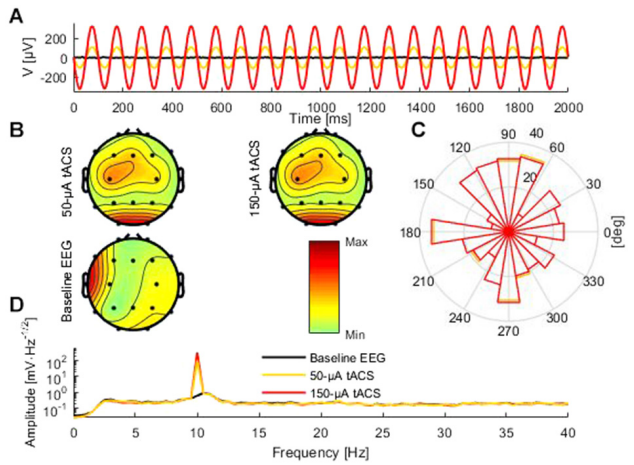

FIGURE 2 | Comparison of baseline data and tACS-contaminated data. **(A)** An illustrative 2-s segment of the baseline (black) and the artifactual data (red and yellow) measured at electrode Pz. **(B)** The topographies showing the average amplitude in the range 8–12 Hz of the artifactual and baseline data. **(C)** Circular histogram of the phase-difference distribution between the artifactual data and the baseline data at 10 Hz across all epochs and channels for the 50-μA (yellow) and 150-μA (red) condition. **(D)** Frequency spectra of the 50-μA (yellow), 150-μA (red), and baseline conditions (black). Because of the logarithmic scale the peak amplitudes at 10 Hz for the 50-μA and 150-μA conditions appear similar regardless of the threefold difference.

Sine Fitting

The most intuitive approach to remove the sinusoidal tACS-artifact is subtracting a sine wave at the stimulation frequency from the recorded data. This method has previously been applied to remove line noise from EEG data (Mitra and Bokil, 2007). We fitted a sine wave at the tACS frequency to non-overlapping time windows, each window having the length of one tACS period. The fitting was done for each channel separately, using the least-squares criterion with amplitude and phase as the fitted parameters. The resulting fits were then subtracted from the artifact-contaminated data in each time window.

Template Subtraction

The template subtraction method was adapted from a technique previously used to remove artifacts in simultaneous EEG + functional magnetic resonance imaging (fMRI) recordings (Allen et al., 2000; Niazy et al., 2005) and has also been applied to remove the tACS artifact from EEG data (Helfrich et al., 2014). Here we used a version of template subtraction that best matches the procedure described in (Kohli and Casson, 2019).

An artifact template was created by averaging data of a given number of tACS cycles (500 cycles in the phantom case) and then subtracting the resulting template from each tACS cycle of the data. We used electrode-specific templates, which were obtained by averaging over all the tACS periods across the data segment of interest. These electrode-specific average artifact templates were then subtracted from the data in non-overlapping windows.

Signal-Space Projection (SSP)

Signal-space projection is a method that separates signals into a set of different components that have constant spatial patterns in a multidimensional signal space, but whose amplitudes may change as a function of time; SSP has been used for separating, e.g., EEG and magnetoencephalography (MEG) signals (Uusitalo and Ilmoniemi, 1997). This feature can be exploited for the combination of EEG and tACS because tACS has a relatively constant spatial pattern, although it may change slightly due to changes in the conductive properties of the scalp. If we are able to estimate this spatial pattern accurately, we can use SSP to suppress the tACS artifact.

First, a maximally pure template of the artifact has to be calculated from the signal. To this end, single cycles of the sinusoidal tACS-artifact are averaged per channel. Thereby the brain signal is mostly removed from the recorded signal and only artifactual signals and noise remain. These remaining data are used to estimate the artifact signal subspace, which enables us to project out the artifact from the contaminated data. Here, the artifact subspace was estimated from the average artifact template (see section "Template Subtraction"), assuming that only little brain activity remains after averaging. The dimension of the artifact subspace was determined qualitatively from the singular value spectrum of the average artifact template. A detailed

description of the SSP method can be found in the Supplementary Section "SSP Details".

One feature of SSP is that it introduces spatial distortions to the signal, which impedes conventional visual interpretation of the resulting signal. To minimize these undesired distortions and keep the corrected data visually interpretable, we used the source-informed reconstruction approach (SIR) introduced by Mutanen et al. (2016). The idea of SIR is to compute from the projected (distorted in a perfectly known manner) signal a brain current distribution and from this current distribution, the corrected signal. For SIR, one needs to compute the lead field matrix of the chosen forward model to explain the measured data in terms of source currents. We used a spherical model that had the same geometry as the phantom containing 5,000 evenly distributed radial dipoles 50 mm away from the origin. From now on, we refer to the combined SSP–SIR approach simply as SSP. Since SIR is not sufficient to correct all the SSP-elicited distortions, we also applied SSP and SIR to the baseline data to make it comparable to the SSP cleaned data (further details in Supplementary section "SSP Details"). The major benefit of this approach is that it allows a direct comparison of the two datasets (e.g., baseline data and artifact-contaminated data) because we are quantifying the change from the baseline to the tACS-contaminated data only in those signal-space dimensions that remain after cleaning. In essence, this approach takes into account the possible unwanted attenuation of the neuronal signals of interest (overcorrection). We want to point out here that comparisons in the case of the sine and template subtractions were done using the original, unmodulated baseline, because with sine or template subtraction, possible overcorrection of signals of interest is typically not known. However, with SSP the removed topographies (signal-space directions) are perfectly known, and to allow an unbiased comparison between two datasets, it is recommended to remove the same directions from both. The approach is analogous with rejecting bad EEG channels; to compare two datasets reliably, the comparison should be done in those channels (signal-space directions) that were identified to be good in both datasets. See the mathematical explanation in the Supplementary Equations SE1–SE8.

Analysis of the Phantom Data

To remove slow drifts and high-frequency noise, the data were bandpass-filtered from 2 to 80 Hz with a 4th-order Butterworth filter. For the artifactual datasets, we identified the exact data point when tACS started and the corresponding time point in the baseline dataset. We discarded the first second of data due to artifacts related to initializing the tACS and extracted a 50-s segment (1–51 s with respect to the tACS onset) for further analysis. We then applied the artifact-correction techniques to these data segments. The resulting data will be referred to as "cleaned data". As indicated above, SSP was also applied to the baseline data prior to comparison. After the cleaned and the baseline data were divided into 2-s epochs, we Fourier-transformed each of these epochs and computed the epoch- and channel-specific amplitudes and phase-angle spectra.

To evaluate the performance of the artifact-rejection techniques, we first quantified the root-means-square error (RMSE) between the ground-truth baseline data and the cleaned data (using all the samples across the whole 50-s time range and all 18 channels) and compared the obtained value with the RMSE between the baseline and artifactual data. The target RMSE (floor value) was calculated using a 6-s segment of the noise in the baseline data before the neural source had been turned on. Next we estimated the degree of tACS-artifact contamination in the cleaned data by calculating the residual artifact (*RA*) for each channel as:

$$RA = \frac{(P_{\text{clean}} - P_{\text{base}})}{(P_{\text{art}} - P_{\text{base}})} \times 100\%$$

where P_{clean} P_{base}, and P_{art} represent the signal power at 10 Hz for the cleaned, baseline, and artifactual data, respectively. A positive *RA* implies that the tACS artifact was not fully removed, whereas a negative *RA* suggests that some additional distortion was introduced in the data (e.g., attenuation of the signal of interest). We quantified spatial distortions elicited by the artifact rejection techniques by computing the topography maps of signal amplitude averaged between 8 and 12 Hz of the baseline and cleaned data. We then computed the relative error (*RE*) between the baseline and the cleaned topographies:

$$RE = \frac{|y_{\text{clean}}| - |y_{\text{base}}|}{|y_{\text{base}}|} \times 100\ \%$$

where y_{clean} and y_{base} are the topography vectors of the cleaned and the baseline data, respectively, and the $|\ |$ represents the Euclidian norm of the topography vector. The level of temporal distortions caused by the artifact-suppression methods was assessed by computing the correlation coefficient (CC) between the baseline and cleaned time courses in each channel and trial.

To further evaluate whether the amplitude spectrum of the neural source was recovered correctly, we computed the average spectrum over the epochs and compared the cleaned and baseline data of each channel separately. We focused the analyses on the individual alpha frequency (IAF: 10.5 Hz), the spectral peak in the range of 8–12 Hz estimated from the baseline spectrum. The IAF amplitude was computed separately for each of the 25 2-s epochs before and after applying the different artifact-removal methods. To test whether the correction methods distort the IAF amplitude, we performed a 2-way ANOVA (factor 1: 18 channels, factor 2: two conditions, i.e., cleaned data and baseline data) and *post hoc t*-tests, the epoch-specific IAF amplitudes serving as samples.

To analyze possible phase distortions, we subtracted for each epoch, channel, and frequency the baseline phase angle from the phase angle of the cleaned data. We visualized the phase difference at 10 Hz, when the artifact was in its maximum (**Figure 2C**). Additionally, we computed the phase-locking value (PLV) (Lachaux et al., 1999) between the baseline and the cleaned data for each channel. To test whether the phase locking between the corrected and the baseline EEG was significant at the IAF, which would indicate preserved phase information, we used Bonferroni-corrected bootstrapping tests (Lachaux et al., 1999). To test whether the artifact removal had significantly improved PLV between the baseline and the tACS-artifact contaminated

TABLE 1 | Comparison of the original and the cleaned datasets with the baseline data in terms of the root-mean-square error (RMSE).

Root-mean-square error (RMSE) with respect to the baseline data [μV]					
	Original	**SSP**	**Template**	**Sine fitting**	**RMSE floor**
50 μA	228.03	0.89	2.38	3.37	1.11
150 μA	683.17	0.81	1.97	3.06	1.11

The RMSE-floor value shows the noise level RMS value of the baseline data prior to switching on the inserted dipolar source.

data, additional bootstrapping tests were performed to compare the PLV between the artifactual and baseline data to the PLV between the cleaned and baseline data. In these tests, the epochs were resampled with replacement 10,000 times, and the resulting distribution for difference between the original PLV and PLV after cleaning was formed. If 95% or more of the probability mass showed that PLV after cleaning was higher, the improvement was considered significant. The same tests were performed to each channel, and cleaning methods and the bootstrap tests were Bonferroni corrected accordingly. All analyses were done using Matlab 2014b (The MathWorks Inc., Natick, MA, United States) and the EEGLAB 13.4.4b toolbox (Delorme and Makeig, 2004).

Results

All artifact-correction methods were able to attenuate the tACS artifact (**Tables 1**, **2**). RMSE was clearly decreased by all the tested methods, SSP-cleaned data showing the smallest discrepancy with the baseline data (less than 0.5% of the original error). SSP was the only method that reached the floor RMSE value (1.1 μV). After applying each method, the amplitude spectra were in the range of the signal of interest (**Figure 3**); however, seemingly at the expense of different degrees of overcorrection, which means that also non-artifact activity had been removed. Sine fitting demonstrated higher overcorrection compared to template-subtraction and SSP (**Table 2**, RA results). Spatial information was distorted by all applied methods, SSP recovering the EEG-topography the best. That said, even SSP failed to recover the spatial information perfectly, as can be seen in the subtle differences in topographies in **Figure 4B**. The spatial information was best recovered by SSP, demonstrating only minor errors compared to template subtraction, whereas sine fitting yielded strong deviations (**Table 2**, RE results). Specifically, sine fitting shows the largest deviation in the frequency range of 5–15 Hz (**Figure 5**, right). On average, SSP and template subtraction performed similarly; however, SSP had less variation across the channels, which can be seen in the more homogeneous topographies of SSP in comparison to Template subtraction (**Figure 5**). Note the comparatively large *RE* in channel P3 after applying SSP, is caused by a very low signal-to-noise ratio in this channel as can be already seen in the baseline condition (see **Figure 2B**). Channel-wise frequency spectra further demonstrate the poor performance of the sine fitting within the 5–15-Hz range (**Figure 3**, left). SSP yielded the best results, especially when comparing SSP-baseline data with SSP-cleaned data: the spectra matched almost perfectly (**Figure 3**, right). Furthermore, SSP was the superior method in recovering the temporal information (phase) of the baseline signal both at the stimulation frequency as well as at IAF, whereas template subtraction and sine fitting poorly recovered the baseline signal in a number of channels (**Figure 5**, left). The difference in preserving the temporal information was also supported by high correlations of the signal between the baseline and the SSP-cleaned data compared to the other methods (**Table 2**, CC results). Additional support comes from the results of the bootstrapping analysis of the PLV at the IAF: After SSP, the PLV between cleaned and baseline data was significant, for all channels and conditions ($p < 0.05$, after Bonferroni correction). After template subtraction, PLV was significant in most of the channels in both conditions ($p < 0.05$) except for three cases (50 μV tACS – P3: $p = 1$; 150 μV tACS – P3: $p = 1$, O1: $p = 0.36$, after Bonferroni correction). After sine fitting,

TABLE 2 | Comparison of the artifact-correction performance.

Relative error (RE) of the topography [%]			
	SSP	**Template**	**Sine fitting**
50 μA	3	5	47
150 μA	3	7	48
Mean residual artifact (RA) across the channels			
	SSP	**Template**	**Sine fitting**
50 μA	−0.01 ± 0.005% (−0.32 ± 0.07 μV)	−0.01 ± 0.005% (−0.24 ± 0.07 μV)	−0.04 ± 0.02% (−0.62 ± 0.12 μV)
150 μA	−0.001 ± 0.001% (−0.33 ± 0.07 μV)	−0.001 ± 0.0005% (−0.23 ± 0.07 μV)	−0.004 ± 0.003% (−0.62 ± 0.12 μV)
Mean time-course match across the channels (CC)			
	SSP	**Template**	**Sine fitting**
50 μA	0.91 ± 0.03	0.72 ± 0.07	0.55 ± 0.05
150 μA	0.93 ± 0.02	0.76 ± 0.06	0.61 ± 0.04

RE, relative error; RA, residual artifact; and CC, correlation. Note that positive RA implies that the tACS artifact was not fully removed, whereas a negative RA indicates overcorrection. Values in parentheses show RA in μV units.

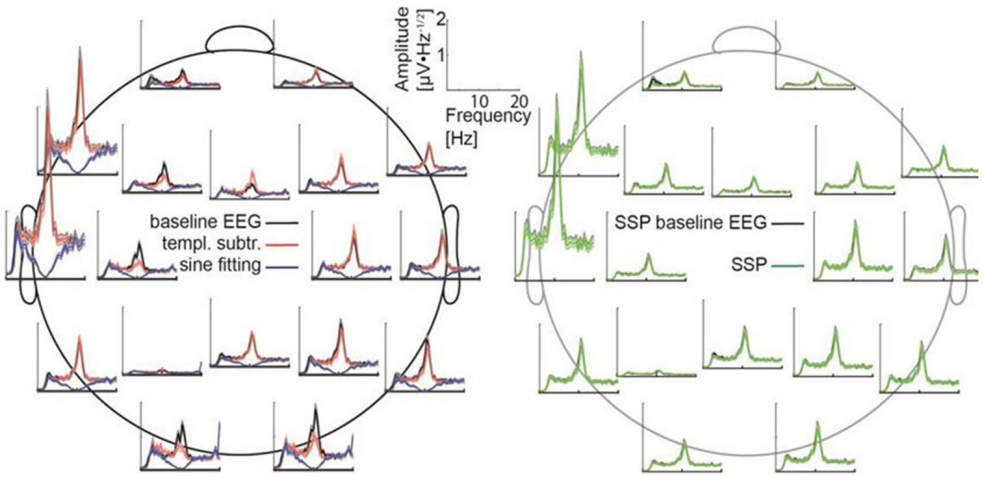

FIGURE 3 | Frequency spectra for each channel. **(Left)** The baseline data (black) are compared with the cleaned data after applying sine fitting (blue) and template subtraction (red). **(Right)** SSP baseline data (black) compared with the SSP cleaned data (green). Here, 150-μV stimulation was delivered at 10 Hz.

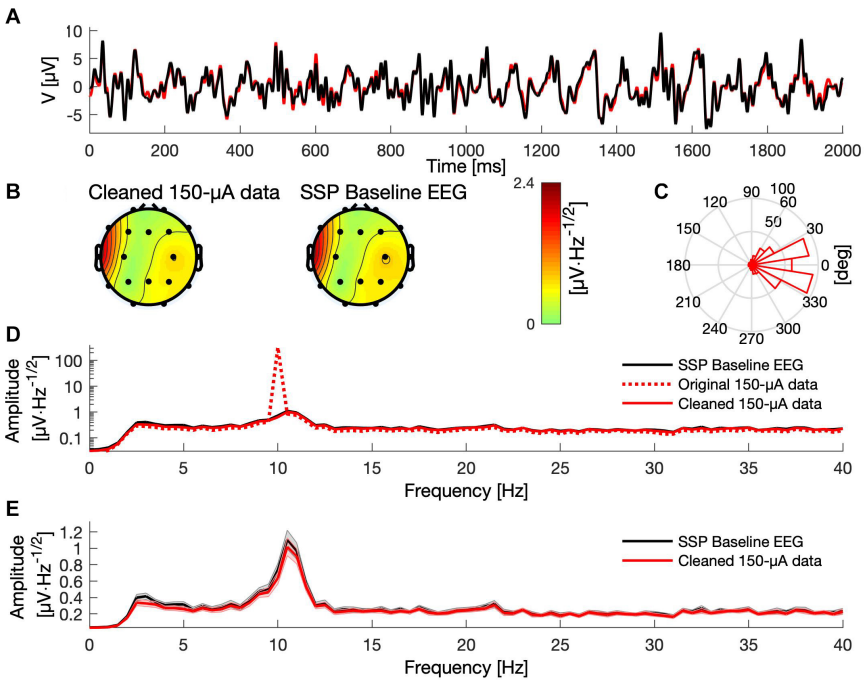

FIGURE 4 | Comparison between baseline and SSP-cleaned data when delivering tACS with 150 μA. **(A)** A 2-s segment of baseline (black) and cleaned data (red) measured at electrode Pz. **(B)** Topographies showing the mean signal amplitude between 8 and 12 Hz of the cleaned and baseline data, respectively. **(C)** Histogram of the phase difference between cleaned artifactual and baseline data at 10 Hz across all epochs and channels. **(D)** The mean frequency spectra (averaged over epochs) for the baseline (black curve), original artifactual (red dashed curve), and cleaned artifactual data (solid red curve), in channel Pz, presented on logarithmic scale. **(E)** The mean frequency spectra of the baseline (black) and the cleaned data (red), in channel Pz, presented on a linear scale. Shaded areas indicate the standard error of the mean.

no results were significant in the 50-μA-tACS condition and only one channel had a significant PLV in the 150-μA-tACS condition (F3: $p < 0.05$, after Bonferroni correction). When comparing the PLV before and after cleaning, only SSP showed significant improvement. In particular, in those channels that originally showed high artifact-power, PLV was significantly improved by SSP ($p < 0.05$ after Bonferroni correction; 50-μV-tACS condition: channels F3, Fz, C3, C4, T5, Pz, O1, and O2; 150-μV-tACS condition: channels Fp2, F3, Fz, F4, C3, C4, T5, Pz, O1, and O2).

For sine fitting, the 2-way ANOVA (factor 1: 18 channels, factor 2: two conditions, i.e., cleaned data and baseline data)

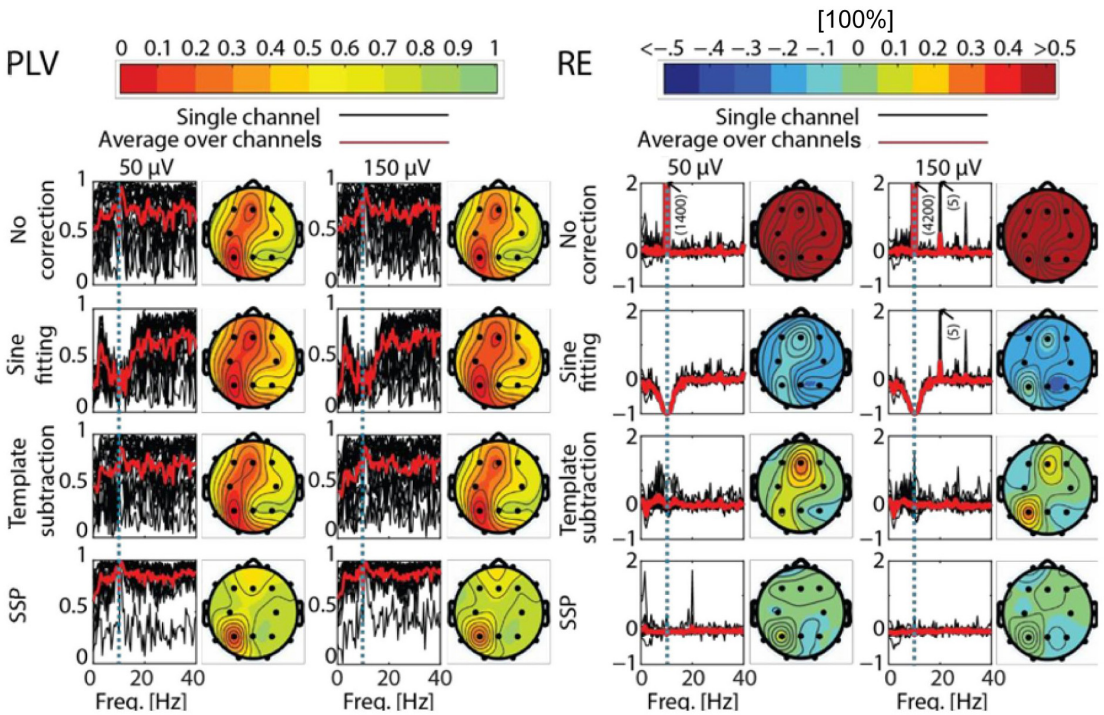

FIGURE 5 | Phase-locking value (PLV) and relative error (RE) as function of frequency and different channels after artifact correction. PLV **(left)** and RE **(right)** for the different correction methods and tACS conditions as compared to the baseline. The black curves show PLV and RE as function of frequency in different channels, the red curve showing the average of the black curves. The dotted blue line depicts the stimulation frequency. Corresponding topographies show the mean value of the channel-specific black curves averaged across frequencies 0–40 Hz. In the PLV column, red indicates low PLV, meaning big distortions between baseline and corrected EEG (Note that PLV is a unitless measure). In the RE column, red means there was artifact left in the data, while blue depicts an overcorrection. Note that the color map of RE is thresholded to 50% absolute error and the plots in the RE section show only values between –1 and 2.

demonstrated that the IAF amplitude depends on the tACS intensity, which additionally interacted with the channel (cf. **Table 3**). Furthermore, the interaction between the channel and condition was significant, which means the artifact suppression is not reliable. Subsequent *post hoc t*-tests indicated significant changes in IAF amplitude in all channels and in both stimulation intensities [$t(24) = 8.96$, $p < 0.001$ for all channels].

Likewise, after template subtraction, the ANOVA revealed a significant main effect of condition in the 150-µA-tACS data, but no interaction between channels and conditions. No such main effect for condition was found in the 50-µA tACS condition. The ANOVAs on the SSP data neither showed effects for the condition nor for the interactions in both tACS conditions (**Table 3**). In general, SSP outperformed sine fitting and template subtraction. A summary of the SSP performance is depicted in **Figure 4**.

EXPERIMENT 2: PROOF OF PRINCIPLE ON HUMAN DATA

After demonstrating in a phantom that a large portion of the tACS artifact can be suppressed with SSP (which is a short form for SSP-SIR), we wanted to give a proof of principle for the applicability of the SSP algorithm to human EEG data. To this end, we recorded EEG-data during the application of tACS while the subject engaged in a mental rotation task. The mental rotation task (Shepard and Metzler, 1971) is known to modulate ongoing alpha activity; while the stimuli are presented, occipital alpha oscillations desynchronize (Michel et al., 1994; Klimesch, 1999). This event-related desynchronization (ERD; Pfurtscheller and Lopes da Silva, 1999) has been used in studies to estimate the performance of methods for tACS artifact correction in MEG (Kasten et al., 2018). We thus employed a mental rotation task highly similar to Kasten and Herrmann (2017) and Kasten et al. (2018) to show the performance of the SSP-correction in one human subject.

We applied tACS concurrently with a mental rotation task using an open-source stimulus set (Ganis and Kievit, 2015; See Supplementary Section "Paradigm of the Human Experiment" for details and an illustration of the task). All experimental procedures were approved by a local ethics committee at the University of Oldenburg (Komission für Forschungsfolgenabschätzung und Ethik) and were in line with the Declaration of Helsinki.

To achieve a high comparability with tACS intensities as used in many previous studies, we decided to apply tACS at 500 and 1,000 µA. Note here that these tACS intensities might seem incomparable to the intensities used in the phantom (50 and 150 µA). The intensity of the stimulator output (in µA), however,

TABLE 3 | Results of the two-way ANOVA on the IAF amplitude changes.

	SSP	Template	Sine fitting
Main effect Condition (baseline/cleaned)	**50-μV:** $F(1) = 1.42$, $p = 0.23$ **150-μV:** $F(1) = 1.21$, $p = 0.27$	**50-μV:** $F(1) = 3.83$, $p = 0.05$ **150-μV:** $F(1) = 4.43$, $p = 0.04$*	**50-μV:** $F(1) = 956$, $p < 0.001$* **150-μV**: $F(1) = 959$, $p < 0.001$*
Main effect Channel	**50-μV:** $F(17) = 78.29$, $p < 0.001$* **150-μV:** $F(17) = 78.74$, $p < 0.001$*	**50-μV:** $F(17) = 77.24$, $p < 0.001$* **150-μV:** $F(17) = 76.53$, $p < 0.001$*	**50-μV:** F(17)=40.78, p<0.001* **150-μV:** F(17)=40.76, p<0.001*
Interaction Channel × Condition	**50-μV:** $F(1,17)=0.06$, p=1 **150-μV:** $F(1,17)=0.06$, p=1	**50-μV:** $F(1,17) = 0.9$, $p = 0.57$ **150-μV:** $F(1,17) = 1.43$, $p = 0.11$	**50-μV:** $F(1,17) = 38.27$, $p < 0.001$* **150-μV:** $F(1,17) = 38.28$, $p < 0.001$*

Asterisks mark statistically significant effects, i.e., the recovered signal deviates from the original signal.

is not as relevant when considering the correction of the artifact strength as measured via the EEG system (in μV). See **Table 4** for a comparison of these values for our study. The artifact strengths for the human study turn out to be higher by a factor of 20 compared to the phantom study. Thus, the artifact correction in the human study is a lot more difficult.

Materials and Methods

Electroencephalography (EEG)

Measurements were performed with a 24-bit battery-powered amplifier (ActiChamp, Brain Products, Munich, Germany) and 24 preamplifier-equipped electrodes mounted in an elastic cap (Acticap, Falk Minow, Munich, Germany) positioned according to the International 10–20 system (see **Supplementary Figure S1** for details). Electrode impedances were kept below 10 kΩ. The EEG was measured against a common reference at position FP1 and sampled at 10 kHz. All recordings were resampled to 1 kHz in a first step before any further processing to match the sampling frequency in experiment 1. The EEG recording was synchronized with the tACS to guarantee an accurate measurement of the tACS artifact. With the ActiChamp system, it is possible to synchronize the two systems conveniently without a SyncBox.

Transcranial Alternating Current Stimulation (tACS)

The tACS current (10 Hz, with an intensity of either 0.5 or 1 mA), was applied using a battery-powered stimulator system (DC stimulator plus, Eldith, Neuroconn, Ilmenau, Germany) positioned next to the subject inside the cabin. EEG recording and tACS were both sampled at 10 kHz. Two rubber electrodes (5 cm × 7 cm), centered at Oz and Cz (corresponding to the stimulation sites of Experiment 1), were attached to the subject's head using adhesive conductive paste (Ten20, Weaver and Company, Aurora, CO, United States). The tACS signal was created digitally in Matlab and transformed into an analog signal by a NI-DAQ before it was fed into the stimulator as in experiment 1. The stimulator then uses a gain of 2 on its external input to forward the external signal to the subjects' head.

TABLE 4 | Comparison of the tACS intensities, as set in the stimulator (left column), and artifact strengths as measured in the EEG signal (right column) between the phantom and the human study.

	Stimulator output	Artifact strength (min – max)
Phantom	50 μA	10–400 μV
	150 μA	30–1200 μV
Human	500 μA	30–10100 μV
	1000 μA	80–19600 μV

Artifact strengths differ considerable between channels. We thus report minimal and maximal values over the different channels in this table.

Correction of the tACS Artifact

Since the phantom data suggested that SSP would be effective in reducing the artifacts, we expected SSP to correct the tACS artifact also in the human EEG. With a few modifications, the method was directly transferred to the human data. The most relevant difference was that we recorded not only 60, but 600 s of tACS + EEG data, which represents a more realistic scenario in an EEG experiment. The SSP method relies on an accurate estimate of the template of the artifact. The accuracy of the template, however, depends on the length of the data taken into account: if more repetitions of the artifact (in our case, cycles of tACS) are averaged for the template, more residual EEG activity in the template is averaged out. It is known that the tACS artifact changes in amplitude over time due to changes in impedances between skin and stimulation as well as EEG electrodes. We therefore decided to apply the SSP procedure on portions of EEG data of 15 s each, while in the phantom data the 50-s segment of interest (of the entire 60-s recording) was corrected at once. After correction, the data were concatenated such that all analysis procedures could be performed as on the raw data. Other parameters, such as for SIR were identical to those used on the phantom data.

Analysis of Human EEG

As expected, the tACS artifact covered brain activity recorded during weak and strong tACS (**Figure 6**) with sharp peaks at the tACS frequency, the amplitude of strong tACS artifact being about 2 times higher than weak tACS (**Figures 6B,C**). The strong impact of the tACS was also visible in the topographies: while the topography of the average FFT amplitudes at 10 Hz of the EEG without tACS showed an occipital maximum, the topographies of the EEG with tACS represented only the centralized tACS artifact (**Figure 6C**). In order to correct the EEG for the tACS artifact, we applied SSP in all conditions, including the tACS-free baseline measurements (see Supplementary section "Amplitude Attenuation After SSP in Human Data" for details and a figure).

After the EEG data were subjected to the SSP algorithm, they were segmented into epochs of 8 s around the onset of a mental rotation stimulus (−4 to +4 s around the stimulus).

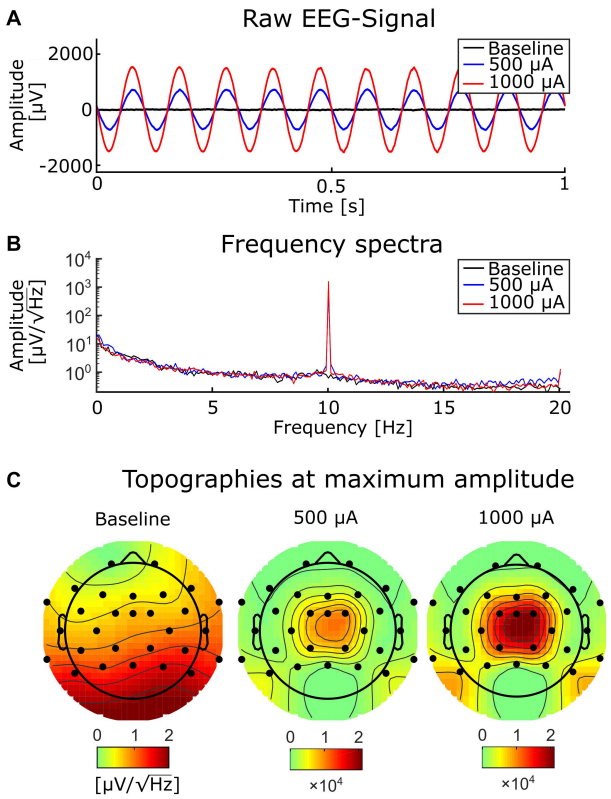

FIGURE 6 | Baseline EEG and tACS-contaminated EEG. **(A)** A representative segment of EEG without tACS (black), and with simultaneous tACS at 500 (blue) and 1,000 μA (red). **(B)** Frequency spectra at 0.2-Hz resolution from the same conditions as in **(A)** and with the same color conventions. **(C)** Topographies of the baseline EEG (left) and the EEG contaminated by tACS with 500 (mid) and 1,000 μA (right).

Time–frequency spectra were calculated of each epoch, using wavelets with 7 cycles over the whole time–frequency range. To increase the performance of the algorithm, data were resampled to 500 Hz before calculating the time-frequency spectra. To show the effectiveness of the SSP algorithm, no baseline correction was applied in the frequency dimension, i.e., the TF data were not normalized to a pre-stimulus baseline period. Thus, pre-stimulus activity is visible in the spectra. Furthermore, event-related (de-) synchronization (ERS/ERD) was calculated for the alpha band (8–12 Hz), by computing the absolute difference between pre- and post-stimulus interval as suggested by Kasten et al. (2018):

$$ERDelta = post - pre$$

Here, 'pre' and 'post' correspond to averaged amplitudes between 200 and 50 ms before stimulus onset and between 100 and 500 ms after stimulus onset, respectively. *ERDelta* is positive when the amplitude is increased after the presentation of an (visual) event (ERS). Negative values represent a decrease of the amplitude, i.e., an event-related desynchronization (ERD). This simple subtraction method is preferable to the more established method by Pfurtscheller and Lopes da Silva (1999) that is based on relative change in oscillatory power. When dealing with tACS-contaminated data, relative change can be strongly biased by residual artifacts in the data, while absolute differences are more robust to such influence. Under the assumption that the strength of the tACS artifact is not systematically modulated by the task, residual artifacts after correction can cancel out (Kasten et al., 2018; Kasten and Herrmann, 2019).

Results

In the time–frequency (TF) spectra before artifact correction (**Figure 7A**), one can see the strong tACS artifact in the second (500 μA tACS) and third row (1,000 μA tACS) as a relatively broad red bar which appears unmodulated throughout the time period depicted. FFT spectra of the uncorrected data can be seen in **Figure 7E**. Due to its high amplitude, the artifact dominates the TF spectrum. In fact, no characteristics of original brain activity can be seen in these plots. Another feature of these plots is the exaggerated 50-Hz line noise artifact. The enormous strength of which can be explained by the experimental setup: the stimulation signal is transmitted from the DAQ to the stimulator through a BNC cable. Even though those cables are shielded, they capture the line noise via electromagnetic induction. Since the stimulator directly transfers the incoming signal to the stimulation electrodes with a gain of 2, the induced line noise is amplified when the signal is conducted to the human scalp. In turn, the 50-Hz noise is amplified in the EEG recordings.

In the baseline tACS condition, the alpha decrease (ERD) after stimulus presentation can be seen by visual inspection. For a better comparison, the color bars for all TF spectra depict the same value range. After artifact correction, time–frequency spectra of the tACS conditions (50-μA tACS and 500-μA tACS) did not show an apparent residual artifact (**Figure 7C**) and natural alpha fluctuations became visible. Data from the baseline tACS condition has also been subjected to the SSP algorithm. Therefore, the difference between the two time–frequency spectra in the first rows of **Figures 7A,C** show the amplitude reduction due to SSP as was described above and which the SIR approach could not restore. The topographies show ERD over parietal areas before artifact correction (**Figure 7B**) and afterward (**Figure 7D**). Note that no occipital electrodes were measured due to the stimulation electrode that covered that area. Thus, shading over occipital areas is extrapolated from other channels. From visually inspecting the topographies, one can clearly identify ERD over parietal areas in all conditions after SSP.

Since ERDelta is a relative measure, one could argue that the correction of the artifact is not even necessary because the calculation of ERDelta is a normalization to a pre-stimulus baseline in the time dimension and would thus be sufficient to cancel out the artifact. However, a recent simulation indicates that strong attenuation of the tACS artifact is necessary to allow the cancelation by computing difference measures to work (Kasten and Herrmann, 2019). To test this assumption on real data, we calculated ERDelta also for the uncorrected data. The resulting topographies are depicted in **Figure 7B**. The range of the ERDelta is strongly reduced in comparison to the data after SSP correction (**Figure 7D**) in the tACS conditions in rows 2

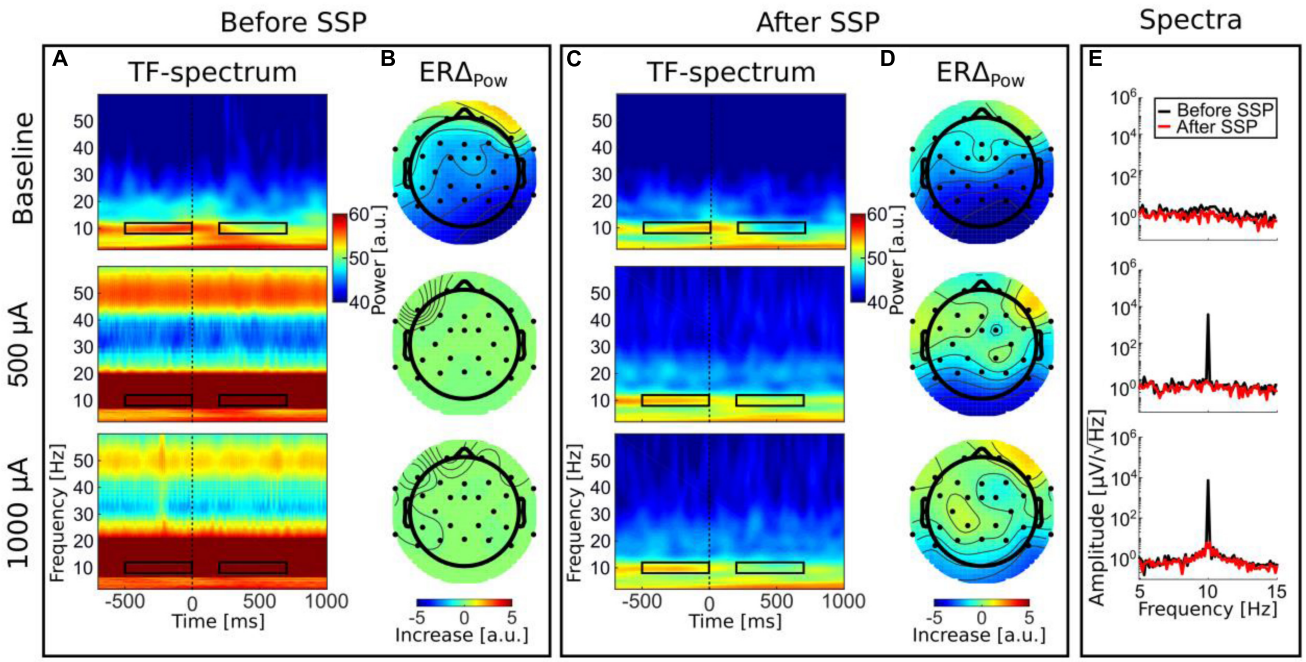

FIGURE 7 | Time–frequency results. Panels **(A,B)** before SSP; panels **(C,D)**; after SSP. TF spectra depict decompositions of event-related EEG data from electrode Pz. Color bars are the same for all TF spectra **(A,C)**. Black rectangles illustrate the time–frequency sub-spectra used to calculate the ERS topographies. Panel **(E)** illustrates the effect of SSP on the frequency spectrum in the alpha range (5–15 Hz) on logarithmic scale. Data for panel **(E)** are identical to the data depicted in the other graphs but were transformed into the frequency domain by an FFT.

and 3. Also the topographies do not show the expected occipito–parietal orientation but appear distorted without a distinctive pattern (**Figure 7B**, row 2 and 3). In line with predictions of the simulation in Kasten and Herrmann (2019) this result indicates that the artifact completely masks the stimulus-related amplitude reduction and that a reduction of the artifact is necessary to recover the underlying brain activity.

DISCUSSION

We evaluated artifact-correction techniques to find a feasible method to remove the tACS artifact from EEG data. By comparing different methods applied to phantom data, we found SSP-SIR ("SSP" in short) to perform the best in recovering the signal of interest. As a proof of concept, we applied SSP to human data from a tACS + EEG experiment and demonstrated to which extent oscillatory parameters such as event-related oscillations can be recovered.

Our initial question was how to estimate that an artifact-correction method does not remove the brain responses of interest and minimizes residual artifacts remaining after correction. We approached this question by applying different methods on a phantom head in which we were in full control over the to-be-recovered EEG signal and the stimulation signal. We found that the SSP method performed best with only minor distortions of the EEG signal compared to template subtraction and sine fitting. For the phantom head, we could quantify this distortion, finding that SSP mildly overcorrects the artifact. However, with SSP this overcorrection can be taken into account when comparing the cleaned signal to the baseline (see Supplementary section "SSP Details" for details). With the phantom, possible physiological effects might be underestimated, because the SSP correction attenuates endogenous amplitudes at the stimulation frequency. For human data, we cannot be entirely sure about the performance of the correction as we do not exactly know the ground truth; however, we compared the same experimental conditions with and without concurrent tACS. Overall, these results suggest that the artifact correction was successful despite an overall reduction of amplitudes; SSP was able to recover subtle changes in alpha amplitude (ERD) relative to a pre-stimulus baseline.

Phantom vs. Human Head

An important question is whether the results obtained in the phantom experiment can be generalized to human data. Obviously, a human head is not three-layered and perfectly spherical. A study by Kim et al. (2015), however, showed that the three-layer spherical model is quite accurate in capturing the essential characteristics of the electric-stimulation-generated ohmic currents in scalp, skull and the brain. Within the typical operating frequency range of tACS, the quasi-static approximation holds in the human head (Opitz et al., 2016). I.e., the conductivity structure of the head, governing the distribution of the ohmic tACS currents, does not change over time or depend on the stimulation frequency. When constructing the phantom, we only measured the impedance

magnitude of the conductive medium. In the next generation phantoms, it is recommended to measure also the impedance phase to makes sure, the phantom perfectly fulfills the quasi-static conditions (Owda and Casson, 2020). However, given the recent measurements in a NaCl based gelatin phantom (Owda and Casson, 2020), it is unlikely that the simple NaCl solution used here would show strong impedance phase within the typical operating frequency range of tACS.

Another difference lies in the sources of activity: contrary to the many sources in a human brain, our phantom only had one neural source. Given that SSP performance depends on the orientation and location of the neural source, the method might further attenuate some neural signals of interest given that their topography can be similar to that of the artifact. This problem can be tackled by evaluating possible signal distortions after SSP (Uusitalo and Ilmoniemi, 1997). A recent work (Yu and Hairston, 2019) provides detailed open-source instructions how to construct a realistic head phantom with several neural sources.

In our phantom study, the dipolar current source oscillated independently of the external stimulation. This might produce over-optimistic results when using template subtraction. If neural activity synchronizes to the tACS, it will be attenuated after subtracting the template; however, perfect phase alignment cannot be expected from real neuronal activity (Van Veen et al., 1997). This also applies to the sine-fitting method: only if the tACS entrains perfectly to the neural frequency at which the brain is stimulated, then sine fitting will also attenuate the entrained brain oscillations.

Another difference of the phantom measurement compared to real human EEG data concerns the electrode–skin impedances: In the phantom head, the artifact amplitude was constant over the course of the stimulation because the electrode–skin impedances remained constant. This allowed us to use all trials to create a template to be subtracted. For real human EEG data, this is not necessarily the ideal approach because the tACS artifact amplitude varies over time due to changes in impedance, elicited by physiological processes in the human body such as heart-beat and respiration (Noury et al., 2016). This poses a problem for the template subtraction method because the subtraction of an incorrectly sized template will result in a residual artifact: the fewer trials are used to create the template, the wider the notch in the Fourier spectrum will be. The problem notably also applies to the SSP method, since the artifact subspace is also calculated based on a data-based template of the artifact. In the human experiment, we tackled the problem of varying impedances by applying the SSP in temporal steps of 15 s.

The tACS current strengths strongly differed between the phantom and the exemplary human data. While in the human subject we applied an intensity comparable to other tACS-studies (1,000 μA), in the phantom we were only able to apply up to 150 μA to avoid clipping artifacts in the data. This limitation of current intensities was less severe in the human experiment, because we were able to use a 24-bit amplifier system in that case, which was not available for the phantom measurements. This general limitation of the phantom experiment may lead to over interpreting the effectiveness of the SSP algorithm. We were, however, able to recover subtle dynamics in the alpha-range even for the 1,000 μA tACS condition in the human. We want to point out here that the artifact, relative to the brain signal was stronger in the human data by a factor of 20 and therefore this condition can be considered more difficult. With this in mind, we argue for the potential of the SSP algorithm to recover EEG in the frequency-band of stimulation also in human subjects at realistic stimulation intensities and encourage a more elaborate examination of the method in further studies. Further on, we would like to add that the conductivity-values used to build the phantom were taken from literature to roughly match the human head (i.e., Gonçalves et al., 2003; Lai et al., 2005). This means that the conductivity of the phantom, even though being comparable to that of a human head, does not perfectly match.

Sine Subtraction

Most commonly, the tACS signal is a sine wave (Herrmann et al., 2013). Therefore, it is an intuitive assumption that one can simply fit and subtract a sine from the contaminated EEG signal and the artifact is removed. An advantage of this method would be that the signal in each electrode can be cleaned separately; this may be beneficial in experimental setups with a small number of electrodes; however, we demonstrated that the sine subtraction method shows a comparatively poor performance. The main problem with sine fitting is that using a least-squares criterion can result in overfitting or underfitting if a significant proportion of the EEG signal of interest phase aligned to the artifact. Another problem with sine fitting is that the tACS artifact is not a perfect sinusoidal wave, but rather a series of analog amplitudes generated by a digital-to-analog converter (DAC), i.e., the sine wave is approximated by a kind of step function and each step is superposed with an exponential due to capacitance inside the DAC. Additionally, the measured artifact is non-sinusoidal due to its interaction with physiological tissues (Noury et al., 2016). A perfect sine wave subtracted from a slightly distorted sine wave will result in a residual artifact. If the artifact is several orders of magnitude larger than the neuronal signals of interest, even small relative differences between the perfect sine-wave model and the actual tACS artifact waveform can cause large absolute errors in the corrected EEG. Overall, our results suggest that this subtraction method cannot be recommended for tACS artifact correction.

Template Subtraction

Like the sine-wave-subtraction method, template subtraction can remove the artifact for each electrode separately. Compared to the sine-fitting approach, template subtraction demonstrated a clearly better performance at recovering the baseline signal in the phantom data; however, especially the temporal fine structure (phase) could not be perfectly recovered. Before applying template subtraction to human tACS + EEG data, several practical considerations should be taken into account.

Typically, the size of the tACS artifact in human EEG can vary due to impedance changes of the tissue (Noury et al., 2016), which can result in improper templates and subsequent residual tACS artifact or a loss of neural EEG signal. Fitting the template to the artifact in the raw EEG by minimizing the sum of squares (Helfrich et al., 2014) can help with the problem of variation

in the amplitude of the artifact; however, this can also result in over- or underfitting. In the phantom-head data, we found that fitting the template to the artifact using least squares resulted in worse recovery of the contaminated signal than simple template subtraction (data not shown). Another solution would be to use temporarily more specific templates by averaging a smaller number of adjacent cycles (moving-average approach); however, the less cycles are included to compute the template, the wider the affected frequency range. A third option is to increase the length of the template (i.e., 2, 3, or more cycles of the artifact). An analysis of how the length of the template and the number of averaged segments influence the resulting EEG recovery can be found in Zebrowska et al. (2020).

Signal-Space Projection (SSP)

We found SSP to yield the best artifact-correction performance. Artifact-contaminated phantom data could be recovered almost perfectly; the application to human data is promising. A major difference between SSP and both sine fitting and template subtraction is that it is based on spatial filtering, thus it may project out artifactual components that are invisible to sine fitting and template subtraction. Even though SSP is able to correct the artifact almost completely in the phantom data, it distorts signals, although in a perfectly known way: the cleaned signals are not meant to be estimates of the signal in the original channels in question (Mäki and Ilmoniemi, 2011). The signals after SSP are known linear combinations of the original EEG signals and can be used without bias in source estimation (Uusitalo and Ilmoniemi, 1997) as long as the data still has a sufficient dimensionality. SIR can correct some of the SSP-induced spatial distortions; however, the original signal amplitudes cannot be perfectly recovered in all channels because some linear components of the signals have been zeroed, leading to overall reduction in amplitude (**Supplementary Figure S2**). We were able to recover time–frequency spectra showing ERD in the alpha range after correction. This indicates that SSP does not completely diminish activity at the stimulation frequency like a notch filter would, but can recover activity even at the stimulation frequency. Comparing tACS-free data with and without the application of SSP–SIR reveals a general decrease of amplitudes in the FFT spectra, which seems to be stronger at higher amplitudes. This is the likely reason why SSP resulted in RMSE of even below the floor value; in addition to the tACS artifact, also other noise located in the artifact subspace was attenuated. Topographic similarity of the artifact and the signals of interest contribute to the unwanted attenuation of the latter; the more similar they are, the higher the attenuation. This is also evident in the human data as the topography of the resting-state alpha and the artifact topographies varied significantly. We advise to apply the SSP–SIR method when comparing data from tACS conditions with tACS-free conditions. Still, most reliable results can be achieved when contrasting experimental conditions combined with the same tACS condition. There is some consensus among different research groups that under the assumption that residual artifacts are present in two experimental conditions to a similar degree, they can cancel out when computing difference measures, such that only the physiological effects remain (Neuling et al., 2015; Kasten et al., 2018; Noury and Siegel, 2018, Herring et al., 2019). In line with predictions of a previous simulation (Kasten and Herrmann, 2019), our data demonstrate that it is insufficient to contrast uncorrected data: although the artifact is constant over time, a baseline correction in the form of a subtraction in the time–frequency space, could not reveal the ERD while the SSP method was able to recover these subtle changes in alpha amplitude.

An open-source MATLAB implementation of a general version of SSP–SIR has been recently added to the transcranial-magnetic-stimulation–EEG signal analyzer code repository (TESA) (Mutanen et al., 2020). The generalized version of SSP–SIR requires evoked control data, containing the artifact topographies to be projected out from the actual data of interest. To reproduce the approach taken here using the TESA functions, one should generate the control data and data of interest by averaging the original data across the tACS cycles and neuronally relevant epochs, respectively.

Technical Requirements for Removing the tACS-Artifact From EEG

A most important requirement during EEG recordings is that the amplifiers do not saturate due to the high amplitudes of the tACS-artifact. If that requirement is not met, no artifact correction is possible. The main feature in this regard is the dynamic range of the amplifier: With a 16-bit EEG amplifier, $2^{16} = 65536$ amplitude values can be digitized. If every amplitude step represents 0.1 μV, as in the phantom experiment, this results in an amplitude range of $\pm$3276 μV. In that case, the amplitude of the artifact can easily exceed the dynamic range, especially at higher impedances. In our measurements on a human subject (using a 24-bit amplifier system), the upper limit of the 16 bit amplifier was already exceeded at 500 μA stimulator output (see **Table 4**).

While this was not a problem for the phantom, it is desirable to use EEG amplifiers with a wider dynamic range for human tACS + EEG experiments, e.g., 24-bit amplifiers, which would allow for an amplitude resolution of 0.05 μV and a dynamic range of $\pm$419430 μV. We therefore used a 24-bit system for the human experiment.

A second factor that has to be taken into account to avoid amplifier saturation is bridging of the tACS electrodes with the recording electrodes. One common technique to reduce the impedance of the tACS electrodes to the scalp is the use of saline-soaked sponge pockets that enclose the tACS electrodes. This bears the danger of leaking saline solution that results in a connection of tACS and EEG electrodes and also of EEG electrodes with each other. To prevent this, we recommend using adhesive paste (e.g., Ten20, D.O. Weaver, Aurora, CO, United States), which does not leak and also prevents electrode movements.

Third, it is of great importance that EEG and tACS are synchronized. Different EEG-systems allow for digital synchronization of the recorder with a different system, e.g., using the BrainVision Syncbox (Brain Products, Munich, Germany). The tACS can by synchronized with the EEG recording by generating the tACS signal digitally and passing that signal

through a digital-to-analog converter (DAQ) into the stimulator as we have done in the phantom experiment. Additionally, the stimulation frequency has to be chosen such that the template estimation can be successful: We used 10 Hz, which has a period duration (100 ms) which is an integer multiple of the period of the EEG sampling interval (i.e., 0.1 ms at 10 kHz sampling frequency). At 11 Hz, the cycle length is $90.\overline{90}$ ms. Thus at 11 Hz, the zero crossings of the artifact cycles do not coincide with one sample. When estimating a template of the tACS artifact based on one cycle, this leads to an unpredictable error in the template, which in turn leads to a failure of the artifact correction.

General

Overall, the results showed that at least in the simplified phantom setup, SSP succeeded well in recovering the underlying oscillatory neuronal activity. Furthermore, our results in human data demonstrate that the SSP method can attenuate the tACS artifact sufficiently to recover task related modulations of endogenous brain oscillations. This is supported by the observation that although the artifact covers brain activity in all EEG channels before correction, after SSP the task induced alpha power modulation is strongest in parietal channels, resembling the topography of the artifact free data. It should be noted, however, that this does not imply that all stimulation artifacts have been removed entirely from the human EEG recordings. Previous studies have shown, that a variety of physiological processes can give rise to non-linear modulations of the tACS artifact, which can hinder complete tACS artifact removal (Noury et al., 2016; Noury and Siegel, 2017). One kind of such additional artifacts are described by Noury et al. (2016) which appear in sidebands of ± 2 Hz around the stimulation frequency. As a possible source Noury and Siegel (2017) identified non-linear modulations of electrode impedance caused by heartbeat and respiration. The SSP-method was not designed to deal with such artifacts resulting from non-linear sources. Future studies will need to evaluate to which degree these non-linearities affect tACS artifact cleaning performance of the SSP method. Nevertheless, our results already indicate that SSP might be a powerful alternative to template subtraction for the analysis of concurrent tACS+EEG data, as the latter suffers from overcorrection (Helfrich et al., 2014) and insufficiently accounts for non-linear modulations of the tACS artifact (Noury et al., 2016).

We have decided for a comparison between three principally different approaches of artifact correction in tACS + EEG data. This concentration was done for the sake of keeping the analysis simple and the interpretation straight-forward. It is of course possible to apply multiple algorithms in combination, or in succession. Helfrich et al. (2014), for example used a sine subtraction method in a first step and a PCA in a second step to correct for the artifact. Other studies have compared different sets of tACS-artifact correction algorithms. Guarnieri et al. (2020) for example have recently compared the approach from Helfrich et al. (2014) to a moving average approach and a time-varying spatial filter using a PCA. The latter method is particularly interesting because it was designed to be computationally efficient to be applied during measurements and thus is able to fulfill closed-loop stimulation settings. In another recent publication, Yan et al. (2020) set out to test three different advanced blind-source separation methods that were combined with an empirical wavelet transform (Gilles, 2013).

We believe that the idea of using realistic phantom heads to test the validity of tACS-artifact correction methods will become a standard technique. One study on a phantom head, comparable to our approach, compared a template subtraction method and adaptive filtering (Kohli and Casson, 2019) as artifact correction techniques. The authors found that both methods yield acceptable results for the recovery of event related potentials. Yet, this study is limited to just one electrode measured on the surface of the phantom and thus cannot evaluate the spatial pattern of the recovered signal in comparison to the original.

Furthermore, our method uses mainly visual inspection and root-means-square error as validation techniques for the tested algorithms. More sophisticated strategies definitely add to the discussion of how good an artifact correction method is. One convincing idea is to use linear discrimination analysis to differentiate between different parts of underlying EEG activity (Kohli and Casson, 2020). With this strategy, the authors were able to differentiate between resting state EEG with eyes open, and EEG from a working memory task after the respective EEG was cleaned from a tACS artificat resulting from 1 mA current.

As the main limitation of our study we want to state that stimulation intensity in the phantom experiment was lower than in regular human studies. Our exemplary human data give rise to the assumption that the method works in human experiments where realistic current intensities are applied. To fully validate the SSP-method it would, however, be desirable to test a realistic phantom also with realistic current strengths.

The SSP method should be further explored in future studies to find the best template the artifact subspace is estimated on. In the current study, the SSP operator was computed from the average template, which might contain entrained brain signals (Thut et al., 2011). As a consequence, this brain activity would also be removed. This issue could be overcome by estimating the artifact subspace based on different tACS conditions (e.g., two or more frequencies and amplitudes), thus minimizing the contribution of brain activity to the template and maximizing the contribution of the artifact.

CONCLUSION

Signal-space projection yielded by far the best performance in removing the tACS artifact at the stimulation frequency and recovering the brain activity in EEG recordings at that frequency in comparison to template and sine-wave subtraction. Even though the performance on the phantom cannot be unequivocally extended to human EEG measurements, SSP is a strong candidate for the correction of the tACS artifact in combined tACS + EEG studies.

DATA AVAILABILITY STATEMENT

The raw data supporting the conclusions of this article will be made available by the authors, without undue reservation, to any qualified researcher.

ETHICS STATEMENT

The studies involving human participants were reviewed and approved by the ethics committee of the University of Oldenberg Kommission für Forschungsfolgenabschätzung und Ethik). The patients/participants provided their written informed consent to participate in this study.

AUTHOR CONTRIBUTIONS

TN, TM, JV, RI, and CH designed the experiments. TN performed the phantom experiment, analyzed the data, and wrote the manuscript. TM built the phantom head, analyzed the data, and wrote the manuscript. JV performed the human experiments, analyzed the data, and wrote the manuscript. RI and CH wrote the manuscript. All authors contributed to the article and approved the submitted version.

FUNDING

This study was supported by the German Research Foundation (Deutsche Forschungsgemeinschaft, DFG) under Germany's Excellence Strategy – EXC 2177/1 – Project ID 390895286, the Academy of Finland (Grant Nos. 283105 and 321631), and the Finnish Cultural Foundation (Grant Nos. 00140634, 00150064, and 00161149).

SUPPLEMENTARY MATERIAL

The Supplementary Material for this article can be found online at: https://www.frontiersin.org/articles/10.3389/fnhum.2020.536070/full#supplementary-material

REFERENCES

Allen, P. J., Josephs, O., and Turner, R. (2000). A method for removing imaging artifact from continuous EEG recorded during functional MRI. *Neuroimage* 12, 230–239. doi: 10.1006/nimg.2000.0599

Cecere, R., Rees, G., and Romei, V. (2015). Individual differences in alpha frequency drive crossmodal illusory perception. *Curr. Biol.* 25, 231–235. doi: 10.1016/j.cub.2014.11.034

Delorme, A., and Makeig, S. (2004). EEGLAB: an open source toolbox for analysis of single-trial EEG dynamics. *J. Neurosci. Methods* 134, 9–21. doi: 10.1016/j.jneumeth.2003.10.009

Dowsett, J., and Herrmann, C. S. (2016). Transcranial alternating current stimulation with sawtooth waves: simultaneous stimulation and EEG recording. *Front. Hum. Neurosci.* 10:135. doi: 10.3389/fnhum.2016.00135

Ganis, G., and Kievit, R. (2015). A new set of three-dimensional shapes for investigating mental rotation processes: validation data and stimulus set. *J. Open Psycholol. Data* 3:e3.

Gilles, J. (2013). Empirical wavelet transform. *IEEE Trans. Signal. Process.* 61, 3999–4010.

Gonçalves, S., De Munck, J. C., Verbunt, J., Bijma, F., Heethaar, R. M., and Lopes da Silva, F. (2003). In vivo measurement of the brain and skull resistivities using an EIT-based method and realistic models for the head. *IEEE Trans. Biomed. Eng.* 50, 754–767. doi: 10.1109/tbme.2003.812164

Guarnieri, R., Brancucci, A., D'Anselmo, A., Manippa, V., Swinnen, S. P., Tecchio, F., et al. (2020). A computationally efficient method for the attenuation of alternating current stimulation artifacts in electroencephalographic recordings. *J. Neural Eng.* 17:e046038.

Helfrich, R. F., Schneider, T. R., Rach, S., Trautmann-Lengsfeld, S. A., Engel, A. K., and Herrmann, C. S. (2014). Entrainment of brain oscillations by transcranial alternating current stimulation. *Curr. Biol.* 24, 333–339. doi: 10.1016/j.cub.2013.12.041

Herring, J. D., Esterer, S., Marshall, T. R., Jensen, O., and Bergmann, T. O. (2019). Low-frequency alternating current stimulation rhythmically suppresses gamma-band oscillations and impairs perceptual performance. *Neuroimage* 184, 440–449. doi: 10.1016/j.neuroimage.2018.09.047

Herrmann, C. S., Rach, S., Neuling, T., and Strüber, D. (2013). Transcranial alternating current stimulation: a review of the underlying mechanisms and modulation of cognitive processes. *Front. Hum. Neurosci.* 7:279. doi: 10.3389/fnhum.2013.00279

Kasten, F. H., and Herrmann, C. S. (2017). Transcranial alternating current stimulation (tACS) enhances mental rotation performance during and after stimulation. *Front. Hum. Neurosci.* 11:2. doi: 10.3389/fnhum.2017.00002

Kasten, F. H., and Herrmann, C. S. (2019). Recovering brain dynamics during concurrent tACS-M/EEG: an overview of analysis approaches and their methodological and interpretational pitfalls. *Brain Topogr.* 32, 1013–1019. doi: 10.1007/s10548-019-00727-7

Kasten, F. H., Maess, B., and Herrmann, C. S. (2018). Facilitated event-related power-modulations during transcranial alternating current stimulation (tACS) revealed by concurrent tACS-MEG. *Eneuro* 5:ENEURO.0069-18.2018.

Kim, D., Jeong, J., Jeong, S., Kim, S., Jun, S. C., and Chung, E. (2015). Validation of 743 computational studies for electrical brain stimulation with phantom head experiments. *Brain Stimulat.* 8, 914–925. doi: 10.1016/j.brs.2015.06.009

Klimesch, W. (1999). EEG alpha and theta oscillations reflect cognitive and memory performance: a review and analysis. *Brain Res. Rev.* 29, 169–195. doi: 10.1016/s0165-0173(98)00056-3

Kohli, S., and Casson, A. J. (2019). Removal of gross artifacts of transcranial alternating current stimulation in simultaneous EEG monitoring. *Sensors* 19:190. doi: 10.3390/s19010190

Kohli, S., and Casson, A. J. (2020). Machine learning validation of EEG+tACS artefact removal. *J. Neur. Eng.* 17:e016034.

Lachaux, J. P., Rodriguez, E., Martinerie, J., and Varela, F. J. (1999). Measuring phase synchrony in brain signals. *Hum. Brain Map.* 8, 194–208. doi: 10.1002/(sici)1097-0193(1999)8:4<194::aid-hbm4>3.0.co;2-c

Lai, Y., Van Drongelen, W., Ding, L., Hecox, K. E., Towle, V. L., Frim, D. M., et al. (2005). Estimation of in vivo human brain-to-skull conductivity ratio from simultaneous extra-and intra-cranial electrical potential recordings. *Clin. Neurophysiol.* 116, 456–465. doi: 10.1016/j.clinph.2004.08.017

Mäki, H., and Ilmoniemi, R. J. (2011). Projecting out muscle artifacts from TMS-evoked EEG. *Neuroimage* 54, 2706–2710. doi: 10.1016/j.neuroimage.2010.11.041

Michel, C. M., Kaufman, L., and Williamson, S. J. (1994). Duration of EEG and MEG α suppression increases with angle in a mental rotation task. *J. Cogn. Neurosci.* 6, 139–150. doi: 10.1162/jocn.1994.6.2.139

Mitra, P., and Bokil, H. (2007). *Observed brain dynamics.* (Oxford: Oxford University Press), 200–202.

Mutanen, T. P., Biabani, M., Sarvas, J., Ilmoniemi, R. J., and Rogasch, N. C. (2020). Source-based artifact-rejection techniques available in TESA, an open-source TMS-EEG toolbox. *Brain Stimulat.* 13, 1349–1351. doi: 10.1016/j.brs.2020.06.079

Mutanen, T. P., Kukkonen, M., Nieminen, J. O., Stenroos, M., Sarvas, J., and Ilmoniemi, R. J. (2016). Recovering TMS-evoked EEG responses masked by muscle artifacts. *Neuroimage* 139, 157–166. doi: 10.1016/j.neuroimage.2016.05.028

Neuling, T., Rach, S., Wagner, S., Wolters, C. H., and Herrmann, C. S. (2012). Good vibrations: oscillatory phase shapes perception. *Neuroimage* 63, 771–778. doi: 10.1016/j.neuroimage.2012.07.024

Neuling, T., Ruhnau, P., Fuscà, M., Demarchi, G., Herrmann, C. S., and Weisz, N. (2015). Friends, not foes: magnetoencephalography as a tool to uncover brain dynamics during transcranial alternating current stimulation. *Neuroimage* 118, 406–413. doi: 10.1016/j.neuroimage.2015.06.026

Neuling, T., Ruhnau, P., Weisz, N., Herrmann, C. S., and Demarchi, G. (2017). Faith and oscillations recovered: on analyzing EEG/MEG signals during tACS. *Neuroimage* 147, 960–963. doi: 10.1016/j.neuroimage.2016.11.022

Niazy, R. K., Beckmann, C. F., Iannetti, G. D., Brady, J. M., and Smith, S. M. (2005). Removal of fMRI environment artifacts from EEG data using optimal basis sets. *Neuroimage* 28, 720–737. doi: 10.1016/j.neuroimage.2005.06.067

Noury, N., Hipp, J. F., and Siegel, M. (2016). Physiological processes non-linearly affect electrophysiological recordings during transcranial electric stimulation. *Neuroimage* 140, 99–109. doi: 10.1016/j.neuroimage.2016.03.065

Noury, N., and Siegel, M. (2017). Phase properties of transcranial electrical stimulation artifacts in electrophysiological recordings. *Neuroimage* 158, 406–416. doi: 10.1016/j.neuroimage.2017.07.010

Noury, N., and Siegel, M. (2018). Analyzing EEG and MEG signals recorded during tES, a reply. *Neuroimage* 167, 53–61. doi: 10.1016/j.neuroimage.2017.11.023

Opitz, A., Falchier, A., Yan, C. G., Yeagle, E. M., Linn, G. S., Megevand, P., et al. (2016). Spatiotemporal structure of intracranial electric fields induced by transcranial electric stimulation in humans and nonhuman primates. *Sci. Rep.* 6, 1–11. doi: 10.1109/tmag.2014.2326819

Owda, A. Y., and Casson, A. J. (2020). Electrical properties, accuracy, and multi-day performance of gelatine phantoms for electrophysiology. *bioRxiv* [Preprint], doi: 10.1101/2020.05.30.125070v1

Pfurtscheller, G., and Lopes da Silva, F. H. (1999). Event-related EEG/MEG synchronization and desynchronization: basic principles. *Clin. Neurophysiol.* 110, 1842–1857. doi: 10.1016/s1388-2457(99)00141-8

Polanía, R., Nitsche, M. A., Korman, C., Batsikadze, G., and Paulus, W. (2012). The importance of timing in segregated theta phase-coupling for cognitive performance. *Curr. Biol.* 22, 1314–1318. doi: 10.1016/j.cub.2012.05.021

Shepard, R. N., and Metzler, J. (1971). Mental rotation of three-dimensional objects. *Science* 171, 701–703. doi: 10.1126/science.171.3972.701

Thut, G., Schyns, P. G., and Gross, J. (2011). Entrainment of perceptually relevant brain oscillations by non-invasive rhythmic stimulation of the human brain. *Front. Psychol.* 2:170. doi: 10.3389/fnhum.2013.00170

Uusitalo, M. A., and Ilmoniemi, R. J. (1997). Signal-space projection method for separating MEG or EEG into components. *Med. Biol. Eng. Comput.* 35, 135–140. doi: 10.1007/bf02534144

Van Veen, B. D., van Drongelen, W., Yuchtman, M., and Suzuki, A. (1997). Localization of brain electrical activity via linearly constrained minimum variance spatial filtering. *IEEE Trans. Biomed. Eng.* 44, 867–880. doi: 10.1109/10.623056

Voss, U., Holzmann, R., Hobson, A., Paulus, W., Koppehele-Gossel, J., Klimke, A., et al. (2014). Induction of self awareness in dreams through frontal low current stimulation of gamma activity. *Nat. Neurosci.* 17, 810–812. doi: 10.1038/nn.3719

Vossen, A., Gross, J., and Thut, G. (2015). Alpha power increase after transcranial alternating current stimulation at alpha frequency (α-tACS) reflects plastic changes rather than entrainment. *Brain Stimulat.* 8, 499–508. doi: 10.1016/j.brs.2014.12.004

Vosskuhl, J., Huster, R. J., and Herrmann, C. S. (2016). BOLD signal effects of transcranial alternating current stimulation (tACS) in the alpha range: a concurrent tACS-fMRI study. *Neuroimage* 140, 118–125. doi: 10.1016/j.neuroimage.2015.10.003

Yan, X., Boudrias, M., and Mitsis, G. D. (2020). "Artifact removal in tACS-EEG recordings: a combined methodology based on the empirical wavelet transform," in *Proceedings of the 42nd Annual International Conference of the IEEE Engineering in Medicine & Biology Society (EMBC)* Montreal, QC.

Yu, A. B., and Hairston, W. D. (2019). *Open EEG Phantom*. Available online at: https://doi.org/10.17605/OSF.IO/QRKA2 (accessed November 23, 2020).

Zaehle, T., Rach, S., and Herrmann, C. S. (2010). Transcranial alternating current stimulation enhances individual alpha activity in human EEG. *PLoS One* 5:e13766. doi: 10.1371/journal.pone.0013766

Zebrowska, M., Dzwiniel, P., and Waleszczyk, W. J. (2020). Removal of the sinusoidal transorbital lternating current stimulation artifact from simultaneous eeg recordings: effects of simple moving average parameters. *Front. Neurosci.* 14:735. doi: 10.3389/fnins.2020.00735

Conflict of Interest: CH has received honoraria as editor from Elsevier Publishers, and has filed a patent application for transcranial electric stimulation.

The remaining authors declare that the research was conducted in the absence of any commercial or financial relationships that could be construed as a potential conflict of interest.

frontiers in Human Neuroscience

REVIEW
published: 14 January 2021
doi: 10.3389/fnhum.2020.586448

Causal Inferences in Repetitive Transcranial Magnetic Stimulation Research: Challenges and Perspectives

Justyna Hobot[1,2]*, *Michał Klincewicz*[3,4], *Kristian Sandberg*[2,5] and *Michał Wierzchoń*[1]

[1]Consciousness Lab, Psychology Institute, Jagiellonian University, Krakow, Poland, [2]Center of Functionally Integrative Neuroscience, Aarhus University, Aarhus, Denmark, [3]Cognitive Science, Institute of Philosophy, Jagiellonian University, Krakow, Poland, [4]Department of Cognitive Science and Artificial Intelligence, Tilburg University, Tilburg, Netherlands, [5]Center of Functionally Integrative Neuroscience, Aarhus University Hospital, Aarhus, Denmark

Transcranial magnetic stimulation (TMS) is used to make inferences about relationships between brain areas and their functions because, in contrast to neuroimaging tools, it modulates neuronal activity. The central aim of this article is to critically evaluate to what extent it is possible to draw causal inferences from repetitive TMS (rTMS) data. To that end, we describe the logical limitations of inferences based on rTMS experiments. The presented analysis suggests that rTMS alone does not provide the sort of premises that are sufficient to warrant strong inferences about the direct causal properties of targeted brain structures. Overcoming these limitations demands a close look at the designs of rTMS studies, especially the methodological and theoretical conditions which are necessary for the functional decomposition of the relations between brain areas and cognitive functions. The main points of this article are that TMS-based inferences are limited in that stimulation-related causal effects are not equivalent to structure-related causal effects due to TMS side effects, the electric field distribution, and the sensitivity of neuroimaging and behavioral methods in detecting structure-related effects and disentangling them from confounds. Moreover, the postulated causal effects can be based on indirect (network) effects. A few suggestions on how to manage some of these limitations are presented. We discuss the benefits of combining rTMS with neuroimaging in experimental reasoning and we address the restrictions and requirements of rTMS control conditions. The use of neuroimaging and control conditions allows stronger inferences to be gained, but the strength of the inferences that can be drawn depends on the individual experiment's designs. Moreover, in some cases, TMS might not be an appropriate method of answering causality-related questions or the hypotheses have to account for the limitations of this technique. We hope this summary and formalization of the

OPEN ACCESS

Edited by:
Nivethida Thirugnanasambandam, National Brain Research Centre (NBRC), India

Reviewed by:
Urvakhsh Meherwan Mehta, National Institutes of Health (NIH), United States
Kyung Mook Choi, Korea University, South Korea

***Correspondence:**
Justyna Hobot
justyna.hobot@doctoral.uj.edu.pl

Specialty section:
This article was submitted to Brain Imaging and Stimulation, a section of the journal Frontiers in Human Neuroscience

Received: *23 July 2020*
Accepted: *30 November 2020*
Published: *14 January 2021*

Citation:
Hobot J, Klincewicz M, Sandberg K and Wierzchoń M (2021) Causal Inferences in Repetitive Transcranial Magnetic Stimulation Research: Challenges and Perspectives. Front. Hum. Neurosci. 14:586448. doi: 10.3389/fnhum.2020.586448

Abbreviations: A_{1C}, a change in A_1 activity is present; BOLD, blood oxygen level-dependent; H, P_X takes place in A_1; P_X, process underlying cognitive function X; P_Y, process underlying cognitive function Y; I_1, inference 1; I_2, inference 2; I_3, inference 3; I_4, inference 4; I_5, inference 5; rTMS, repetitive Transcranial magnetic stimulation (TMS); S_0, a sham rTMS protocol; $rTMS_1$, an active rTMS protocol 1; S_{1A}, $rTMS_1$ is applied to A_1; $rTMS_2$, an active rTMS protocol 2; TMS, transcranial magnetic stimulation; T_X, task X; T_{XD}, an observed difference in T_X performance; T_Y, task Y.

reasoning behind rTMS research can be of use not only for scientists and clinicians who intend to interpret rTMS results causally but also for philosophers interested in causal inferences based on brain stimulation research.

Keywords: causal inferences, brain plasticity, brain excitability, repetitive TMS, TMS-neuroimaging

INTRODUCTION

A fundamental issue in human neuroscience is how to make causal inferences based on research data. Traditional use of neuroimaging methods limits experimental conclusions to correlational inferences (though, the methods of effective connectivity are used to postulate causal inferences; see Valdes-Sosa et al., 2011). Following their introduction, brain stimulation methods, especially TMS, started to be considered as a remedy for this limitation. TMS was developed over thirty years ago and is based on electromagnetic induction (Barker et al., 1985). A TMS coil induces an electric field which might influence the activity of brain tissue. It was originally thought that TMS would make it possible to conclude the causal relations between brain activity, cognitive functions, and behaviors. However, it has since become clearer that the brain cannot simply be parceled into regions responsible for certain functions, and the impact of brain lesions and non-invasive brain stimulation is not necessarily limited to a single area but extends to networks. Currently, TMS is often used to test hypotheses about how short-term changes in the excitability of a stimulated brain area affect cognitive functions. In online TMS paradigms, electromagnetic pulses are applied concurrently with the experimental measurement. The physiological consequences of a single electromagnetic pulse can be detected for over a dozen seconds (Furubayashi et al., 2013). In repetitive (rTMS) paradigms, pulses with a particular frequency pattern are applied during or before experimental measurement because they often lead to neuroplasticity-like changes (Chung et al., 2015). The neuromodulatory rTMS effect can be assessed with standard experimental procedures or neuroimaging techniques (for a review of combined TMS-EEG studies, see Thut and Pascual-Leone, 2010); it can be observed even for up to 45 min after a single protocol application (Huang et al., 2005), or it can last for months after multiple protocol applications over repeated TMS sessions in longitudinal studies (Speer et al., 2000, 2009; Li et al., 2004; Choi et al., 2014, 2019; Kang et al., 2016). Thus, TMS is often considered to be an extension of neuroimaging, which (due to its influence on brain activity) allows causal relations to be tested.

TMS is frequently used to decompose the functional organization of the brain. Multiple scientific articles contain statements that TMS can be used to draw both causal brain-behavior inferences (Sack, 2006; Śliwińska et al., 2014) and causal relationships between brain structure and function (Schutter et al., 2004; Bolognini and Ro, 2010; Hartwigsen, 2015; Veniero et al., 2019). In research practice, this often leads to implicit assumptions that TMS can selectively influence the area of interest, therefore its role can be established. Consequently, multiple studies have presented rTMS-based conclusions on the causal role of certain brain areas in certain cognitive functions (e.g., Carmel et al., 2010; Philiastides et al., 2011; Zanto et al., 2011; Bourgeois et al., 2013; Izuma et al., 2015; Schaal et al., 2015; Siuda-Krzywicka et al., 2016; Montefinese et al., 2017), often without describing alternative explanations or making a distinction between direct and indirect causal effects of an rTMS-induced change in activity in a certain area on a certain behavior or brain process.

Employing chronometry (tracking the time course of functional relevance), online single-pulse, double-pulse, or short-burst TMS protocols (including double-coil approaches) allow investigation of the causal relations between the activity of certain brain areas and behaviors or cognitive functions especially when effective connectivity measures are also employed (e.g., de Graaf et al., 2009). These protocol types might be used to influence cognitive functions or perturb brain activity to track the signal propagation and analyze the topographic pattern of TMS-evoked changes in brain activity. This allows researchers to: (1) identify the brain areas involved in certain behavior; (2) assess the impact of the stimulated brain area upon interconnected areas *via* direct connections or intermediate areas, including inter-hemispheric interactions (Blankenburg et al., 2008); (3) reveal bottom-up and top-down influences between brain areas; and (4) dissect the specific functional contributions of different cortical areas of an investigated network. Crucially, the propagation of TMS-evoked activity can depend on the degree of wakefulness (Massimini et al., 2005), which in some studies may act as a confound but in others may allow the state-dependence of interactions among remote and interconnected brain regions to be investigated. However, this use of TMS is limited to specific experimental designs, and some TMS effects (as in the case of all active TMS protocols) may be side effects of the stimulation procedure (Holmes and Meteyard, 2018; for a review, see Bestmann et al., 2008a).

The rTMS approach is more limited than single-pulse, double-pulse, and burst-pulse TMS in terms of helping to understand the causal relationships between brain areas and cognitive functions (however, in certain designs rTMS can be used for chronometry, see Rossi et al., 2011). Online rTMS does not allow concurrent brain activity registration using neuroimaging techniques, while offline rTMS effects depend on neuroplasticity-like changes which might occur at various time points after the start or the end of rTMS. Thus, rTMS does not allow tracking of the direct influence of perturbation to determine the time point at which an area makes a critical contribution to a given behavior or to investigate effective connectivity between brain areas. Although most non-invasive stimulation methods share the same limitations

as rTMS, for purposes of clarity we narrow the scope of the discussion below to rTMS. Most of the issues, that are mentioned below, related to the pitfalls of TMS have already been selectively discussed (e.g., Siebner and Rothwell, 2003; Robertson et al., 2003; Thickbroom, 2007; Bestmann et al., 2008a; Siebner et al., 2009). The current article aims to combine, organize, and analyze these insights at the theoretical level and indicate their possible consequences for inferences based on rTMS evidence. Below, we first analyze several known methodological issues that can invalidate inferences about direct causal relations between brain areas, brain processes, and cognitive functions investigated with TMS. Second, we discuss the special role that neuroimaging plays in rTMS-based inferences and approaches to creating TMS control conditions.

INFERENCES BASED ON CONDITIONAL STATEMENTS

Causal inference, and specifically inference based on interventions in the operation of a complex system such as the brain, fall within the theoretical framework of the general theory of causality that was developed by Pearl (2000). We use a small part of Pearl's Structural Causal Model. This is because unlike causal frameworks such as Bradford Hill's criteria (Hill, 1965), Pearl's framework is resistant to counterexamples and makes sense of probabilistic causal inferences about specific mechanisms that are parts of complex systems. In this view, to characterize a relationship between event A and event B as causal is to say that a selective intervention on A might lead to a change in the distribution of B. We assume a causal influence of one event on another is direct if none of the variables included in a given causal model mediates this effect; otherwise, it is indirect. In a setting such as a TMS experiment, where intervention is randomized, we compare the intervention-related distribution of variables with a control distribution and expect to find suitable neuronal candidates that cause the response. For clarity purposes, we address TMS-related inferences with the use of conditional logic.

To consider a simple type of TMS-based inference, assume that a researcher is interested in cognitive function X. To investigate the process (P_X) that underlies this function, the researcher aims to determine whether brain area 1 (A_1), which is typically associated with P_X, is engaged during a task that is assumed to engage cognitive function X (T_X). For example, one may investigate the involvement of the dorsolateral prefrontal cortex in decision confidence by measuring the effect of rTMS on confidence ratings. In such a case, the hypothesis (H) often states that P_X takes place in A_1 and is tested with the application of an active rTMS protocol 1 ($rTMS_1$) to A_1. We can formally represent this pattern of reasoning in the following way (the logic symbol $\wedge$ represents the logical conjunction, i.e., "and," and the $\rightarrow$ represents implication, i.e., "if <antecedent> then <consequent>"):

H – P_X takes place in A_1
S_{1A}—$rTMS_1$ is applied to A_1
T_{XD}—a difference in T_X performance is observed (as compared to a control condition)

$$I_1(((H \wedge S_{1A}) \rightarrow T_{XD}) \wedge (S_{1A} \wedge T_{XD})) \rightarrow H$$

Inference 1 (I_1) states that the statement that P_X takes place in A_1 is true if the following two premises are true: (1) if P_X takes place in A_1 and $rTMS_1$ is applied to A_1 then a difference in T_X performance is observed; and (2) $rTMS_1$ is applied to A_1 and a difference in T_X performance is observed.

I_1 depicts the basic form of reasoning used in rTMS research. However, like any inductive inference, this form of reasoning does not always lead to true conclusions. For example, the occurrence of the difference in T_X performance may be unrelated to $rTMS_1$, in which case, two independent factors contribute to falsely interpreting the consequent of the condition as true. Thus, causal reasoning based on misuse of I_1 may lead to false conclusions. Possible overconfidence in I_1-based inferences might also stem from overlooking both how TMS and brains work. First, the assumption that TMS selectively influences a targeted area is not always true. The strength of the induced electric field decreases together with the distance from the coil, so the brain areas above or adjacent to the targeted area are likely to be stimulated more than the intended one (Heller and van Hulsteyn, 1992). Second, applying TMS to one area can indirectly influence multiple brain areas that are structurally connected to it and lead to an alteration of the functional state of the targeted network, as pointed out in several reviews (Ruff et al., 2009; Bolognini and Ro, 2010; Ziemann, 2010; Beynel et al., 2020). In sum, TMS applied to a specific brain region can influence other regions directly (e.g., due to stimulation of an area above or adjacent to the area investigated) or indirectly *via* neural connections (e.g., indirect stimulation of an area that is connected to the investigated area or activity alteration in another area due to excitability alteration in the investigated area). These factors limit the strength of causal conclusions based on I_1.

Accordingly, $rTMS_1$ may be responsible for a difference in T_X performance *via* unintended stimulation of an area other than A_1. For example, assume that A_1 is structurally connected to brain area 2 (A_2). Then, there is a possibility that A_2 activity is influenced: (1) directly by $rTMS_1$ when A_1 is targeted (**Figure 1A**); or (2) indirectly by $rTMS_1$ *via* an alteration of A_1 activity. At the same time, A_2 is responsible or more important than A_1 for executing P_X (**Figure 1B**). Unintentional direct stimulation of A_2 may occur in several ways. First, the physical spread of an electrical field may reach areas adjacent to the targeted one. Second, since electrical current follows the path of least resistance, the electric field distribution is highly dependent on cerebrospinal fluid distribution and brain folding, thus the peak of the electric field can occur in gray matter regions located some distance from the electric field's expected peak, which is judged based on the location of the center of the (figure-of-eight) coil. This might result in greater stimulation of area/s other than the targeted one (Bijsterbosch et al., 2012). Third, it is challenging to distinguish

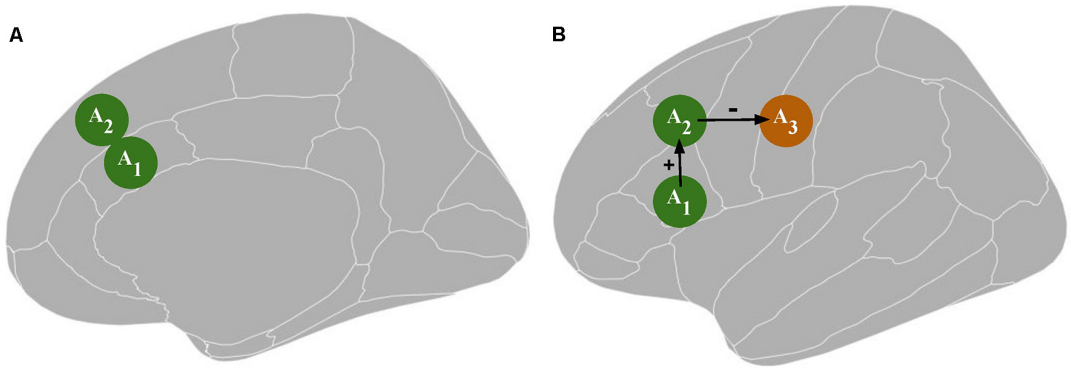

FIGURE 1 | Panel **(A)** depicts a possible direct influence of transcranial magnetic stimulation [TMS; an excitability alteration in the brain tissue surrounding the targeted area A_1, i.e., area 2 (A_2)]. Panel **(B)** depicts a possible indirect TMS influence: an excitability alteration in A_2 or area 3 (A_3) resulting from an excitability alteration in A_1. A_1 represents the targeted area; A_2 and A_3 represent the areas directly and indirectly connected to A_1, respectively, which together constitute a functional network. The green color indicates an increase in neuronal excitation while the orange color indicates a decrease in neuronal excitation.

whether the rTMS effect stems from excitability alteration in the targeted area or an area above it that possibly has a distinct specialization. These concerns may be raised especially when deeper structures such as the anterior cingulate cortex (Hayward et al., 2007) or insula (Pollatos et al., 2016) are investigated. The vast majority of TMS studies target superficial structures; however, the rule that the strongest electrical field is generated within the outermost areas applies even if the distances (which might be the consequences of brain folding) are small. Because a large part of the cortex lies within sulci, targeted brain coordinates in numerous TMS studies have to be placed within sulci (Busan et al., 2009; Cappelletti et al., 2009; Salillas et al., 2009). Additionally, stimulation of deeper brain structures is obtained at the expense of inducing wider electrical field spread in the brain (Roth et al., 2007; Deng et al., 2013; Downar et al., 2016). For example, metabolic and physiological effects on the primary motor cortex and the primary somatosensory cortex can be observed after rTMS to premotor areas (Siebner et al., 2003). This may compound the difficulty in distinguishing the contribution of direct vs. indirect rTMS effects. The network effects may produce remote activity alteration in cortical areas *via* cortico-cortical routes and in subcortical structures *via* cortico-subcortical projections (Strafella et al., 2003; Lefaucheur et al., 2020). The extent of the network effects depends on rTMS protocol parameters (Bestmann et al., 2003). Additionally, the assumption that a difference in T_X performance is caused by an $rTMS_1$-induced change in A_1 activity may be misleading due to the occurrence of placebo and sensory side effects (Abler et al., 2005). Moreover, rTMS may influence areas related to general cognitive resources (e.g., regions engaged in attentional or working memory processing) or the observed effect may be specific to the T_X design (e.g., resulting from $rTMS_1$ influence on brain regions involved in response generation during T_X), which is not related to the influence on the investigated cognitive function. In sum, overconfidence in I_1 has multiple ways to lead researchers to overinterpret their data as evidence that P_X takes place in A_1.

Since statements that follow I_1 cannot fully support the conclusion that P_X takes place in A_1, can some other inference be used to show that P_X is not executed in A_1? This would provide independent evidence for excluding that region from the area of research interest. This way of reasoning is indeed found in TMS literature: based on the lack of an observed effect, some authors postulate a lack of rTMS influence on investigated cognitive functions (e.g., Ghabra et al., 1999; Poulet et al., 2004; Jung et al., 2010; Bor et al., 2017), which might suggest that an investigated area is not involved in the process underlying the investigated cognitive function. Consider then the inference of the following structure (the logic symbol ¬ represents negation, i.e., "not"):

H – P_X takes place in A_1
S_{1A}—$rTMS_1$ is applied to A_1

T_{XD}—a difference in T_X performance is observed (as compared to a control condition)

$$I_2(((H \wedge S_{1A}) \rightarrow T_{XD}) \wedge (S_{1A} \wedge \neg T_{XD})) \rightarrow \neg H$$

Inference 2 (I_2) states that the statement that P_X is not executed in A_1 is true if the following two premises are also true: (1) a difference in T_X performance is observed if P_X takes place in A_1 and $rTMS_1$ is applied to A_1; (2) $rTMS_1$ is applied to A_1 and a difference in T_X performance is not observed.

In research practice, $rTMS_1$ does not always lead to a change in A_1 activity and/or a difference in T_X performance. $rTMS_1$ may have no factual effect because: (1) the $rTMS_1$ frequency pattern is inadequate for investigating P_X (e.g., theta burst stimulation is applied but P_X is independent of theta-gamma coupling; De Ridder et al., 2007); (2) $rTMS_1$ parameters are set too low (e.g., intensity or current direction) to influence P_X (Valero-Cabré et al., 2017); (3) brain-intrinsic factors such as neurochemical and neurophysiological properties of A_1 prevent an alteration in its excitability (e.g., it is impossible to facilitate or inhibit A_1 to

a greater extent than it is before $rTMS_1$ application; Karabanov et al., 2015); and (4) to influence A_1, $rTMS_1$ should be applied with greater precision (e.g., based on individual functional brain images; Hannula and Ilmoniemi, 2017). Altogether, this is enough evidence to assume that I_2 is not a stronger form of reasoning than I_1. I_1 and I_2 include a hidden assumption that $rTMS_1$ leads to an alteration in A_1 activity but not all active rTMS applications have neural effects. To claim that A_1 has changed, the assertion based on the inference presented below has to be true:

S_{1A}—$rTMS_1$ is applied to A_1
A_{1C}—a change in A_1 activity is present

$$I_3((S_{1A} \rightarrow A_{1C}) \wedge S_{1A}) \rightarrow A_{1C}$$

I_3 states that the statement that A_1 activity is changed if the following two premises are true: (1) a change in A_1 activity is present if $rTMS_1$ is applied to A_1; and (2) $rTMS_1$ is applied to A_1.

The issue of the impact of $rTMS_1$ on the activity of A_1 might be addressed with the use of neuroimaging.

TMS AND NEUROIMAGING

A way of strengthening TMS-based inferences is to combine TMS with neuroimaging, the advantages of which have already been exhaustively described (e.g., Sack, 2006; Bestmann et al., 2008b; Bergmann et al., 2016). Multiple studies have already successfully employed neuroimaging to determine whether a particular rTMS protocol leads to a change in A_1 activity (e.g., Bestmann et al., 2008c; Ruff et al., 2008; Capotosto et al., 2012). Despite the advantage of neuroimaging methods in allowing detection of a change in A_1 activity, confirmation that the change in A_1 activity accompanies TMS_1 cannot fully confirm H. Importantly, even if the change in A_1 activity can be confirmed with neuroimaging, it does not always lead to a difference in T_X performance (Reithler et al., 2011). TMS_1 may have no observable effect because: (1) TMS_1 could have additional consequences that hinder the original stimulation effect, such as the occurrence of compensatory effects that diminish the TMS-induced alteration in A_1 activity or that fulfill the function of A_1 (Andoh and Martinot, 2008); and (2) T_X may not provide an adequate measure of P_X because T_X or its performance level is not demanding enough to be influenced by TMS_1, or T_X is not sensitive enough to capture the impact of TMS_1. Nevertheless, this does not imply that null TMS results are not meaningful because they are crucial to proving the functional irrelevance of a brain region to performing a particular function (de Graaf and Sack, 2011).

Next, assume that the influence of TMS_1 on A_1 can be effectively measured by neuroimaging methods and T_X, and both a change in A_1 activity and a difference in T_X performance is observed. This leads to stronger reasoning than I_1 (inference 4; I_4):

H – P_X takes place in A_1
S_{1A}—$rTMS_1$ is applied to A_1
T_{XD}—a difference in T_X performance is observed (as compared to a control condition)
A_{1C}—a change in A_1 activity is present

$$I_4((((H \wedge S_{1A}) \rightarrow T_{XD}) \wedge (S_{1A} \wedge T_{XD})) \wedge (((S_{1A} \rightarrow A_{1C}) \wedge S_{1A}) \rightarrow T_{XD})) \rightarrow H$$

I_4 states that the statement that P_X takes place in A_1 is true if the following two premises are true: (1) the antecedent of I_1; and (2) a difference in T_X performance is observed if the antecedent of I_3 is true (analogous reasoning including $\neg T_{XD}$ instead of T_{XD} can be used to infer about the lack of A_1 involvement in P_X).

Again, since the inference is inductive, I_4 is not immune to error and H might be false. Even if it is not, I4 merely adds to I_1 that whenever $rTMS_1$ is applied to A_1, its activity is changed, and if this occurs then a difference in T_X performance is observed. However, this reasoning pattern does not guarantee the correctness of the conclusion that the change in A_1 activity is a cause of the difference in T_X performance, and therefore that P_X takes place in A_1. It may be the case that TMS_1 is a cause of both the change in A_1 activity and the difference in T_X performance, but the change in A_1 activity is not a cause of the difference in T_X performance. Thus, the causal inference between $rTMS_1$ to A_1 and the difference in T_X performance is stronger when the purported cause is brain stimulation but not when the purported cause is the change in brain activity, i.e., TMS causes are not analogs of neural causes. To strengthen I_4 inference one might additionally provide evidence that whenever the difference in T_X performance is observed the change in A_1 activity is present (inference 5; I_5):

H – P_X takes place in A_1
S_{1A}—$rTMS_1$ is applied to A_1
T_{XD}—a difference in T_X performance is observed (as compared to a control condition)
A_{1C}—a change in A_1 activity is present

$$I_5(((((H \wedge S_{1A}) \rightarrow T_{XD}) \wedge (S_{1A} \rightarrow T_{XD})) \wedge (((S_{1A} \rightarrow A_{1C}) \wedge S_{1A}) \rightarrow T_{XD})) \wedge (T_{XD} \rightarrow A_{1C})) \rightarrow H$$

I_5 states that the statement that P_X takes place in A_1 is true if the following two premises are true: (1) the antecedent of I_4; and (2) a change in A_1 activity is present if a difference in T_X performance is observed.

I_4 and I_5 are improvements over I_1, and I_2 and provide more confidence in TMS results. However, the limits of TMS-based conclusions also strongly depend on the complexity of the brain processes/cognitive functions investigated. The assumption that P_X takes place in A_1 may be simply inadequate because the complexity of P_X may require it to be executed by a network rather than a single area (Pessoa, 2014), i.e., a brain area determined with TMS to be "responsible" for a certain cognitive function may be necessary but not sufficient for the realization of this cognitive function. Thus, instead of focusing on the functional properties of a single brain area, often it is necessary to investigate the functional interactions between remote but interconnected brain regions (for a review of different

paradigms, see Romei et al., 2016). However, even though H might alternatively state that A_1 is partly (not fully) responsible for P_X, all the above issues related to the described inferences still hold.

In essence, the employment of neuroimaging may allow the following questions to be answered: (1) Does $rTMS_1$ applied to A_1 lead to a detectable change in A_1 activity (Siebner et al., 2000)?; (2) How big is the influence of $rTMS_1$ on areas adjacent to A_1?; (3) Which areas are functionally connected to A_1, and are they involved in P_X and/or T_X (Bestmann et al., 2005)?; (4) How does $rTMS_1$ affect connectivity between certain brain areas or networks (Gratton et al., 2013)?; (5) What is the relation between the effects of $rTMS_1$ and the other brain activations that occur during T_X?; (6) What is the relation between the effects of $rTMS_1$ and the difference in T_X performance?; and (7) Which kind of neuroplastic changes arise, and when (Poeppl et al., 2018)? These investigations might be supported by the use of effective connectivity measures (Iwabuchi et al., 2019) based on the application of causal dynamic modeling, Granger causality (Friston et al., 2013), or graph theory (Farahani et al., 2019). Additionally, novel modeling approaches that can localize cortical TMS effects might be employed to determine whether the cortical area is effectively stimulated by TMS (Weise et al., 2020). At the same time, neuroimaging evidence can include confounding activations rather than clearly represent the network responsible for the cognitive function X because: (1) TMS_1 may serve as a common cause that has several transcranial and non-transcranial consequences (Conde et al., 2019), thus some of the brain activations (including compensatory mechanisms) may be unrelated to P_X; and (2) engagement in T_X may activate processes unrelated to P_X (which can be addressed with appropriate control conditions). Therefore, determining whether observed changes in brain activity are associated more with activity change in A_1 or its adjacent areas and differentiating between network effects related to P_X and compensatory effects is both challenging. In sum, the above patterns of reasoning may still lead to false conclusions, especially if no adequate control condition is employed.

rTMS CONTROL CONDITIONS

TMS might result in various psychological, auditory, and somatosensory side effects that might trigger shifts of attention, influence alertness, or interact with elements of the experimental task. Factors like the placement of the TMS coil or the occurrence of a clicking sound can influence task performance. For example, Duecker et al. (2013) showed that lateralized sham TMS pulses caused automatic shifts of spatial attention towards the location of the TMS coil. The use of sham TMS is intended to account for the impact of active TMS's placebo and sensory side effects. The former is related to behavioral and cognitive changes (including certain expectations) that result from a person's belief that their brain is being stimulated, while the latter is related to somatosensory effects (e.g., muscle twitches), peripheral nerve stimulation, and auditory effects (perception of a clicking sound). The sham approach might induce placebo effects of different magnitude (Burke et al., 2019). The mismatch between active TMS and the sensory effects of control TMS can form participants' beliefs about the effectiveness of brain stimulation. The sham approaches can to a certain degree reproduce the sensory effects of active TMS without meaningfully influencing brain activity. They are based on the employment of either regular but tilted TMS coils, in which case, the electric field can still be sufficiently strong to result in somatosensory effects and peripheral nerve stimulation (Loo et al., 2000; Lisanby et al., 2001) or purpose-built sham TMS coils which have a magnetic shield that attenuates the electromagnetic field and prevents stimulation of the brain concurrently limiting somatosensory and peripheral nerve stimulation effects (for a review, see Duecker and Sack, 2015). To mitigate the trade-off between invoking somatosensory effects and not stimulating the brain, Duecker and Sack (2015) recommend the use of surface electrodes for skin stimulation in combination with a sham TMS coil.

However, sham TMS approaches do not demonstrate area specificity. Thus, Duecker and Sack (2015) recommend it might be beneficial to use sham TMS over each brain area where active TMS is applied to ensure that all stimulation sites have a control condition for the sensory side effects of TMS. Proper choice of control condition/s involves taking into account the difference between clinical and experimental research as well as whether and how the investigated process can be influenced by participants' beliefs. While single-blinding seems to be feasible in between-subject designs, due to distinctive TMS effects, double-blinding is difficult to perform (Broadbent et al., 2011). However, it is practiced to use the sham and active TMS coils that are indistinguishable to the researcher carrying out the stimulation, and/or this researcher is not informed about the hypothesis of the study (Basil et al., 2005). One might also minimize the placebo effect-related issues by the employment of between-subject designs (on the cost of increasing interindividual variability). Despite the chosen design, the researcher might gather from participants information on blinding success or how the TMS was experienced in a form of a short questionnaire which can further inform the study results (Flanagan et al., 2019). An alternative to the control stimulations (including active and sham TMS control strategies) might be an investigation of interindividual differences in the response to TMS measured with neuroimaging techniques and correlating them with the chosen behavioral measure.

The probabilistic strength of inferences based on experimental studies largely depends on the type of control condition used. Below, we discuss how considerations regarding control condition/s apply to TMS research designs. In general, when investigating whether P_X underlies cognitive function X, the simplest study designs consist of investigating a difference in T_X performance between pre-and post-TMS conditions or between the application of TMS1 and a sham rTMS protocol ($rTMS_0$) to the same area (Duecker and Sack, 2015).

Suppose that TMS_1 ab $rTMS_0$ protocols were applied to A_1. If a difference in TX performance is observed between $rTMS_1$ and $rTMS_0$ conditions, besides explanations based on sensory and placebo TMS effects (Duecker and Sack, 2015) there are alternative explanations that should be taken into consideration

that is related to the direct and indirect influence of TMS on: (1) the areas surrounding A_1; (2) excitability of A_2, which could be more important for executing P_X; (3) processes responsible for general cognitive functions; and (4) processes not specific to cognitive function X but to T_X execution. Given this, eliminating these possible alternative explanations should guide the designs of TMS studies.

Protocol Control

Ideally, $rTMS_0$ should account for sensory and placebo effects of $rTMS_1$ but does not cause a change in A_1 activity (Duecker and Sack, 2015). Typically used $rTMS_0$ that attempts not to influence brain activity fail to control for all the effects that are not specific to the change in A_1 activity because we might assume the ideal control should influence areas which are stimulated when A_1 is targeted with TMS to separate the consequence of the change in A_1 activity from the consequences of influencing other brain areas. For example, if an area is embedded in brain folds or lies relatively deep in the brain, then distal cortical areas which are situated above that area are affected by the electrical field, most likely more strongly (Heller and van Hulsteyn, 1992). This issue (a direct stimulation influence on the areas surrounding A_1) can be partly addressed with a control condition by diminishing the intensity of the used protocol to account for the stimulation of the areas lying above A_1, i.e., influencing cerebrospinal fluid distribution or superior areas while not reaching A_1 in a significant manner. However, it has to be taken into account that the relationship between TMS protocol intensity and its outcome might not be linear (e.g., Chung et al., 2018). Additionally, active protocols with certain frequency patterns are often classified in TMS literature as "inhibitory" or "excitatory". Thus, sometimes the protocol patterns of $rTMS_1$ and another active rTMS protocol 2 ($rTMS_2$) differ and might be commonly conceived as being inhibitory and excitatory, respectively; thus, they are used to obtain a difference in T_X performance directly (e.g., Gann et al., 2020) or to prime cortex excitability before the application of other protocols (e.g., Todd et al., 2009). It is important to note that inhibitory and excitatory rTMS properties are extrinsic to the protocol pattern and may vary depending on, e.g., protocol length, current direction, intensity, genome, and the targeted area characteristics, including its tissue excitability history and tissue excitability before protocol application (Polanía et al., 2018). Therefore, applying TMS_1 and TMS_2 separately to A_1 cannot inform what change or difference in A_1 activity is represented by a difference in T_X performance unless it is previously known how the activity of A_1 is related to the difference in T_X performance, or the change in A_1 activity was recorded with neuroimaging methods that can differentiate between an increase or a decrease of A_1 activity.

Area Control

The following, previously mentioned, issues can be addressed with a control condition that includes a control area: (1) stimulation of areas next to A_1; (2) an indirect network effect on A_2 activity that is more important for executing P_X; and (3) influence on processes responsible for more general cognitive functions than cognitive function X issue that undermine the strength of TMS-based inferences. In TMS studies, it is often assumed that an adequate control condition employs a stimulation protocol that affects an area that has the lowest possibility of playing a role in P_X or does not influence the brain at all.

For a long time, the vertex was conceived to be such a site because it was presumed that its stimulation does not affect the brain at all. Nonetheless, several years ago it was shown that the blood oxygen level-dependent (BOLD) signal decreases in the default mode network after applying 1 Hz rTMS to the vertex, and this is not accompanied by any significant BOLD increases throughout the brain (Jung et al., 2016). The authors concluded that this supports the use of vertex simulation as a control condition. However, such a conclusion is problematic for several reasons. First, it presumes that an increase in the BOLD signal, which determines which parts of the brain are most active, will be observed after the application of a protocol that predominantly acts in an inhibitory manner (Fitzgerald et al., 2002). Second, there is an assumption that a decrease in the BOLD signal cannot indicate a change in neuronal activity (which could represent an increase in the activity of inhibitory neurons). Also, distinctly increasing and decreasing neuronal activity in an area is not equivalent to improving and impairing a cognitive function that depends on this area. Some brain processes require a decrease in local brain activity, e.g., deactivation has often been observed in the hippocampus during encoding and retrieval tasks believed to recruit this brain structure (Axmacher et al., 2009). Third, there is an assumption that the adequate control area is the one with the lowest possibility of affecting P_X. Targeting A_2 (an area which is not anticipated to carry out P_X) does not confirm the specificity of A_1 for carrying out P_X, i.e., that P_X is carried out exclusively in A_1. Since the evidence in favor of the specificity of A_1 is based on inductive reasoning, in theory, it would be required to effectively stimulate all brain areas to conclude that A_1 and only A_1 is responsible for P_X. Conceivably, an opposite approach should be adopted: adequate control for the site requires the selection of a control site that has a high probability of influencing P_X. However, this approach is challenged by consideration of possible indirect network influences on A_1 due to the possibility of the control site's involvement in processes interacting with P_X. Furthermore, assume that P_X requires activation in areas A_1 and A_2. When a difference in T_X performance between the conditions with $rTMS_1$ to A_1 and $rTMS_1$ to A_2 is analyzed and $rTMS_1$ in the first condition resulted in impairment of T_X performance but in the second condition resulted in improvement of T_X performance, one might erroneously conclude that only one area is crucial for X. Similarly, if $rTMS_1$ in both conditions influenced T_X performance in the same manner, one might erroneously conclude that $rTMS_1$ was ineffective. Thus, limiting control conditions to area control might be not sufficient to adequately explain the TMS effect.

Task Control

The issues of influencing processes responsible for more general cognitive functions rather than cognitive function X and influencing processes specific to T_X but not to cognitive function X, both of which weaken the strength of TMS-based inferences,

can be addressed with task control. Dissociations may help reduce the probability of drawing erroneous conclusions on the neural bases of cognitive functions (Machery, 2012). To solve complex issues regarding certain cognitive functions or to include a task control condition in a study, e.g., to demonstrate that a certain brain area is selectively engaged in the execution of P_X but not in the execution of the neuronal process that underlies a different cognitive function Y (P_Y), rTMS can be employed to determine whether the neural underpinnings of cognitive functions X and Y differ. In this case, inferences can be based on a single dissociation that is observed whenever TMS influences T_X and influences T_Y to a lesser extent. This may lead to the conclusion that A_1 plays a role in P_X but not P_Y.

However, the results of studies employing task control may still be confounded by the confounds already mentioned. Additionally, the following confounds might be present: (1) a task that taps into one of two processes (T_X into P_X) might be less sensitive than a task that taps into another one (T_Y into P_Y); (2) due to its characteristics, P_X might be more difficult to measure than P_Y; (3) the relative difficulties of T_X and T_Y are likely to require a different amount of available cognitive resources (e.g., memory, attention); (4) when cognitive resources are limited, different brain networks may be engaged in T_X or T_Y execution than when they are available; and (5) a discrepancy between how T_X and T_Y engage A_1 and A_2 can be observed, even when they recruit the same area or network, e.g., carrying out T_X may require a decrease in A_1 activity, while carrying out T_Y may require an increase in A_1 activity. In all the above circumstances, it would be erroneous to conclude with certainty that cognitive functions X and Y are based on two distinct brain substrates. The solution may consist of designs that combine different control approaches and allow double dissociation (Dunn and Kirsner, 2003), e.g., T_X but not T_Y performance is impaired when $rTMS_0$ application and $rTMS_1$ application outcomes are compared after stimulation to A_1, while T_Y but not T_X performance is impaired when the $rTMS_0$ and $rTMS_1$ outcomes are compared after stimulation to A_2. In the case of an uncrossed double dissociation, a difference in T_X performance and a difference in T_Y performance is observed when A_1 condition and A_2 condition are compared (when pre-and post- $rTMS_1$ or $rTMS_1$ and $rTMS_0$ are compared) but one condition is associated with higher performance in both tasks. A cross-over double dissociation is observed when $rTMS_1$ to A_1 influences T_X performance more than $rTMS_1$ to A_2, and $rTMS_1$ to A_2 influences T_Y performance more than $rTMS_1$ to A_1 (for a summary of the solutions that aim to control for TMS confounds, see **Figure 2**).

Can it then be concluded that P_X takes place in A_1 while P_Y takes place in A_2? Unfortunately, most of the mentioned confounds also apply to double dissociations (e.g., $rTMS_1$ to A_1 reduces the available cognitive resources to T_X, while S_2 to A_2 reduces them to T_Y). In the case of uncrossed double dissociations, the additional confound may be that the task demand function for A_1 increases monotonically, while the task demand function for A_2 is U-shaped: A_2 is more active when a task requires fewer or more cognitive resources. In such circumstances, if T_X and T_Y recruit a single process whose neural correlate includes A_1 and A_2, for A_1 the greater task demands may correspond to the increase in its activity, while for A_2 the greater task demands can correspond to its inactivation. Such an issue can be avoided when a cross-over double dissociation is observed, but the following confounds may still be present: (1) neuroplasticity-like effects occur at a different rate in A_1 and A_2 (e.g., depending on the type of brain cells affected by the stimulation); (2) $rTMS_1$ and $rTMS_2$ protocols applied to different areas may differently influence excitability in these areas; (3) an increase in A_1 excitability results in a decrease in A_2 activity, which is necessary to perform T_Y, while an increase in A_2 excitability results in inactivation of A_1, which is the area necessary to perform T_X; (4) the execution of P_X may correspond to A_1 activity increase while the execution of P_Y may correspond to A_1 inactivation; and (5) both A_1 and A_2 are recruited depending on the available cognitive resources, and the processes recruited when the amount of available resources is greater differ from the processes recruited when fewer resources are available. In all the above circumstances, it would be premature to conclude with certainty that cognitive functions X and Y are based on two distinct brain substrates.

In certain types of research (mostly preclinical and clinical studies), rTMS effects might be studied using longitudinal designs. The effect of longitudinal rTMS studies can be long-lasting, thus they can be used to investigate stable neuroplastic changes and determine whether the observed rTMS effect consistently arises over the time course of a study (Auriat et al., 2015). They also reduce the erroneous identification of side effect-associated changes as the brain stimulation effect, and they enable the employment of multiple testing measures. Similar to single-session rTMS effects, the rTMS effects in longitudinal studies might be related to individual excitability of brain areas, but they are less prone to the influence of day-to-day fluctuations in cortex excitability (Huber et al., 2013). However, there is still a possibility that the long-term effects of neuroplasticity in longitudinal studies might be related to placebo effects or be influenced by confounding factors that occur over the time course of the study.

CONCLUSIONS

TMS has traditionally been used to provide evidence for functional brain specialization. Nevertheless—as has been getting clearer over the past two decades—the application of rTMS alone does not allow causal inferences to be drawn on neural causes without additional assumptions. A change in the execution of an experimental task might be a consequence of rTMS but at the same time not a consequence of a change in the excitability of a targeted area. However, this might be avoided when: (1) the research question is grounded in previous research and accounts for the complexity of the investigated cognitive function; (2) neuroimaging/neurophysiological techniques are employed to monitor the direct and indirect influence of rTMS; and (3) more than one control condition is employed in a single experiment to reduce the number of possible interpretations. On one hand, functional neuroimaging could make it possible to determine whether the process responsible for the investigated

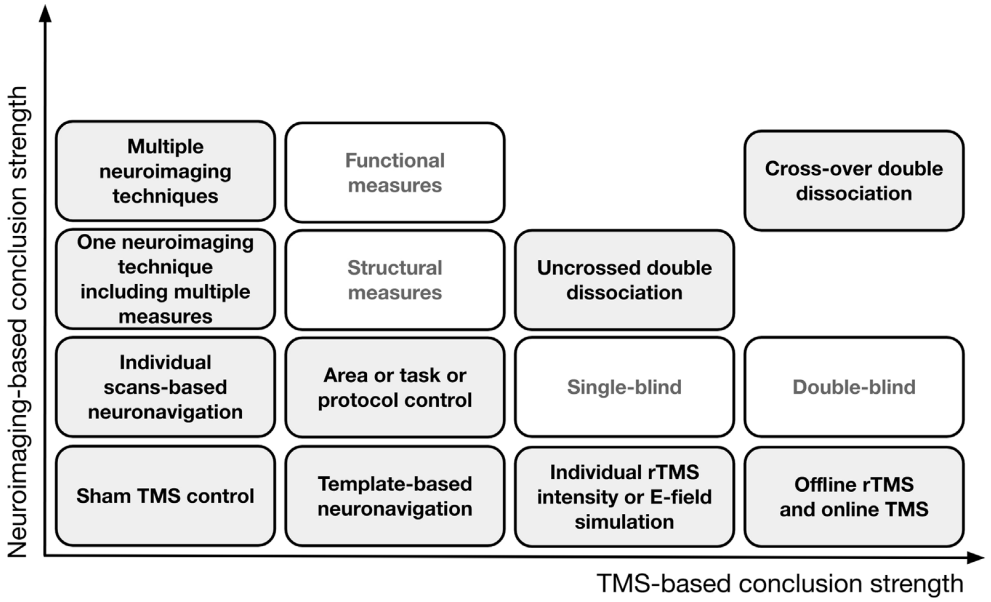

FIGURE 2 | A theoretical representation of the solutions that aim to control for confounds in TMS research and improve the logical strength of the premises behind the conclusions. On the horizontal axis, progress in TMS-based conclusion strength is depicted when only TMS is employed; the vertical axis represents conclusion strength when neuroimaging is involved.

cognitive function has local or network characteristics and can be used to study the spread of TMS effects throughout the brain networks. On the other hand, confounding factors of neuronal correlates of investigated cognitive processes need to be addressed within each TMS-neuroimaging study. Although TMS has been proven to be a very effective brain stimulation method, its characteristic features have to be considered in reasoning based on its employment. In this article, we have clarified the difference between the causal effects of TMS and structure-related causal effects, and we have pointed out that the latter can be divided into direct and network effects. We have also outlined issues related to TMS-based inferences. Taking them into account requires limiting the extent of TMS-based reasoning but at the same time may support analysis of possible confounds and improve research designs to alleviate these confounds. Although the aforementioned issues are often addressed by experts in the field of non-invasive brain stimulation, we hope that the presented summary and theoretical analysis will help researchers who are developing the field of human-neuroscience based on TMS-based inferences. Even though rTMS without neuroimaging cannot unequivocally prove structure-related causal claims concerning direct relations between brain processes carried out in certain areas and certain behaviors/cognitive functions, it might be used for probabilistic statements about causal influences if its limitations are kept in mind. The fact that combining rTMS with neuroimaging techniques allows stronger inferences to be made does not imply that one should use rTMS only in combination with neuroimaging or/and multiple control conditions. The need for neuroimaging or/and multiple control conditions depends on the research question guiding the study and how its results are intended to be interpreted. There is a trade-off between the inferential limit and experimental feasibility; therefore, when feasible, combining rTMS with neuroimaging, multiple control conditions, and/or perturbational TMS is recommended and might provide further support for conclusions regarding experimental outcomes.

AUTHOR CONTRIBUTIONS

JH drafted the manuscript. MK, KS, and MW suggested changes and provided comments on the manuscript. JH improved the manuscript. All authors contributed to the article and approved the submitted version.

FUNDING

This work was supported by the National Science Centre, Poland under grants HARMONIA (2014/14/M/HS6/00911) and OPUS [2017/27/B/HS6/00937] given to MW and grant SONATA (2015/17/D/HS1/01705) given to MK. The publication was funded by the Priority Research Area Society of the Future under the program "Excellence Initiative—Research University" at the Jagiellonian University in Krakow.

ACKNOWLEDGMENTS

We thank Borysaw Paulewicz for providing comments on our manuscript and Michael Timberlake for proofreading. This article is based upon work from COST Action CA18106, supported by COST (European Cooperation in Science and Technology).

REFERENCES

Abler, B., Walter, H., Wunderlich, A., Grothe, J., Schönfeldt-Lecuona, C., Spitzer, M., et al. (2005). Side effects of transcranial magnetic stimulation biased task performance in a cognitive neuroscience study. *Brain Topogr.* 17, 193–196. doi: 10.1007/s10548-005-6028-y

Andoh, J., and Martinot, J.-L. (2008). Interhemispheric compensation: a hypothesis of TMS-induced effects on language-related areas. *Eur. Psychiatry* 23, 281–288. doi: 10.1016/j.eurpsy.2007.10.012

Auriat, A. M., Neva, J. L., Peters, S., Ferris, J. K., and Boyd, L. A. (2015). A review of transcranial magnetic stimulation and multimodal neuroimaging to characterize post-stroke neuroplasticity. *Front. Neurol.* 6:226. doi: 10.3389/fneur.2015.00226

Axmacher, N., Elger, C. E., and Fell, J. (2009). The specific contribution of neuroimaging versus neurophysiological data to understanding cognition. *Behav. Brain Res.* 200, 1–6. doi: 10.1016/j.bbr.2009.01.028

Barker, A. T., Jalinous, R., and Freeston, I. L. (1985). Non-invasive magnetic stimulation of human motor cortex. *Lancet* 1, 1106–1107. doi: 10.1016/s0140-6736(85)92413-4

Basil, B., Mahmud, J., Mathews, M., Rodriguez, C., and Adetunji, B. (2005). Is there evidence for effectiveness of transcranial magnetic stimulation in the treatment of psychiatric disorders? *Psychiatry* 2, 64–69.

Bergmann, T. O., Karabanov, A., Hartwigsen, G., Thielscher, A., and Siebner, H. R. (2016). Combining non-invasive transcranial brain stimulation with neuroimaging and electrophysiology: current approaches and future perspectives. *NeuroImage* 140, 4–19. doi: 10.1016/j.neuroimage.2016.02.012

Bestmann, S., Baudewig, J., Siebner, H. R., Rothwell, J. C., and Frahm, J. (2003). Subthreshold high-frequency TMS of human primary motor cortex modulates interconnected frontal motor areas as detected by interleaved fMRI-TMS. *NeuroImage* 20, 1685–1696. doi: 10.1016/j.neuroimage.2003.07.028

Bestmann, S., Baudewig, J., Siebner, H. R., Rothwell, J. C., and Frahm, J. (2005). BOLD MRI responses to repetitive TMS over human dorsal premotor cortex. *NeuroImage* 28, 22–29. doi: 10.1016/j.neuroimage.2005.05.027

Bestmann, S., Ruff, C. C., Blankenburg, F., Weiskopf, N., Driver, J., and Rothwell, J. C. (2008a). Mapping causal interregional influences with concurrent TMS-fMRI. *Exp. Brain Res.* 191, 383–402. doi: 10.1007/s00221-008-1601-8

Bestmann, S. R., Ruff, C. C., Driver, J., and Blankenburg, F. (2008b). "Concurrent TMS and functional magnetic resonance imaging: methods and current advances," in *Oxford Handbook of Transcranial Stimulation*, eds E. Wasserman, C. Epstein and U. Ziemann (Oxford, UK: Oxford University Press), 569–592.

Bestmann, S., Swayne, O., Blankenburg, F., Ruff, C. C., Haggard, P., Weiskopf, N., et al. (2008c). Dorsal premotor cortex exerts state-dependent causal influences on activity in contralateral primary motor and dorsal premotor cortex. *Cereb. Cortex* 18, 1281–1291. doi: 10.1093/cercor/bhm159

Beynel, L., Powers, J. P., and Appelbaum, L. G. (2020). Effects of repetitive transcranial magnetic stimulation on resting-state connectivity: a systematic review. *NeuroImage* 211:116596. doi: 10.1016/j.neuroimage.2020.116596

Bijsterbosch, J. D., Barker, A. T., Lee, K.-H., and Woodruff, P. W. R. (2012). Where does transcranial magnetic stimulation (TMS) stimulate? Modelling of induced field maps for some common cortical and cerebellar targets. *Med. Biol. Eng. Comput.* 50, 671–681. doi: 10.1007/s11517-012-0922-8

Blankenburg, F., Ruff, C. C., Bestmann, S., Bjoertomt, O., Eshel, N., Josephs, O., et al. (2008). Interhemispheric effect of parietal TMS on somatosensory response confirmed directly with concurrent TMS-fMRI. *J. Neurosci.* 28, 13202–13208. doi: 10.1523/JNEUROSCI.3043-08.2008

Bolognini, N., and Ro, T. (2010). Transcranial magnetic stimulation: disrupting neural activity to alter and assess brain function. *J. Neurosci.* 30, 9647–9650. doi: 10.1523/JNEUROSCI.1990-10.2010

Bor, D., Schwartzman, D. J., Barrett, A. B., and Seth, A. K. (2017). Theta-burst transcranial magnetic stimulation to the prefrontal or parietal cortex does not impair metacognitive visual awareness. *PLoS One* 12:e0171793. doi: 10.1371/journal.pone.0171793

Bourgeois, A., Chica, A. B., Valero-Cabré, A., and Bartolomeo, P. (2013). Cortical control of Inhibition of Return: exploring the causal contributions of the left parietal cortex. *Cortex* 49, 2927–2934. doi: 10.1016/j.cortex.2013.08.004

Broadbent, H. J., van den Eynde, F., Guillaume, S., Hanif, E. L., Stahl, D., David, A. S., et al. (2011). Blinding success of rTMS applied to the dorsolateral prefrontal cortex in randomised sham-controlled trials: a systematic review. *The World Journal of Biological Psychiatry: The Official Journal of the World Federation of Societies of Biological Psychiatry* 12, 240–248. doi: 10.3109/15622975.2010.541281

Burke, M. J., Kaptchuk, T. J., and Pascual-Leone, A. (2019). Challenges of differential placebo effects in contemporary medicine: the example of brain stimulation. *Ann. Neurol.* 85, 12–20. doi: 10.1002/ana.25387

Busan, P., Barbera, C., Semenic, M., Monti, F., Pizzolato, G., Pelamatti, G., et al. (2009). Effect of transcranial magnetic stimulation (TMS) on parietal and premotor cortex during planning of reaching movements. *PLoS One* 4:e4621. doi: 10.1371/journal.pone.0004621

Capotosto, P., Babiloni, C., Romani, G. L., and Corbetta, M. (2012). Differential contribution of right and left parietal cortex to the control of spatial attention: a simultaneous EEG-rTMS study. *Cereb. Cortex* 22, 446–454. doi: 10.1093/cercor/bhr127

Cappelletti, M., Muggleton, N., and Walsh, V. (2009). Quantity without numbers and numbers without quantity in the parietal cortex. *NeuroImage* 46, 522–529. doi: 10.1016/j.neuroimage.2009.02.016

Carmel, D., Walsh, V., Lavie, N., and Rees, G. (2010). A causal role for right parietal cortex in binocular rivalry demonstrated with TMS. *J. Vision* 8:790. doi: 10.1167/8.6.790

Choi, K. M., Choi, S.-H., Lee, S. M., Jang, K.-I., and Chae, J.-H. (2019). Three weeks of rTMS treatment maintains clinical improvement but not electrophysiological changes in patients with depression: a 6-week follow-up pilot study. *Front. Psychiatry* 10:351. doi: 10.3389/fpsyt.2019.00351

Choi, K. M., Jang, K.-M., Jang, K. I., Um, Y. H., Kim, M.-S., Kim, D.-W., et al. (2014). The effects of 3 weeks of rTMS treatment on P200 amplitude in patients with depression. *Neurosci. Lett.* 577, 22–27. doi: 10.1016/j.neulet.2014.06.003

Chung, S. W., Rogasch, N. C., Hoy, K. E., and Fitzgerald, P. B. (2015). Measuring brain stimulation induced changes in cortical properties using TMS-EEG. *Brain Stimul.* 8, 1010–1020. doi: 10.1016/j.brs.2015.07.029

Chung, S. W., Rogasch, N. C., Hoy, K. E., Sullivan, C. M., Cash, R. F. H., and Fitzgerald, P. B. (2018). Impact of different intensities of intermittent theta burst stimulation on the cortical properties during TMS-EEG and working memory performance. *Hum. Brain Mapp.* 39, 783–802. doi: 10.1002/hbm.23882

Conde, V., Tomasevic, L., Akopian, I., Stanek, K., Saturnino, G. B., Thielscher, A., et al. (2019). The non-transcranial TMS-evoked potential is an inherent source of ambiguity in TMS-EEG studies. *NeuroImage* 185, 300–312. doi: 10.1016/j.neuroimage.2018.10.052

de Graaf, T. A., Jacobs, C., Roebroeck, A., and Sack, A. T. (2009). FMRI effective connectivity and TMS chronometry: complementary accounts of causality in the visuospatial judgment network. *PLoS One* 4:e8307. doi: 10.1371/journal.pone.0008307

de Graaf, T. A., and Sack, A. T. (2011). Null results in TMS: from absence of evidence to evidence of absence. *Neurosci. Biobehav. Rev.* 35, 871–877. doi: 10.1016/j.neubiorev.2010.10.006

Deng, Z.-D., Lisanby, S. H., and Peterchev, A. V. (2013). Electric field depth-focality tradeoff in transcranial magnetic stimulation: simulation comparison of 50 coil designs. *Brain Stimul.* 6, 1–13. doi: 10.1016/j.brs.2012.02.005

De Ridder, D., De Mulder, G., Verstraeten, E., Sunaert, S., and Moller, A. (2007). Somatosensory cortex stimulation for deafferentation pain. *Acta Neurochir. Suppl.* 97, 67–74. doi: 10.1007/978-3-211-33081-4_8

Downar, J., Blumberger, D. M., and Daskalakis, Z. J. (2016). The neural crossroads of psychiatric illness: an emerging target for brain stimulation. *Trends Cogn. Sci.* 20, 107–120. doi: 10.1016/j.tics.2015.10.007

Duecker, F., de Graaf, T. A., Jacobs, C., and Sack, A. T. (2013). Time- and task-dependent non-neural effects of real and sham TMS. *PLoS One* 8:e73813. doi: 10.1371/journal.pone.0073813

Duecker, F., and Sack, A. T. (2015). Rethinking the role of sham TMS. *Front. Psychol.* 6:210. doi: 10.3389/fpsyg.2015.00210

Dunn, J. C., and Kirsner, K. (2003). What can we infer from double dissociations? *Cortex* 39, 1–7. doi: 10.1016/s0010-9452(08)70070-4

Farahani, F. V., Karwowski, W., and Lighthall, N. R. (2019). Application of graph theory for identifying connectivity patterns in human brain networks: a systematic review. *Front. Neurosci.* 13:585. doi: 10.3389/fnins.2019.00585

Fitzgerald, P. B., Brown, T. L., Daskalakis, Z. J., Chen, R., and Kulkarni, J. (2002). Intensity-dependent effects of 1 Hz rTMS on human corticospinal excitability. *Clin. Neurophysiol.* 113, 1136–1141. doi: 10.1016/s1388-2457(02)00145-1

Flanagan, S. D., Beethe, A. Z., Eagle, S. R., Proessl, F., Connaboy, C., Dunn-Lewis, C., et al. (2019). Blinding success of sham-controlled motor cortex intermittent theta burst stimulation based on participant perceptions. *Brain Stimul.* 12, 1058–1060. doi: 10.1016/j.brs.2019.03.004

Friston, K., Moran, R., and Seth, A. K. (2013). Analysing connectivity with Granger causality and dynamic causal modelling. *Curr. Opin. Neurobiol.* 23, 172–178. doi: 10.1016/j.conb.2012.11.010

Furubayashi, T., Mochizuki, H., Terao, Y., Arai, N., Hanajima, R., Hamada, M., et al. (2013). Cortical hemoglobin concentration changes underneath the coil after single-pulse transcranial magnetic stimulation: a near-infrared spectroscopy study. *J. Neurophysiol.* 109, 1626–1637. doi: 10.1152/jn.00980.2011

Gann, M. A., King, B. R., Dolfen, N., Veldman, M. P., Chan, K. L., Puts, N. A. J., et al. (2020). Hippocampal and striatal responses during motor learning are modulated by prefrontal cortex stimulation. *bioRxiv* [Preprint]. doi: 10.1101/2020.06.05.136531

Ghabra, M. B., Hallett, M., and Wassermann, E. M. (1999). Simultaneous repetitive transcranial magnetic stimulation does not speed fine movement in PD. *Neurology* 52, 768–770. doi: 10.1212/wnl.52.4.768

Gratton, C., Lee, T. G., Nomura, E. M., and D'Esposito, M. (2013). The effect of theta-burst TMS on cognitive control networks measured with resting state fMRI. *Front. Syst. Neurosci.* 7:124. doi: 10.3389/fnsys.2013.00124

Hannula, H., and Ilmoniemi, R. J. (2017). "Basic principles of navigated TMS," in *Navigated Transcranial Magnetic Stimulation in Neurosurgery*, ed S. M. Krieg (Cham: Springer), 3–29. doi: 10.1007/978-3-319-54918-7_1

Hartwigsen, G. (2015). The neurophysiology of language: insights from non-invasive brain stimulation in the healthy human brain. *Brain Lang.* 148, 81–94. doi: 10.1016/j.bandl.2014.10.007

Hayward, G., Mehta, M. A., Harmer, C., Spinks, T. J., Grasby, P. M., and Goodwin, G. M. (2007). Exploring the physiological effects of double-cone coil TMS over the medial frontal cortex on the anterior cingulate cortex: an H215O PET study. *Eur. J. Neurosci.* 25, 2224–2233. doi: 10.1111/j.1460-9568.2007.05430.x

Heller, L., and van Hulsteyn, D. B. (1992). Brain stimulation using electromagnetic sources: theoretical aspects. *Biophys. J.* 63, 129–138. doi: 10.1016/S0006-3495(92)81587-4

Hill, A. B. (1965). The environment and disease: association or causation? *Proc. R. Soc. Med.* 58, 295–300.

Holmes, N. P., and Meteyard, L. (2018). Subjective discomfort of TMS predicts reaction times differences in published studies. *Front. Psychol.* 9:1989. doi: 10.3389/fpsyg.2018.01989

Huang, Y.-Z., Edwards, M. J., Rounis, E., Bhatia, K. P., and Rothwell, J. C. (2005). Theta burst stimulation of the human motor cortex. *Neuron* 45, 201–206. doi: 10.1016/j.neuron.2004.12.033

Huber, R., Mäki, H., Rosanova, M., Casarotto, S., Canali, P., Casali, A. G., et al. (2013). Human cortical excitability increases with time awake. *Cereb. Cortex* 23, 332–338. doi: 10.1093/cercor/bhs014

Iwabuchi, S. J., Auer, D. P., Lankappa, S. T., and Palaniyappan, L. (2019). Baseline effective connectivity predicts response to repetitive transcranial magnetic stimulation in patients with treatment-resistant depression. *Eur. Neuropsychopharmacol.* 29, 681–690. doi: 10.1016/j.euroneuro.2019.02.012

Izuma, K., Akula, S., Murayama, K., Wu, D.-A., Iacoboni, M., and Adolphs, R. (2015). A causal role for posterior medial frontal cortex in choice-induced preference change. *J. Neurosci.* 35, 3598–3606. doi: 10.1523/JNEUROSCI.4591-14.2015

Jung, J., Bungert, A., Bowtell, R., and Jackson, S. R. (2016). Vertex stimulation as a control site for transcranial magnetic stimulation: a concurrent TMS/fMRI study. *Brain Stimul.* 9, 58–64. doi: 10.1016/j.brs.2015.09.008

Jung, N. H., Delvendahl, I., Kuhnke, N. G., Hauschke, D., Stolle, S., and Mall, V. (2010). Navigated transcranial magnetic stimulation does not decrease the variability of motor-evoked potentials. *Brain Stimul.* 3, 87–94. doi: 10.1016/j.brs.2009.10.003

Kang, J. I., Lee, H., Jhung, K., Kim, K. R., An, S. K., Yoon, K.-J., et al. (2016). Frontostriatal connectivity changes in major depressive disorder after repetitive transcranial magnetic stimulation: a randomized sham-controlled study. *J. Clin. Psychiatry* 77, e1137–e1143. doi: 10.4088/JCP.15m10110

Karabanov, A., Ziemann, U., Hamada, M., George, M. S., Quartarone, A., Classen, J., et al. (2015). Consensus paper: probing homeostatic plasticity of human cortex with non-invasive transcranial brain stimulation. *Brain Stimul.* 8, 442–454. doi: 10.1016/j.brs.2015.01.404

Lefaucheur, J.-P., Aleman, A., Baeken, C., Benninger, D. H., Brunelin, J., Di Lazzaro, V., et al. (2020). Evidence-based guidelines on the therapeutic use of repetitive transcranial magnetic stimulation (rTMS): an update (2014–2018). *Clin. Neurophysiol.* 131, 474–528. doi: 10.1016/j.clinph.2019.11.002

Li, X., Nahas, Z., Kozel, F. A., Anderson, B., Bohning, D. E., and George, M. S. (2004). Acute left prefrontal transcranial magnetic stimulation in depressed patients is associated with immediately increased activity in prefrontal cortical as well as subcortical regions. *Biol. Psychiatry* 55, 882–890. doi: 10.1016/j.biopsych.2004.01.017

Lisanby, S. H., Gutman, D., Luber, B., Schroeder, C., and Sackeim, H. A. (2001). Sham TMS: intracerebral measurement of the induced electrical field and the induction of motor-evoked potentials. *Biol. Psychiatry* 49, 460–463. doi: 10.1016/s0006-3223(00)01110-0

Loo, C. K., Taylor, J. L., Gandevia, S. C., McDarmont, B. N., Mitchell, P. B., and Sachdev, P. S. (2000). Transcranial magnetic stimulation (TMS) in controlled treatment studies: are some "sham" forms active? *Biol. Psychiatry* 47, 325–331. doi: 10.1016/s0006-3223(99)00285-1

Machery, E. (2012). Dissociations in neuropsychology and cognitive neuroscience. *Philos. Sci.* 79, 490–518. doi: 10.1086/668002

Massimini, M., Ferrarelli, F., Huber, R., Esser, S. K., Singh, H., and Tononi, G. (2005). Breakdown of cortical effective connectivity during sleep. *Science* 309, 2228–2232. doi: 10.1126/science.1117256

Montefinese, M., Turco, C., Piccione, F., and Semenza, C. (2017). Causal role of the posterior parietal cortex for two-digit mental subtraction and addition: a repetitive TMS study. *NeuroImage* 155, 72–81. doi: 10.1016/j.neuroimage.2017.04.058

Pearl, J. (2000). *Causality: Models, Reasoning, and Inference.* New York, NY: Cambridge University Press.

Pessoa, L. (2014). Understanding brain networks and brain organization. *Phys. Life Rev.* 11, 400–435. doi: 10.1016/j.plrev.2014.03.005

Philiastides, M. G., Auksztulewicz, R., Heekeren, H. R., and Blankenburg, F. (2011). Causal role of dorsolateral prefrontal cortex in human perceptual decision making. *Curr. Biol.* 21, 980–983. doi: 10.1016/j.cub.2011.04.034

Poeppl, T. B., Langguth, B., Lehner, A., Frodl, T., Rupprecht, R., Kreuzer, P. M., et al. (2018). Brain stimulation-induced neuroplasticity underlying therapeutic response in phantom sounds. *Hum. Brain Mapp.* 39, 554–562. doi: 10.1002/hbm.23864

Polanía, R., Nitsche, M. A., and Ruff, C. C. (2018). Studying and modifying brain function with non-invasive brain stimulation. *Nat. Neurosci.* 21, 174–187. doi: 10.1038/s41593-017-0054-4

Pollatos, O., Herbert, B. M., Mai, S., and Kammer, T. (2016). Changes in interoceptive processes following brain stimulation. *Philos. Trans. R. Soc. B Biol. Sci.* 371:20160016. doi: 10.1098/rstb.2016.0016

Poulet, E., Brunelin, J., Boeuve, C., Lerond, J., D'Amato, T., Dalery, J., et al. (2004). Repetitive transcranial magnetic stimulation does not potentiate antidepressant treatment. *Eur. Psychiatry* 19, 382–383. doi: 10.1016/j.eurpsy.2004.06.021

Reithler, J., Peters, J. C., and Sack, A. T. (2011). Multimodal transcranial magnetic stimulation: using concurrent neuroimaging to reveal the neural network dynamics of noninvasive brain stimulation. *Prog. Neurobiol.* 94, 149–165. doi: 10.1016/j.pneurobio.2011.04.004

Robertson, E. M., Théoret, H., and Pascual-Leone, A. (2003). Studies in cognition: the problems solved and created by transcranial magnetic stimulation. *J. Cogn. Neurosci.* 15, 948–960. doi: 10.1162/089892903770007344

Romei, V., Thut, G., and Silvanto, J. (2016). Information-based approaches of noninvasive transcranial brain stimulation. *Trends Neurosci.* 39, 782–795. doi: 10.1016/j.tins.2016.09.001

Rossi, S., Innocenti, I., Polizzotto, N. R., Feurra, M., De Capua, A., Ulivelli, M., et al. (2011). Temporal dynamics of memory trace formation in the human prefrontal cortex. *Cereb. Cortex* 21, 368–373. doi: 10.1093/cercor/bhq103

Roth, Y., Amir, A., Levkovitz, Y., and Zangen, A. (2007). Three-dimensional distribution of the electric field induced in the brain by transcranial magnetic stimulation using figure-8 and deep H-coils. *J. Clin. Neurophysiol.* 24, 31–38. doi: 10.1097/WNP.0b013e31802fa393

Ruff, C. C., Bestmann, S., Blankenburg, F., Bjoertomt, O., Josephs, O., Weiskopf, N., et al. (2008). Distinct causal influences of parietal versus frontal areas on human visual cortex: evidence from concurrent TMS-fMRI. *Cereb. Cortex* 18, 817–827. doi: 10.1093/cercor/bhm128

Ruff, C. C., Driver, J., and Bestmann, S. (2009). Combining TMS and fMRI: from "virtual lesions" to functional-network accounts of cognition. *Cortex* 45, 1043–1049. doi: 10.1016/j.cortex.2008.10.012

Sack, A. T. (2006). Transcranial magnetic stimulation, causal structure-function mapping and networks of functional relevance. *Curr. Opin. Neurobiol.* 16, 593–599. doi: 10.1016/j.conb.2006.06.016

Salillas, E., Basso, D., Baldi, M., Semenza, C., and Vecchi, T. (2009). Motion on numbers: transcranial magnetic stimulation on the ventral intraparietal sulcus alters both numerical and motion processes. *J. Cogn. Neurosci.* 21, 2129–2138. doi: 10.1162/jocn.2008.21157

Schaal, N. K., Williamson, V. J., Kelly, M., Muggleton, N. G., Pollok, B., Krause, V., et al. (2015). A causal involvement of the left supramarginal gyrus during the retention of musical pitches. *Cortex* 64, 310–317. doi: 10.1016/j.cortex.2014.11.011

Schutter, D. J. L. G., Van Honk, J., and Panksepp, J. (2004). Introducing transcranial magnetic stimulation (TMS) and its property of causal inference in investigating brain–function relationships. *Synthese* 141, 155–173. doi: 10.1023/b:synt.0000042951.25087.16

Siebner, H. R., Filipovic, S. R., Rowe, J. B., Cordivari, C., Gerschlager, W., Rothwell, J. C., et al. (2003). Patients with focal arm dystonia have increased sensitivity to slow-frequency repetitive TMS of the dorsal premotor cortex. *Brain* 126, 2710–2725. doi: 10.1093/brain/awg282

Siebner, H. R., Hartwigsen, G., Kassuba, T., and Rothwell, J. C. (2009). How does transcranial magnetic stimulation modify neuronal activity in the brain? Implications for studies of cognition. *Cortex* 45, 1035–1042. doi: 10.1016/j.cortex.2009.02.007

Siebner, H. R., Peller, M., Willoch, F., Minoshima, S., Boecker, H., Auer, C., et al. (2000). Lasting cortical activation after repetitive TMS of the motor cortex: a glucose metabolic study. *Neurology* 54, 956–963. doi: 10.1212/wnl.54.4.956

Siebner, H. R., and Rothwell, J. (2003). Transcranial magnetic stimulation: new insights into representational cortical plasticity. *Exp. Brain Res.* 148, 1–16. doi: 10.1007/s00221-002-1234-2

Siuda-Krzywicka, K., Bola, Ł., Paplińska, M., Sumera, E., Jednoróg, K., Marchewka, A., et al. (2016). Massive cortical reorganization in sighted Braille readers. *eLife* 5:e10762. doi: 10.7554/eLife.10762

Śliwińska, M. W., Vitello, S., and Devlin, J. T. (2014). Transcranial magnetic stimulation for investigating causal brain-behavioral relationships and their time course. *J. Vis. Exp.* 89:51735. doi: 10.3791/51735

Speer, A. M., Benson, B. E., Kimbrell, T. K., Wassermann, E. M., Willis, M. W., Herscovitch, P., et al. (2009). Opposite effects of high and low frequency rTMS on mood in depressed patients: relationship to baseline cerebral activity on PET. *J. Affect. Disord.* 115, 386–394. doi: 10.1016/j.jad.2008.10.006

Speer, A. M., Kimbrell, T. A., Wassermann, E. M., Repella, J. D., Willis, M. W., Herscovitch, P., et al. (2000). Opposite effects of high and low frequency rTMS on regional brain activity in depressed patients. *Biol. Psychiatry* 48, 1133–1141. doi: 10.1016/s0006-3223(00)01065-9

Strafella, A. P., Paus, T., Fraraccio, M., and Dagher, A. (2003). Striatal dopamine release induced by repetitive transcranial magnetic stimulation of the human motor cortex. *Brain* 126, 2609–2615. doi: 10.1093/brain/awg268

Thickbroom, G. W. (2007). Transcranial magnetic stimulation and synaptic plasticity: experimental framework and human models. *Exp. Brain Res.* 180, 583–593. doi: 10.1007/s00221-007-0991-3

Thut, G., and Pascual-Leone, A. (2010). A review of combined TMS-EEG studies to characterize lasting effects of repetitive TMS and assess their usefulness in cognitive and clinical neuroscience. *Brain Topogr.* 22, 219–232. doi: 10.1007/s10548-009-0115-4

Todd, G., Flavel, S. C., and Ridding, M. C. (2009). Priming theta-burst repetitive transcranial magnetic stimulation with low- and high-frequency stimulation. *Exp. Brain Res.* 195, 307–315. doi: 10.1007/s00221-009-1791-8

Valdes-Sosa, P. A., Roebroeck, A., Daunizeau, J., and Friston, K. (2011). Effective connectivity: influence, causality and biophysical modeling. *NeuroImage* 58, 339–361. doi: 10.1016/j.neuroimage.2011.03.058

Valero-Cabré, A., Amengual, J. L., Stengel, C., Pascual-Leone, A., and Coubard, O. A. (2017). Transcranial magnetic stimulation in basic and clinical neuroscience: a comprehensive review of fundamental principles and novel insights. *Neurosci. Biobehav. Rev.* 83, 381–404. doi: 10.1016/j.neubiorev.2017.10.006

Veniero, D., Strüber, D., Thut, G., and Herrmann, C. S. (2019). Noninvasive brain stimulation techniques can modulate cognitive processing. *Organ. Res. Methods* 22, 116–147. doi: 10.1177/1094428116658960

Weise, K., Numssen, O., Thielscher, A., Hartwigsen, G., and Knösche, T. R. (2020). A novel approach to localize cortical TMS effects. *NeuroImage* 209:116486. doi: 10.1016/j.neuroimage.2019.116486

Zanto, T. P., Rubens, M. T., Thangavel, A., and Gazzaley, A. (2011). Causal role of the prefrontal cortex in top-down modulation of visual processing and working memory. *Nat. Neurosci.* 14, 656–661. doi: 10.1038/nn.2773

Ziemann, U. (2010). TMS in cognitive neuroscience: virtual lesion and beyond. *Cortex* 46, 124–127. doi: 10.1016/j.cortex.2009.02.020

Conflict of Interest: The authors declare that the research was conducted in the absence of any commercial or financial relationships that could be construed as a potential conflict of interest.

frontiers in Human Neuroscience

SYSTEMATIC REVIEW
published: 21 January 2021
doi: 10.3389/fnhum.2020.616054

Resting State Functional Connectivity of Brain With Electroconvulsive Therapy in Depression: Meta-Analysis to Understand Its Mechanisms

Preeti Sinha[1,2]*, *Himanshu Joshi*[2,3] *and Dhruva Ithal*[1,4]

[1] *ECT Services, Noninvasive Brain Stimulation (NIBS) Team, Department of Psychiatry, Bengaluru, India,* [2] *Geriatric Clinic and Services, Department of Psychiatry, National Institute of Mental Health and Neurosciences, Bengaluru, India,* [3] *Multimodal Brain Image Analysis Laboratory, Department of Psychiatry, National Institute of Mental Health and Neurosciences, Bengaluru, India,* [4] *Accelerated Program for Discovery in Brain Disorders, Department of Psychiatry, National Institute of Mental Health and Neurosciences, Bengaluru, India*

Introduction: Electroconvulsive therapy (ECT) is a commonly used brain stimulation treatment for treatment-resistant or severe depression. This study was planned to find the effects of ECT on brain connectivity by conducting a systematic review and coordinate-based meta-analysis of the studies performing resting state fMRI (rsfMRI) in patients with depression receiving ECT.

Methods: We systematically searched the databases published up to July 31, 2020, for studies in patients having depression that compared resting-state functional connectivity (rsFC) before and after a course of pulse wave ECT. Meta-analysis was performed using the activation likelihood estimation method after extracting details about coordinates, voxel size, and method for correction of multiple comparisons corresponding to the significant clusters and the respective rsFC analysis measure with its method of extraction.

Results: Among 41 articles selected for full-text review, 31 articles were included in the systematic review. Among them, 13 articles were included in the meta-analysis, and a total of 73 foci of 21 experiments were examined using activation likelihood estimation in 10 sets. Using the cluster-level interference method, one voxel-wise analysis with the measure of amplitude of low frequency fluctuations and one seed-voxel analysis with the right hippocampus showed a significant reduction ($p < 0.0001$) in the left cingulate gyrus (dorsal anterior cingulate cortex) and a significant increase ($p < 0.0001$) in the right hippocampus with the right parahippocampal gyrus, respectively. Another analysis with the studies implementing network-wise (posterior default mode network: dorsomedial prefrontal cortex) resting state functional connectivity showed a significant increase ($p < 0.001$) in bilateral posterior cingulate cortex. There was considerable variability as well as a few key deficits in the preprocessing and analysis of the neuroimages and the reporting of results in the included studies. Due to lesser studies, we could not do further analysis to address the neuroimaging variability and subject-related differences.

OPEN ACCESS

Edited by:
Nivethida Thirugnanasambandam, National Brain Research Centre (NBRC), India

Reviewed by:
Christopher C. Abbott, University of New Mexico Health Science Center, United States
Jinping Xu, Chinese Academy of Sciences (CAS), China

***Correspondence:**
Preeti Sinha
preetisinha@nimhans.ac.in

Specialty section:
This article was submitted to Brain Imaging and Stimulation, a section of the journal Frontiers in Human Neuroscience

Received: *10 October 2020*
Accepted: *15 December 2020*
Published: *21 January 2021*

Citation:
Sinha P, Joshi H and Ithal D (2021) Resting State Functional Connectivity of Brain With Electroconvulsive Therapy in Depression: Meta-Analysis to Understand Its Mechanisms. Front. Hum. Neurosci. 14:616054. doi: 10.3389/fnhum.2020.616054

Conclusion: The brain regions noted in this meta-analysis are reasonably specific and distinguished, and they had significant changes in resting state functional connectivity after a course of ECT for depression. More studies with better neuroimaging standards should be conducted in the future to confirm these results in different subgroups of depression and with varied aspects of ECT.

Keywords: electroconvulsive therapy, depression, resting state functional neuroimaging, meta- analysis, activation likelihood estimation, hippocampus, dorsal anterior cingulate cortex, posterior cingulate cortex

INTRODUCTION

Electroconvulsive therapy (ECT) as a non-invasive brain stimulation treatment holds an important place in the management of depression (Hermida et al., 2018); it is more clinically and cost effective than other non-invasive brain stimulation methods in pharmacotherapy-resistant depression (Magnezi et al., 2016). The opening of different avenues of investigational modalities in the last 20 years has promoted a detailed examination of mechanisms of the effects of ECT vis-à-vis the neurobiology of depression to improve its applicability and tolerability (Li et al., 2020). Resting state functional magnetic resonance imaging (rsfMRI) is one such technique of neuroimaging, with which the spontaneous activities of the brain during rest are recorded through blood oxygen level dependent (BOLD) signals (Biswal et al., 1995). In comparison to stimulus-based acquisition protocols (task based) of fMRI, this is not only simpler, but it also can identify functionally and spatially distinct modes with greater biological interpretability (Fox and Raichle, 2007; Van Dijk et al., 2010). There are different analysis strategies/measures available for rsfMRI to understand the intrinsic functional connectivity at rest such as regional homogeneity (ReHo) (Zang et al., 2004), amplitude of low frequency fluctuations (ALFF) (Cordes et al., 2001) or fractional amplitude of low frequency fluctuations (fALFF) (Zou et al., 2008), resting state network based functional connectivity (FC) (Raichle et al., 2001; Beckmann et al., 2005), global measures-FC (Friston, 1994; Salvador et al., 2005), and graph theory and network (GTN) analysis (Bullmore and Sporns, 2009; Farahani et al., 2019). Under these strategies, many additional methodological approaches for extracting data are possible based on the research question, such as seed-voxel analysis, voxel-wise analysis, and local and global measures of network in graph theory (Smith, 2012). Each of them provides a window of opportunity to examine the FC of the brain noninvasively.

The rsfMRI studies using the abovementioned measures and methods and other kinds of neuroimaging studies have helped us to understand the disease mechanisms of depression. A recent meta-analysis on structural MRI–based studies in a depressed population established evidence of global atrophy of bilateral hippocampus (HC) (Santos et al., 2018). This finding adds to the integrated model of neurobiological, cognitive, and psychological construct toward the theory of neuronal loss and reduction of synaptic plasticity in HC and probably in the region of medial prefrontal cortex (PFC) in patients with depression (Price and Duman, 2020). Task-based fMRI in depression shows increased FC of the amygdala with HC and that of subgenual anterior cingulate cortex (sgACC) and insula and middle frontal gyrus with dorsal anterior cingulate cortex (dACC) during emotional/pain-related tasks (Helm et al., 2018). The sgACC could differentiate depressed patients from healthy controls in an rsfMRI study with both group-level clustering consistency and individual-level classification consistency of 92.5% (Zeng et al., 2014). In general, rsfMRI-based studies support the involvement of frontal, prefrontal, and limbic structures in depression with lesser consistency for a specific region (Helm et al., 2018). Other areas showing increased resting state FC (rsFC) in patients with depression include the right amygdala with ventral anterior putamen and reduced rsFC in middle occipital gyrus, inferior temporal gyrus, and retrosplenial cortex in the left hemisphere (Gray et al., 2020).

The neurobiological processes involved in the treatment of depression are said to be better understood with antidepressants than with different brain stimulation treatments and psychotherapy. Different antidepressants in task-based fMRI studies are found to normalize the increased activation of the amygdala and ACC, particularly sgACC, to negative emotional tasks and also to improve the activation of these regions to positive emotions (Arnone, 2019). In a few studies, antidepressants also reduced the activation in the dorsolateral PFC (dlPFC) with anticipatory cues/self-referential tasks and in the insula with negative emotions/pain-related tasks. The findings of rsfMRI studies, on the other hand, are too variable to give specific interpretations for the effects of antidepressants

Abbreviations: ACC, Anterior Cingulate Cortex; ALFF, Amplitude of Low-Frequency Fluctuation; ALE, Activation Likelihood Estimation; BA, Brodmann Area; BF, Bifrontal; BT, Bitemporal; CBMA, Coordinate based meta-analysis; CG, Cingluate Gyrus; DMN, Default Mode Network; dACC, dorsal Anterior Cingulate Cortex; dlPFC, dorsolateral Prefrontal Cortex; dmPFC, dorsomedial Prefrontal Cortex; ECT, Electroconvulsive therapy; fALFF, fractional Amplitude of Low-Frequency Fluctuation; FC, Functional Connectivity; FCD, Functional Connectivity Density; FcHo, Functional connectivity Homogeneity; FD, Framewise Displacement; FDR, False Discovery Rate; FCS, Functional Connectivity Strength; fMRI, functional magnetic resonance imaging; FWER, Family-wise Error Rate; FWHM, Full Width Half Maximum; gFCD, global Functional Connectivity Density; GMV, Gray matter volume; GTN, Graph Theory and Network analysis; HC, Hippocampus; IBMA, Image based meta-analysis; L., Left; MNI, Montreal Neuroimaging Institute; PCC, Posterior Cingulate Cortex; PFC, Prefrontal Cortex; PHG, Parahippocampal Gyrus; R., Right; ReHo, Regional Homogeneity; rsFC, resting state Functional Connectivity; rsfMRI, Resting state functional magnetic resonance imaging; ROI, Region of Interest with resting state functional connectivity; RUL, Right Unilateral; SDM, Signed differential mapping; SDM-PSI, Seed-based d mapping- permutation of subject imaging; sgACC, subgenual Anterior Cingulate Cortex; sbFC, Seed-based Functional Connectivity.

beyond the involvement of prefrontal and limbic structures and the default mode network (DMN) (Fonseka et al., 2018; Arnone, 2019). The neuroimaging predictors considered for response to antidepressants include HC, amygdala, ACC, posterior cingulate cortex (PCC), insula, orbitofrontal cortex, dlPFC, and dorsomedial prefrontal cortex (dmPFC); however, there is less consensus about the direction of change in these predictor regions (Fonseka et al., 2018).

ECT-associated structural changes in the brain in patients with depression are probably more reliable than similar changes with other treatments for depression (Enneking et al., 2020). These findings are also more consistent than the other neuroimaging modality–related findings in ECT. According to a recent systematic review, gray matter volume (GMV) of the amygdala, HC, and ACC increases in patients with depression following administration of ECT (Enneking et al., 2020). This review did not find these changes to be associated with the response to ECT. However, an earlier systematic review focusing only on limbic structures notes a negative association of the left HC GMV with a better clinical response to ECT (Takamiya et al., 2018). Similarly, another systematic review on baseline predictors reports that reduced GMV of HC and increased GMV of the amygdala and sgACC are predictive of a better ECT response in depression (Levy et al., 2019). Reviews are available that looked at changes in rsFC with ECT in depression. They include the other studies related to either other treatments for depression (Brakowski et al., 2017; Fonseka et al., 2018) or using other neuroimaging modalities with ECT (Abbott et al., 2014a; Bolwig, 2014; Zhuo and Yu, 2014; Yrondi et al., 2018). These reviews provide a broad notion about rsfMRI effects of ECT as altered FC in DMN, sgACC, central executive network, and dlPFC.

The above description of neuroimaging findings of depression and its various treatments, including ECT, is inferred from the narrative and systematic reviews. Another systematic approach of review, the meta-analysis, can correct the distorting effects of sampling error, measurement error, and other artifacts that produce the illusion of conflicting findings (Schmidt and Hunter, 2015). A meta-analysis may, thus, better integrate the findings across studies to reveal the specific patterns of relationships. This is particularly relevant in the fMRI field, considering the low power of individual studies and the variability present in scanning, preprocessing, and analysis of neuroimages in these studies (Samartsidis et al., 2017; Muller et al., 2018). With the development and progress in methods of coordinate based meta-analysis (CBMA) in the last 10 years, the meta-analytic approach of review has become increasingly common. Unlike image-based meta-analysis (IBMA), which requires the sharing of full image data, CBMA requires mainly information related to cluster size, its peak voxel coordinates, and related statistical methods used for analyzing neuroimages. Activation likelihood estimation (ALE), one of the most common methods described under CBMA (Samartsidis et al., 2017), has been utilized in meta-analysis for fMRI studies in depression. One such meta-analysis, focusing on the treatment of depression, finds a series of regions having altered FC with psychotherapy and activation in insula with antidepressants (Boccia et al., 2016), and a recent study using ALE on rsFC in all treatments for depression, including non-invasive brain stimulation, finds predictors for response to rTMS but not for ECT (Long et al., 2020). The major issues with both these papers and many other neuroimaging meta-analyses exploring the neurobiology of depressive disorders (Sacher et al., 2012; Kuhn and Gallinat, 2013) is they include the inappropriate combining of studies with different measures/extraction methods of rsfMRI (seed-based, ICA, ALFF, ReHo, FCD) (Zang et al., 2015) and inadequate qualitative analysis of the whole neuroimaging process of the included studies (Poldrack et al., 2008; Weber et al., 2015; Roiser et al., 2016; Soares et al., 2016).

Thus, we planned a systematic review and CBMA using ALE of the studies performing rsfMRI before and after a course of ECT in patients having depression. The primary objective of this meta-analysis was to provide definite and specific patterns of rsFC associated with ECT in depression by synthesizing the findings of different modalities of rsfMRI.

MATERIALS AND METHODS

Search Strategies and Study Selection

In this systematic review, we follow the recommendations provided in the Preferred Reporting Items for Systematic reviews and Meta-Analysis (PRISMA) statement (Moher et al., 2009). A systematic literature search was performed in the following four electronic databases: PubMed, Medline, Pro Quest, and Web of Science library. The terms put together for this search are shown below:

- (electroconvulsive) OR (electroconvulsive therapy) OR (ECT) OR (Shock therapy)

AND

- (depression) OR (depressive disorder)

AND

- (resting state functional connectivity) OR (rsfMRI) OR (rs-fMRI) OR (bold rest) OR (rest fMRI) OR (functional connectivity at rest) OR (fMRI)

The search was conducted initially on April 1, 2020, and then it was repeated on July 31, 2020. A total of 477 studies were obtained, and they were then entered into the reference citation manager (Endnote X9) to remove the duplicates. Further selection of the articles was done on the basis of the following criteria.

Inclusion Criteria

1. Prospective observational/ randomized study
2. Subjects in the study having an episode of depression of any severity based on either DSM-IV/5 or ICD-10 irrespective of whether it is part of bipolar affective disorder or major depressive disorder, i.e., unipolar (single episode or recurrent depressive disorder)
3. Subjects in the study received constant current, pulse-wave modified ECT with any electrode placement and any set of electrical parameters

4. Subjects in the study at least underwent rsfMRI of brain on 2 occasions: (1) Prior to the beginning of the ECT course or (2) either at the end of the ECT course or after any fixed number of sessions.

There was no constraint in this review on the concurrent use of any medications for the treatment of depressive episodes.

Exclusion Criteria

1. Case reports or case series
2. Single ECT session
3. Simultaneous treatment with any other brain stimulation technique
4. Comorbid severe mental illness or neurological illness.

All 3 authors (PS, HJ, DI) of this manuscript reviewed the title and abstract of each article independently as per the abovementioned criteria. The studies that clearly satisfy the criteria or whose exclusion could not be confirmed based on review of the abstract, they were selected for acquisition of the full text. The final inclusion to the meta-analysis and systematic review was made after reviewing the full text. In case of any disagreement between any two reviewers during any step of the review, the third reviewer's decision was considered.

Data Extraction

The data was extracted for each study under 2 major categories: subject characteristics and neuroimaging characteristics. The study was identified by its first author, journal, and year of publication. The details noted for the study sample included demography, psychiatry diagnosis along with specifically used clinical features as inclusion criteria (if present), pre- and post-ECT scores on rating scales used for depression, all standard ECT procedure–related information, and details of the concurrent psychotropics. Under the neuroimaging category, details about both scanning and preprocessing of rsfMRI, particulars of measures and methods of extraction undertaken to process the rsfMRI images, the statistical approaches adopted to analyze the differences between pre- and post-ECT neuroimages, and results of the analysis pertaining to rsfMRI were recorded.

Unlike the availability of tools for assessing the quality of general epidemiological, diagnostic, and intervention-related studies, we could not find any specific tool to rate the quality of fMRI aspects of a study. However, there are reviews (Waheed et al., 2016) and a few guidelines (Poldrack et al., 2008; Weber et al., 2015; Roiser et al., 2016; Soares et al., 2016) available focusing on how to conduct and report fMRI-based clinical studies. Based on these recommendations, we prepared a set of variables related to the process and analysis of rsfMRI as well as the display of results in the text, tables, and figures. There were a few articles for which the required information about the coordinates of peak voxel and cluster size of the significant regions were unavailable in their full text and **Supplementary Material**. We sought that information by writing to the respective corresponding authors.

Activation Likelihood Estimation Analysis

CBMA of rsfMRI data was performed using a revised version of the ALE algorithm (Laird et al., 2005; Eickhoff et al., 2009, 2012; Turkeltaub et al., 2012) implemented in GingerALE 3.0.2. The consistency of the coordinates was assured using either Montreal Neuroimaging Institute (MNI) coordinates or converting them into an MNI-based coordinate system. Studies having a similar measure of rsFC were compiled together, followed by putting those results that had a change in one direction (either pre-ECT > post-ECT or post-ECT > pre-ECT) in one set for ALE analysis. The estimates thus obtained had the above-chance convergence of rsFC patterns, independently distributed, between common experiments/studies in a random effects model. The resulting ALE maps and ALE score corresponding to the experiments studied were extracted. Multiple comparisons were performed accordingly, either at a statistical ($p < 0.05$; 1,000 permutations) threshold using a cluster-level familywise error rate (FWER) or at a statistical threshold of $p < 0.05$ (minimum volume threshold in mm^3 equal to the volume of the lowest cluster having significant difference) using the false discovery rate (FDR) as a correction measure.

RESULTS

Search Results

The flow diagram of the process depicting the literature search and study selection is shown in **Figure 1**. Among the 258 articles found in the literature search, 217 were excluded after reviewing the abstract, and another 10 were rejected after reviewing their full text. Their details and reasons for exclusion from the systematic review are shown in **Supplementary Table 1**. We identified a total of 31 articles to be included in the systematic review. Among them, 13 articles were considered for ALE analysis. One of them had 2 different samples (Bai et al., 2018b), which were considered separately for meta-analysis. Contrary to it, there was one sample that was used for different kinds of neuroimaging analysis in different articles (Wang et al., 2017, 2018a,b; Wang J. et al., 2020; Wang L. et al., 2020). We considered those articles to be separate entities as the different measures of rsFC were undertaken separately for meta-analysis. The studies reporting ALFF, fALFF, and ReHo as a measure of rsFC with the voxel-wise method of extracting image data were analyzed using ALE. All of them used FWER for correcting multiple comparisons. Further, ALE was conducted for 3 seed-based FC. Here, the 2 studies reporting right HC (R. HC) as seed were considered separately during ALE because one used FWER (Abbott et al., 2014b) and the other used FDR (Takamiya et al., 2020) for handling multiple comparisons. Last, 2 studies reporting rsFC between the posterior DMN (constituting PCC and precuneus) and dmPFC using network-based analysis with FDR as the multiple comparisons correction method were included for ALE. The details of all these studies are presented in **Table 1** with their measures that were included in ALE analysis as well as the excluded measures. The remaining 18 studies that were excluded completely from the meta-analysis are shown in **Table 2** with all measures of rsFC used in these studies and reasons for their exclusion. The most common

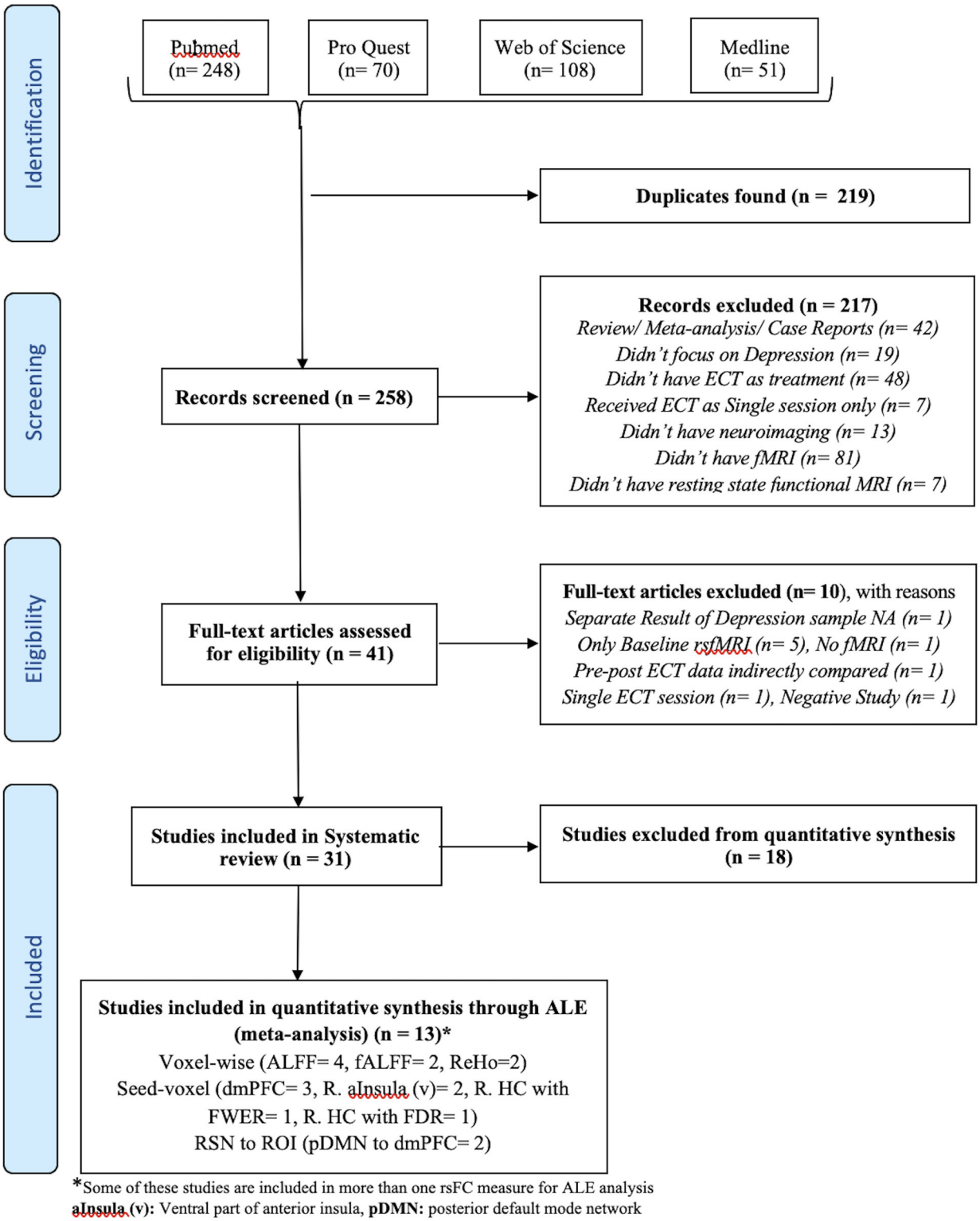

FIGURE 1 | Flow diagram of literature search and study selection. *Some of these studies are included in more than one rsFC measure for ALE analysis. aInsula (v), Ventral part of anterior insula; pDMN, posterior default mode network.

reason for the exclusion of studies was the absence of any other study using same measure or using same region of interest (ROI) for seed-/network-based rsFC analysis. In addition, some other studies were also not included due to the unavailability of information regarding coordinates and cluster size needed to conduct ALE analysis.

ALE Results

A total of 73 foci were analyzed from 21 experiments through 10 sets of ALE analysis. Among the analysis exploring ECT-associated rsFC changes using FWER, one voxel-wise analysis with the measure of ALFF and one seed-voxel analysis with R. HC showed a significant reduction of rsFC ($p < 0.0001$) in the left cingulate gyrus (L. CG) in the area of L. dACC and a significant increase ($p < 0.0001$) in R. HC with right parahippocampal gyrus (R. PHG) using cluster-level interference method, respectively. Another combination of studies implementing network-based (posterior DMN- dmPFC) rsFC analysis using FDR as a multiple comparisons correction procedure showed a statistically significant increase ($p < 0.001$) in the left posterior cingulate cortex (L. PCC) and R. PCC using FDR. The results are presented in **Table 3**, and images of significant clusters are shown in **Figure 2**.

Articles Included in Meta-Analysis-Quality Assessment of Neuroimaging Process

The detailed qualitative assessment of neuroimaging was done for those studies that were included in ALE analysis (**Supplementary Table 2**). We did not rate the overall neuroimaging quality of a study. Instead, we highlighted the aspects by which the study lacked the relevant information or missed the concerned step of the neuroimaging process. These lacunae definitely bring down the quality of studies.

Scanning Procedure

- Most of the studies provided almost all relevant information about it although some did not document a few characteristics, such as orientation of image acquisition, matrix size, and the presence of interslice skip.
- Although many articles provided the name of the software/s used for preprocessing and further analysis of images, detail about the version was missing in most of them.

Image Preprocessing

- The information about the distortion correction related to the artifacts of the EPI sequence was available only in Leaver et al. (2016b). In this study, artifacts retrieved through ICA were then used as regressors during denoising to get rid of them, an approach suggested for handling the distortions (Griffanti et al., 2016; Soares et al., 2016). None of the other papers reported this or any other method of correction, such as reversed phase encoding, field map correction, or point spread function (Hong et al., 2015; Caballero-Gaudes and Reynolds, 2017; Nunes and Hajnal, 2018).
- All studies except Argyelan et al. (2016) provided information about realignment parameters for head motion correction, but a description about transformation functions used during realignment was specified only in Abbott et al. (2013); Abbott et al. (2014b).
- Outlier detection was performed through framewise displacement (FD) in only 4 studies (Argyelan et al., 2016; Bai et al., 2018b; Takamiya et al., 2020; Wang J. et al., 2020) with the threshold as 0.5 or 5 mm. Other studies did not give any account of outlier detection.
- The normalization of the functional images was indirect through the structural image and its associated template in 3 articles (Liu et al., 2015; Kong et al., 2017; Zhang et al., 2020). In other studies, the normalization was probably direct. The name of the template with or without further specification was provided by all except Bai et al. (2018b). An EPI template was used only by Qiu et al. (2016), whereas others used a standard structural template.
- FWHM for smoothing varied from 3.33 times the slice thickness (Abbott et al., 2013, 2014b) to <1.33 times (Qiu et al., 2016; Kong et al., 2017; Bai et al., 2018b; Zhang et al., 2020). They had smoothing with FWHM at 3 times (Leaver et al., 2016b), 2.67 times (Qiu et al., 2019), 2 times (Argyelan et al., 2016), and 1.5 times (Wang J. et al., 2020; Wang L. et al., 2020).
- Some of the recommended models/measures for denoising were reported in few studies here. tCompCor was adopted by Abbott et al. (2013, 2014b) and aCompCor by Takamiya et al. (2020), and FD-related motion parameters were scrubbed by Takamiya et al. (2020) and Wang J. et al. (2020). Nonetheless, cerebrospinal fluid, white matter, and motion parameters from realignment were considered by all during linear regression for denoising along with the frequency band filtering. Leaver et al. (2016b) did not use these parameters for denoising providing statistical justification, and Takamiya et al. (2020) did not provide information about the number of motion parameters used during denoising. No study recorded physiological parameters specifically to be used as regressors. The global brain signal was used as a regressor by Liu et al. (2015) and Zhang et al. (2020), whereas a few studies did not consider it (Abbott et al., 2013, 2014b; Argyelan et al., 2016; Bai et al., 2018b; Wang J. et al., 2020; Wang L. et al., 2020). No study provided any information about detrending. There were two studies that did not have any information about denoising (Qiu et al., 2016, 2019).

Statistical Analysis

Studies had a few shortfalls in this area compared with the standards required (Poldrack et al., 2008; Roiser et al., 2016).

- Although most of them used FWER for handling multiple comparison issues, a few did not write about the model used to consider the cluster size and significance threshold for FWER (Abbott et al., 2014b; Argyelan et al., 2016; Zhang et al., 2020).
- Among the studies that used random field theory for FWER, none of them provided the information about resolution element (RESEL) count (Leaver et al., 2016b; Kong et al., 2017; Bai et al., 2018b). A RESEL is defined as a block of pixels of the same size as the FWHM of the smoothness of the image and is a crucial factor in the application of random field theory for FWER (Brett et al., 2003).

TABLE 1 | List of studies with their different measures of rsFC included in ALE analysis examining the effect of ECT in depression.

References	ALFF based rsFC	fALFF based rsFC	ReHo based rsFC	Seed based rsFC	Seed taken	RSN/ROI to RSN/ ROI	RSN taken	ROI taken	Other measures of rsFC	Correction for multiple comparisons	rsFC measure/ROI used in ALE analysis	Other studies included in ALE analysis of the respective rsFC measure/ROI
Abbott et al. (2013)	-	-	-	-	-	RSN to RSN	*pDMN to dmPFC, L. dlPFC*	-	-	FDR	pDMN (PCC, Precuneus) with dmPFC	Leaver et al., 2016b
Abbott et al. (2014b)	-	-	-	Yes	*HC*	-	-	-	-	FWER	R. HC to R. TL	None
Liu et al. (2015)	Yes	-	-	Yes	L. sgACC	-	-	-	-	FWER	ALFF	Kong et al., 2017; Bai et al., 2018b
Argyelan et al. (2016)	-	Yes	-	Yes	SCC(peak coordinate on R. side)	-	-	-	-	FWER (fALFF); FDR (sbFC)	fALFF	Qiu et al., 2019
Leaver et al. (2016b)	-	-	-	-	-	RSNs to ROI	*mdTh/ vBGN, pDMN, aDMN, vDMN, SAL, OFN, AMTN*	*dACC, PCC, R. a TL, Precuneus, mdTh,*	GTN	FDR	pDMN (PCC, Precuneus) with dmPFC	Abbott et al., 2013
Qiu et al. (2016)	-	-	Yes	-	-	-	-	-	-	FWER	ReHo	Kong et al., 2017
Kong et al. (2017)	Yes	-	Yes	-	-	-	-	-	-	FWER	ALFF ReHo	Liu et al., 2015; Qiu et al., 2016; Bai et al., 2018b
Bai et al. (2018b)	Yes	-	-	Yes	*dmPFC*	-	-	-	-	FWER	ALFF Seed (dmPFC) to voxel	Liu et al., 2015; Qiu et al., 2016; Kong et al., 2017; Wang J. et al., 2020
Qiu et al. (2019)		Yes	-	-	-	-	-	-	-	FWER	fALFF	Argyelan et al., 2016
Wang L. et al. (2020)	-	-	-	Yes	*R. aInsula (v)*	-	-	-	-	FWER	Seed [R. aInsula (v)] to voxel	Zhang et al., 2020
Takamiya et al. (2020)	-	-	-	Yes	*R. HC, L. HC*	-	-	-	-	FDR	Seed (R. HC) to voxel	None
Wang J. et al. (2020)	-	-	-	Yes	*L. AG, dmPFC*	-	-	-	FcHo	FWER	Seed (dmPFC) to voxel	Bai et al., 2018b
Zhang et al. (2020)	-	-	-	Yes	*R. & L. aInsula (v)*	-	-	-	-	FWER	Seed [R. aInsula (v)] to voxel	Wang L. et al., 2020

aDMN, anterior DMN; AMTN, Anteromedial Temporal network; mdTh, medio dorsal thalamus; OFN, Orbitofrontal network; pDMN, posterior DMN; SCC, Subcallosal cingulate cortex; SAL, Salience network; vBGN, ventral basal ganglia network; aTL, anterior Temporal lobe; GTN, Graph Theory and Network analysis; FcHo, Functional connectivity Homogeneity; FDR, False Discovery Rate; FWER, Family-wise Error Rate.

TABLE 2 | List of studies with their different measures of rsFC excluded from ALE analysis examining the effect of ECT in depression and the reasons for exclusion.

References	Seed based rsFC	Seed taken	RSN/ROI to RSN/ ROI rsFC	RSN taken	ROI taken	Other measures of rsFC	Correction for multiple comparisons	Reason for exclusion from ALE analysis
Beall et al. (2012)	-	-	ROI to ROI	-	*B/L ACC to OFC, Caudate*	-	Bonferroni	No other study has matching ROI to ROI in result, Coordinates information NA
Perrin et al. (2012)	-	-	-	-	-	weighted FC for voxel to voxel	FWER	No other study used same measure of rsFC analysis
Wei et al. (2014)	-	-	-	-	-	VMHC for voxel to voxel	FWER	No other study used same measure of rsFC analysis
Cano et al. (2016)	Yes	*R. cm/ sfAmyg*	-	-	-	-	FWER	No other study used same seed for Seed-voxel rsFC analysis
Leaver et al. (2016a)	-	-	RSN to ROI		*aDMN & vDMN to VS*	-	FWER	No other study has matching RSN to ROI in result
Mulders et al. (2016)	-	-	-	-	-	Variance ratio of FC within DMN mask for voxel to voxel	FDR	No other study used same measure of rsFC analysis
Wang et al. (2017)	Yes	*L. sfAmyg*					FWER	No other study used same seed for Seed-voxel rsFC analysis
Bai et al. (2018a)	Yes	*L. aHC, L. midHC*	-	-	-	-	FWER	No other study used same seed for Seed-voxel rsFC analysis
Wang et al. (2018a)	-	-	RSN to RSN, ROI to ROI	Details in Table 5	Details in Table 5	-	Bonferroni	No other study has matching RSN/ROI in result, Coordinates information NA
Wang et al. (2018b)	Yes	*R. supTG*	-	-	-	FCD	FWER	No other study used same measure of rsFC or used same seed for Seed-voxel rsFC analysis
Wei et al. (2018)	-	-	-	-	-	Person's correlation of FC for voxel to voxel	FWER	No other study used same measure of rsFC analysis
Li et al. (2019)	-	-	-	-	-	gFCD	FWER	No other study used same measure of rsFC analysis
Sinha et al. (2019)	-	-	-	-	-	GTN	FDR	GTN is not analyzed with ALE
Leaver et al. (2020)	-	-	-	-	-	GTN within HC	FDR	GTN is not analyzed with ALE
Qi et al. (2020)	-	-	-	-	-	GMV (sMRI) + fALFF (rsfMRI)	FDR	Guidelines for combining different modality of MRI in meta-analysis: NA
Sun et al. (2020)	-	-	ROI to ROI	-	Details in Table 5	-	FDR	No other study has matching ROI to ROI in result, Coordinates information NA
Wei et al. (2020b)	Yes (within cerebellum)	*L. sgACC*	-	-	-	-	FWER	No other study used similar mask
Wei et al. (2020a)	Within Thalamus	*Parietal Cortex, L. Pulvinar*	-	-	-	-	FWER	No other study used same seed for Seed-voxel rsFC analysis

ACC, Anterior Cingulate Cortex; OFC, Orbito Frontal Cortex; aDMN, anterior DMN; cm/sfAmyg, centromedian/superficial amygdala; midHC, middle hippocampus; supTG, superior temporal gyrus; vDMN, ventral DMN; VMHC, Voxel-Mirrored Homotopic Connectivity; VS, Ventral striatum; sgACC, subgenual Anterior Cingulate Cortex; gFCD, global Functional Connectivity Density; FDR, False Discovery Rate; FWER, Family-wise Error Rate.

- In some studies, the difference between pre- and post-ECT rsfMRI was analyzed without adding any study sample-based characteristic as a covariate (Liu et al., 2015; Argyelan et al., 2016; Kong et al., 2017; Wang J. et al., 2020; Wang L. et al., 2020).
- The correlation of ECT-associated rsFC with the clinical characteristics was carried out in most of the studies as a *post hoc* analysis of the significant results without any correction for multiple comparisons. In one study only, we found the percentage change in depression scores during the course of ECT to be incorporated as between-subjects contrast in the primary model of analysis of significant change in seed-based rsFC (Takamiya et al., 2020).
- The display of the results in tabular format was mostly as per the standards in all the studies included for meta-analysis although some had a deficiency in a few aspects in their figures, such as absence of thresholds, *t*-scores, naming, and coordinate details of significant regions. In addition, there

TABLE 3 | ALE results for studies using different measures of rsFC to study the effect of ECT in depression.

Analysis	ECT	FDR/ FWER	Brain region	Cluster size (mm^3)	Peak MNI Coordinates (x, y, z)	ALE value	*Z* score	*P*
ALFF voxel wise	Pre > post	FWER*	L. CG, BA 32	584	−8, 24, 32	0.011	4.715	<0.0001
ALFF voxel wise	Post > pre	FWER*	No significant clusters found					
ReHo voxel cluster	Pre > post	FWER*	No significant clusters found					
Network Based	Post > pre	FDR	L. PCC, BA 31 R. PCC, BA 31	600	2, −56,32 8, −56, 24	0.014 0.013	5.378 5.165	<0.001 <0.001
fALFF voxel to voxel	Pre > post	FWER	No significant clusters found					
Seed (R. HC) to voxel	Post > pre	FWER*	R. HC and R. PHG	8864	42, −22, −11	0.008	4.296	<0.0001
Seed (R. HC) to voxel	Post > pre	FDR	No significant clusters found					
Seed (R. HC) to voxel	Pre > post	FDR	No significant clusters found					
Seed (dmPFC) to voxel	Post > pre	FWER*	No significant clusters found					
Seed (L. anterior Insula (ventral) to voxel	Post > pre	FWER#	No significant clusters found					

**Cluster level FWER; #Voxel level FWER.*
pre> post, Greater before the ECT course; post> pre, Greater after the ECT course/specified number of ECT sessions.

were some studies that could not be included in the meta-analysis due to unavailability of all required parameters of the significant results.

Articles Included for Systematic Review: Clinical and ECT Characteristics

Articles Included in Meta-Analysis: Clinical Characteristics

The clinical characteristics were reported adequately by all studies. Among the 13 studies (**Table 4**) included in the meta-analysis, the sample size was limited to 12–30 subjects except for one study by Zhang et al. (2020) with 45 subjects. Half of these studies had patients with unipolar depression only, whereas the rest included subjects with bipolar depression as well. Three studies focused only on patients having treatment-resistant depression (Abbott et al., 2013; Argyelan et al., 2016; Leaver et al., 2016b), and four had older adults only as their participants (Abbott et al., 2013, 2014b; Kong et al., 2017; Takamiya et al., 2020). Except for a few (Argyelan et al., 2016; Leaver et al., 2016b; Qiu et al., 2016, 2019), patients in all studies had pharmacotherapy concurrently during the course of ECT.

Articles Excluded From Meta-Analysis: Clinical Characteristics

The clinical characteristics of the 18 articles that were excluded from meta-analysis were partially similar to those of articles included in the meta-analysis. Among these studies (**Supplementary Table 4**), all had a sample size of <30 subjects except for 3 studies with sample sizes of 45 (Bai et al., 2018a), 118 (Qi et al., 2020), and 122 (Sun et al., 2020), respectively. Ten of them recruited patients with unipolar depression only, and six of them solely focused on treatment-resistant depression. However, none of these studies specifically studied the geriatric population.

Articles Included for Systematic Review: ECT Characteristics

The treatment aspects related to ECT are presented here together for the articles included in the meta-analysis and those excluded. The details about ECT were provided sufficiently in most of the 31 articles for systematic review. However, the ratio of the administered electrical charge to the seizure threshold is mentioned only in some studies. This information is important as the electrical stimulus dosing influences the rate of improvement and total response in depressive symptoms with ECT (Murugesan, 1994). A few studies also fail to provide anesthetic medications details. An almost equal number of studies used bifrontal (BF), bitemporal (BT), and right unilateral (RUL) as electrode placements during ECT. Some had provision to switch to BT (Leaver et al., 2020; Qi et al., 2020; Sun et al., 2020) or BF (Leaver et al., 2016b) if RUL did not provide significant improvement. Except for Leaver et al. (2020) (ultra-brief pulse-wave ECT), all studies used brief pulse-wave ECT. Most of them had conducted post-ECT neuroimaging after the last session of ECT except in some studies, in which it was done after a predetermined number of ECT sessions (Liu et al., 2015; Cano et al., 2016; Qiu et al., 2016, 2019; Li et al., 2019; Sinha et al., 2019).

Articles Included for Systematic Review: Neuroimaging Findings

Here, we briefly present the resting state neuroimaging findings of all 31 articles that studied ECT-associated changes in rsFC in the depressed patient group. The detailed findings are shown in

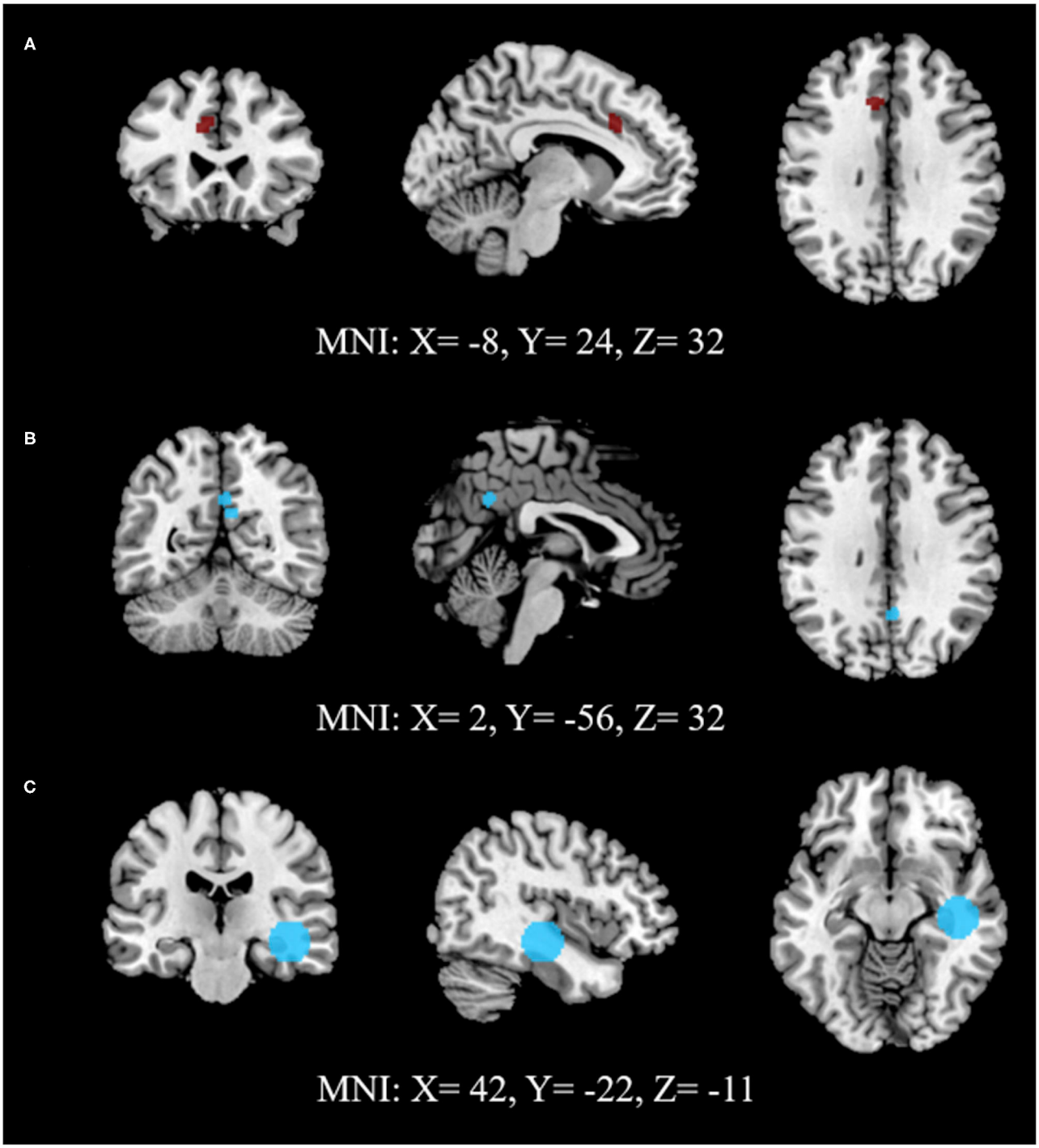

FIGURE 2 | Activation likelihood estimate results for studies measuring **(A)** ALFF, **(B)** network connectivity and **(C)** seed (RHC) to voxels to study the effect of ECT on rsFC. **(A)** shows lower (dark red) and **(B,C)** show higher (light blue) rsFC after ECT intervention. **(A,C)** use FWE (cluster-level extent thresholding) unlike **(B)**, which used FDR as correction for multiple comparisons during reporting significant changes between pre- and post-intervention (Refer to **Table 3** for details).

Supplementary Tables 3, 4. Among studies based on the voxel-wise method of data analysis, CG was often noted as a significant region to be associated with ECT. Although the ACC (L > R) is a more common region of the CG to show a significant change in rsFC after ECT, the concurrence was low for the specific part of the ACC. The other regions that had significant findings

post-ECT in voxel-wise analysis of rsFC belonged to the frontal cortex and parietal cortex as well as the temporal cortex. It included dmPFC, bilateral precentral gyrus, bilateral superior frontal gyrus, left angular gyrus, left precuneus, bilateral HC, right superior temporal gyrus, and right insula. In addition, the cerebellum (L > R) in a few studies showed significant change in rsFC with ECT.

In seed-based analysis, rsFC of the sgACC/subcallosal cingulate cortex with ipsilateral PHG and contralateral temporal pole significantly changed with ECT in two studies but had contrast in the direction of change (Liu et al., 2015; Argyelan et al., 2016). Superficial amygdala was used in two studies for seed-based rsFC analysis. One study found a significant decrease in rsFC post-ECT between the centromedial/superficial amygdala and sgACC on the right side (Cano et al., 2016) although the other study noted an increase in rsFC of the superficial amygdala with a fusiform area on the left side (Wang et al., 2017). In network-based and ROI (with rsFC) to ROI analysis, ACC, PCC, different regions of DMN (PCC, precuneus, medial PFC, intraparietal sulcus), and left cerebellum more often had prominent changes in rsFC with ECT. In the study that jointly analyzed structural MRI and rsfMRI images using HAM-D scores as a reference, FC in PFC, HC, insula, and left caudate were found to be reduced after ECT (Qi et al., 2020).

DISCUSSION

Advancement in neuroimaging in the last 20 years has been seen as a hope to reduce the enigma associated with mechanisms of actions of ECT. Structural neuroimaging shows stronger evidence of change in the brain with ECT compared with other treatments for depression (Enneking et al., 2020). We focus on CBMA of rsfMRI-based studies conducted on patients receiving ECT for treating depression. A meta-analytic approach helped us to achieve reliable and strong results instead of a gamut of less reproducible findings of the individual studies. We conducted ALE analysis on 7 measures of rsFC, including ALFF, fALFF, and ReHo for the voxel-wise, ventral part of the anterior insula, dmPFC and R. HC as seed-based and pDMN-dmPFC as network-based data extraction methods from the rsfMRI data.

Findings of Meta-Analysis and Systematic Review

The significant regions in our meta-analysis were associated with cingulate gyrus (L > R) and included the dorsal part of the ACC (Left), BA 32, and PCC (bilateral), BA 31. There was a reduction in rsFC of the L. dACC after the course of ECT. Neuroimaging studies suggest increased activity in the ACC as an important biomarker for depression (Helm et al., 2018; Lai, 2019), which normalizes after treatment with antidepressants and serves as a predictor for the response (Arnone, 2019; Dunlop et al., 2019; Tian et al., 2020). However, sgACC/rACC are implicated here more often than dACC. Studies exploring dACC found increased FC of dACC within the frontocingular network during emotional/cognitive control–related tasks in patients with depression (Schlösser et al., 2008), which also predicts response to both antidepressants (Crane et al., 2017; Godlewska et al., 2018) and psychotherapy (Beevers et al., 2015; Fonseka et al., 2018). Although Fu et al. (2004) found a decrease in FC of dACC with fluoxetine during the task of "sadness" recognition, most of the other studies on rsFC or task-based FC failed to observe a change in FC of dACC with the treatment of depression through either antidepressants or psychotherapy. Thus, the effect on the dACC in patients having depression, as noted in our meta-analysis, may be a specific mechanism of action of ECT. The dACC is implicated in the salience network along with the anterior insula (Seeley et al., 2007; Enneking et al., 2020). In fact, the dACC is being considered as a part of the neural alarm system and seems to be involved in both detecting performance in a cognitive task and social behavior as well as providing a negative affect to, thus, perceive errors and social rejection, respectively (Spunt et al., 2012). The exaggerated pattern of this aspect is associated with depression (Slavich et al., 2010; Kupferberg et al., 2016).

In our pDMN- and dmPFC-related network analysis, we found increased rsFC of PCC by the end of the ECT course. PCC is considered to be an important part of pDMN and is found to have increased FC with dmPFC in people having depression compared with controls (Mulders et al., 2015; Helm et al., 2018). Increased rsFC of PCC has been shown to be a predictor for response to antidepressants (Goldstein-Piekarski et al., 2018; Dunlop et al., 2019), psychotherapy (Dunlop et al., 2019), and ECT (van Waarde et al., 2015). Although there is evidence of reduction in FC of PCC with antidepressants in response to a negative emotional task in some studies, the evidence is limited in rsFC studies to overall increased activity in pDMN rather than in PCC specifically (Arnone, 2019; Ichikawa et al., 2020). An increase in glucose metabolism in PCC in unipolar depressed patients receiving fluoxetine was, however, noted in an earlier PET study (Mayberg et al., 2000). The possible reasons for the difference in brain regions affected by ECT and antidepressants may be related to their duration of action. The reduction in depressive symptoms achieved by the antidepressants is not by their direct pharmacological actions but through the brain's compensatory responses to those actions, hence, needing a longer time for the clinical improvement with antidepressants (Schatzberg and DeBattista, 2019). Considering that response to ECT is faster, its mechanism of action might be different from that of antidepressants.

The link of global atrophy of HC to the pathology of depression is reasonably recognized, and so is the improvement in its size and associated neurogenesis with antidepressants and other treatment for depression (Helm et al., 2018; Santos et al., 2018; Lai, 2019; Price and Duman, 2020). However, the knowledge about FC of HC during the depressive episode and post response to antidepressants or ECT is ambiguous (Fonseka et al., 2018; Dunlop et al., 2019). Hence, our result of increased FC between R. HC and R. PHG after a course of ECT is valuable. HC is considered to be part of the limbic system with PHG and amygdala and is involved in emotional perception, forming an integral part of the frontolimbic network (Yeo et al., 2011; Lindquist et al., 2012). Our result is based on a single-study

TABLE 4 | List of studies included in ALE analysis: clinical characteristics.

1st Author (year)	Sample characteristics • **Total No., Age as Mean (SD), M: F** • **Disease details** • **Medication details (Class, Frequency in %)** • **Depression scale [Name: Pre ECT score Mean (SD), Post ECT score Mean (SD)]**	ECT characteristics • **Pulse width, electrode placement, charge as times ST** • **Frequency of ECT session, session with Post ECT MRI- [Fixed no/ Last session as Mean (SD)]** • **Anesthetic (Name, Dose), Muscle relaxant (Name, Dose)**
Abbott et al. (2013)	• 12, 66.42 (9.78), 4:8 • Treatment resistance depression • AD (100%), AP (66.67%), MS (16.67%) • HAM-D: 34.56 (10.03), 2.89 (2.93) s	• Brief, RUL (10) & BT (2), 6 times (RUL) 2 times (BT) • 3 times a week, > 5 days (21.13 ± 13.90) • after Last session- 11.17 (3.33) • Methohexital, S Ch
Abbott et al. (2014b)	• 19, 65.3 (8.0), 6:13 • UPD • AD (94.7%), AP (63.2%) • HAM-D: 32.6 (8.5), 8.4 (8.6)	• **NA**, RUL (17) & BT (2), 6 times (RUL) 2 times (BT) • 3 times a week, > 5 days (11 ± 8.4) after Last session- 11 (2.7) • Methohexital, S Ch
Liu et al. (2015)	• 23, 30.57 (9.43), 9:1z • UPD with Active suicidal risk • 1 AD (68.2%), 2 AD (27.3%), AP (13.6%); SSRI (68.2%), SNRI (18.2%), NaSSA (36.4%) • HAM-D: 28.45 (4.93), 8.23 (4.55)	• Brief, BT, 1.5–2 • 1st 3 daily, then 3times a week, After 8th session • Propofol (1.5–2 mg/kg), S. Ch (0.5–1 mg/kg)
Argyelan et al. (2016)	• 16, 48.5 (13. 6), 10:6 • Treatment resistance Depression (UPD = 13, BPD = 3) • All medications stopped except lorazepam • HAM-D: 28.2 (5.6), 10.3	• Brief, BF, 1.5 • 3 times a week, Last or 8th session- 6.4 (1.5) • Ketamine (1mg/kg)/ Methohexital 1mg/kg, S Ch. 1mg/kg
Leaver et al. (2016b)	• 30, 40.90 (12.45), 16:14 • Treatment resistance Depression (UPD = 24, BPD = 6) • Medications stopped 48–72 h prior to ECT course • HAM-D: 26.3 (5.8), 9.3 (5.5)	• **NA**, RUL, 5 times • 3 times a week, Last session- 10.04 (2.93) • Short acting anesthetic, **NA**
Qiu et al. (2016)	• 12, 34.4 (10.1), 4:8 • UPD • No medications • HAM-D: 35.9±1.3, **NA**	• Brief, BT, **NA** • 1st 2weeks as 3times a week, then twice in 1 week; After 8th session • Thiopentone (3.0–5.0 mg/kg) and S. Ch (0.5–1.0 mg/kg)
Kong et al. (2017)	• 13, 63.0 (4.9), 2:11 • Severe depressive episode without psychotic symptoms • 1 AD (53.8%), 2 AD (46.2%), AP = 0, MS = 0; SSRI (92.3%), NaSSA (46.2%), SNRI (7.7%) • HAM-D: 38.6(3.3), 3.1(2.9)	• Brief, BF, **NA** • 3 times a week, Last session: 5.8(0.4) • Propofol, S. Ch
Bai et al. (2018b) (AMHU)	• 33, 35.97 (11.11), 15:18 • UPD = 25, BPD = 8 • SSRI (66.7%), SNRI (33.3%), NaSSA (6.1%), SARI (6.1%), AP (51.5%); AC (Stopped) • HAM-D: 22.42 (4.12), 5.24 (5.09)	• **NA**, BF, **NA** • 3 times a week, Last session- 8.03 (1.91) • Propofol, S. Ch
Bai et al. (2018b) (USTC)	• 28, 35.25 (11.48), 6:22 • UPD = 23, BPD = 5 • SSRI (64.3%), SNRI (39.3%), NaSSA (28.6%), SARI (7.1%), AP (46.4%); AC (Stopped) • HAM-D: 21.54 (4.73), 8.36 (5.62)	• **NA**, BF, **NA** • 3 times a week, Last session- 8.71 (1.80) • Propofol, S. Ch
Qiu et al. (2019)	• 24, 31.33 (10.79), 10:14 • Severe UPD • No medication in last 1 month and during the ECT course • HAM-D: 31.33 (4.55), 8.58 (5.62) s	• Brief, BT, 1.5–2 times • 1st 2 weeks as 3 times a week & 2 times a week in 3rd week, After 8th session • Thiopentone 3–5 mg/kg, S Ch (0.5–1mg/kg)
Wang L. et al. (2020)	• 23, 38.74 (11.02), 11:12 • UPD (Treatment resistance or for suicide) • 1 AD (86.9%), 2 AD (13.1%), AP (39.1%); SSRI (82.3%), SNRI (21.7%), NaSSa/ SARI (8.6%) • HAM-D: 22.22 (4.74), 3.83 (2.15)	• **NA**, BF, **NA** • 1st 3 daily, then 3 times a week; Last session- 7.36 (2) • Propofol, S Ch
Takamiya et al. (2020)	• 27, 67.5 (8.1), 8:19 • Depression with melancholic features (UPD = 22, BPD = 5) • AD (88.9%), AP (77.8%), MS (7.4%) • HAM-D: 32.0 (6.6), 6.0 (5.3)	• Brief, BL, **NA** • 2-3 times a week, Last session: 10.8 (1.8) • Propofol (1 mg/kg), S. Ch (0.5–1 mg/kg)

(Continued)

TABLE 4 | Continued

1st Author (year)	Sample characteristics	ECT characteristics
Wang J. et al. (2020)	• 23, 38.74 (11.02), 11:12 • UPD (Treatment resistance/ suicide) • 1 AD (86.9%), 2 AD (13.1%), AP (39.1%); SSRI (82.6%), SNRI (21.7%), NaSSA (4.34%) • HAM-D: 22.22 (4.74), 3.83 (2.15)	• **NA**, BF, **NA** • 1st 3 daily, then 3 times a week; Last session: 7.26 (2) • Propofol, S. Ch
Zhang et al. (2020)	• 45, 39.07(12.29), 11:34 • UPD = 36, BPD = 9 • SSRI (62.22%), SNRI (31.11%), AP (55.55%) • HAM-D: 24.11(5.63), **NA**	• Brief, BF, **NA** • 1st 3 daily, then 3times a week, Last Session: Range (6–12) • Propofol (0.2–0.5 mg/kg), S. Ch (0.5–1 mg/kg)

AD, Antidepressants; AMHU, Anhui Mental Health Center as Study site; AP, Antipsychotics; BPD, Bipolar depression; BT, Bitemporal; HAM-D, Hamilton Depression Rating Scale; MS, Mood Stabilizer; NA, Information Not Available; NaSSA, Noradrenergic and specific serotonergic antidepressants; SARI, Serotonin antagonist and reuptake inhibitor; S. Ch, Succinylcholine; SD, Standard Deviation; SNRI, Serotonin-norepinephrine reuptake inhibitor; SSRI, Selective serotonin reuptake inhibitor; UPD, Unipolar depression; USTC, University of Science and Technology of China as Study site.

ALE analysis using FWER; ALE analysis with multiple studies is definitely needed to confirm this finding and to examine the connectivity of HC of each hemisphere with prefrontal areas. There is also a need for a greater number of studies to evaluate the effect of ECT on other important areas that were noted during systematically reviewing existing studies. These possible regions include sgACC, dlPFC, precuneus, precentral gyrus, superior frontal gyrus, superior temporal gyrus, and anterior insula.

Strengths of Our Meta-Analytic Approach

We analyzed the studies with different rsFC measures/extraction methods of rsfMRI separately for CBMA as recommended (Zhang et al., 2015). In fact, the studies having different seed regions in seed-voxel or RSN analysis were also analyzed separately. Combining seed-based connectivity studies with different seeds can be a problem because it represents selection bias at the time of choosing seeds and, hence, is not recommended (Cortese et al., 2020). This approach is distinct from that considered by earlier studies using gingerALE based meta-analysis, in which they had combined results of different kinds of neuroimaging (Chen et al., 2017; Disner et al., 2018; Mothersill and Donohoe, 2019), different approaches to fMRI (resting state and task based) (Ayoub et al., 2018), different extraction methods and measures for rsFC (Disner et al., 2018; Gu and Zhang, 2019; Lau et al., 2019), and different seed regions and networks (Lau et al., 2019; Ramsay, 2019; Xu et al., 2019). We also analyzed the studies separately that derived results using FDR and that using FWER as these statistical methods of correcting for multiple comparisons are fundamentally distinguished and need different handling during ALE analysis (Roiser et al., 2016; Eickhoff et al., 2017). Our results can be trusted with a greater degree of confidence considering that our $p < 0.0001$. Because foci with only the same direction of change was considered together in our analysis, our results could indicate significant regions with precision and the associated direction of effects with ECT unlike other neuroimaging meta-analyses using the ALE method (Mothersill and Donohoe, 2019; Gray et al., 2020).

Limitations of the Studies Included in Meta-Analysis

Limitations in Clinical Characteristics

The most important limitation of the studies included in the meta-analysis is their small sample size. Half of the studies had a sample size fewer than 20, and the remainder of the studies except one (Wang L. et al., 2020) had sizes within 30. Small sample-sized studies have limited power and are more likely to miss the regions with significant FC or else to get spurious results if less stringent cutoff p value or lower voxel/cluster thresholds are used (Carter et al., 2016). The clinical population varied across the studies with inclusion of different categories of depression (unipolar vs. bipolar, with or without psychotic symptoms, presence of treatment resistance), age groups of both young and older adults, and varied status of pharmacotherapy. Studies also varied with the electrode placement used for administering ECT. All this variability in clinical and treatment characteristics might have added to the disparity in study findings and, hence, to the insignificant results in ALE analysis.

Limitations in Neuroimaging Characteristics

In addition, there were differences in acquisition and analysis of neuroimaging in the included studies. Because there is no scale/instrument available that rates the neuroimaging aspects of studies, many meta-analysis-based papers either had not commented on the quality of neuroimaging (Disner et al., 2018; Gu and Zhang, 2019; Ramsay, 2019) or did partly (Chen et al., 2017; Ayoub et al., 2018; Xu et al., 2019). We reviewed in detail the procedure, preprocessing, and analysis of neuroimaging; their documentation; and the reporting style of the results presented in the studies to assess the quality and understand the variability. Many features in the included studies were present as per the recommendations and opinions of experts (Poldrack et al., 2008; Weber et al., 2015; Soares et al., 2016), yet they had a few important omissions. Along with flip angle during scanning, the slice thickness varied; both would affect the image intensity. A few recommended steps of preprocessing were missing in many studies, thus reducing the validity of the respective neuroimaging study findings. These included a specific distortion correction method for scanner-related artifacts, outlier

detection through DVARS (the temporal derivative of time courses for FC variance over voxels)/FD for further motion correction, and denoising with extensive variables and scrubbing using appropriate functions (aCompCor, ICA based) (Behzadi et al., 2007; Poldrack et al., 2011; Power et al., 2015; Griffanti et al., 2016; Caballero-Gaudes and Reynolds, 2017). We could not ascertain whether the unreported steps were carried out as many studies did not provide the version of software used for neuroimage preprocessing and analysis. The inadequate information provided about FWER in some studies further casts a concern about the accuracy of their results (Poldrack et al., 2008; Weber et al., 2015; Soares et al., 2016). Last, most of the studies correlated results with depressive symptoms as *post hoc* analysis, which increases the type-1 error (Vul et al., 2009).

Limitations of Our Meta-Analytic Approach

Our study has few limitations as well. CBMA applied in our study has disadvantages, including less consistency and reliability of findings and less flexibility than IBMA, which relies on statistical parametric maps of raw images of the included studies (Salimi-Khorshidi et al., 2009). In addition, the role of the different demographic and clinical characteristics of study samples as covariates in explaining the significant results is still in its nascent phase in CBMA (Tench et al., 2020). This came as an important drawback for our analysis as we had significant heterogeneity in the included studies. However, using CBMA enabled us to include more studies than what was possible with image-based meta-analysis.

Among the available kernel-based techniques of CBMA [multilevel kernel density analysis, ALE, and signed differential mapping (SDM)], ALE is the most widely used and popular method (The BrainMap Project, 2020). With recent updates, ALE addresses the limitations cited with respect to multilevel kernel density analysis (Wager et al., 2007). The newer version of SDM as a seed-based d mapping permutation of subject imaging (SDM-PSI) is able to provide a good estimate of effect size of voxel clusters with a significant change in activity if the peak coordinates and *t*-values are reported (Albajes-Eizagirre et al., 2019). Unfortunately, many studies do not report *t*-values or associated *z*-values, and SDM-PSI is less sensitive and has more uncertainty than anisotropic effect-size seed-based d mapping (AES-SDM) (Radua et al., 2012). Other limitations exist with SDM-PSI, some of which are related to the principle of CBMA. These include the handling of studies using multiple comparisons, the presence of a fewer number of studies, and focusing on correlation among only those voxels that are completely in line with each other rather than partly. A recent meta-analysis of task-based fMRI for language comprehension in children found the same brain regions of significant activation peaks with both ALE and SDM-PSI (Enge et al., 2020). We applied the ALE as recommended and avoided mixing of the studies with differences in neuroimaging techniques and analysis (Zang et al., 2015).

We did not explore the data using model-based methods, such as the Bayesian hierarchical cluster process model, which could have provided more accurate spatial results (Kang et al., 2011). We hope that our results and future studies would lead to model-based CBMA of rsFC in ECT with a valid a priori assumption (Samartsidis et al., 2017). We also had to exclude studies using GTN due to restriction in ALE analysis. With these results, we also did not comment on either the neuroimaging predictors of improvement in depression with ECT or on the association of regions with significant change in rsFC with cognitive deficits developed after ECT. These aims need to be explored in separate meta-analyses.

CONCLUSION AND FUTURE DIRECTIONS

This meta-analysis aimed to understand the mechanisms of action of ECT in patients having depression. We focus on different measures of rsFC used in this group of patients and find those regions of cingulate gyrus showing a significant change with ECT, which has not changed often with other treatments for depression in earlier studies. These include reduction in rsFC in L. dACC and increase in rsFC of bilateral PCC. They are also noted in the literature as important predictors of improvement in depression with different treatments. In addition, we find increased rsFC in R. HC and R. PHG. Thus, our meta-analysis supports the argument of distinct mechanisms of action of ECT. The constraint in sample size and limitations in different aspects of neuroimaging of the studies included for this meta-analysis need to be addressed in future neuroimaging studies of ECT in depression. We also recommend the use of these regions to explore seed-based rsFC and to apply common measures of rsFC as rsfMRI studies in ECT are still in their early phase. Nonetheless, dynamic FC and GTN can be explored further on the rsfMRI data for studying the effect of ECT.

DATA AVAILABILITY STATEMENT

The original contributions presented in the study are included in the article/**Supplementary Material**, further inquiries can be directed to the corresponding author/s.

AUTHOR CONTRIBUTIONS

HJ did the ALE analysis and prepared figure and table related to ALE analysis. DI prepared the introduction. PS prepared other parts of manuscript including tables and figures, which was then reviewed by all of the authors. All three authors contributed to the systematic search and final selection of the articles and extraction of the data.

SUPPLEMENTARY MATERIAL

The Supplementary Material for this article can be found online at: https://www.frontiersin.org/articles/10.3389/fnhum.2020.616054/full#supplementary-material

REFERENCES

Abbott, C. C., Gallegos, P., Rediske, N., Lemke, N. T., and Quinn, D. K. (2014a). A review of longitudinal electroconvulsive therapy: neuroimaging investigations. *J. Geriatr. Psychiatr. Neurol.* 27, 33–46. doi: 10.1177/0891988713516542

Abbott, C. C., Jones, T., Lemke, N. T., Gallegos, P., McClintock, S. M., Mayer, A. R., et al. (2014b). Hippocampal structural and functional changes associated with electroconvulsive therapy response. *Transl. Psychiatr.* 4:e483. doi: 10.1038/tp.2014.124

Abbott, C. C., Lemke, N. T., Gopal, S., Thoma, R. J., Bustillo, J., Calhoun, V. D., et al. (2013). Electroconvulsive therapy response in major depressive disorder: a pilot functional network connectivity resting state FMRI investigation. *Front. Psychiatr.* 4:10. doi: 10.3389/fpsyt.2013.00010

Albajes-Eizagirre, A., Solanes, A., Vieta, E., and Radua, J. (2019). Voxel-based meta-analysis via permutation of subject images (PSI): theory and implementation for SDM. *Neuroimage* 186, 174–184. doi: 10.1016/j.neuroimage.2018.10.077

Argyelan, M., Lencz, T., Kaliora, S., Sarpal, D. K., Weissman, N., Kingsley, P. B., et al. (2016). Subgenual cingulate cortical activity predicts the efficacy of electroconvulsive therapy. *Transl. Psychiatr.* 6:e789. doi: 10.1038/tp.2016.54

Arnone, D. (2019). Functional MRI findings, pharmacological treatment in major depression and clinical response. *Prog. Neuropsychopharmacol. Biol. Psychiatr.* 91, 28–37. doi: 10.1016/j.pnpbp.2018.08.004

Ayoub, L. J., Seminowicz, D. A., and Moayedi, M. (2018). A meta-analytic study of experimental and chronic orofacial pain excluding headache disorders. *NeuroImage* 20, 901–912. doi: 10.1016/j.nicl.2018.09.018

Bai, T., Wei, Q., Xie, W., Wang, A., Wang, J., Ji, G. J., et al. (2018a). Hippocampal-subregion functional alterations associated with antidepressant effects and cognitive impairments of electroconvulsive therapy. *Psychol. Med.* 49, 1357–1364. doi: 10.1017/S0033291718002684

Bai, T., Wei, Q., Zu, M., Xie, W., Wang, J., Gong-Jun, J., et al. (2018b). Functional plasticity of the dorsomedial prefrontal cortex in depression reorganized by electroconvulsive therapy: validation in two independent samples. *Hum. Brain Mapp.* 40, 465–473. doi: 10.1002/hbm.24387

Beall, E. B., Malone, D. A., Dale, R. M., Muzina, D. J., Koenig, K. A., Bhattacharrya, P. K., et al. (2012). Effects of electroconvulsive therapy on brain functional activation and connectivity in depression. *J. ECT* 28, 234–241. doi: 10.1097/YCT.0b013e31825ebcc7

Beckmann, C. F., DeLuca, M., Devlin, J. T., and Smith, S. M. (2005). Investigations into resting-state connectivity using independent component analysis. *Philos. Trans. R. Soc. Lond. B. Biol. Sci.* 360, 1001–1013. doi: 10.1098/rstb.2005.1634

Beevers, C. G., Clasen, P. C., Enock, P. M., and Schnyer, D. M. (2015). Attention bias modification for major depressive disorder: Effects on attention bias, resting state connectivity, and symptom change. *J. Abnorm. Psychol.* 124, 463–475. doi: 10.1037/abn0000049

Behzadi, Y., Restom, K., Liau, J., and Liu, T. T. (2007). A component based noise correction method (CompCor) for BOLD and perfusion based fMRI. *Neuroimage* 37, 90–101. doi: 10.1016/j.neuroimage.2007.04.042

Biswal, B., Yetkin, F. Z., Haughton, V. M., and Hyde, J. S. (1995). Functional connectivity in the motor cortex of resting human brain using echo-planar MRI. *Magn. Reson. Med.* 34, 537–541. doi: 10.1002/mrm.1910340409

Boccia, M., Piccardi, L., and Guariglia, P. (2016). How treatment affects the brain: meta-analysis evidence of neural substrates underpinning drug therapy and psychotherapy in major depression. *Brain Imaging Behav.* 10, 619–627. doi: 10.1007/s11682-015-9429-x

Bolwig, T. G. (2014). Neuroimaging and electroconvulsive therapy: a review. *J. ECT* 30, 138–142. doi: 10.1097/YCT.0000000000000140

Brakowski, J., Spinelli, S., Dorig, N., Bosch, O. G., Manoliu, A., Holtforth, M. G., et al. (2017). Resting state brain network function in major depression - depression symptomatology, antidepressant treatment effects, future research. *J. Psychiatr. Res.* 92, 147–159. doi: 10.1016/j.jpsychires.2017.04.007

Brett, M., Penny, W., and Kiebel, S. (2003). "An Introduction to Random Field Theory," in *Human Brain Function,* eds K. J. Friston, C. Frith, R. Dolan, C. Price, S. Zeki, J. Ashburner and W. Penny. 2nd ed (London: Academic Press), 1144.

Bullmore, E., and Sporns, O. (2009). Complex brain networks: graph theoretical analysis of structural and functional systems. *Nat. Rev. Neurosci.* 10, 186–198. doi: 10.1038/nrn2575

Caballero-Gaudes, C., and Reynolds, R. C. (2017). Methods for cleaning the BOLD fMRI signal. *Neuroimage* 154, 128–149. doi: 10.1016/j.neuroimage.2016.12.018

Cano, M., Cardoner, N., Urretavizcaya, M., Martinez-Zalacain, I., Goldberg, X., Via, E., et al. (2016). Modulation of limbic and prefrontal connectivity by electroconvulsive therapy in treatment-resistant depression: a preliminary study. *Brain Stimul.* 9, 65–71. doi: 10.1016/j.brs.2015.08.016

Carter, C. S., Lesh, T. A., and Barch, D. M. (2016). Thresholds, Power, and sample sizes in clinical neuroimaging. *Biol. Psychiatry Cogn. Neurosci. Neuroimaging* 1, 99–100. doi: 10.1016/j.bpsc.2016.01.005

Chen, Y. C., Wang, F., Wang, J., Bo, F., Xia, W., Gu, J. P., et al. (2017). Resting-state brain abnormalities in chronic subjective tinnitus: a meta-analysis. *Front. Hum. Neurosci.* 11:22. doi: 10.3389/fnhum.2017.00022

Cordes, D., Haughton, V. M., Arfanakis, K., Carew, J. D., Turski, P. A., Moritz, C. H., et al. (2001). Frequencies contributing to functional connectivity in the cerebral cortex in "resting-state" data. *AJNR Am. J. Neuroradiol.* 22, 1326–1333.

Cortese, S., Aoki, Y. Y., Itahashi, T., Castellanos, F. X., and Eickhoff, S. B. (2020). Systematic review and meta-analysis: resting state functional magnetic resonance imaging studies of attention-deficit/hyperactivity disorder. *J. Am. Acad. Child. Adolesc. Psychiatry.* 15;S0890-8567(20)31414-3. doi: 10.1016/j.jaac.2020.08.014

Crane, N. A., Jenkins, L. M., Bhaumik, R., Dion, C., Gowins, J. R., Mickey, B. J., et al. (2017). Multidimensional prediction of treatment response to antidepressants with cognitive control and functional MRI. *Brain* 140, 472–486. doi: 10.1093/brain/aww326

Disner, S. G., Marquardt, C. A., Mueller, B. A., Burton, P. C., and Sponheim, S. R. (2018). Spontaneous neural activity differences in posttraumatic stress disorder: a quantitative resting-state meta-analysis and fMRI validation. *Human Brain Mapp.* 39, 837–850. doi: 10.1002/hbm.23886

Dunlop, K., Talishinsky, A., and Liston, C. (2019). Intrinsic brain network biomarkers of antidepressant response: a review. *Curr. Psychiatr. Rep.* 21:87. doi: 10.1007/s11920-019-1072-6

Eickhoff, S. B., Bzdok, D., Laird, A. R., Kurth, F., and Fox, P. T. (2012). Activation likelihood estimation meta-analysis revisited. *Neuroimage* 59, 2349–2361. doi: 10.1016/j.neuroimage.2011.09.017

Eickhoff, S. B., Laird, A. R., Fox, P. M., Lancaster, J. L., and Fox, P. T. (2017). Implementation errors in the GingerALE Software: description and recommendations. *Human Brain Mapp.* 38, 7–11. doi: 10.1002/hbm.23342

Eickhoff, S. B., Laird, A. R., Grefkes, C., Wang, L. E., Zilles, K., and Fox, P. T. (2009). Coordinate-based activation likelihood estimation meta-analysis of neuroimaging data: a random-effects approach based on empirical estimates of spatial uncertainty. *Hum. Brain Mapp.* 30, 2907–2926. doi: 10.1002/hbm.20718

Enge, A., Friederici, A. D., and Skeide, M. A. (2020). A meta-analysis of fMRI studies of language comprehension in children. *Neuroimage* 215:116858. doi: 10.1016/j.neuroimage.2020.116858

Enneking, V., Leehr, E. J., Dannlowski, U., and Redlich, R. (2020). Brain structural effects of treatments for depression and biomarkers of response: a systematic review of neuroimaging studies. *Psychol. Med.* 50, 187–209. doi: 10.1017/S0033291719003660

Farahani, F. V., Karwowski, W., and Lighthall, N. R. (2019). Application of graph theory for identifying connectivity patterns in human brain networks: a systematic review. *Front. Neurosci.* 13:585. doi: 10.3389/fnins.2019.00585

Fonseka, T. M., MacQueen, G. M., and Kennedy, S. H. (2018). Neuroimaging biomarkers as predictors of treatment outcome in major depressive disorder. *J. Affect. Disord.* 233, 21–35. doi: 10.1016/j.jad.2017.10.049

Fox, M. D., and Raichle, M. E. (2007). Spontaneous fluctuations in brain activity observed with functional magnetic resonance imaging. *Nat. Rev. Neurosci.* 8, 700–711. doi: 10.1038/nrn2201

Friston, K. J. (1994). Functional and effective connectivity in neuroimaging: a synthesis. *Human Brain Mapp.* 2, 56–78. doi: 10.1002/hbm.460020107

Fu, C. H. Y., Williams, S. C. R., Cleare, A. J., Brammer, M. J., Walsh, N. D., Kim, J., et al. (2004). Attenuation of the neural response to sad faces in major depressionby antidepressant treatment: a prospective, event-related functional magnetic resonance imaging study. *Arch. General Psychiatr.* 61, 877–889. doi: 10.1001/archpsyc.61.9.877

Godlewska, B. R., Browning, M., Norbury, R., Igoumenou, A., Cowen, P. J., and Harmer, C. J. (2018). Predicting treatment response in depression: the role of anterior cingulate cortex. *Int. J. Neuropsychopharmacol.* 21, 988–996. doi: 10.1093/ijnp/pyy069

Goldstein-Piekarski, A. N., Staveland, B. R., Ball, T. M., Yesavage, J., Korgaonkar, M. S., and Williams, L. M. (2018). Intrinsic functional connectivity predicts remission on antidepressants: a randomized controlled trial to identify clinically applicable imaging biomarkers. *Transl. Psychiatr.* 8:57. doi: 10.1038/s41398-018-0100-3

Gray, J. P., Müller, V. I., Eickhoff, S. B., and Fox, P. T. (2020). Multimodal abnormalities of brain structure and function in major depressive disorder: a meta-analysis of neuroimaging studies. *Am. J. Psychiatr.* 177, 422–434. doi: 10.1176/appi.ajp.2019.19050560

Griffanti, L., Rolinski, M., Szewczyk-Krolikowski, K., Menke, R. A., Filippini, N., Zamboni, G., et al. (2016). Challenges in the reproducibility of clinical studies with resting state fMRI: an example in early Parkinson's disease. *NeuroImage* 124, 704–713. doi: 10.1016/j.neuroimage.2015.09.021

Gu, L., and Zhang, Z. (2019). Exploring structural and functional brain changes in mild cognitive impairment: a whole brain ALE meta-analysis for multimodal MRI. *ACS Chem. Neurosci.* 10, 2823–2829. doi: 10.1021/acschemneuro.9b00045

Helm, K., Viol, K., Weiger, T. M., Tass, P. A., Grefkes, C., Del Monte, D., et al. (2018). Neuronal connectivity in major depressive disorder: a systematic review. *Neuropsychiatr. Dis. Treat*. 14, 2715–2737. doi: 10.2147/NDT.S170989

Hermida, A. P., Glass, O. M., Shafi, H., and McDonald, W. M. (2018). Electroconvulsive therapy in depression: current practice and future direction. *Psychiatr. Clin. North Am*. 41, 341–353. doi: 10.1016/j.psc.2018.04.001

Hong, X., To, X. V., Teh, I., Soh, J. R., and Chuang, K. H. (2015). Evaluation of EPI distortion correction methods for quantitative MRI of the brain at high magnetic field. *Magnetic Resonance Imaging* 33, 1098–1105. doi: 10.1016/j.mri.2015.06.010

Ichikawa, N., Lisi, G., Yahata, N., Okada, G., Takamura, M., and Hashimoto, R., et al. (2020). Primary functional brain connections associated with melancholic major depressive disorder and modulation by antidepressants. *Sci. Rep.* 10:3542. doi: 10.1038/s41598-020-60527-z

Kang, J., Johnson, T. D., Nichols, T. E., and Wager, T. D. (2011). Meta analysis of functional neuroimaging data via bayesian spatial point processes. *J. Am. Stat. Assoc*. 106, 124–134. doi: 10.1198/jasa.2011.ap09735

Kong, X. M., Xu, S. X., Sun, Y., Wang, K. Y., Wang, C., Zhang, J., et al. (2017). Electroconvulsive therapy changes the regional resting state function measured by regional homogeneity (ReHo) and amplitude of low frequency fluctuations (ALFF) in elderly major depressive disorder patients: an exploratory study. *Psychiatr. Res*. 264, 13–21. doi: 10.1016/j.pscychresns.2017.04.001

Kuhn, S., and Gallinat, J. (2013). Resting-state brain activity in schizophrenia and major depression: a quantitative meta-analysis. *Schizophr. Bull*. 39, 358–365. doi: 10.1093/schbul/sbr151

Kupferberg, A., Bicks, L., and Hasler, G. (2016). Social functioning in major depressive disorder. *Neurosci. Biobehav. Rev*. 69, 313–332. doi: 10.1016/j.neubiorev.2016.07.002

Lai, C. H. (2019). Promising neuroimaging biomarkers in depression. *Psychiatr. Investig* 16, 662–670. doi: 10.30773/pi.2019.07.25.2

Laird, A. R., Fox, P. M., Price, C. J., Glahn, D. C., Uecker, A. M., Lancaster, J. L., et al. (2005). ALE meta-analysis: controlling the false discovery rate and performing statistical contrasts. *Hum. Brain Mapp*. 25, 155–164. doi: 10.1002/hbm.20136

Lau, W. K. W., Leung, M.-K., and Lau, B. W. M. (2019). Resting-state abnormalities in Autism spectrum disorders: a meta-analysis. *Sci. Rep.* 9:3892. doi: 10.1038/s41598-019-40427-7

Leaver, A. M., Espinoza, R., Joshi, S. H., Vasavada, M., Njau, S., Woods, R. P., et al. (2016a). Desynchronization and Plasticity of Striato-frontal connectivity in major depressive disorder. *Cereb. Cortex* 26, 4337–4346. doi: 10.1093/cercor/bhv207

Leaver, A. M., Espinoza, R., Pirnia, T., Joshi, S. H., Woods, R. P., and Narr, K. L. (2016b). Modulation of intrinsic brain activity by electroconvulsive therapy in major depression. *Biol. Psychiatr. Cogn. Neurosci. Neuroimag.* 1, 77–86. doi: 10.1016/j.bpsc.2015.09.001

Leaver, A. M., Vasavada, M., Kubicki, A., Wade, B., Loureiro, J., Hellemann, G., et al. (2020). Hippocampal subregions and networks linked with antidepressant response to electroconvulsive therapy. *Mol. Psychiatr.* 6:10.1038/s41380-020-0666-z. doi: 10.1038/s41380-020-0666-z

Levy, A., Taib, S., Arbus, C., Peran, P., Sauvaget, A., Schmitt, L., et al. (2019). Neuroimaging biomarkers at baseline predict electroconvulsive therapy overall clinical response in depression: a systematic review. *J. ECT* 35, 77–83. doi: 10.1097/YCT.0000000000000570

Li, M., Yao, X., Sun, L., Zhao, L., Xu, W., Zhao, H., et al. (2020). Effects of electroconvulsive therapy on depression and its potential mechanism. *Front. Psychol.* 11:80. doi: 10.3389/fpsyg.2020.00080

Li, X., Meng, H., Fu, Y., Du, L., Qiu, H., Qiu, T., et al. (2019). The impact of whole brain global functional connectivity density following MECT in major depression: a follow-up study. *Front. Psychiatr.* 10:7. doi: 10.3389/fpsyt.2019.00007

Lindquist, K. A., Wager, T. D., Kober, H., Bliss-Moreau, E., and Barrett, L. F. (2012). The brain basis of emotion: a meta-analytic review. *Behav. Brain Sci.* 35, 121–143. doi: 10.1017/S0140525X11000446

Liu, Y., Du, L., Li, Y., Liu, H., Zhao, W., Liu, D., et al. (2015). Antidepressant effects of electroconvulsive therapy correlate with subgenual anterior cingulate activity and connectivity in depression. *Medicine* 94:e2033. doi: 10.1097/MD.0000000000002033

Long, Z., Du, L., Zhao, J., Wu, S., Zheng, Q., and Lei, X. (2020). Prediction on treatment improvement in depression with resting state connectivity: a coordinate-based meta-analysis. *J. Affect Disord*. 276, 62–68. doi: 10.1016/j.jad.2020.06.072

Magnezi, R., Aminov, E., Shmuel, D., Dreifuss, M., and Dannon, P. (2016). Comparison between neurostimulation techniques repetitive transcranial magnetic stimulation vs electroconvulsive therapy for the treatment of resistant depression: patient preference and cost-effectiveness. *Patient Prefer. Adherence* 10, 1481–1487. doi: 10.2147/PPA.S105654

Mayberg, H. S., Brannan, S. K., Tekell, J. L., Silva, J. A., Mahurin, R. K., McGinnis, S., et al. (2000). Regional metabolic effects of fluoxetine in major depression: serial changes and relationship to clinical response. *Biol. Psychiatr.* 48, 830–843. doi: 10.1016/S0006-3223(00)01036-2

Moher, D., Liberati, A., Tetzlaff, J., Altman, D. G., and Group, P. (2009). Preferred reporting items for systematic reviews and meta-analyses: the PRISMA statement. *PLoS Med*. 6:e1000097. doi: 10.1371/journal.pmed.1000097

Mothersill, D., and Donohoe, G. (2019). Neural effects of cognitive training in schizophrenia: a systematic review and activation likelihood estimation meta-analysis. *Biol Psychiatr.* 4, 688–696. doi: 10.1016/j.bpsc.2019.03.005

Mulders, P. C., van Eijndhoven, P. F., Pluijmen, J., Schene, A. H., Tendolkar, I., and Beckmann, C. F. (2016). Default mode network coherence in treatment-resistant major depressive disorder during electroconvulsive therapy. *J. Affect. Disord*. 205, 130–137. doi: 10.1016/j.jad.2016.06.059

Mulders, P. C., van Eijndhoven, P. F., Schene, A. H., Beckmann, C. F., and Tendolkar, I. (2015). Resting-state functional connectivity in major depressive disorder: a review. *Neurosci. Biobehav. Rev*. 56, 330–344. doi: 10.1016/j.neubiorev.2015.07.014

Muller, V. I., Cieslik, E. C., Laird, A. R., Fox, P. T., Radua, J., Mataix-Cols, D., et al. (2018). Ten simple rules for neuroimaging meta-analysis. *Neurosci. Biobehav. Rev*. 84, 151–161. doi: 10.1016/j.neubiorev.2017.11.012

Murugesan, G. (1994). Electrode placement, stimulus dosing and seizure monitoring during ECT. *Aust. N. Z. J. Psychiatr.* 28, 675–683. doi: 10.1080/00048679409080791

Nunes, R. G., and Hajnal, J. V. (2018). Distortion correction of echo planar images applying the concept of finite rate of innovation to point spread function mapping (FRIP). *Magnet. Resonance Mater. Phys. Biol. Med.* 31, 449–456. doi: 10.1007/s10334-017-0669-1

Perrin, J. S., Merz, S., Bennett, D. M., Currie, J., Steele, D. J., Reid, I. C., et al. (2012). Electroconvulsive therapy reduces frontal cortical connectivity in severe depressive disorder. *Proc. Natl. Acad. Sci. U.S.A.* 109, 5464–5468. doi: 10.1073/pnas.1117206109

Poldrack, R. A., Fletcher, P. C., Henson, R. N., Worsley, K. J., Brett, M., and Nichols, T. E. (2008). Guidelines for reporting an fMRI study. *Neuroimage* 40, 409–414. doi: 10.1016/j.neuroimage.2007.11.048

Poldrack, R. A., Mumford, J. A., and Nichols, T. E. (2011). *Handbook of Functional MRI Data Analysis*. Cambridge: Cambridge University Press.

Power, J. D., Schlaggar, B. L., and Petersen, S. E. (2015). Recent progress and outstanding issues in motion correction in resting state fMRI. *Neuroimage* 105, 536–551. doi: 10.1016/j.neuroimage.2014.10.044

Price, R. B., and Duman, R. (2020). Neuroplasticity in cognitive and psychological mechanisms of depression: an integrative model. *Mol. Psychiatr.* 25, 530–543. doi: 10.1038/s41380-019-0615-x

Qi, S., Abbott, C. C., Narr, K. L., Jiang, R., Upston, J., McClintock, S. M., et al. (2020). Electroconvulsive therapy treatment responsive multimodal brain networks. *Hum. Brain Mapp*. 41, 1775–1785. doi: 10.1002/hbm.24910

Qiu, H., Li, X., Luo, Q., Li, Y., Zhou, X., Cao, H., et al. (2019). Alterations in patients with major depressive disorder before and after electroconvulsive therapy measured by fractional amplitude of low-frequency fluctuations (fALFF). *J. Affect. Disord*. 244, 92–99. doi: 10.1016/j.jad.2018.10.099

Qiu, H., Li, X., Zhao, W., Du, L., Huang, P., Fu, Y., et al. (2016). Electroconvulsive therapy-induced brain structural and functional changes in major depressive disorders: a longitudinal study. *Med. Sci. Monit*. 22, 4577–4586. doi: 10.12659/MSM.898081

Radua, J., Mataix-Cols, D., Phillips, M. L., El-Hage, W., Kronhaus, D. M., Cardoner, N., et al. (2012). A new meta-analytic method for neuroimaging studies that combines reported peak coordinates and statistical parametric maps. *Eur. Psychiatr*. 27, 605–611. doi: 10.1016/j.eurpsy.2011.04.001

Raichle, M. E., MacLeod, A. M., Snyder, A. Z., Powers, W. J., Gusnard, D. A., and Shulman, G. L. (2001). A default mode of brain function. *Proc. Natl. Acad. Sci. U.S.A*. 98, 676–682. doi: 10.1073/pnas.98.2.676

Ramsay, I. S. (2019). An activation likelihood estimate meta-analysis of thalamocortical dysconnectivity in psychosis. *Biol. Psychiatr. Cogn. Neurosci. Neuroimaging* 4, 859–869. doi: 10.1016/j.bpsc.2019.04.007

Roiser, J. P., Linden, D. E., Gorno-Tempinin, M. L., Moran, R. J., Dickerson, B. C., and Grafton, S. T. (2016). Minimum statistical standards for submissions to Neuroimage: clinical. *Neuroimage Clin*. 12, 1045–1047. doi: 10.1016/j.nicl.2016.08.002

Sacher, J., Neumann, J., Funfstuck, T., Soliman, A., Villringer, A., and Schroeter, M. L. (2012). Mapping the depressed brain: a meta-analysis of structural and functional alterations in major depressive disorder. *J. Affect. Disord*. 140, 142–148. doi: 10.1016/j.jad.2011.08.001

Salimi-Khorshidi, G., Smith, S. M., Keltner, J. R., Wager, T. D., and Nichols, T. E. (2009). Meta-analysis of neuroimaging data: a comparison of image-based and coordinate-based pooling of studies. *Neuroimage* 45, 810–823. doi: 10.1016/j.neuroimage.2008.12.039

Salvador, R., Suckling, J., Coleman, M. R., Pickard, J. D., Menon, D., and Bullmore, E. (2005). Neurophysiological architecture of functional magnetic resonance images of human brain. *Cereb. Cortex* 15, 1332–1342. doi: 10.1093/cercor/bhi016

Samartsidis, P., Montagna, S., Nichols, T. E., and Johnson, T. D. (2017). The coordinate-based meta-analysis of neuroimaging data. *Stat. Sci*. 32, 580–599. doi: 10.1214/17-STS624

Santos, M. A. O., Bezerra, L. S., Carvalho, A., and Brainer-Lima, A. M. (2018). Global hippocampal atrophy in major depressive disorder: a meta-analysis of magnetic resonance imaging studies. *Trends Psychiatr. Psychother*. 40, 369–378. doi: 10.1590/2237-6089-2017-0130

Schatzberg, A. F., and DeBattista, C. (2019). *Manual of Clinical Psychopharmacology, 9th Ed.* Arlington, VA, US: American Psychiatric Publishing, Inc.

Schlösser, R. G., Wagner, G., Koch, K., Dahnke, R., Reichenbach, J. R., and Sauer, H. (2008). Fronto-cingulate effective connectivity in major depression: a study with fMRI and dynamic causal modeling. *Neuroimage* 43, 645–655. doi: 10.1016/j.neuroimage.2008.08.002

Schmidt, F. L., and Hunter, J. E. (2015). *Methods of Meta-Analysis: Correcting Error and Bias in Research Findings.* 55 City Road, London: SAGE Publications, Ltd.

Seeley, W. W., Menon, V., Schatzberg, A. F., Keller, J., Glover, G. H., Kenna, H., et al. (2007). Dissociable intrinsic connectivity networks for salience processing and executive control. *J. Neurosci.* 27, 2349–2356. doi: 10.1523/JNEUROSCI.5587-06.2007

Sinha, P., Reddy, R. V., Srivastava, P., Mehta, U. M., and Bharath, R. D. (2019). Network neurobiology of electroconvulsive therapy in patients with depression. *Psychiatr. Res.* 287, 31–40. doi: 10.1016/j.pscychresns.2019.03.008

Slavich, G. M., O'Donovan, A., Epel, E. S., and Kemeny, M. E. (2010). Black sheep get the blues: a psychobiological model of social rejection and depression. *Neurosci. Biobehav. Rev*. 35, 39–45. doi: 10.1016/j.neubiorev.2010.01.003

Smith, S. M. (2012). The future of FMRI connectivity. *Neuroimage* 62, 1257–1266. doi: 10.1016/j.neuroimage.2012.01.022

Soares, J. M., Magalhaes, R., Moreira, P. S., Sousa, A., Ganz, E., Sampaio, A., et al. (2016). A Hitchhiker's guide to functional magnetic resonance imaging. *Front. Neurosci*. 10:515. doi: 10.3389/fnins.2016.00515

Spunt, R. P., Lieberman, M. D., Cohen, J. R., and Eisenberger, N. I. (2012). The phenomenology of error processing: the dorsal ACC response to stop-signal errors tracks reports of negative affect. *J. Cognit. Neurosci.* 24, 1753–1765. doi: 10.1162/jocn_a_00242

Sun, H., Jiang, R., Qi, S., Narr, K. L., Wade, B. S., Upston, J., et al. (2020). Preliminary prediction of individual response to electroconvulsive therapy using whole-brain functional magnetic resonance imaging data. *Neuroimage Clin*. 26:102080. doi: 10.1016/j.nicl.2019.102080

Takamiya, A., Chung, J. K., Liang, K. C., Graff-Guerrero, A., Mimura, M., and Kishimoto, T. (2018). Effect of electroconvulsive therapy on hippocampal and amygdala volumes: systematic review and meta-analysis. *Br. J. Psychiatr.* 212, 19–26. doi: 10.1192/bjp.2017.11

Takamiya, A., Kishimoto, T., Hirano, J., Nishikata, S., Sawada, K., Kurokawa, S., et al. (2020). Neuronal network mechanisms associated with depressive symptom improvement following electroconvulsive therapy. *Psychol. Med*. 1, 1–8. doi: 10.1017/S0033291720001518

Tench, C. R., Tanasescu, R., Constantinescu, C. S., Cottam, W. J., and Auer, D. P. (2020). Coordinate based meta-analysis of networks in neuroimaging studies. *Neuroimage* 205:116259. doi: 10.1016/j.neuroimage.2019.116259

The BrainMap Project (2020). *BrainMap Publications*. Available online at: http://brainmap.org/pubs/ (accessed November 11, 2020).

Tian, S., Sun, Y., Shao, J., Zhang, S., Mo, Z., Liu, X., et al. (2020). Predicting escitalopram monotherapy response in depression: the role of anterior cingulate cortex. *Hum. Brain Mapp*. 41, 1249–1260. doi: 10.1002/hbm.24872

Turkeltaub, P. E., Eickhoff, S. B., Laird, A. R., Fox, M., Wiener, M., and Fox, P. (2012). Minimizing within-experiment and within-group effects in Activation Likelihood Estimation meta-analyses. *Hum. Brain Mapp*. 33, 1–13. doi: 10.1002/hbm.21186

Van Dijk, K. R., Hedden, T., Venkataraman, A., Evans, K. C., Lazar, S. W., and Buckner, R. L. (2010). Intrinsic functional connectivity as a tool for human connectomics: theory, properties, and optimization. *J. Neurophysiol.* 103, 297–321. doi: 10.1152/jn.00783.2009

van Waarde, J. A., Scholte, H. S., van Oudheusden, L. J. B., Verwey, B., Denys, D., and van Wingen, G. A. (2015). A functional MRI marker may predict the outcome of electroconvulsive therapy in severe and treatment-resistant depression. *Mol. Psychiatr.* 20, 609–614. doi: 10.1038/mp.2014.78

Vul, E., Harris, C., Winkielman, P., and Pashler, H. (2009). Puzzlingly high correlations in fMRI studies of emotion, personality, and social cognition. *Perspect. Psychol. Sci*. 4, 274–290. doi: 10.1111/j.1745-6924.2009.01125.x

Wager, T. D., Lindquist, M., and Kaplan, L. (2007). Meta-analysis of functional neuroimaging data: current and future directions. *Soc. Cogn. Affect. Neurosci*. 2, 150–158. doi: 10.1093/scan/nsm015

Waheed, S. H., Mirbagheri, S., Agarwal, S., Kamali, A., Yahyavi-Firouz-Abadi, N., Chaudhry, A., et al. (2016). Reporting of resting-state functional magnetic resonance imaging preprocessing methodologies. *Brain Connect* 6, 663–668. doi: 10.1089/brain.2016.0446

Wang, J., Ji, Y., Li, X., He, Z., Wei, Q., Bai, T., et al. (2020). Improved and residual functional abnormalities in major depressive disorder after electroconvulsive therapy. *Prog. Neuropsychopharmacol. Biol. Psychiatr.* 100:109888. doi: 10.1016/j.pnpbp.2020.109888

Wang, J., Wei, Q., Bai, T., Zhou, X., Sun, H., Becker, B., et al. (2017). Electroconvulsive therapy selectively enhanced feedforward connectivity from fusiform face area to amygdala in major depressive disorder. *Soc. Cogn. Affect. Neurosci*. 12, 1983–1992. doi: 10.1093/scan/nsx100

Wang, J., Wei, Q., Wang, L., Zhang, H., Bai, T., Cheng, L., et al. (2018a). Functional reorganization of intra- and internetwork connectivity in major depressive disorder after electroconvulsive therapy. *Hum. Brain Mapp*. 39, 1403–1411. doi: 10.1002/hbm.23928

Wang, J., Wei, Q., Yuan, X., Jiang, X., Xu, J., Zhou, X., et al. (2018b). Local functional connectivity density is closely associated with the response of electroconvulsive therapy in major depressive disorder. *J. Affect. Disord.* 225, 658–664. doi: 10.1016/j.jad.2017.09.001

Wang, L., Wei, Q., Wang, C., Xu, J., Wang, K., Tian, Y., et al. (2020). Altered functional connectivity patterns of insular subregions in major depressive disorder after electroconvulsive therapy. *Brain Imaging Behav*. 14, 753–761. doi: 10.1007/s11682-018-0013-z

Weber, R., Mangus, J. M., and Huskey, R. (2015). Brain imaging in communication research: a practical guide to understanding and evaluating fMRI studies. *Commun. Methods Measures* 9, 5–29. doi: 10.1080/19312458.2014.999754

Wei, Q., Bai, T., Brown, E. C., Xie, W., Chen, Y., Ji, G., et al. (2020a). Thalamocortical connectivity in electroconvulsive therapy for major depressive disorder. *J. Affect. Disord*. 264, 163–171. doi: 10.1016/j.jad.2019.11.120

Wei, Q., Bai, T., Chen, Y., Ji, G., Hu, X., Xie, W., et al. (2018). The changes of functional connectivity strength in electroconvulsive therapy for depression: a longitudinal study. *Front. Neurosci*. 12:661. doi: 10.3389/fnins.2018.00661

Wei, Q., Ji, Y., Bai, T., Zu, M., Guo, Y., Mo, Y., et al. (2020b). Enhanced cerebro-cerebellar functional connectivity reverses cognitive impairment following electroconvulsive therapy in major depressive disorder. *Brain Imaging Behav*. doi: 10.1007/s11682-020-00290-x

Wei, Q., Tian, Y., Yu, Y., Zhang, F., Hu, X., Dong, Y., et al. (2014). Modulation of interhemispheric functional coordination in electroconvulsive therapy for depression. *Translational Psychiatr.* 4:e453. doi: 10.1038/tp.2014.101

Xu, J., Van Dam, N. T., Feng, C., Luo, Y., Ai, H., Gu, R., et al. (2019). Anxious brain networks: a coordinate-based activation likelihood estimation meta-analysis of resting-state functional connectivity studies in anxiety. *Neurosci. Biobehav. Rev.* 96, 21–30. doi: 10.1016/j.neubiorev.2018.11.005

Yeo, B. T., Krienen, F. M., Sepulcre, J., Sabuncu, M. R., Lashkari, D., Hollinshead, M., et al. (2011). The organization of the human cerebral cortex estimated by intrinsic functional connectivity. *J. Neurophysiol*. 106, 1125–1165. doi: 10.1152/jn.00338.2011

Yrondi, A., Peran, P., Sauvaget, A., Schmitt, L., and Arbus, C. (2018). Structural-functional brain changes in depressed patients during and after electroconvulsive therapy. *Acta Neuropsychiatr*. 30, 17–28. doi: 10.1017/neu.2016.62

Zang, Y., Jiang, T., Lu, Y., He, Y., and Tian, L. (2004). Regional homogeneity approach to fMRI data analysis. *Neuroimage* 22, 394–400. doi: 10.1016/j.neuroimage.2003.12.030

Zang, Y.-F., Zuo, X.-N., Milham, M., and Hallett, M. (2015). Toward a meta-analytic synthesis of the resting-state fMRI literature for clinical populations. *BioMed. Res. Int.* 2015:435265. doi: 10.1155/2015/435265

Zeng, L. L., Shen, H., Liu, L., and Hu, D. (2014). Unsupervised classification of major depression using functional connectivity MRI. *Hum. Brain Mapp*. 35, 1630–1641. doi: 10.1002/hbm.22278

Zhang, T., Bai, T., Xie, W., Wei, Q., Lv, H., Wang, A., et al. (2020). Abnormal connectivity of anterior-insular subdivisions and relationship with somatic symptom in depressive patients. *Brain Imaging Behav*. doi: 10.1007/s11682-020-00371-x

Zhang, Y. F., Han, Y., Wang, Y. Z., Zhang, Y. F., Jia, H. X., Jin, E. H., et al. (2015). Characterization of resting-state fMRI-derived functional connectivity in patients with deficiency versus excess patterns of major depression. *Complementary Ther. Med.* 23, 7–13. doi: 10.1016/j.ctim.2014.12.010

Zhuo, C., and Yu, C. (2014). Functional neuroimaging changes subsequent to electroconvulsive therapy in unipolar depression: a review of the literature. *J. ECT* 30, 265–274. doi: 10.1097/YCT.0000000000000114

Zou, Q. H., Zhu, C. Z., Yang, Y., Zuo, X. N., Long, X. Y., Cao, Q. J., et al. (2008). An improved approach to detection of amplitude of low-frequency fluctuation (ALFF) for resting-state fMRI: fractional ALFF. *J. Neurosci. Methods* 172, 137–141. doi: 10.1016/j.jneumeth.2008.04.012

Conflict of Interest: The authors declare that the research was conducted in the absence of any commercial or financial relationships that could be construed as a potential conflict of interest.

frontiers in Human Neuroscience

ORIGINAL RESEARCH
published: 25 February 2021
doi: 10.3389/fnhum.2021.639274

Multimodal Assessment of Precentral Anodal TDCS: Individual Rise in Supplementary Motor Activity Scales With Increase in Corticospinal Excitability

Anke Ninija Karabanov[1,2†], Keiichiro Shindo[1,3*†], Yuko Shindo[1,3], Estelle Raffin[1,4] and Hartwig Roman Siebner[1,5,6]*

[1] Danish Research Centre for Magnetic Resonance, Centre for Functional and Diagnostic Imaging and Research, Copenhagen University Hospital Hvidovre, Hvidovre, Denmark, [2] Department of Nutrition, Exercise and Sports, University of Copenhagen, Copenhagen, Denmark, [3] Department of Rehabilitation Medicine, Keio University School of Medicine, Shinjyuku-ku, Japan, [4] Center for Neuroprosthetics and Brain Mind Institute, Swiss Federal Institute of Technology, Geneva, Switzerland, [5] Institute for Clinical Medicine, University of Copenhagen, Copenhagen, Denmark, [6] Department of Neurology, Copenhagen University Hospital Bispebjerg, Copenhagen, Denmark

OPEN ACCESS

Edited by:
Nivethida Thirugnanasambandam, National Brain Research Centre (NBRC), India

Reviewed by:
Masashi Hamada, The University of Tokyo, Japan
Maxciel Zortea, Federal University of Rio Grande Do Sul, Brazil

***Correspondence:**
Keiichiro Shindo
krugreims@yahoo.co.jp;
Anke Ninija Karabanov
ankenk@drcmr.dk

† These authors have contributed equally to this work

Specialty section:
This article was submitted to Brain Imaging and Stimulation, a section of the journal Frontiers in Human Neuroscience

Received: 08 December 2020
Accepted: 01 February 2021
Published: 25 February 2021

Citation:
Karabanov AN, Shindo K, Shindo Y, Raffin E and Siebner HR (2021) Multimodal Assessment of Precentral Anodal TDCS: Individual Rise in Supplementary Motor Activity Scales With Increase in Corticospinal Excitability. Front. Hum. Neurosci. 15:639274. doi: 10.3389/fnhum.2021.639274

Background: Transcranial direct current stimulation (TDCS) targeting the primary motor hand area (M1-HAND) may induce lasting shifts in corticospinal excitability, but after-effects show substantial inter-individual variability. Functional magnetic resonance imaging (fMRI) can probe after-effects of TDCS on regional neural activity on a whole-brain level.

Objective: Using a double-blinded cross-over design, we investigated whether the individual change in corticospinal excitability after TDCS of M1-HAND is associated with changes in task-related regional activity in cortical motor areas.

Methods: Seventeen healthy volunteers (10 women) received 20 min of real (0.75 mA) or sham TDCS on separate days in randomized order. Real and sham TDCS used the classic bipolar set-up with the anode placed over right M1-HAND. Before and after each TDCS session, we recorded motor evoked potentials (MEP) from the relaxed left first dorsal interosseus muscle after single-pulse transcranial magnetic stimulation(TMS) of left M1-HAND and performed whole-brain fMRI at 3 Tesla while participants completed a visuomotor tracking task with their left hand. We also assessed the difference in MEP latency when applying anterior-posterior and latero-medial TMS pulses to the precentral hand knob (AP-LM MEP latency).

Results: Real TDCS had no consistent aftereffects on mean MEP amplitude, task-related activity or motor performance. Individual changes in MEP amplitude, measured

directly after real TDCS showed a positive linear relationship with individual changes in task-related activity in the supplementary motor area and AP-LM MEP latency.

Conclusion: Functional aftereffects of classical bipolar anodal TDCS of M1-HAND on the motor system vary substantially across individuals. Physiological features upstream from the primary motor cortex may determine how anodal TDCS changes corticospinal excitability.

Keywords: functional magnetic resonance imaging (fMRI), inter-individual variability, motor evoked potentials, primary motor cortex (M1), supplementary motor area (SMA), transcranial direct current stimulation (tDCS), non-invasive brain stimulation, transcrancial magnetic stimulation (TMS)

INTRODUCTION

Transcranial Direct Current Stimulation (TDCS) can non-invasively induce plasticity in the human brain by de- or hyperpolarizing neuronal membranes through the application of weak direct, electrical current. TDCS-induced plasticity is often demonstrated by bi-directional, polarity-specific effects on corticospinal excitability (Nitsche and Paulus, 2011). Using the amplitude of the motor evoked potential (MEP) as a measure of corticospinal excitability, many studies have demonstrated that corticospinal excitability increases when the anodal electrode (anodal TDCS) is placed over the primary motor hand area (M1-HAND) while it decreases when the cathodal electrode (cathodal TDCS) is placed over M1-HAND (Nitsche and Paulus, 2000; Liebetanz et al., 2002). Even though TDCS induced MEP changes have been replicated various times (for review Nitsche and Paulus, 2011), many recent reports, including a large double-blind, placebo-controlled trial, did not show significant effects of anodal TDCS on corticospinal excitability. These recent studies consistently found that the individual change in MEP amplitude was highly variable (Horvath et al., 2014; Lopez-Alonso et al., 2014; Wiethoff et al., 2014; Chew et al., 2015; Strube et al., 2016; Ammann et al., 2017; Lefebvre et al., 2019; Jonker et al., 2020). The number of participants displaying the "classical" anodal TDCS-induced increase ranging only between 30 and 50%, while the other participants showed no or the opposite effect (Lopez-Alonso et al., 2014; Wiethoff et al., 2014). The large variability in response patterns illustrates the need for a better understanding of the neurophysiological mechanisms that drive the changes in corticospinal excitability as well as the need to identify clinically applicable markers that can predict the individual response to TDCS in order to individualize stimulation (Karabanov et al., 2016).

Neuroimaging techniques like functional magnetic resonance imaging (fMRI) or (15)O-water positron emission tomography [(15)O-PET] can investigate the effects of non-invasive brain stimulation (NTBS), by using cerebral blood flow as a proxy for neural activity (Karabanov and Siebner, in press). Early investigations in the neurovascular response to brain stimulation demonstrated that changes are not restricted to the target site but that M1 stimulation affects activity and connectivity in a network of sensorimotor areas, most prominently the premotor cortex (PMC) and the supplementary motor area (SMA; Siebner et al., 2001; Lee et al., 2003). Early (15)O-PET studies used repetitive transcranial magnetic stimulation (TMS) to induce plasticity in M1-HAND, but more recent work using TDCS in combination with fMRI has shown similar effects: Anodal TDCS over M1-HAND modulates activity in M1 and SMA when applied at rest (Jang et al., 2009; Stagg et al., 2009) or when given during a motor task (Antal et al., 2011; Kwon and Park, 2011) and can impact functional coupling between the target region and remote network nodes (Antonenko et al., 2018). However, it is unclear whether the strength of TDCS-induced modulations in sensorimotor areas determines the individual change in corticospinal excitability measured by the MEP.

Improving the individual response to TDCS is important as TDCS-induced plasticity also modulates performance (Nitsche and Paulus, 2011): Several studies suggest that anodal TDCS of M1-HAND during motor training can improve training outcome (Reis and Fritsch, 2011) and TDCS is increasingly used to augment motor training (Buch et al., 2017). However, also performance improvements are reported to be highly variable (Ammann et al., 2016), limiting the use of TDCS as a tool in motor rehabilitation and highlighting the need for markers that can explain variability and guide personalization of stimulation protocols.

Several studies have identified physiological factors that influence variability of NTBS effects (Ridding and Ziemann, 2010; Guerra et al., 2020). One intriguing marker, that also implicates the responsiveness of areas upstream of M1-HAND in mediating corticospinal excitability changes after TDCS can be derived with single-pulse TMS of M1-HAND. It was shown that the latency difference between MEPs induced by anterior-posterior (AP) and lateral-medial (LM) current directions (i.e., AP-LM MEP latency), may predict the individual change in corticospinal excitability following TDCS (Wiethoff et al., 2014; McCambridge et al., 2015). While it was initially thought to reflect individual differences in inter-neuronal networks within M1-HAND (Hamada et al., 2013), the AP-LM MEP latency difference may alternatively reflect the preferential responsiveness of different parts of the precentral gyrus to transcranial electrical stimulation: Long AP-latencies indicate that AP-TMS targets more rostral parts of the precentral crown that are more upstream

Abbreviations: AP, anterior-to-posterior (current direction); BOLD, blood oxygenation level dependent; FDI, first dorsal interosseous; fMRI, functional magnetic resonance imaging; LM, latero-medial (current direction); M1, primary motor cortex; M1-HAND, primary motor hand area; MEP, motor evoked potential; PA, posterior-to-anterior (current direction); RMT, resting motor threshold; VoI, volume of interest; S1, primary sensory cortex; SMA, supplementary motor area; TDCS, transcranial direct current stimulation; TMS, transcranial magnetic stimulation; PEST, parameter Estimation by Sequential Testing.

to M1-HAND (Aberra et al., 2020; Siebner, 2020). Conversely, short LM-latencies indicate that LM-TMS targets deeper parts of the precentral wall close to M1-HAND. Therefore, the latency difference between MEPs evoked by AP-TMS vs LM-TMS can be considered a physiological marker of individual microstructural properties of the precentral gyrus and their susceptibility to transcranial electrical stimulation.

Using a double-blinded placebo-controlled study design, we prospectively assessed the aftereffects of bipolar anodal TDCS targeting right M1-HAND on corticospinal excitability and task-related activation of frontal motor cortex. We complemented this interventional approach with singe-pulse TMS of M1-HAND to determine the individual AP-LM difference in MEP latency. This put us in a position to test whether TDCS-related changes in cortical motor activity in a broader set of sensory-motor areas scaled with the aftereffects of anodal TDCS on corticospinal excitability, accounting for interindividual differences in the susceptibility of the precentral gyrus to transcranial electrical stimulation.

MATERIALS AND METHODS

Subjects

Twenty healthy volunteers were recruited via an advertisement posted on an open-access website for subject recruitment[1] and completed both experimental sessions. All participants (10 women) were consistently right-handed (85.5 ± 15.3 points on Edenborough handedness Scale), non-smokers (Grundey et al., 2012) and had no history of previous neurological or psychiatric illness and no contraindication to NTBS or magnetic resonance imaging (MRI; Oldfield, 1971). The age ranged between 20 and 35 years (mean age. 25.0 ± 3.7). All participants gave informed consent for the purpose and procedures of the study. The study was conducted in accordance with the Declaration of Helsinki and approved by the Research Ethics Committees of the Capital Region (H-2-2013-040). Three participants were excluded because of missing data in the sham TDCS session. Another participant was excluded from fMRI analyses because of inability to correctly perform the behavioral task. Seventeen participants were included in the analyses of the MEP data and 16 participants were included in the analysis that included fMRI data.

Experimental Procedures

Figure 1 provides a synopsis of the experimental procedures. Using a double-blinded cross-over design, we investigated how individual TDCS-induced changes in corticospinal excitability, as reflected by MEP amplitude evoked by single-pulse TMS, are associated with individual changes in regional cortical activity, as reflected by task-related BOLD-fMRI. Each participant received 20 min of real (0.75 mA) or sham (0 mA) TDCS on separate days in randomized order at least a week apart. Real and sham TDCS used the classic bipolar set-up with the anode placed over the right primary motor hand area (M1-HAND) and the cathode over the left supraorbital region. To avoid circadian fluctuations within participants both sessions were scheduled at the same time of day (Ridding and Ziemann, 2010).

Each experimental session started with a BOLD-fMRI run during which participants performed a visuospatial tracking (Raffin and Siebner, 2019). After baseline BOLD-fMRI, participants were moved out of the scanner and were placed in a comfortable chair in a laboratory adjacent to the MR-scanner, where MEPs were recorded to obtain a baseline measure of corticospinal excitability. Participants remained seated and received 20 minutes of real or sham TDCS. Immediately after the end of the TDCS-intervention corticospinal excitability was reassessed (T0) followed by task-related BOLD-fMRI using the same fMRI sequence and visuomotor task as at baseline. Thereafter, we measured brain perfusion using Arterial Spin Labeling (ASL) and performed resting-state fMRI (rs-fMRI). Sixty minutes after the TDCS intervention corticospinal excitability was reassessed (T60). At the end of the second and final session, we performed a comparison of MEP latencies in response to single-pulse TMS evoking an anterior-to-posterior or a medial-to-lateral current in the precentral gyrus using different coil orientations. During all TMS and TDCS procedures the participants were asked to remain seated comfortably, with resting hands and open eyes.

MRI Measurements

Magnetic resonance imaging was performed using a Phillips 3 Tesla MR Achieva scanner (Philips Healthcare, The Netherland). BOLD signal during a visuomotor tracking task was assessed by a 10-min EPI-sequence (TR/TE = 1580/30 ms, field of view (FOV) 200 × 212 × 90, voxel size = 2.94 × 2.94 × 3mm, flip angle = 71°, number of slices = 30, no slice gap). The baseline scan in Session1 also included a high-resolution structural T1- and T2-weighted brain scan, which was used for neuronavigation of TMS. During the baseline scan of session 2, these scans were exchanged with a Diffusion Weighted MRI scan. Post-intervention MRI scans included, besides the EPI-sequence during visuomotor tracking, a resting-state fMRI (rs-fMRI) and a perfusion scan using ASL. The diffusion MRI, rs-fMRI, and ASL measurements were not included in this manuscript.

Visuomotor Tracking During fMRI

The study was designed to delineate whether TDCS of right M1-HAND would produce lasting changes in task-related activity in the motor system. Therefore, participants performed a visuomotor tracking task during the fMRI session (Raffin and Siebner, 2019). The task was chosen because visuomotor tracking reliably activates the motor network including the SMA and the PMC (Ogawa et al., 2007) and required the participants to follow a continuously moving target line using an fMRI-compatible joystick (Hybridmojo, San Mateo, CA, United States). The joystick was operated by the left index finger and modified only to allow horizontal movements. The subjects' left hand was placed palm down on the joystick using a foam wrist support to ensure that they had full index finger abduction and adduction range of motion. The joystick was attached to the subject's left forearm such that they could only to move their left index to manipulate the joystick, with the remaining part of the arm completely still. The voltage signal representing joint motion

[1] www.forsogsperson.dk

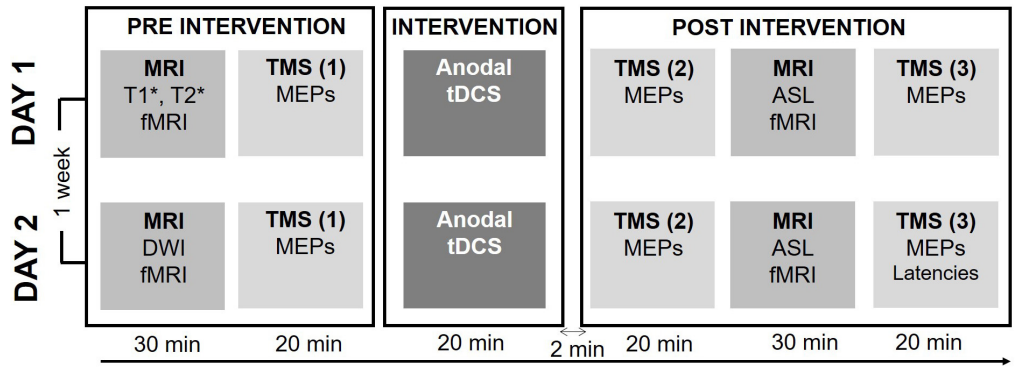

FIGURE 1 | Experimental procedure. Each session started by a baseline measure consisting of a structural and functional MRI (fMRI) exam and baseline physiological measures of corticospinal excitability. Baseline behavioral measures of motor performance during a visuomotor tracking task were recorded during the fMRI sequence. After baseline measures, 20 min of either active or sham TDCS was applied. Directly after the intervention corticospinal excitability was reassessed, followed by the post-intervention run of the fMRI, Arterial Spin Labeling (ALS) and Resting-state fMRI (rs-fMRI) sequences. The post-intervention was concluded by the second measure of corticospinal excitability. In the second session, the individual latency profile was assessed by measuring the MEP latency following stimulation with different coil orientations.

was sent to a computer (Dell Computer Company, Round Rock, TX, United States) through an analog-to-digital converter that sampled the signal at 60 Hz. The peak of the target waveform was set at 85% of the standard range of motion (with 100% defined as a full extension), and the lower peak of the wave was set at 15% of the standard range of motion (with 0% defined as a full flexion). Thus, the upper and lower peaks of the target were within each subject's range of motion. Before entering the scanner, the subjects were familiarized with the task and had the chance to practice the task for a few minutes.

Each fMRI run consisted of 30 blocks (block length approx. 20 s) during which, a target line continuously moved in the middle of the screen. Each block was preceded by a 2 to 4-s baseline with the target line being at a start position. Three different conditions were randomly alternating (resulted in from 8 to 12 blocks per condition): During *complex tracking,* the target line represented an unpredictable pattern that participants had to track using the joystick. During *simple tracking,* subjects had to track a highly predictable pattern. During *visual tracking,* participants had only to visually follow the target line. The line length was equal between conditions. The task was implemented in PsychoPy 2 (Version 1.8) (Peirce, 2008) and displayed on a 17-inch monitor with a resolution of 1280 × 1024 pixel situated at the end of the MRI tunnel that subjects viewed through a 45° oriented mirror placed above the eyes.

Neurophysiological Measures

Transcranial magnetic stimulation measures were collected using a MagVenture MagPro R30 Stimulator (MagVentureA/S, Farum, Denmark) connected to a MC-B70 coil (MagVenture A/S, Farum, Denmark).TMS pulses were monophasic, induced a P-A current direction in the brain and were given with an inter-pulse interval of 0.2Hz. Correct positioning was continuously mirrored using a stereotaxic frameless neuronavigation system (LOCALITE GmbH, Sankt Augustin, Germany). Corticospinal excitability was evaluated before TDCS intervention (baseline), and 2 min and 1 h after the intervention (T0 and T60). Corticospinal excitability was measured by recording MEP amplitudes in response to an individually constant stimulation intensity (MEP amplitude): At the beginning of the experiment the individual stimulator intensity was set to evoke MEPs with a mean amplitude of 0.5 mV while at rest ($Threshold_{0.5}$). Baseline recordings started with the identification of the motor hotspot for the left first dorsal interosseus (FDI) muscle. The motor hot spot was marked for online monitoring using neuronavigation and for re-identification of the hotspot during post-intervention recordings. In all sessions (pre and post) the $Threshold_{0.5}$ was determined using the adaptive, parameter estimation by sequential testing method (adaptive PEST) (Awiszus, 2003; Karabanov et al., 2015). The initial output intensity for $Threshold_{0.5}$ was used during both pre- and post-intervention measures to collect 20 MEPs. We also measured corticomotor latency of the MEP at the end of the experimental session at the second day (Hamada et al., 2013). To determine corticomotor MEP latency, we applied a single monophasic TMS pulse at motor hot spot. Stimulus intensity was adjusted to evoke a mean MEP amplitude of approximately 0.5 mV in the FDI muscle. MEPs were evoked with single monophasic TMS pulses inducing either a posterior-to-anterior (PA), anterior-to-posterior (AP), or latero-to-medial (LM) current direction in the precentral gyrus, while participants maintained a tonic contraction of the FDI muscle at 10% of maximal force level. To evaluate inter-individual differences in MEP latency, 20 MEPs were recorded for each coil orientation in a randomized order.

TDCS Interventions

Direct current was generated by a DC-stimulator (NeuroCohn, GmbH, Ilmenau, Germany) via a pair of electrodes prepared with Ten20 Conductive Paste (Weaver and Company, CO, United States). The anodal electrode (3 cm × 4 cm) was placed over right M1-HAND with its center corresponding to the motor hot spot of the left FDI muscle. The motor hot spot was also marked on the scalp with the help of an individual anatomical MR scan of the whole brain and stereotaxic frameless

neuronavigation. The cathodal electrode (5 cm × 7 cm) was attached to the left forehead above the orbit. Anodal TDCS was applied with an intensity of 0.75 mA for 20 min. We chose a small anodal electrode to be able to stimulate M1-HAND more focally, the relatively low current intensity was chosen to match the mA/cm^2 current density usually achieved by the conventional 5 cm × 7 cm electrode at an intensity of 2 mV (0.625 mA/cm^2 at 0.75 mV with 12 cm^2 compared to 0.57 mA/cm^2 at2 mA with 35 cm^2).

The fade-in fade-out period lasted 15 s. Sham TDCS consisted of the fade-in and fade-out phases only without any constant stimulation in between. A visualization of the applied montage and a calculation of the induced electric field was conducted with SimNIBS software (Thielscher et al., 2015) and a mean map of the electrical field distribution can be seen in **Figure 2**. After each interventional session, participants completed a questionnaire about TDCS-induced sensory effects (Brunoni et al., 2011). The study was double blinded since both, the participants and the examiner, responsible for the pre-post measures (MRI, TMS) were not aware of the type of stimulation in each session (sham or active).

Statistical Analysis

Corticospinal Excitability

The mean MEP amplitude of the left FDI muscle was used as index of corticospinal excitability. Baseline $MEP_{PreSham}$ and $MEP_{PreTDCS}$ amplitudes were compared using a paired *t*-test to test whether corticospinal excitability was matched before the sham and real TDCS. For further investigation of TDCS-induced effects, the mean MEP_{Post} amplitudes were normalized to the pre-TDCS amplitudes of the same session by dividing MEP_{Post} by MEP_{Pre}. The normalized MEPs of post1 and post2 measurements were entered as dependent variable in a two-way repeated measure analysis of variance (ANOVA) to investigate the effects of "Stimulation" (sham/TDCS) and Time (Post1/Post2).

MEP Latency

To investigate potential effects of TDCS on the MEP latency, two examiners independently measured the shortest latency of the superimposed MEP waveforms for each separate coil orientation (Hamada et al., 2013). We computed the Pearson correlation coefficient to test for correlations between the normalized amplitudes of MEP_{Post1} and MEP_{Post2} and the orientation-related differences in MEP latency (PA-LM and AP-LM orientations).

Behavioral Data

The absolute mean of the tracking error was calculated for both movement conditions (complex tracking versus simple tracking). If (*xt*) is the instantaneous horizontal coordinate of the target line and (*xj*) the instantaneous horizontal coordinate of the joystick, then the instantaneous error at that time point was defined as:

$$Instantaneous\ error \ = \sqrt{(xt - xj)^2} - r$$

where *r* is the radius of the circle around the joystick (i.e the tolerance area). The improvement ($Errror_{Imp}$) across the pre- and post-intervention scan was calculated by subtracting the absolute mean $Error_{\%Post}$ from the absolute mean $Error_{pre}$ for each participant. A two-factorial ANOVA with the dependent factor $Errror_{Imp}$ and the independent factors "Stimulation" (real TDCS/sham TDCS) and "Task" (complex/simple), was calculated to focus on potential TDCS-induced performance changes. Effects were considered significant at $p < 0.05$.

Analysis of Task-Based fMRI Data

Functional magnetic resonance imaging data analysis was performed using SPM8 (Wellcome Department of Cognitive

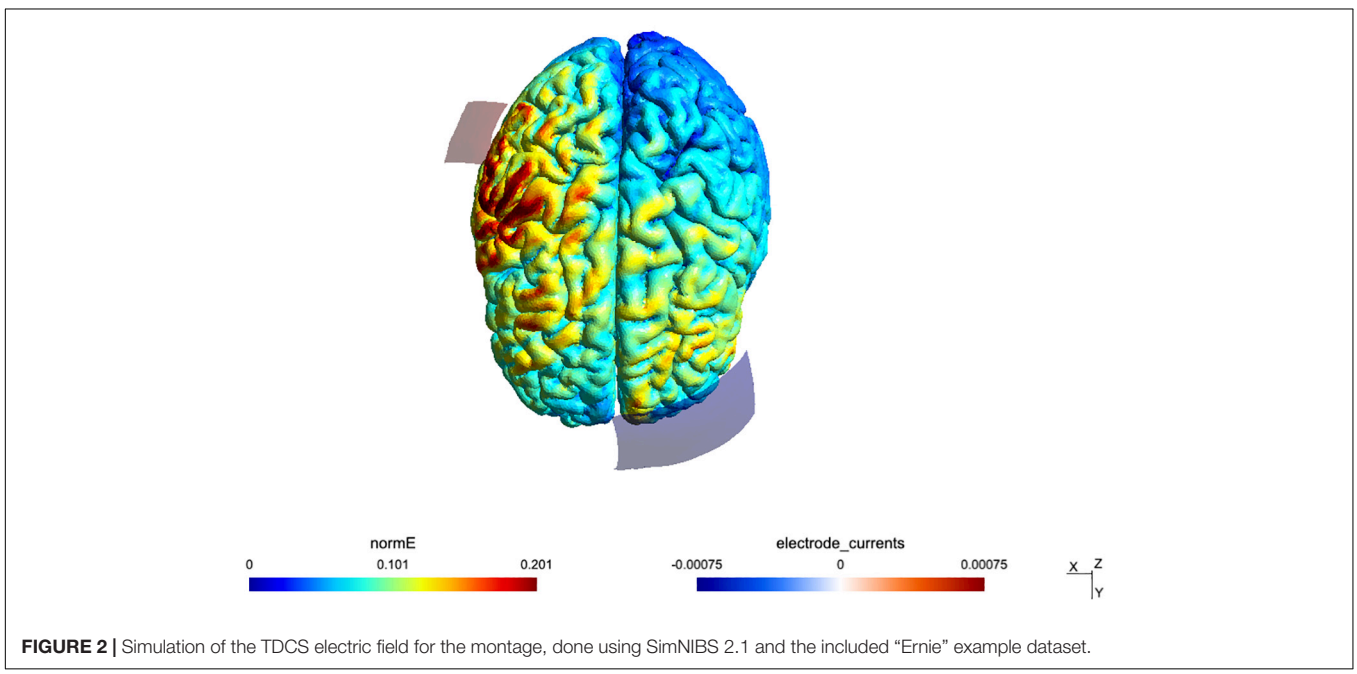

FIGURE 2 | Simulation of the TDCS electric field for the montage, done using SimNIBS 2.1 and the included "Ernie" example dataset.

Neurology, London, UK) and MATLAB R2012a (Mathworks, Natick, MA, United States). Data from each participant were motion-corrected, realigned and smoothed with an 8-mm isotropic Gaussian kernel. At the first level, images related to the amplitude of the hemodynamic response were entered into the full factorial ANOVA model in each subject modeling "Stimulation," "Task," and "Time." At the second level, contrast images were collected into one sample *t*-test. To investigate correlations between TDCS-induced effects on movement-related BOLD activity and TDCS-induced effects on corticospinal excitability, the contrast images "*simple tracking and complex tracking* versus rest" were entered into an SPM regression with the normalized MEP as covariates (i.e., independent variable). A statistical threshold of $p < 0.05$ (FWE corrected at the cluster level) was used to identify significantly activated regions on the group level, applying a non-corrected cluster extent threshold of $p < 0.001$). For nodes of the sensorimotor network known to be affected by TDCS (SMA, PMd, and M1-HAND) we constructed spherical volume-of-interest (VoI) with a 10 mm radius. The center of the spherical VoI matched peak coordinates was center coordinates based on task-based peak activations reported in a previous fMRI study (Lee et al., 2003). Small volume correction was applied for voxels within the VoIs.

Multiple Regression Analysis

We tested whether a combination of predictor variables (BOLD change in SMA and MEP latency difference depending on AP-LM current orientation) could predict TDCS-induced change in MEP amplitude. We computed a multiple regression analysis in which the normalized MEP at post1 was treated as dependent variable. The change in task-related BOLD signal in SMA and the AP-LM latency difference were entered as explanatory variables. The linear regression model was calculated in R and used the lm function (R Core Team, 2017). The relative importance of each predictor was determined using bootstrap confidence intervals for relative importance (function boot.relimp) (R Core Team, 2017).

Questionnaires

Feedback about the sensory side effects of real and sham TDCS stimulation was analyzed using a questionnaire (Brunoni et al., 2011). A Fisher's exact test was performed to differences in questionnaire ratings between TDCS and sham sessions. Statistical analyses were performed with SPSS version 19.0, with exception of the Multiple Regression analysis.

RESULTS

Data from the post-stimulation questionnaire (see Appendix) indicated that participants could not distinguish between the sham and real TDCS intervention. There was no significant difference ratings of any item ($p > 0.05$, Fisher's exact test).

Corticospinal Excitability

The mean MEP amplitudes at baseline and after TDCS are shown in **Figure 3**. At baseline, there was a significant difference in MEP amplitudes between the real and sham TDCS sessions ($p = 0.034$, paired *t*-test. This difference was caused by higher baseline MEP amplitudes in the sham TDCS session **Figure 3A**. Using the non-normalized MEPs in a 3 × 2 ANOVA with the factors Stimulation (anodal/sham) and Time (pre/T0/T60) a main effect of Stimulation [$p = 0.002$, $F(16) = 9.99$] was detected, indicating a difference in MEP amplitude between the sham and real TDCS sessions but the ANOVA showed neither a significant main effect of Time [$p = 0.32$, $F(16) = 0.99$] nor an interaction between Time and Stimulation [$p = 0.71$, $F(16) = 0.17$]. To check if the baseline difference in MEP amplitude affected the results, we ran a post-hoc analysis where the same ANOVA was repeated after removing the three individuals with the highest MEP amplitudes during sham. This analysis ($N = 14$), confirmed that there was no significant effect of TDCS or Time x TDCS interaction when the baseline difference between groups was eliminated (all *p*-values >0.13). In an additional analysis ($N = 17$), we normalized post-TDCS MEP amplitudes at T0 and T60 to individual mean MEP amplitude at baseline. Normalized MEP amplitudes were entered in a 2 × 2 ANOVA with the factors Stimulation (anodal/sham) and Time (T0/T60). No main effect or interaction was detected by this analysis ($p > 0.5$ for all). The normalized group data are illustrated in **Figure 3**.

Orientation Dependency of MEP Latency and TDCS Aftereffect on MEP Amplitudes

Mean corticomotor latencies of the MEPs were 22.1 ms (±1.7) for the PA current direction, 24.5 ms (±2.0) for the AP current direction and 21.6 ms (±1.8) for the LM current direction. There was a significant positive correlation between the individual difference between the MEP latency evoked with AP versus LM current orientation and the individual change in normalized MEP amplitude immediately after the anodal TDCS (post1) ($R = 0.57$, $p = 0.018$, **Figure 4A**). The larger the relative delay in MEP latency at AP versus LM current direction, the larger the individual increase in MEP amplitude after real anodal TDCS. No such relationship was found for the sham TDCS session ($R = -0.15$, $p = 0.56$, **Figure 4B**). There was no significant correlation between AP-LM latency and normalized amplitudes of MEPs one hour after either the anodal TDCS ($R = 0.24$, $p = 0.36$) or the sham ($R = -0.15$, $p = 0.56$). There was no significant correlation between PA-LM latencies and normalized amplitudes of MEPs just after the anodal TDCS ($R = 0.26$, $p = 0.31$) or the sham ($R = 0.05$, $p = 0.86$).

Task Performance During Visuomotor Tracking

We computed a two-factorial ANOVA to investigate the effects of sham and anodal TDCS on task performance. We found a main effect of Task [$F(16) = 1.5396$, $p = 0.02$] of the tracking error, showing better performance during the simple tracking condition. There was no main effect of Stimulation [$F(16) = 1.53$, $p = 0.21$] and no Task × Stimulation interaction [$F(16) = 0.02$, $p = 0.88$], indicating that TDCS did not modify visuomotor tracking performance.

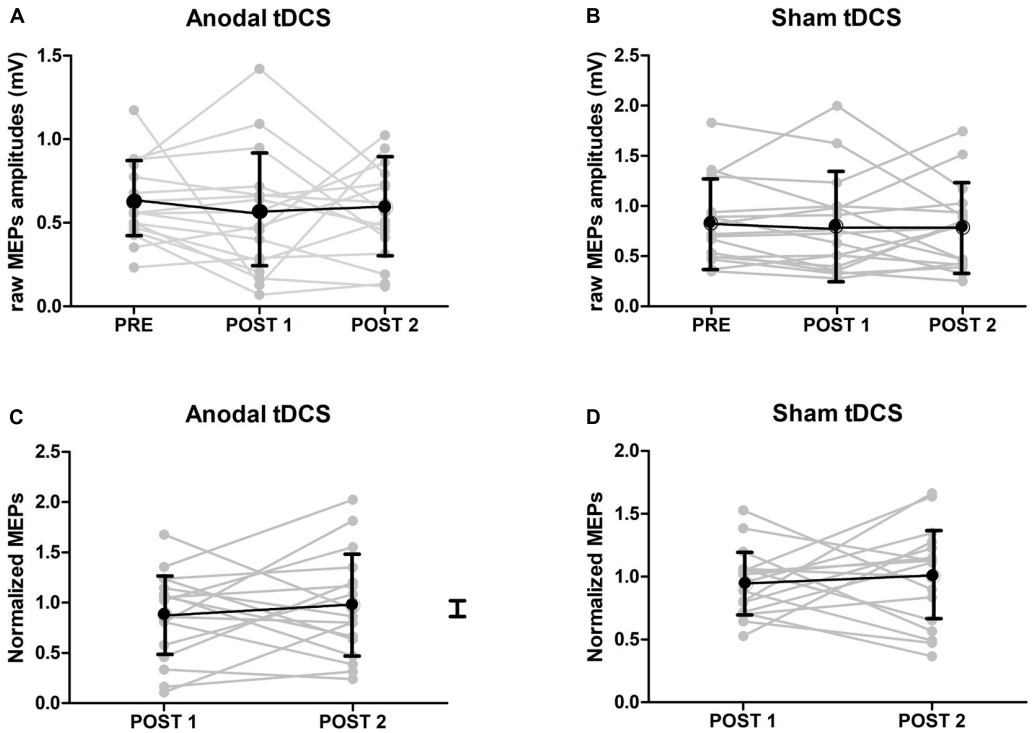

FIGURE 3 | MEP results. **(A)** Raw amplitudes of MEPs after either anodal or sham TDCS (mean ± SE). At baseline, there was a significant difference in MEP amplitudes between TDCS and sham sessions ($p < 0.05$, paired t-test). **(B)** Group results of normalized amplitudes of MEPs after either anodal or sham TDCS (mean ± SE, $n = 17$). Normalized amplitudes were calculated by dividing the amplitudes of MEPs just after or 1 hour after TDCS by ones at baseline. No interaction could be detected.

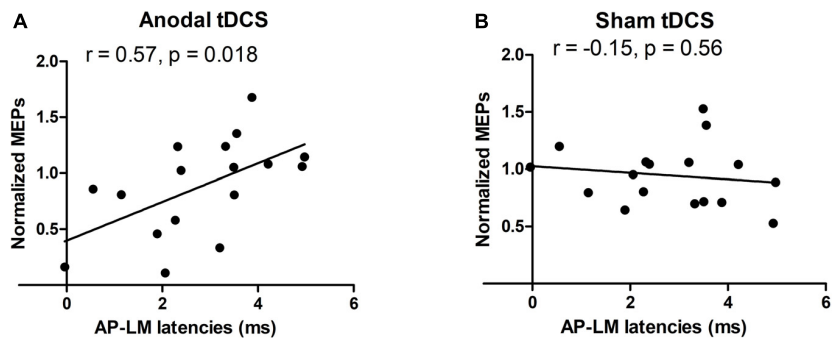

FIGURE 4 | Relationships between the normalized TMS amplitudes and AP-LM latency. A positive correlation was found just after the anodal session **(A)**, but neither just after the sham session (B), nor 1 h after each stimulation. For the *y*-axis a value of 1 is equivalent to no change from baseline.

Task-Based BOLD Signal Changes

The post-TDCS fMRI session started on average 20 (±3.3) minutes after TDCS. The complex and simple visuomotor finger tracking tasks induced significant BOLD signal increases in the right precentral cortex and in a broad bilateral network, including the SMA, ventral premotor and parietal cortex (IPC) (FWE, $p < 0.05$), when compared to visual tracking alone (**Table 1** and **Figure 5A**). The complex visuomotor tracking task induced more activation in the right middle occipital gyrus, bilateral parietal cortex, right dorsal PMC and SMA when compared to the simple task (FWE, $p < 0.05$) (**Table 2** and **Figure 5B**. *Anodal TDCS* induced no significant change in task-related fMRI activity compared to sham TDCS. There was also no significant interaction between Stimulation and Task (at FWE < 0.05, whole brain or small volume corrected in VOIs).

Relationship Between Corticospinal Excitability and BOLD Response

The normalized MEP immediately after real anodal TDCS (T0) was positively correlated with BOLD signal change during the visual-motor tracking task (complex and simple combined) after anodal TDCS. Significant correlations were found in the bilateral SMA ($x = 6$, $y = -12$, $z = 60$, kE 374, T score = 5.95, $p = 0.014$, FWE, small volume corrected, **Figure 6**). There were

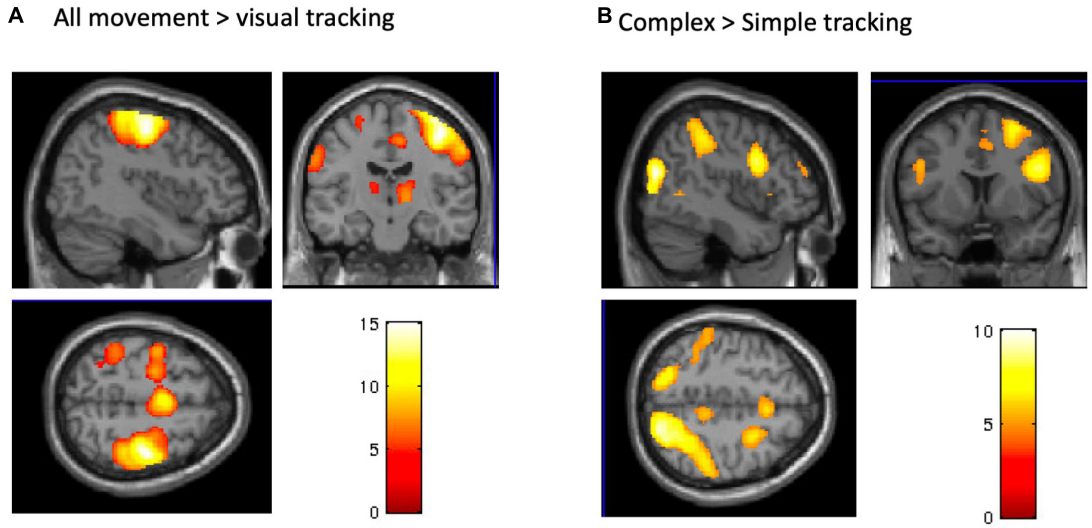

FIGURE 5 | BOLD signals during the tracking task. **(A)** A conjunction analysis between complex and simple visuomotor tasks. The significant regions were the right precentral gyrus, bilateral SMA, contralateral postcentral gyrus, and IPC and SPL ($p < 0.05$, FWE). **(B)** A contrast (complex > simple visuomotor tasks). The significant regions were the right middle occipital gyrus, bilateral SPL, right IPC and premotor cortex, and bilateral SMA ($p < 0.05$, FWE).

no significant correlations just after sham stimulation, or 1 h after anodal TDCS, or using the pre-TDCS MEP values or AP-LM latency difference of the MEPs.

Multiple Regression Analysis

In a follow-up analysis, we specified a multiple regression model combining explanatory variables (AP-LM MEP latency and BOLD signal change in SMA). The combined model explained 54% of the variance in normalized MEP amplitude immediately after real TDCS: (Multiple $R^2 = 0.54$; R^2-adjusted = 0.47; $p = 0.005$). Both explanatory variables had an independent predictive value (signal change in SMA; $p = 0.043$, AP-LM latency; $p = 0.007$) but the AP-LM latency had a higher relative importance (0.65) compared to the task-related BOLD change in the SMA (0.34) (R Core Team, 2017). Both explanatory variables had a variance inflation factor (VIF) of 1.00 indicating that collinearity was not an issue in the model.

TABLE 1 | Task activations for the conjunction analysis between complex and simple task.

Coordinates			Brain region	Cluster size
x	y	z		
42	**−16**	56	**R primary motor cortex**	**6924**
44	−32	64	R superior parietal lobule	
0	0	54	R supplementary motor cortex	
44	−32	64	R superior parietal cortex	
−52	**−24**	**40**	**L inferior parietal lobule**	**1538**
−40	−36	48	L superior parietal lobule	
−34	−37	61	L primary sensory cortex	
−58	**6**	**32**	**L ventral premotor cortex**	**378**
−54	8	18	L inferior frontal gyrus	
−2	**−56**	**−2**	**L cerebellar vermis**	**32**
14	**−16**	**2**	**R thalamus**	**366**
−12	**−4**	**−14**	**L thalamus**	**160**
60	**10**	**28**	**R inferior frontal gyrus**	**268**
−26	**−2**	**2**	**L putamen**	**129**
−44	**−2**	**6**	**L Insula**	**57**

Bold values: correction for multiple comparisons used the FWE method at a corrected $p < 0.05$.

DISCUSSION

In this double-blinded, placebo-controlled study, we prospectively assessed the functional aftereffects of low-intensity anodal TDCS over M1-HAND on corticospinal

TABLE 2 | Task activations when the complex motor task was compared to the simple motor task.

Coordinates			Brain region	Cluster size
x	y	z		
44	**−76**	**18**	**R superior parietal cortex**	**2018**
30	−70	44	R middle occipital cortex	
50	34	44	R inferior parietal cortex	647
−50	**−34**	**42**	**L inferior parietal cortex**	647
46	**8**	**28**	**R inferior frontal gyrus**	**243**
−46	**6**	**28**	**L inferior frontal gyrus**	**204**
30	6	60	R dorsal premotor cortex	955
6	**18**	**46**	**R supplementary motor cortex**	**468**

Bold values: correction for multiple comparisons used the FWE method at a corrected $p < 0.05$. Cluster size is indicated in voxel.

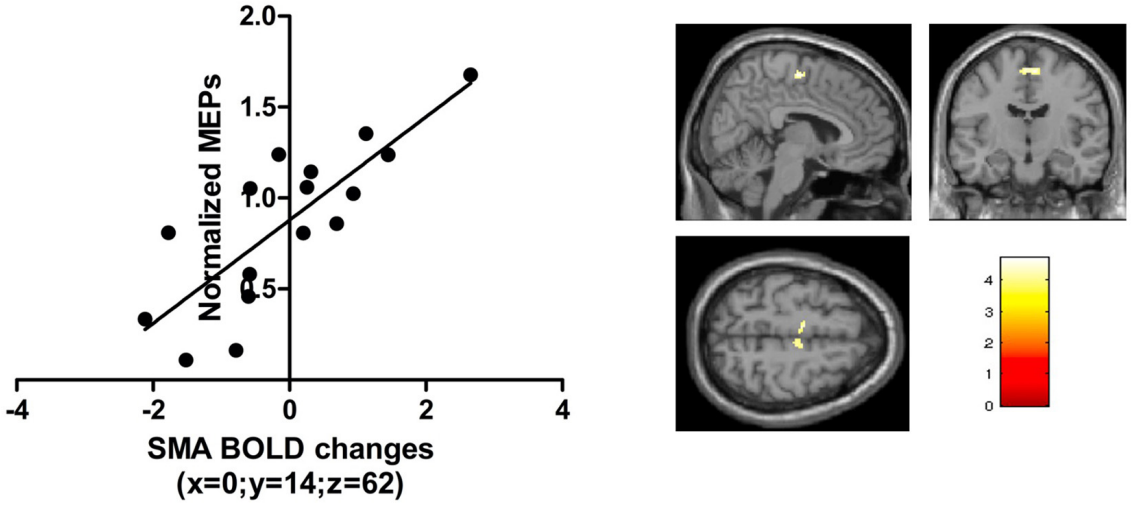

FIGURE 6 | The *t*-scores in the contrast visuomotor tracking vs visual baseline correlated with the normalized TMS amplitudes just after anodal TDCS in a region in the bilateral SMA [peak activation [0, -14, 62]; $p < 0.05$ FWE; small volume correction; 10 mm sphere based on Lee et al. (2003)].

excitability at rest as well as functional cortical activation and performance during visuomotor tracking. At a current intensity of 0.75 mA, 20 min of anodal TDCS did not trigger a consistent modulation of corticospinal excitability, task-related cortical activity or motor performance on a group level. We found that the individual increase in MEP amplitude shortly after anodal TDCS correlated positively with a stronger functional recruitment of SMA during the visuomotor task shortly after TDCS. This correlation was not present after sham stimulation.

Our null finding that anodal TDCS did not have a consistent group effect on corticospinal excitability fits with other studies reporting high variability and a high non-responder rate (Horvath et al., 2014; Lopez-Alonso et al., 2014; Ammann et al., 2017). Together, this recent work suggests that current intensities up to 2 mA may be below the intensity needed to efficiently affect intrinsic neural spiking activity in the cortical target, at least when using the classical bipolar M1-supraorbital montage (Voroslakos et al., 2018). The positive linear relationship between the TDCS-induced increase in task-related SMA activity and TDCS-induced MEP amplitude change suggests that low-intensity TDCS may influence the cortical motor system upstream from M1-HAND.

Several studies have demonstrated that stimulation-induced alterations in corticospinal excitability are associated with more widespread changes in the sensorimotor network (Lang et al., 2005; Jang et al., 2009; Stagg et al., 2009; Gao et al., 2020). Non-invasive transcranial stimulation of the M1-HAND results in stronger functional coupling between the SMA and the sensorimotor cortex (Lee et al., 2003) and leads to increased regional activity in the SMA (Jang et al., 2009; Stagg et al., 2009; R Core Team, 2017; Voroslakos et al., 2018). Our results are in good agreement with these studies, showing a linear relationship between the TDCS effects on corticospinal excitability and changes in task-related activity of the SMA. The results may be accounted for by two mechanisms. On the one hand, the TDCS effect on corticospinal excitability may have triggered a compensatory increase in SMA activity in order to maintain overall network balance despite a change in the corticospinal output function. On the other hand, the TDCS-induced change in corticospinal excitability may have been mediated by an upstream modulation of SMA activation. While the present study cannot differentiate between the two mechanisms, our findings add evidence to a relevant role of the SMA in mediating the neuromodulatory effects of classical bipolar TDCS with the anode placed over the M1-HAND.

Our multiple regression analysis indicated that the AP-LM latency differences had a higher predictive power than the task related SMA activity even though both variables uniquely contributed to explain inter-subject variations in corticospinal facilitation after anodal TDCS. The electrophysiological results confirm the well-known dependency of MEP latencies on the TMS-induced current orientation in the precentral gyrus (Hamada et al., 2013). The larger the latency difference between AP and LM oriented TMS, the more rostrally the AP-TMS stimulus excites cortical neurons in the precentral crown and the more caudally the LM-TMS stimulus excites cortical neurons in the depth of the precentral wall (Hamada et al., 2013; Siebner, 2020). Several previous studies have investigated if individual differences in orientation-dependent MEP latencies relate to TDCS-induced aftereffects and our work is the third study showing a linear relationship between orientation dependency of AP-LM MEP latency and anodal TDCS aftereffects on corticospinal excitability (Wiethoff et al., 2014; Davidson et al., 2016). However, while previous studies reported negative correlations our study found a positive relationship between the orientation-depended latency difference and MEP amplitudes. One possible reason of the discrepancy is the difference in current intensity between studies: Studies that report negative correlations used stronger currents (2mA) than the present study and it may be that that stimulation intensities interact with

the AP-LM latency to differentially determine the efficacy to induce LTP or LTD-like aftereffects. Using transcranial magnetic stimulation (TMS) to stimulate the M1-HAND, Hamada and colleagues found that a large AP-LM MEP latency favors a "canonic" plasticity response, being associated with a large MEP increase after a "facilitatory" TMS protocol (intermittent theta burst stimulation) and a larger MEP decrease after an "inhibitory" TMS protocol (continuous theta burst stimulation) (Hamada et al., 2013). This shows that the sign of the linear relationship between AP-LM MEP latency and the stimulation-induced MEP change may flip when changing a variable of the interventional protocol such as the temporal pattern of stimulation, but possibly also the intensity of stimulation. Hence, the impact of AP-LM latency may "flip" when the intensity of anodal TDCS is increased.

The timing of measurements relative to the administration of TDCS may also have contributed to the discrepant findings regarding the relationship between AP-LM MEP latency and the TDCS-induced change in MEP amplitude. The two studies that reported a negative relationship did measure the AP-LM latencies prior to the TDCS-intervention, whereas our study found a positive relationship and AP-LM latencies were measured at the very end of the second testing day. Indeed, it has been shown that the AP-LM latency itself can be modulated by plasticity-inducing NTBS interventions (Volz et al., 2019). Although the timing of latency measurement relative to TDCS may play a role in determining the relationship between AP-LM MEP latency and TDCS-induced MEP changes, we consider it unlikely that latency measures were significantly influenced by TDCS in this study. We measured latencies approximately one hour after the end of stimulation to minimize the influence of TDCS aftereffects. Further, measurements were performed on the second experimental day, on which half of the participants received sham TDCS. However, more research is needed to clarify how stimulation variables and the relative timing between stimulation and measurements influence the aftereffects of TDCS.

The method to assess the difference in AP-LM MEP latency may also be relevant. While we used the shortest MEP latency out of 20 superimposed MEP waveforms for each separate coil orientation to determine the AP and LM latency, others calculate the AP and LM latency based on an averaging procedure that takes into account all MEPs (Jonker et al., 2020). Using the latter procedure, a recent larger double-blind trial did not find AP-LM MEP latency differences to reliably predict TDCS-induced aftereffects when using a stimulation intensity of 2 mA (Jonker et al., 2020). Together, the existing data on, the predictive value of the individual difference in AP-LM MEP latency on TDCS-related aftereffects on corticomotor excitability are highly interesting, but more research on the impact of methodological factors and specific features of the TDCS protocol, such as intensity or montage, is needed to assess the usefulness of the AP-LM MEP latency as predictive variable in future TDCS studies.

Anodal TDCS over M1-HAND did not affect performance during the visuomotor tracking task. Previous literature on the effects of TDCS on motor performance has suggested that behavioral effects are most prominent when TDCS is applied concurrently with the training task or when the motor task and stimulation are interleaved (Reis and Fritsch, 2011; Buch et al., 2017). This may explain why we were not able to show a measurable effect of anodal TDCS on motor performance. Alternatively, continuous visuomotor tracking may be a motor skill that may not benefit from anodal TDCS or would require a higher current intensity to show consistent effects of TDCS at the behavioral level.

A strength of this study is its double-blinded, placebo-controlled study design. MEP measurements are strongly dependent on the investigator holding the coil, even if neuro-navigation and other standard methods are applied. Knowledge about the session type might lead the experimenter to unconsciously influence study outcome and thereby artificially increasing the effect size and studies with a similarly rigorous design have also not shown effects of anodal TDCS on corticospinal excitability, even at significantly higher stimulation intensities (2 mA) (Jonker et al., 2020). A limitation of this study was that mean MEP amplitudes at pre-TDCS baseline were not matched between the real and sham TDCS conditions. This between-session difference emerged despite of our attempts to keep variability between sessions as small as possible by choosing a within-subject design, MRI-guided neuronavigation and controlling for circadian variations by scheduling both sessions at the same time of day. However, we don't think that these differences in baseline MEP between sessions challenge the main conclusions of this study as a post-hoc analysis, in which the individuals that caused the baseline difference, were removed did not alter our conclusions.

CONCLUSION

The after-effects of weak-current (0.75 mA) anodal TDCS stimulation targeting M1-HAND are highly variable, confirming several anodal TDCS studies, using the same electrode set-up but higher current intensities. Individual susceptibility to the neuromodulatory effects of TDCS on corticospinal excitability is likely to be determined by various physiological factors, including physiological properties of the precentral gyrus – as reflected by the orientation-dependent effect of single TMS on MEP latency and by the fact that the response pattern was predicted by individual differences in sensitivity to coil orientation. Further, the magnitude of TDCS-induced changes in corticospinal excitability correlated positively with the TDCS-induced increase in BOLD activity in the SMA. This linear relationship suggests that physiological features upstream from the primary motor cortex may mediate how anodal TDCS changes corticospinal excitability.

DATA AVAILABILITY STATEMENT

The raw data supporting the conclusions of this article will be made available by the authors, without undue reservation.

ETHICS STATEMENT

The studies involving human participants were reviewed and approved by Research Ethics Committees of the Capital Region H-2-2013-040. The patients/participants provided their written informed consent to participate in this study.

AUTHOR CONTRIBUTIONS

AK, KS, ER, and HS designed the study. KS, YS, and AK collected the data. KS and AK analyzed the data. AK, KS, YS, ER, and HS wrote the manuscript. All authors contributed to the article and approved the submitted version.

FUNDING

The study was supported by a Grant of Excellence "Mapping, Modulation and Modeling the Control of Actions" from Lundbeckfonden (grant nr. R59 A5399) awarded to HS. HS holds a 5-year professorship in precision medicine at the Faculty of Health Sciences and Medicine, University of Copenhagen which is sponsored by the Lundbeck Foundation (Grant Nr. R186-2015-2138).

REFERENCES

Aberra, A. S., Wang, B., Grill, W. M., and Peterchev, A. V. (2020). Simulation of transcranial magnetic stimulation in head model with morphologically-realistic cortical neurons. *Brain Stimul.* 13, 175–189. doi: 10.1016/j.brs.2019.10.002

Ammann, C., Lindquist, M. A., and Celnik, P. A. (2017). Response variability of different anodal transcranial direct current stimulation intensities across multiple sessions. *Brain Stimul.* 10, 757–763. doi: 10.1016/j.brs.2017.04.003

Ammann, C., Spampinato, D., and Marquez-Ruiz, J. (2016). Modulating Motor learning through transcranial direct-current stimulation: an integrative view. *Front. Psychol.* 7:1981. doi: 10.3389/fpsyg.2016.01981

Antal, A., Polania, R., Schmidt-Samoa, C., Dechent, P., and Paulus, W. (2011). Transcranial direct current stimulation over the primary motor cortex during fMRI. *NeuroImage* 55, 590–596. doi: 10.1016/j.neuroimage.2010.11.085

Antonenko, D., Nierhaus, T., Meinzer, M., Prehn, K., Thielscher, A., Ittermann, B., et al. (2018). Age-dependent effects of brain stimulation on network centrality. *Neuroimage* 176, 71–82. doi: 10.1016/j.neuroimage.2018.04.038

Awiszus, F. (2003). TMS and threshold hunting. *Suppl. Clin. Neurophysiol.* 56, 13–23. doi: 10.1016/s1567-424x(09)70205-3

Brunoni, A. R., Amadera, J., Berbel, B., Volz, M. S., Rizzerio, B. G., and Fregni, F. (2011). A systematic review on reporting and assessment of adverse effects associated with transcranial direct current stimulation. *Int. J. Neuropsychopharmacol. Off. Sci. J. Colleg. Int. Neuropsychopharmacol.* 14, 1133–1145. doi: 10.1017/s1461145710001690

Buch, E. R., Santarnecchi, E., Antal, A., Born, J., Celnik, P. A., Classen, J., et al. (2017). Effects of tDCS on motor learning and memory formation: a consensus and critical position paper. *Clin. Neurophysiol.* 128, 589–603. doi: 10.1016/j.clinph.2017.01.004

Chew, T., Ho, K. A., and Loo, C. K. (2015). Inter- and Intra-individual variability in response to transcranial direct current stimulation (tDCS) at varying current intensities. *Brain Stimul.* 8, 1130–1137. doi: 10.1016/j.brs.2015.07.031

Davidson, T. W., Bolic, M., and Tremblay, F. (2016). Predicting modulation in corticomotor excitability and in transcallosal inhibition in response to anodal transcranial direct current stimulation. *Front. Hum. Neurosci.* 10:49. doi: 10.3389/fnhum.2016.00049

Gao, Y., Cavuoto, L., Schwaitzberg, S., Norfleet, J. E., Intes, X., and De, S. (2020). The Effects of transcranial electrical stimulation on human motor functions: a comprehensive review of functional neuroimaging studies. *Front. Neurosci.* 14:744. doi: 10.3389/fnins.2020.00744

Grundey, J., Thirugnanasambandam, N., Kaminsky, K., Drees, A., Skwirba, A. C., Lang, N., et al. (2012). Neuroplasticity in cigarette smokers is altered under withdrawal and partially restituted by nicotine exposition. *J. Neurosci.* 32, 4156–4162. doi: 10.1523/jneurosci.3660-11.2012

Guerra, A., Lopez-Alonso, V., Cheeran, B., and Suppa, A. (2020). Variability in non-invasive brain stimulation studies: reasons and results. *Neurosci. Lett.* 719:133330. doi: 10.1016/j.neulet.2017.12.058

Hamada, M., Murase, N., Hasan, A., Balaratnam, M., and Rothwell, J. C. (2013). The role of interneuron networks in driving human motor cortical plasticity. *Cerebral Cortex* 23, 1593–1605. doi: 10.1093/cercor/bhs147

Horvath, J. C., Carter, O., and Forte, J. D. (2014). Transcranial direct current stimulation: five important issues we aren't discussing (but probably should be). *Frontiers in systems neuroscience* 8:2. doi: 10.3389/fnsys.2014.00002

Jang, S. H., Ahn, S. H., Byun, W. M., Kim, C. S., Lee, M. Y., and Kwon, Y. H. (2009). The effect of transcranial direct current stimulation on the cortical activation by motor task in the human brain: an fMRI study. *Neurosci. Lett.* 460, 117–120. doi: 10.1016/j.neulet.2009.05.037

Jonker, Z. D., Gaiser, C., Tulen, J. H. M., Ribbers, G. M., Frens, M. A., and Selles, R. W. (2020). No effect of anodal tDCS on motor cortical excitability and no evidence for responders in a large double-blind placebo-controlled trial. *Brain Stimul.* 14, 100–109. doi: 10.1016/j.brs.2020.11.005

Karabanov, A., Thielscher, A., and Siebner, H. R. (2016). Transcranial brain stimulation: closing the loop between brain and stimulation. *Curr. Opin. Neurol.* 29, 397–404. doi: 10.1097/wco.0000000000000342

Karabanov, A. N., Raffin, E., and Siebner, H. R. (2015). The resting motor threshold–restless or resting? A repeated threshold hunting technique to track dynamic changes in resting motor threshold. *Brain stimulation* 8, 1191–1194. doi: 10.1016/j.brs.2015.07.001

Karabanov, A. N., and Siebner, H. (in press). "A conceptional framework for combining brain mapping and brain stimulation," in *Oxford Handbook of Transcranial Stimulation*, ed. E. M. Wassermann (Oxford: Oxford University Press).

Kwon, Y. H., and Park, J. W. (2011). Different cortical activation patterns during voluntary eccentric and concentric muscle contractions: an fMRI study. *NeuroRehabilitation* 29, 253–259. doi: 10.3233/nre-2011-0701

Lang, N., Siebner, H. R., Ward, N. S., Lee, L., Nitsche, M. A., Paulus, W., et al. (2005). How does transcranial DC stimulation of the primary motor cortex alter regional neuronal activity in the human brain? *Eur. J. Neurosci.* 22, 495–504. doi: 10.1111/j.1460-9568.2005.04233.x

Lee, L., Siebner, H. R., Rowe, J. B., Rizzo, V., Rothwell, J. C., Frackowiak, R. S., et al. (2003). Acute remapping within the motor system induced by low-frequency repetitive transcranial magnetic stimulation. *J. Neurosci.* 23, 5308–5318. doi: 10.1523/jneurosci.23-12-05308.2003

Lefebvre, S., Jann, K., Schmiesing, A., Ito, K., Jog, M., Schweighofer, N., et al. (2019). Differences in high-definition transcranial direct current stimulation over the motor hotspot versus the premotor cortex on motor network excitability. *Sci. Rep.* 9:17605.

Liebetanz, D., Nitsche, M. A., Tergau, F., and Paulus, W. (2002). Pharmacological approach to the mechanisms of transcranial DC-stimulation-induced after-effects of human motor cortex excitability. *Brain* 125(Pt 10), 2238–2247. doi: 10.1093/brain/awf238

Lopez-Alonso, V., Cheeran, B., Rio-Rodriguez, D., and Fernandez-Del-Olmo, M. (2014). Inter-individual variability in response to non-invasive brain stimulation paradigms. *Brain Stimul.* 7, 372–380. doi: 10.1016/j.brs.2014.02.004

McCambridge, A. B., Stinear, J. W., and Byblow, W. D. (2015). 'I-wave' recruitment determines response to tDCS in the upper limb, but only so far. *Brain Stimul.* 8, 1124–1129. doi: 10.1016/j.brs.2015.07.027

Nitsche, M. A., and Paulus, W. (2000). Excitability changes induced in the human motor cortex by weak transcranial direct current stimulation. *J. Physiol.* 527(Pt 3), 633–639. doi: 10.1111/j.1469-7793.2000.t01-1-00633.x

Nitsche, M. A., and Paulus, W. (2011). Transcranial direct current stimulation–update 2011. *Restor. Neurol. Neurosci.* 29, 463–492. doi: 10.3233/rnn-2011-0618

Ogawa, K., Inui, T., and Sugio, T. (2007). Neural correlates of state estimation in visually guided movements: an event-related fMRI study. *Cortex* 43, 289–300. doi: 10.1016/s0010-9452(08)70455-6

Oldfield, R. C. (1971). The assessment and analysis of handedness: the Edinburgh inventory. *Neuropsychologia* 9, 97–113. doi: 10.1016/0028-3932(71)90067-4

Peirce, J. W. (2008). Generating stimuli for neuroscience using PsychoPy. *Front. Neuroinform.* 2:10.

R Core Team (2017). *R: A Language and Environment for Statistical Computing*. Vienna: R Foundation for Statistical Computing.

Raffin, E., and Siebner, H. R. (2019). Use-dependent plasticity in human primary motor hand area: synergistic interplay between training and immobilization. *Cereb Cortex* 29, 356–371. doi: 10.1093/cercor/bhy226

Reis, J., and Fritsch, B. (2011). Modulation of motor performance and motor learning by transcranial direct current stimulation. *Curr. Opin. Neurol.* 24, 590–596. doi: 10.1097/wco.0b013e32834c3db0

Ridding, M. C., and Ziemann, U. (2010). Determinants of the induction of cortical plasticity by non-invasive brain stimulation in healthy subjects. *J. Physiol.* 588(Pt 13), 2291–2304. doi: 10.1113/jphysiol.2010.190314

Siebner, H. R. (2020). Does TMS of the precentral motor hand knob primarily stimulate the dorsal premotor cortex or the primary motor hand area? *Brain Stimul.* 13, 517–518. doi: 10.1016/j.brs.2019.12.015

Siebner, H. R., Takano, B., Peinemann, A., Schwaiger, M., Conrad, B., and Drzezga, A. (2001). Continuous transcranial magnetic stimulation during positron emission tomography: a suitable tool for imaging regional excitability of the human cortex. *Neuroimage* 14, 883–890. doi: 10.1006/nimg.2001.0889

Stagg, C. J., O'Shea, J., Kincses, Z. T., Woolrich, M., Matthews, P. M., and Johansen-Berg, H. (2009). Modulation of movement-associated cortical activation by transcranial direct current stimulation. *Eur. J. Neurosci.* 30, 1412–1423. doi: 10.1111/j.1460-9568.2009.06937.x

Strube, W., Bunse, T., Nitsche, M. A., Nikolaeva, A., Palm, U., Padberg, F., et al. (2016). Bidirectional variability in motor cortex excitability modulation following 1 mA transcranial direct current stimulation in healthy participants. *Physiol. Rep.* 4:e12884. doi: 10.14814/phy2.12884

Thielscher, A., Antunes, A., and Saturnino, G. B. (2015). Field modeling for transcranial magnetic stimulation: a useful tool to understand the physiological effects of TMS? *Annu. Int. Conf. IEEE Eng. Med. Biol. Soc.* 2015, 222–225.

Volz, L. J., Hamada, M., Michely, J., Pool, E. M., Nettekoven, C., Rothwell, J. C., et al. (2019). Modulation of I-wave generating pathways by theta-burst stimulation: a model of plasticity induction. *J. Physiol.* 597, 5963–5971. doi: 10.1113/jp278636

Voroslakos, M., Takeuchi, Y., Brinyiczki, K., Zombori, T., Oliva, A., Fernandez-Ruiz, A., et al. (2018). Direct effects of transcranial electric stimulation on brain circuits in rats and humans. *Nat. Commun.* 9:483.

Wiethoff, S., Hamada, M., and Rothwell, J. C. (2014). Variability in response to transcranial direct current stimulation of the motor cortex. *Brain Stimul.* 7, 468–475.

Conflict of Interest: HS has received honoraria as speaker from Sanofi Genzyme, Denmark and Novartis, Denmark, as consultant from Sanofi Genzyme, Denmark, Lophora, Denmark, and Lundbeck AS, Denmark, and as editor-in-chief (Neuroimage Clinical) and senior editor (NeuroImage) from Elsevier Publishers, Amsterdam, The Netherlands. He has received royalties as book editor from Springer Publishers, Stuttgart, Germany and from Gyldendal Publishers, Copenhagen, Denmark.

The remaining authors declare that the research was conducted in the absence of any commercial or financial relationships that could be construed as a potential conflict of interest.

APPENDIX

Appendix Side Effects of TDCS

There was not a significant difference in the items rating two (mild) or more points on the questionnaire ($p > 0.05$, Fisher's exact test).

	Anodal (n = 17)	**Sham (n = 17)**	**Fisher's exact test**
Headache	3	2	1.000
Neck pain	2	2	1.000
Scalp pain	3	1	0.601
Tingling	5	10	0.166
Itching	7	5	0.721
Burning	9	11	0.728
Redness	2	0	0.485
Sleepness	11	9	0.728
Trouble concentraining	7	4	0.465
Acute mood change	0	0	–

frontiers in Human Neuroscience

MINI REVIEW
published: 12 May 2021
doi: 10.3389/fnhum.2021.661396

Tapping the Potential of Multimodal Non-invasive Brain Stimulation to Elucidate the Pathophysiology of Movement Disorders

*Sakshi Shukla and Nivethida Thirugnanasambandam**

National Brain Research Centre (NBRC), Manesar, India

This mini-review provides a detailed outline of studies that have used multimodal approaches in non-invasive brain stimulation to investigate the pathophysiology of the three common movement disorders, namely, essential tremor, Parkinson's disease, and dystonia. Using specific search terms and filters in the PubMed® database, we finally shortlisted 27 studies in total that were relevant to this review. While two-thirds (Brittain et al., 2013) of these studies were performed on Parkinson's disease patients, we could find only three studies that were conducted in patients with essential tremor. We clearly show that although multimodal non-invasive brain stimulation holds immense potential in unraveling the physiological mechanisms that are disrupted in movement disorders, the technical challenges and pitfalls of combining these methods may hinder their widespread application by movement disorder specialists. A multidisciplinary team with clinical and technical expertise may be crucial in reaping the fullest benefits from such novel multimodal approaches.

Keywords: non-invasive brain stimulation, movement disorder, transcranial magnetic stimulation, magnetic resonance imaging, positron emission tomograghy, essential tremor, Parkinson's disease, dystonia

OPEN ACCESS

Edited by:
Filippo Brighina,
University of Palermo, Italy

Reviewed by:
Robert LeMoyne,
Northern Arizona University, United States
Antonella Conte,
Sapienza University of Rome, Italy

***Correspondence:**
Nivethida Thirugnanasambandam
dr.nivethida@gmail.com;
nivethida@nbrc.ac.in

Specialty section:
This article was submitted to Brain Imaging and Stimulation, a section of the journal Frontiers in Human Neuroscience

Received: *30 January 2021*
Accepted: *30 March 2021*
Published: *12 May 2021*

Citation:
Shukla S and Thirugnanasambandam N (2021) Tapping the Potential of Multimodal Non-invasive Brain Stimulation to Elucidate the Pathophysiology of Movement Disorders. Front. Hum. Neurosci. 15:661396. doi: 10.3389/fnhum.2021.661396

INTRODUCTION

Movement disorders are a class of neurological syndromes that are characterized by uncontrollable, abnormally increased, or decreased movements. They rank among the most common neurological diseases with a prevalence of about 28% in middle-aged and elderly populations (Wenning et al., 2005). The most common movement disorders include essential tremor, Parkinson's disease, and dystonia (Wichmann, 2018). These disorders are often progressive, increasing in severity, thereby causing considerable disability over time. Little is known about the pathophysiology of these disorders, and a lot still remains to be explored. Understanding their pathophysiological mechanisms is crucial to developing novel diagnostic tools and therapeutic strategies. Non-invasive brain stimulation (NIBS) methods have played a key role in understanding the neurophysiological mechanisms underlying clinical phenomena in patients with movement disorders (Quartarone, 2013; Rothwell, 2007; Ugawa et al., 2020). Transcranial magnetic stimulation (TMS), is a painless, non-invasive brain stimulation technique that has been used to study motor physiology for over three decades (Hallett, 2000; Chail et al., 2018). Novel TMS paradigms have been developed

over the years to unravel the physiology of human motor control in health and disease. TMS has contributed significantly to our understanding of the altered neurophysiology in patients with movement disorders, for example, in dissociating the neural networks causing essential and parkinsonian tremors (Hanajima et al., 2016; Shih and Pascual-Leone, 2017), in identifying the impaired cortical inhibition in dystonia and Parkinson's disease (Rothwell, 2007), and in differentiating the diagnosis of organic and functional dystonia (Quartarone et al., 2009). Recently, other NIBS methods such as transcranial direct/alternating current stimulation (tDCS/tACS) have also gained attention (Antal et al., 2017). These techniques, although in their infancy, offer great promise in exploring the pathophysiology of movement disorders. A more efficient approach is to combine the use of different NIBS with neuroimaging/neurophysiological methods such as Positron emission tomography (PET), magnetic resonance imaging (MRI), and magneto-/electro-encephalography (M/EEG). The knowledge gained from such a multimodal approach could be manifold as compared with employing individual techniques. **Figure 1** shows the different non-invasive brain stimulation and neuroimaging/neurophysiological methods that can be combined effectively for studying movement disorders.

In this mini review, we describe the different multimodal NIBS approaches that have been used to study the pathophysiology of movement disorders and also discuss the immense potential such an approach offers in enhancing our understanding of these disorders. We discuss the three most common movement disorders—essential tremor, Parkinson's disease, and dystonia—and how multimodal NIBS studies have enhanced our knowledge and understanding of these disorders. We also propose future research directions for movement disorder specialists by discussing the scope of some of the most recent advancements in the field of NIBS.

MATERIALS AND METHODS

This mini-review includes research studies conducted to date that have used a multimodal approach using non-invasive brain stimulation techniques for movement disorders such as Parkinson's disease, dystonia, and essential tremor. Related research studies were searched on the PubMed® database[1] using the advanced search builder feature. Within the "All fields" category, search terms were added in the following pattern: ([(Disease name) OR (Disease Acronym)] AND [(Non-invasive brain technique) OR (Acronym)] AND [(other technique) OR (Acronym)]). An example of a search terms sequence used for Parkinson's Disease was: "([(Parkinson's Disease) OR (PD)] AND [(Transcranial Magnetic Stimulation) OR (TMS)] AND [(Magnetic Resonance Imaging) OR (MRI)])." Similarly, various different combinations of NIBS techniques and other modalities were searched for each of the three diseases. A total of 1,416, 506, and 86 results were obtained for PD, Dystonia, and ET, respectively. Out of the total number of results, studies with a multimodal approach were filtered out for each disease, which counted about 86 for PD, 14 for dystonia, and 3 for ET. Furthermore, case reports and review articles were excluded. Finally, the number of research articles included in qualitative synthesis were 18, 6, and 3 for PD, dystonia, and ET, respectively. The relevant papers were then thoroughly read and reread, with the aim of determining key methods used and their advantages. Their results were analyzed as to how different multimodal approaches help in elucidating the pathophysiology of movement disorders.

[1]http://pubmed.ncbi.nlm.nih.gov

Essential Tremor

Essential tremor (ET) is a brain disorder that causes uncontrollable and rhythmic shaking of one or more body parts, most commonly the upper limbs. It is the most common movement disorder affecting approximately 4% of adults over the age of 40 years (Zesiewicz et al., 2010). Although about half of the patients with ET have a positive family history, an equal percentage of them are idiopathic (Elble, 2013). The diagnosis is often confused with Parkinsonian tremor or dystonic tremor (Tarakad and Jankovic, 2018; Panyakaew et al., 2020). It is important to differentiate among these tremor types for their effective management. However, little is known about the pathophysiology underlying tremors of different etiologies. We found only a few studies in literature that employed multimodal NIBS to investigate ET. A notable study by Popa et al. (2013) showed that low frequency (1 Hz) repetitive TMS (rTMS) applied over bilateral posterior cerebellar cortices for a week successfully reduced the overall amplitude of the tremors. Furthermore, this clinical effect, which lasted for about 3 weeks, was associated with an improvement in the functional connectivity of the cerebello-thalamo-cortical network and there was no change in the functional connectivity within other networks such as the default mode network. These results clearly indicate that ET may be caused by abnormal connectivity in the cerebello-thalamo-cortical circuit and that suppressing the excitability of the bilateral cerebellum using rTMS could be an effective treatment option for patients with severe ET. Another study by Lu et al. (2016) investigated the effect of an associative plasticity-inducing TMS protocol, on the structural connectivity of the corticospinal tract in patients with ET and Parkinson's disease with intention tremor. The authors found that the microstructure of the corticospinal tract was intact in both these patient groups, suggesting that the corticospinal tract may not be relevant to the deficient motor plasticity seen in them (Lu et al., 2016). Fox and colleagues showed, using resting-state functional connectivity MRI, that NIBS was effective only if applied to cortical regions with good functional connectivity to effective deep brain stimulation sites. This reiterates the importance of combining information from neuroimaging to effectively target NIBS.

ET, although the most common movement disorder, has not been studied enough using multimodal approaches. Novel NIBS methods, especially transcranial alternating current stimulation (tACS) administered in a closed-loop pattern, have proven to be beneficial in reducing the tremor amplitude in ET patients (Brittain et al., 2013; Schreglmann et al., 2021). Investigating the

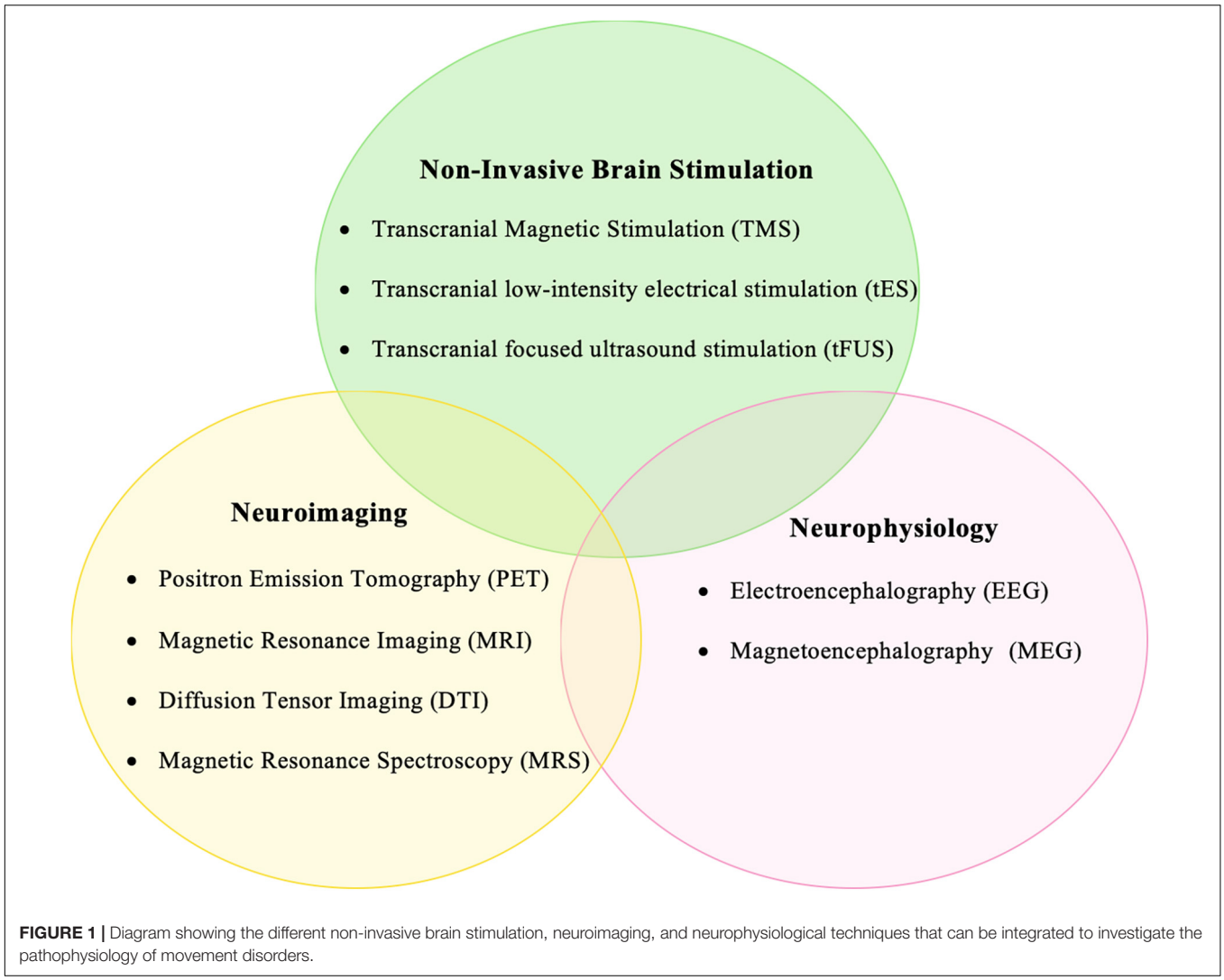

FIGURE 1 | Diagram showing the different non-invasive brain stimulation, neuroimaging, and neurophysiological techniques that can be integrated to investigate the pathophysiology of movement disorders.

pathophysiology of ET using concurrent tACS with M/EEG is likely to shed light on the contribution of key neurophysiological mechanisms in the disease process.

Parkinson's Disease

Parkinson's disease (PD) is a neurodegenerative disorder characterized by loss of dopaminergic neurons in the substantia nigra of the basal ganglia, manifesting itself as bradykinesia, rigidity, rest tremor, postural imbalance, and other non-motor features (Poewe et al., 2017). Although some of the primary disease symptoms respond to dopamine supplementation, not all features of the disease are mediated by a dopaminergic deficit (Miguelez et al., 1460). The neurophysiological mechanisms underlying several of the clinical features of PD still remain to be explored (Jankovic and Sherer, 2014). Here we discuss some of the multimodal NIBS approaches that have been employed to study the pathophysiology of PD.

Positron emission tomography (PET) is a functional neuroimaging technique that uses radioactive tracer elements to visualize and measure changes in cerebral blood flow resulting from metabolic processes. The combination of PET and TMS to study PD was already used as recently as 2001. Strafella et al. (2001) used [^{11}C] raclopride (a dopamine receptor ligand) to measure the dopamine release in the human striatum following rTMS to the dorsolateral prefrontal cortex (DLPFC). rTMS was also applied to the occipital region as a control. Low frequency (1 Hz) rTMS to DLPFC but not to the occipital cortex decreased the [^{11}C] raclopride binding potential in the ipsilateral caudate nucleus, implying that activation of corticostriatal fibers originating in the DLPFC is involved in dopamine release at the respective projection site in the striatum. In a follow-up study, it was also shown that rTMS in the primary motor cortex induced dopamine release in the ipsilateral putamen (Strafella et al., 2003). Furthermore, the same combination of TMS and PET was used to identify potential differences in corticostriatal dopamine release between the symptomatic and presymptomatic hemispheres. A frequency of 10 Hz rTMS to the primary motor cortex on the symptomatic hemisphere revealed less striatal dopamine release; however, with a significantly larger cluster size. This spatially enlarged area of dopamine

release in the symptomatic hemisphere possibly indicates a loss of functional segregation and abnormal corticostriatal transmission in early PD (Strafella et al., 2005). Sacheli et al. (2019) conducted a multimodal study combining PET and fMRI during TMS to investigate the effects of exercise in PD patients. They aimed to evaluate the effect of exercise on dorsal striatal dopamine release and the ventral striatal response to reward anticipation. The results of this study showed that exercise in PD patients enhances the dopaminergic function and reward-related responsivity in both nigrostriatal and mesolimbic projections, thereby contributing to improvements in motor function, mood, and apathy. Fregni et al. (2006) also studied depression in PD using rTMS and SPECT, which measured the changes in regional cerebral blood flow (rCBF). They reported significantly lower rCBF in the left prefrontal, posterior cingulate gyrus, and left insula and right parietal cortex in PD patients as compared with healthy controls. Furthermore, rTMS improved depression significantly associated with increased rCBF in the posterior cingulate cortex, indicating that depression in PD is associated with a dysfunction of the fronto-limbic network connectivity that can be effectively modulated by rTMS.

Magnetic resonance spectroscopy (MRS) is used to measure the different metabolite concentrations in the brain. Flamez et al. (2019) applied 1Hz rTMS over the right pre-supplementary motor area (SMA) and assessed the change in choline/creatine ratio in PD patients. They found that low frequency (1 Hz) rTMS significantly increased the choline/creatine ratio but only when disease duration was taken into account, that is, the shorter the duration of disease, the stronger the observed effects were. This implies that in the early stages of PD, membrane turnover at the pre-SMA could still be influenced by a single session of rTMS suggesting that at least some brain plasticity is preserved. In addition to primary motor deficits, PD patients have abnormal sensory processing (Hwang et al., 2016). Functional MRI combined with somatosensory stimulation in the form of vibrotactile stimulation (Nelson et al., 2018) or laser-induced nociceptive stimulation (Petschow et al., 2016) revealed deficient activation of the somatosensory cortex in the former and the nodes of the central pain matrix in the latter for PD patients. A TMS-fMRI study revealed that depression in PD patients may result from increased activity of the medial prefrontal cortex (Cardoso et al., 2008).

One of the recent advances in the field of NIBS is the successful coupling of TMS and EEG (Tremblay et al., 2019). Both these techniques have an excellent temporal resolution that makes it an excellent combination to examine the neurophysiological processes that take place within a millisecond. Although the field of TMS-EEG is still in its infancy, it has already been used successfully to study PD. Concurrent TMS-EEG has yielded a wealth of new information on the pathophysiology of PD, which neither of the techniques did when used individually. One of the earliest TMS-EEG studies in PD patients by Casarotto et al. (2019) showed that levodopa intake increased the cortical reactivity over the SMA ipsilateral to the more affected putamen. TMS-EEG has also been used to study the role of the motor cortex in re-emergent tremor in PD (Leodori et al., 2020). TMS over the primary motor cortex caused stable resetting of the re-emergent tremor, which suggests that the primary motor cortex is a crucial node in the cortico-subcortical network that generates a re-emergent tremor and is more than just an output region. TMS-induced oscillatory activity was studied by Van Der Werf et al. (2006) in PD patients who underwent unilateral thalamotomy. They reported that the TMS-induced beta oscillatory power was lower in the operated hemisphere, indicating that thalamotomy successfully reduced the pathological beta oscillations in the cortico-subcortical network in PD patients. NIBS methods other than TMS have also been used in combination with neuroimaging to study PD. Pereira et al. (2013) integrated tDCS and fMRI to study phonemic and semantic fluency, another non-motor feature in PD patients. They observed that tDCS over DLPFC, but not the temporo-parietal cortex, enhanced functional connectivity in the verbal fluency and the deactivation task-related network.

Levodopa-induced dyskinesias (LID) are a common complication of PD (Espay et al., 2018). Although there are a few hypotheses, the exact etiology of LID is unknown (Pandey and Srivanitchapoom, 2017). A resting-state fMRI revealed impaired functional connectivity between the right inferior frontal cortex, contralateral primary motor cortex, and ipsilateral putamen with levodopa intake. Furthermore, continuous theta-burst stimulation applied over the right inferior frontal cortex reduced dyskinesia severity suggesting that the pathophysiological mechanisms underlying LID may extend beyond the basal ganglia and possibly involve neural networks centered on the inferior frontal cortex (Cerasa et al., 2015). Another study by Brusa et al. (2012) showed improvement of dyskinetic symptoms associated with a reduction of ^{18}fluorodeoxyglucose (FDG) metabolism in the cerebellum following 1 week of daily bilateral cerebellar continuous theta-burst stimulation. These findings suggest that the interventional TMS protocol modulated the activity of neural pathways connecting the cerebellar cortex with deep cerebellar nuclei.

In summary, PD has been the most investigated movement disorder using multimodal NIBS approaches. These studies have been able to successfully identify novel neurophysiological mechanisms that are likely to contribute to the pathophysiology of PD.

Dystonia

Dystonia is a complex and highly variable movement disorder characterized by involuntary muscle contractions that cause slow, repetitive, twisting movements or abnormal postures affecting any body part such as the arms, legs, trunk, face, or vocal cords (Phukan et al., 2011). The etiology of primary/idiopathic dystonia is not known; hence, treatment options are also very limited (Balint et al., 2018). The most common form of idiopathic dystonia is focal (involving a single body part) and therefore is also the most studied form of dystonia, using multimodal NIBS. Neuroimaging studies suggest that dystonia is likely to be a disorder of abnormal functional connectivity (van Wijk et al., 2017). Bharath et al. (2015) using fMRI showed that resting-state functional connectivity within the network comprising the contralateral premotor cortex,

intraparietal sulcus, cerebellum, bilateral thalamus, putamen, globus pallidus, and the bilateral supplementary motor area was lower in patients with writer's cramp (WC) and that low-frequency (1 Hz) rTMS administered over the primary motor cortex-improved functional connectivity within the motor network. The authors, using a combination of rTMS and fMRI, concluded that WC is probably a network disorder involving subcortical and trans-hemispheric brain regions with widespread dysfunction much larger than is clinically evident. From several studies, we know that impaired sensorimotor integration also plays a role in the pathophysiology of dystonia. Schneider et al. (2010) applied high-frequency rTMS over the left primary somatosensory cortex in WC patients and measured its effects on tactile discrimination accuracy and hemodynamic activity. Their findings revealed that tactile discrimination in patients was lower than that in healthy controls and that 5 Hz rTMS did not improve the condition. On fMRI, rTMS-induced improvement in discrimination in healthy controls that was associated with enhanced basal ganglia activation was absent in WC patients. This may reflect impaired basal ganglia-somatosensory connectivity in WC patients. An rTMS interventional study (Havrankova et al., 2010) also supports the hypothesis that clinical improvement in writer's cramp patients following multiple rTMS sessions over the primary somatosensory cortex is associated with enhanced connectivity in the sensorimotor network comprising the primary somatosensory, supplementary motor, and posterior parietal cortices. Apart from the primary motor and somatosensory cortices, the multimodal approach enabled us to study the role of upstream brain regions such as the premotor and parietal cortices in the pathophysiology of dystonia. In a very recent study by Merchant et al. (2020), the authors demonstrated significant interactions between the principal nodes of fine motor control namely, the ventral premotor cortex, the anterior and dorsal inferior parietal lobules, and the motor cortex by integrating TMS, structural and functional MRI methods. They found that the parieto-motor interactions as assessed by TMS were abnormal in WC patients. Although there was no significant change in the structural connectivity within the parietal-premotor-motor network in these patients, the dorsal inferior parietal lobule-premotor connectivity in the resting state was abnormally high in them. By suppressing the activity of the dorsal inferior parietal lobule using continuous theta burst stimulation, the parieto-motor interactions were restored to levels similar to healthy controls. The findings of this study indicate that the dorsal inferior parietal lobule, a region that is crucial for multimodal sensory association, could be interfering with the fine motor control network in WC patients and the same can possibly be restored by appropriate non-invasive brain stimulation methods. de Vries et al. (2012) studied the impact of low-frequency rTMS over the left superior parietal cortex on the fMRI activation patterns during executed and imagined wrist movement in cervical dystonia patients. Cervical dystonia patients showed similar but weaker activation patterns especially in the angular gyrus, suggesting poor compensatory ability of the superior parietal cortex in these patients. To add more evidence to the hypothesis of impaired compensatory mechanisms, Odorfer et al. (2019) used continuous theta burst stimulation over bilateral cerebellum to interfere with finger-tapping ability in cervical dystonia patients. They reported that finger movements, although clinically unaffected in these patients, were associated with increased activation of the lateral cerebellum on fMRI, which is likely due to compensatory disinhibitory effect on the Purkinje cells, resulting in inhibition of cerebello-thalamo-cortical circuits in cervical dystonia. Another study in adductor spasmodic dysphonia patients also suggests a possible imbalance of inhibitory processes during phonation and its correlation with hemodynamic activation of the left laryngeal motor cortex on

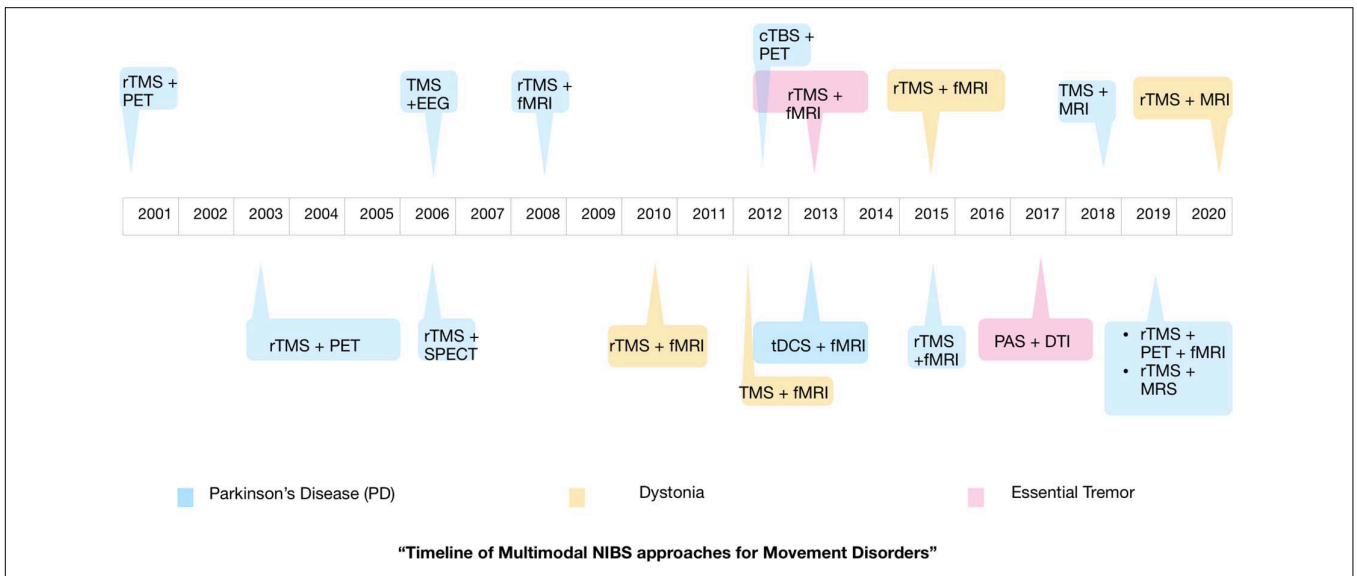

FIGURE 2 | Timeline showing the publication of multimodal non-invasive brain stimulation (NIBS) studies investigating movement disorders. Parkinson's disease is the most studied movement disorder using multimodal NIBS. The majority of studies used a combination of repetitive TMS and MRI.

fMRI (Chen et al., 2020). Lumsden et al. (2015) studied children with acquired dystonia in whom they performed diffusion tensor imaging (DTI) and also measured central motor conduction time (CMCT) using TMS. They found that over half of the patients had normal CMCT in spite of white matter damage. Moreover, CMCT in these patients did not correlate with DTI parameters, and, also, changes in CMCT were not reflected as changes in DTI measures. This implies that the pathology involved disruptions in the sensory connections rather than in the corticospinal tract (Mcclelland et al., 2011). Studies using multimodal approaches other than TMS-MRI, such as TMS-M/EEG could be more informative but are very few.

Thirugnanasambandam et al. (2021) aimed at exploring the neurophysiological mechanisms that underlie sensory trick in cervical dystonia patients using concurrent TMS and EEG. The study results reveal a long-latency component of TMS-evoked potential from primary motor cortex stimulation that correlated with disease duration and was exclusively present only in cervical dystonia patients who exhibited an effective sensory trick. This component, which corresponds to cortical excitation levels, is reduced during a sensory trick in patients thereby, implying that the sensory trick is likely to occur from the reduction of abnormal cortical facilitation observed in cervical dystonia patients.

DISCUSSION

From this mini-review, the dearth of multimodal NIBS studies conducted in movement disorders patients, especially ET and dystonia, is clearly evident. **Figure 2** shows the timeline of the various multimodal NIBS studies investigating movement disorders that have been published up to now. Although NIBS and neuroimaging studies independently have been useful in our understanding of disease pathophysiology, well-designed multimodal NIBS studies can yield a wealth of new information that may not be obtained from these methods used in isolation. There is growing evidence in the literature to support the notion that movement disorders are associated with aberrant cortical and subcortical functional connectivity (Poston and Eidelberg, 2012). Integrating non-invasive brain stimulation and functional neuroimaging methods could be an ideal approach to investigating these connectivity changes and possibly restoring normal connectivity in patients with movement disorders (Brittain and Cagnan, 2018). Particularly, tACS seems to be a promising modality to modulate functional connectivity and therefore could have therapeutic implications for movement disorders (Brittain et al., 2013; Schreglmann et al., 2021). The field of NIBS is progressing rapidly, and more innovative techniques and novel implications of existing techniques are being introduced (di Biase et al., 2019). Multimodal NIBS approaches can enrich our knowledge on the pathophysiology of movement disorders by discerning the causal role of specific brain regions in the disease pathophysiology and outlining the changes in functional brain connectivity that contribute to the disease process. This is likely to help us in developing new diagnostic tools and treatment strategies for movement disorders.

However, the multimodal NIBS approach is not without challenges and pitfalls, which may account for the low number of studies performed. One of the main challenges of combining NIBS with functional neuroimaging methods is the issue of artifacts. Although there are novel developments in the data acquisition and analysis methods, they are not without shortcomings and therefore require judicious implementation by investigators. The combination of methods should also be carefully chosen so as to best answer the primary research question. Moreover, the experiments should be designed carefully with appropriate controls to rule out any confounders from irrelevant cortical responses (Conde et al., 2019; Rocchi et al., 2021). Although the multimodal NIBS approach is likely to yield a wealth of information, unless these data are properly channeled and results carefully interpreted, there are high chances of misinterpretation or overinterpretation of the results. Recent studies have highlighted the potential of machine learning algorithms to extract hidden information from NIBS data that may also prove beneficial (Schreglmann et al., 2021). These challenges could best be overcome by having a multidisciplinary team with both clinical and technical expertise.

In summary, it is obvious that the potential of multimodal NIBS has not been adequately leveraged for the study of movement disorders due to several challenges associated with this approach. The movement disorders community should capitalize on the immense potential that novel multimodal NIBS approaches offer and exploit them to their fullest. This could be made possible by fostering multidisciplinary collaborations.

AUTHOR CONTRIBUTIONS

NT: conception, first draft, and review. SS: execution, first draft, and review. Both authors contributed to the article and approved the submitted version.

FUNDING

This work was supported by the DBT/Wellcome Trust India Alliance Fellowship (IA/CPHI/16/1/502624) awarded to NT. SS was supported by Ph.D. fellowship from the National Brain Research Centre.

REFERENCES

Antal, A., Alekseichuk, I., Bikson, M., Brockmöller, J., Brunoni, A. R., Chen, R., et al. (2017). Low intensity transcranial electric stimulation: Safety, ethical, legal regulatory and application guidelines. *Clin. Neurophys.* 128, 1774–1809. doi: 10.1016/j.clinph.2017.06.001

Balint, B., Mencacci, N. E., Valente, E. M., Pisani, A., Rothwell, J., Jankovic, J., et al. (2018). Dystonia. *Nat. Rev. Dis. Primers* 4:25.

Bharath, R. D., Biswal, B. B., Bhaskar, M. V., Gohel, S., Jhunjhunwala, K., Panda, R., et al. (2015). Repetitive transcranial magnetic stimulation induced modulations of resting state motor connectivity in writer's cramp. *Eur. J. Neurol.* 22, e53–e54.

Brittain, J. S., Probert-Smith, P., Aziz, T. Z., and Brown, P. (2013). Tremor suppression by rhythmic transcranial current stimulation. *Curr. Biol. CB.* 23, 436–440. doi: 10.1016/j.cub.2013.01.068

Brittain, J.-S., and Cagnan, H. (2018). Recent Trends in the Use of Electrical Neuromodulation in Parkinson's Disease. *Curr. Behav. Neurosci. Rep.* 5, 170–178. doi: 10.1007/s40473-018-0154-9

Brusa, L., Ceravolo, R., Kiferle, L., Monteleone, F., Iani, C., Schillaci, O., et al. (2012). Metabolic changes induced by theta burst stimulation of the cerebellum in dyskinetic Parkinson's disease patients. *Parkinson. Relat. Dis.* 18, 59–62. doi: 10.1016/j.parkreldis.2011.08.019

Cardoso, E. F., Fregni, F., Martins Maia, F., Boggio, P. S., Luis Myczkowski, M., Coracini, K., et al. (2008). rTMS treatment for depression in Parkinson's disease increases BOLD responses in the left prefrontal cortex. *Internat. J. Neuropsychopharm.* 11, 173–183.

Casarotto, S., Turco, F., Comanducci, A., Perretti, A., Marotta, G., Pezzoli, G., et al. (2019). Excitability of the supplementary motor area in Parkinson's disease depends on subcortical damage. *Brain Stimul.* 12, 152–160. doi: 10.1016/j.brs.2018.10.011

Cerasa, A., Koch, G., Donzuso, G., Mangone, G., Morelli, M., Brusa, L., et al. (2015). A network centred on the inferior frontal cortex is critically involved in levodopa-induced dyskinesias. *Brain* 138(Pt 2), 414–427. doi: 10.1093/brain/awu329

Chail, A., Saini, R. K., Bhat, P. S., Srivastava, K., and Chauhan, V. (2018). Transcranial magnetic stimulation: A review of its evolution and current applications. *Ind. Psychiatr. J.* 27, 172–180. doi: 10.4103/ipj.ipj_88_18

Chen, M., Summers, R. L. S., Prudente, C. N., Goding, G. S., Samargia-Grivette, S., Ludlow, C. L., et al. (2020). Transcranial magnetic stimulation and functional magnet resonance imaging evaluation of adductor spasmodic dysphonia during phonation. *Brain Stimulat.* 13, 908–915. doi: 10.1016/j.brs.2020.03.003

Conde, V., Tomasevic, L., Akopian, I., Stanek, K., Saturnino, G. B., Thielscher, A., et al. (2019). The non-transcranial TMS-evoked potential is an inherent source of ambiguity in TMS-EEG studies. *Neuroimage* 185, 300–312. doi: 10.1016/j.neuroimage.2018.10.052

de Vries, P. M., de Jong, B. M., Bohning, D. E., Hinson, V. K., George, M. S., and Leenders, K. L. (2012). Reduced parietal activation in cervical dystonia after parietal TMS interleaved with fMRI. *Clin. Neurol. Neurosurg.* 114, 914–921. doi: 10.1016/j.clineuro.2012.02.006

di Biase, L., Falato, E., and Di Lazzaro, V. (2019). Transcranial Focused Ultrasound (tFUS) and Transcranial Unfocused Ultrasound (tUS) Neuromodulation: From Theoretical Principles to Stimulation Practices. *Front. Neurol.* 10:549. doi: 10.3389/fneur.2019.00549

Elble, R. J. (2013). What is essential tremor? *Curr. Neurol. Neurosci. Rep.* 13:353.

Espay, A. J., Morgante, F., Merola, A., Fasano, A., Marsili, L., Fox, S. H., et al. (2018). Levodopa-induced dyskinesia in Parkinson disease: Current and evolving concepts. *Ann. Neurol.* 84, 797–811. doi: 10.1002/ana.25364

Flamez, A., Wiels, W., Van Schuerbeek, P., De Mey, J., De Keyser, J., and Baeken, C. (2019). The influence of one session of low frequency rTMS on pre-supplementary motor area metabolites in late stage Parkinson's disease. *Clin. Neurophys.* 130, 1292–1298. doi: 10.1016/j.clinph.2019.04.720

Fregni, F., Ono, C. R., Santos, C. M., Bermpohl, F., Buchpiguel, C., Barbosa, E. R., et al. (2006). Effects of antidepressant treatment with rTMS and fluoxetine on brain perfusion in PD. *Neurology* 66, 1629–1637. doi: 10.1212/01.wnl.0000218194.12054.60

Hallett, M. (2000). Transcranial magnetic stimulation and the human brain. *Nature* 406, 147–150.

Hanajima, R., Tsutsumi, R., Shirota, Y., Shimizu, T., Tanaka, N., and Ugawa, Y. (2016). Cerebellar dysfunction in essential tremor. *Move. Dis.* 31, 1230–1234.

Havrankova, P., Jech, R., Walker, N. D., Operto, G., Tauchmanova, J., Vymazal, J., et al. (2010). Repetitive TMS of the somatosensory cortex improves writer's cramp and enhances cortical activity. *Neuro Endocrinol. Lett.* 31, 73–86.

Hwang, S., Agada, P., Grill, S., Kiemel, T., and Jeka, J. J. A. (2016). central processing sensory deficit with Parkinson's disease. *Exp. Brain Res.* 234, 2369–2379. doi: 10.1007/s00221-016-4642-4

Jankovic, J., and Sherer, T. (2014). The future of research in Parkinson disease. *JAMA Neurol.* 71, 1351–1352. doi: 10.1001/jamaneurol.2014.1717

Leodori, G., Belvisi, D., De Bartolo, M. I., Fabbrini, A., Costanzo, M., Vial, F., et al. (2020). Re-emergent Tremor in Parkinson's Disease: The Role of the Motor Cortex. *Move. Dis.* 35, 1002–1011. doi: 10.1002/mds.28022

Lu, M. K., Chen, C. M., Duann, J. R., Ziemann, U., Chen, J. C., Chiou, S. M., et al. (2016). Investigation of Motor Cortical Plasticity and Corticospinal Tract Diffusion Tensor Imaging in Patients with Parkinsons Disease and Essential Tremor. *PLoS One* 11:e0162265. doi: 10.1371/journal.pone.0162265

Lumsden, D. E., McClelland, V., Ashmore, J., Charles-Edwards, G., Mills, K., and Lin, J.-P. (2015). Central Motor Conduction Time and Diffusion Tensor Imaging metrics in children with complex motor disorders. *Clin. Neurophysiol.* 126, 140–146. doi: 10.1016/j.clinph.2014.04.005

Mcclelland, V., Mills, K., Siddiqui, A., Selway, R., and Lin, J.-P. (2011). Central motor conduction studies and diagnostic magnetic resonance imaging in children with severe primary and secondary dystonia. *Dev. Med. Child Neurol.* 53, 757–763. doi: 10.1111/j.1469-8749.2011.03981.x

Merchant, S. H. I., Frangos, E., Parker, J., Bradson, M., Wu, T., Vial-Undurraga, F., et al. (2020). The role of the inferior parietal lobule in writer's cramp. *Brain* 143, 1766–1779. doi: 10.1093/brain/awaa138

Miguelez, C., De Deurwaerdère, P., and Sgambato, V. (1460). Editorial: Non-Dopaminergic Systems in Parkinson's Disease. *Front. Pharm.* 2020:11. doi: 10.3389/fphar.2020.593822

Nelson, A. J., Hoque, T., Gunraj, C., and Chen, R. (2018). Altered somatosensory processing in Parkinson's disease and modulation by dopaminergic medications. *Parkinson. Relat. Dis.* 53, 76–81. doi: 10.1016/j.parkreldis.2018.05.002

Odorfer, T., Homola, G., Reich, M., Volkmann, J., and Zeller, D. (2019). Increased Finger-Tapping Related Cerebellar Activation in Cervical Dystonia, Enhanced by Transcranial Stimulation: An Indicator of Compensation? *Front. Neurol.* 2019:10.

Pandey, S., and Srivanitchapoom, P. (2017). Levodopa-induced Dyskinesia: Clinical Features. *Pathophysiol. Med. Manag. Ann. Indian Acad. Neurol.* 20, 190–198.

Panyakaew, P., Cho, H. J., Lee, S. W., Wu, T., and Hallett, M. (2020). The Pathophysiology of Dystonic Tremors and Comparison With Essential Tremor. *J. Neurosci.* 40, 9317–9326. doi: 10.1523/jneurosci.1181-20.2020

Pereira, J. B., Junqué, C., Bartrés-Faz, D., Martí, M. J., Sala-Llonch, R., Compta, Y., et al. (2013). Modulation of verbal fluency networks by transcranial direct current stimulation (tDCS) in Parkinson's disease. *Brain Stimul.* 6, 16–24. doi: 10.1016/j.brs.2012.01.006

Petschow, C., Scheef, L., Paus, S., Zimmermann, N., Schild, H. H., Klockgether, T., et al. (2016). Central Pain Processing in Early-Stage Parkinson's Disease: A Laser Pain fMRI Study. *PLoS One* 11:e0164607. doi: 10.1371/journal.pone.0164607

Phukan, J., Albanese, A., Gasser, T., and Warner, T. (2011). Primary dystonia and dystonia-plus syndromes: clinical characteristics, diagnosis, and pathogenesis. *Lancet Neurol.* 10, 1074–1085. doi: 10.1016/s1474-4422(11)70232-0

Poewe, W., Seppi, K., Tanner, C. M., Halliday, G. M., Brundin, P., Volkmann, J., et al. (2017). Parkinson disease. *Nat. Rev. Dis. Primers* 3:17013.

Popa, T., Russo, M., Vidailhet, M., Roze, E., Lehéricy, S., Bonnet, C., et al. (2013). Cerebellar rTMS stimulation may induce prolonged clinical benefits in essential tremor, and subjacent changes in functional connectivity: an open label trial. *Brain Stimul.* 6, 175–179. doi: 10.1016/j.brs.2012.04.009

Poston, K. L., and Eidelberg, D. (2012). Functional brain networks and abnormal connectivity in the movement disorders. *Neuroimage* 62, 2261–2270.

Quartarone, A. (2013). Transcranial magnetic stimulation in dystonia. *Handbook Clin. Neurol.* 116, 543–553. doi: 10.1016/b978-0-444-53497-2.00043-7

Quartarone, A., Rizzo, V., Terranova, C., Morgante, F., Schneider, S., Ibrahim, N., et al. (2009). Abnormal sensorimotor plasticity in organic but not in psychogenic dystonia. *Brain* 132(Pt 10), 2871–2877. doi: 10.1093/brain/awp213

Rocchi, L., Di Santo, A., Brown, K., Ibáñez, J., Casula, E., Rawji, V., et al. (2021). Disentangling EEG responses to TMS due to cortical and peripheral activations. *Brain Stimul.* 14, 4–18. doi: 10.1016/j.brs.2020.10.011

Rothwell, J. (2007). Transcranial magnetic stimulation as a method for investigating the plasticity of the brain in Parkinson's disease and dystonia. *Parkinson. Relat. Dis.* 13(Suppl. 3), S417–S420.

Sacheli, M. A., Neva, J. L., Lakhani, B., Murray, D. K., Vafai, N., Shahinfard, E., et al. (2019). Exercise increases caudate dopamine release and ventral striatal activation in Parkinson's disease. *Move. Dis.* 34, 1891–1900. doi: 10.1002/mds.27865

Schneider, S. A., Pleger, B., Draganski, B., Cordivari, C., Rothwell, J. C., Bhatia, K. P., et al. (2010). Modulatory effects of 5Hz rTMS over the primary somatosensory cortex in focal dystonia—An fMRI-TMS study. *Movement Dis.* 25, 76–83. doi: 10.1002/mds.22825

Schreglmann, S. R., Wang, D., Peach, R. L., Li, J., Zhang, X., Latorre, A., et al. (2021). Non-invasive suppression of essential tremor via phase-locked disruption of its temporal coherence. *Nat. Comm.* 12:363.

Shih, L. C., and Pascual-Leone, A. (2017). Non-invasive Brain Stimulation for Essential Tremor. *Tremor Other HyperKinet. Movements* 7:458. doi: 10.5334/tohm.377

Strafella, A. P., Ko, J. H., Grant, J., Fraraccio, M., and Monchi, O. (2005). Corticostriatal functional interactions in Parkinson's disease: a rTMS/[11C]raclopride PET study. *Eur. J. Neurosci.* 22, 2946–2952. doi: 10.1111/j.1460-9568.2005.04476.x

Strafella, A. P., Paus, T., Barrett, J., and Dagher, A. (2001). Repetitive transcranial magnetic stimulation of the human prefrontal cortex induces dopamine release in the caudate nucleus. *J. Neurosci. Offi. J. Soc. Neurosci.* 21:Rc157. doi: 10.1523/jneurosci.21-15-j0003.2001

Strafella, A. P., Paus, T., Fraraccio, M., and Dagher, A. (2003). Striatal dopamine release induced by repetitive transcranial magnetic stimulation of the human motor cortex. *Brain* 126(Pt 12), 2609–2615. doi: 10.1093/brain/awg268

Tarakad, A., and Jankovic, J. (2018). Essential Tremor and Parkinson's Disease: Exploring the Relationship. *Tremor Other Hyperkinetic Move.* 8:589. doi: 10.5334/tohm.441

Thirugnanasambandam, N., Singh, S., Cho, H., Shitara, H., Panyakaew, P., Lee, S., et al. (2021). Site-specific decrease in cortical reactivity during sensory trick in cervical dystonia patients. *Medrxiv*. doi: 10.1101/2021.02.01.21250820

Tremblay, S., Rogasch, N. C., Premoli, I., Blumberger, D. M., Casarotto, S., Chen, R., et al. (2019). Clinical utility and prospective of TMS-EEG. *Clin. Neurophys. Offi. J. Internat. Federat. Clin. Neurophys.* 130, 802–844.

Ugawa, Y., Shimo, Y., and Terao, Y. (2020). Future of Tanscranial Magnetic Stimulation in Movement Disorders: Introduction of Novel Methods. *J. Mov. Disord.* 13, 115–117. doi: 10.14802/jmd.19083

Van Der Werf, Y. D., Sadikot, A. F., Strafella, A. P., and Paus, T. (2006). The neural response to transcranial magnetic stimulation of the human motor cortex. II. Thalamocortical contributions. *Exp. Brain Res.* 175, 246–255. doi: 10.1007/s00221-006-0548-x

van Wijk, B. C. M., Neumann, W.-J., Schneider, G.-H., Sander, T. H., Litvak, V., and Kühn, A. A. (2017). Low-beta cortico-pallidal coherence decreases during movement and correlates with overall reaction time. *Neuroimage* 159, 1–8. doi: 10.1016/j.neuroimage.2017.07.024

Wenning, G. K., Kiechl, S., Seppi, K., Müller, J., Högl, B., Saletu, M., et al. (2005). Prevalence of movement disorders in men and women aged 50–89 years (Bruneck Study cohort): a population-based study. *Lancet Neurol.* 4, 815–820.

Wichmann, T. (2018). Pathophysiologic Basis of Movement Disorders. *Prog. Neurol. Surg.* 33, 13–24. doi: 10.1159/000480718

Zesiewicz, T. A., Chari, A., Jahan, I., Miller, A. M., and Sullivan, K. L. (2010). Overview of essential tremor. *Neuropsychiatr. Dis. Treat.* 6, 401–408. doi: 10.2147/ndt.s4795

Conflict of Interest: The authors declare that the research was conducted in the absence of any commercial or financial relationships that could be construed as a potential conflict of interest.

frontiers in Human Neuroscience

METHODS
published: 28 May 2021
doi: 10.3389/fnhum.2021.637080

Investigating Nuisance Effects Induced in EEG During tACS Application

Romain Holzmann[1]*, *Judith Koppehele-Gossel*[2], *Ursula Voss*[2,3]* and *Ansgar Klimke*[2,4]

[1] GSI Helmholtzzentrum für Schwerionenforschung GmbH, Darmstadt, Germany, [2] Vitos Hochtaunuskliniken, Friederichsdorf, Germany, [3] Department of Psychology, J. W. Goethe-Universität, Frankfurt am Main, Germany, [4] Department of Psychiatry, Heinrich-Heine-Universität Düsseldorf, Düsseldorf, Germany

Transcranial alternating-current stimulation (tACS) in the frequency range of 1–100 Hz has come to be used routinely in electroencephalogram (EEG) studies of brain function through entrainment of neuronal oscillations. It turned out, however, to be highly non-trivial to remove the strong stimulation signal, including its harmonic and non-harmonic distortions, as well as various induced higher-order artifacts from the EEG data recorded during the stimulation. In this paper, we discuss some of the problems encountered and present methodological approaches aimed at overcoming them. To illustrate the mechanisms of artifact induction and the proposed removal strategies, we use data obtained with the help of a schematic demonstrator setup as well as human-subject data.

Keywords: EEG, tACS, modulation, hardware demonstrator, artifact removal

OPEN ACCESS

Edited by:
Kaviraja Udupa,
National Institute of Mental Health and Neurosciences, India

Reviewed by:
Burkhard Maess,
Max Planck Institute for Human Cognitive and Brain Sciences, Germany
Alexander James Casson,
The University of Manchester, United Kingdom
Andrea Guerra,
Sapienza University of Rome, Italy

***Correspondence:**
Ursula Voss
voss@psych.uni-frankfurt.de
Romain Holzmann
r.holzmann@gsi.de

Specialty section:
This article was submitted to Brain Imaging and Stimulation, a section of the journal Frontiers in Human Neuroscience

Received: *02 December 2020*
Accepted: *17 March 2021*
Published: *28 May 2021*

Citation:
Holzmann R, Koppehele-Gossel J, Voss U and Klimke A (2021) Investigating Nuisance Effects Induced in EEG During tACS Application. Front. Hum. Neurosci. 15:637080. doi: 10.3389/fnhum.2021.637080

1. INTRODUCTION

Low-current electrical stimulation of the human brain is a powerful technique developed in applied and experimental neuroscience (Herrmann et al., 2013; Paulus et al., 2013). Especially transcranial alternating current stimulation (tACS) is a unique form of non-invasive brain stimulation in which sinusoidal currents are delivered to the scalp to affect mostly cortical neurons. Among other things, tACS has been used for the entrainment of brain activity at specific frequencies, aiming at a synchronization of cortical oscillators (Helfrich et al., 2014b; Witkowski et al., 2016) and at localized increases in specific targeted frequencies, e.g., alpha (Zaehle et al., 2010) or gamma power (Voss et al., 2014). Moreover, Elyamany et al. (2020) showed in a recent review that tACS may also have the potential to reset disturbed brain oscillations, and thereby be able to support pharmacotherapy and psychotherapy in various mental disturbances, like obsessive-compulsive disorder (OCD), depression, bipolar disorder, dementia, and attention-deficit/hyperactivity disorder (ADHD). In many research studies, the neural response is inferred from the characteristics of the recorded electroencephalogram (EEG). Also from a clinical viewpoint, it would be of special interest to determine whether a regional modulation of neuronal circuits takes place during the tACS stimulation itself. This might be useful, both as a predictor and a quantitative correlator of the clinical efficacy of the treatment. However, analyzing and interpreting the EEG during concurrent tACS are very demanding tasks because of the extensive artifacts induced in the data, in both the time and frequency domains. To remove the stimulation artifacts from the recorded EEG or, at least, minimize their impact in the subsequent analysis, various schemes have been proposed; see Caldwell et al. (2020) for a brief review. Common approaches are to either (1) filter the artifact in the frequency domain (Helfrich et al., 2014a; Kohli and Casson, 2019), (2) subtract an artifact template in the time domain (Helfrich et al., 2014b; Voss et al., 2014; Caldwell et al., 2020), or (3) apply spatial filters constructed by modal decomposition

of the EEG signals (Neuling et al., 2017; Guarnieri et al., 2020; Haslacher et al., 2020; Vosskuhl et al., 2020). Spatial filtering relies on concurrent information from a sufficiently large number of EEG sites and it requires, therefore, a high-density EEG montage. Note that combinations of several methods have been used as well; for example, Fehér et al. (2017) have subtracted a moving-average template followed by a principal component analysis (PCA). While most of these artifact-removal techniques are now quite well-established, recent investigations by Noury et al. (2016) and Noury and Siegel (2017) have revealed that unavoidable quasi-periodic physiological processes, like heartbeat and respiration, can induce additional, non-linear effects in the EEG through a rhythmic modulation of the main tACS frequency. Indeed, Noury et al. observed in EEG data both an amplitude modulation (AM) and a phase modulation (PM) of the stimulation artifact, which they attributed to periodic changes of the body-tissue impedance. They also posited that these changes would be caused by the pulsating blood flow and the regular breathing movements imprinting a modulation at frequencies in the range of 1–2 and 0.2–0.5 Hz, respectively, and thus provoking a corresponding spread in the EEG frequency spectrum. As a consequence, the possible occurrence of such spreads must be carefully considered in any artifact-removal procedure used, especially when the stimulation is applied in the frequency band targeted by the investigation.

In the present paper, we focus on the AM of the stimulation artifact in EEG recordings. We first recapitulate how the modulation of the signal amplitude produces side bands in the EEG power spectrum and we also illustrate the effect with a schematic simulation. We then suggest a novel cleaning procedure that allows to remove the modulation from the recorded EEG signals. We provide proof of principle by applying the proposed scheme to mock EEG data measured with the help of a demonstrator, i.e., an experimental setup based on a simple phantom scalp. Finally, we demonstrate the procedure and its performance on data recorded from a human subject in a realistic laboratory setting. In doing so, we focus on stimulation frequencies applied in the EEG low and high gamma bands (30–140 Hz) where modulation artifacts are most liable to impact the overall descending intrinsic EEG power spectrum.

2. AMPLITUDE MODULATION AND DEMODULATION

2.1. AM Signal Modulation

AM of a sinusoidal signal introduces periodic changes of its maximum value as a function of time, i.e., it imprints those changes onto the signal envelope. In AM broadcasting, the information transported by the radio signal, e.g., voice, music or data, is hence encoded in its envelope. To illustrate the modulation process in tACS, let us first consider a sinusoidal signal $V(t)$, of amplitude $A_\circ$, frequency f_s, and phase $\varphi_s = 0$, expressed as a function of time t by

$$V_\circ(t) = A_\circ \sin \omega_s t\,, \tag{1}$$

where $\omega_s = 2\pi f_s$. Introducing furthermore a periodic change of the amplitude at a frequency f_m, realized here as $A(t) = A_\circ[1 + m\cos\omega_m t]$, we arrive at the following, amplitude-modulated signal

$$V(t) = A(t)\sin\omega_s t = A_\circ[1 + m\cos\omega_m t]\sin\omega_s t\,, \tag{2}$$

with $\omega_m = 2\pi f_m$ and $m \in [0, 1]$ being the so-called modulation index. Applying the trigonometric identity $2\sin A\cos B = \sin(A + B) + \sin(A - B)$, this expression can be rewritten as

$$V(t) = A_\circ \sin\omega_s t + \frac{1}{2} m A_\circ \left[\sin(\omega_s + \omega_m)t + \sin(\omega_s - \omega_m)t\right]. \tag{3}$$

Note that, due to the modulation, two additional terms appear at frequencies $f_s \pm f_m$, i.e., equally spaced above and below the main signal frequency. For a more complex periodic modulation signal, e.g., specified as $A(t) = \sum_{k=1}^{\infty} a_k \cos k\omega_m t$, the relation expressed by Equation (2) can be generalized[1] to the form

$$V(t) = A(t)\sin\omega_s t = A_\circ[1 + m\sum_{k=1}^{\infty} a_k \cos k\omega_m t]\sin\omega_s t\,, \tag{4}$$

which in turn expands into the expression

$$V(t) = A_\circ \sin\omega_s t + \frac{1}{2} m A_\circ \left[\sum_{k=1}^{\infty} a_k \sin(\omega_s + k\omega_m)t + \sum_{k=1}^{\infty} a_k \sin(\omega_s - k\omega_m)t\right]. \tag{5}$$

It appears from Equation (5) that the full Fourier spectrum characterizing the modulation signal $A(t)$ is added on either side of the central frequency. The same result follows directly from the convolution theorem of the Fourier transformation $\mathcal{F}$. In fact, by applying the operator $\mathcal{F}$ to Equation (4), one finds

$$\begin{aligned}\mathcal{F}[V(t)] &= \mathcal{F}[A(t)\times\sin\omega_s t)] = \mathcal{F}[\sin\omega_s t]\otimes\mathcal{F}[A(t)] \\ &= \delta(f - f_s)\otimes\mathcal{F}[A(t)]\,,\end{aligned} \tag{6}$$

where $\otimes$ stands for the convolution, or folding, operation. The right side of Equation (6) corresponds to the comb-spectrum expressed by Equation (5).

2.2. AM Signal Demodulation

Conversely, by demodulating an amplitude-modulated signal, one can recover the information encoded in its envelope; mathematically, this corresponds to reversing the modulation operation expressed by Equation (2). In more practical terms, e.g., in an AM radio receiver, the envelope can be retrieved by multiplying the (amplified) captured signal $V(t)$ with a local

[1] Again, for the sake of clarity, we have set all phase angles to zero. In the most general case, where $\varphi_k \neq 0$, the expansion of Equation (3) will lead to additional terms in Equation (5) involving also the corresponding cosine functions. This restriction does, however, not curtail our line of argumentation.

oscillator signal, tuned and phase-locked to the central frequency f_s of $V(t)$, giving the product

$$\begin{aligned} V(t) \times \sin \omega_s t &= A(t) \sin \omega_s t \times \sin \omega_s t \\ &= A(t) \sin^2 \omega_s t \\ &= \frac{1}{2} A(t)[1 - \cos 2\omega_s t] \,. \end{aligned} \tag{7}$$

After having removed the $2\,\omega_s$ harmonic with an appropriate low-pass filter, this procedure yields the low-frequency AM signal $A(t)$. This demodulation principle, called product detector, is typically implemented in analog radio receivers. A more effective separation of the harmonics is achieved with higher-order product detectors, using the following scheme:

$$\begin{aligned} V(t) \times \sin \omega_s t \, \cos^2 \omega_s t &= A(t) \sin^2 \omega_s t \, \cos^2 \omega_s t \\ &= \frac{1}{8} A(t)[1 - \cos 4\omega_s t] \,. \end{aligned} \tag{8}$$

Again, the signal to be demodulated is multiplied with a phase-locked local oscillator signal as well as with the square of a 90° phase-shifted derivation of the latter, leading now to a high-frequency term at $4\,\omega_s$ that can be filtered more easily from the low-frequency envelope $A(t)$. Note that yet more sophisticated schemes can be devised, but are then implemented most conveniently by software in a digital receiver.

In the present context, namely the modeling of artifacts generated by tACS in electrophysiological signals, the data are usually available as digitized signal samples that can readily be subjected to more sophisticated signal analysis procedures. In particular, the analytical representation of a signal can be computed as $V_a(t) = V(t) + i\mathcal{H}[V(t)]$, where $\mathcal{H}$ represents the Hilbert transformation operator (Bendat and Piersol, 2010). From this, the envelope $A(t)$ can be directly obtained as the norm of $V_a(t)$, namely

$$A(t) = |V_a(t)| = \sqrt{V(t)^2 + \mathcal{H}[V(t)]^2}. \tag{9}$$

Figure 1 illustrates all of the AM concepts discussed above by showing a stable 10-Hz sine wave **(A)** modulated with a slow saw tooth **(B)**. The latter was approximated as the sum of a 0.5-Hz sine and contributions of its first four harmonics at 1, 1.5, 2, and 2.5 Hz. The modulation index was set to $m = 0.1$, i.e., large enough to make the AM envelope clearly visible in the modulated signal **(C)**. The power spectral density (PSD)

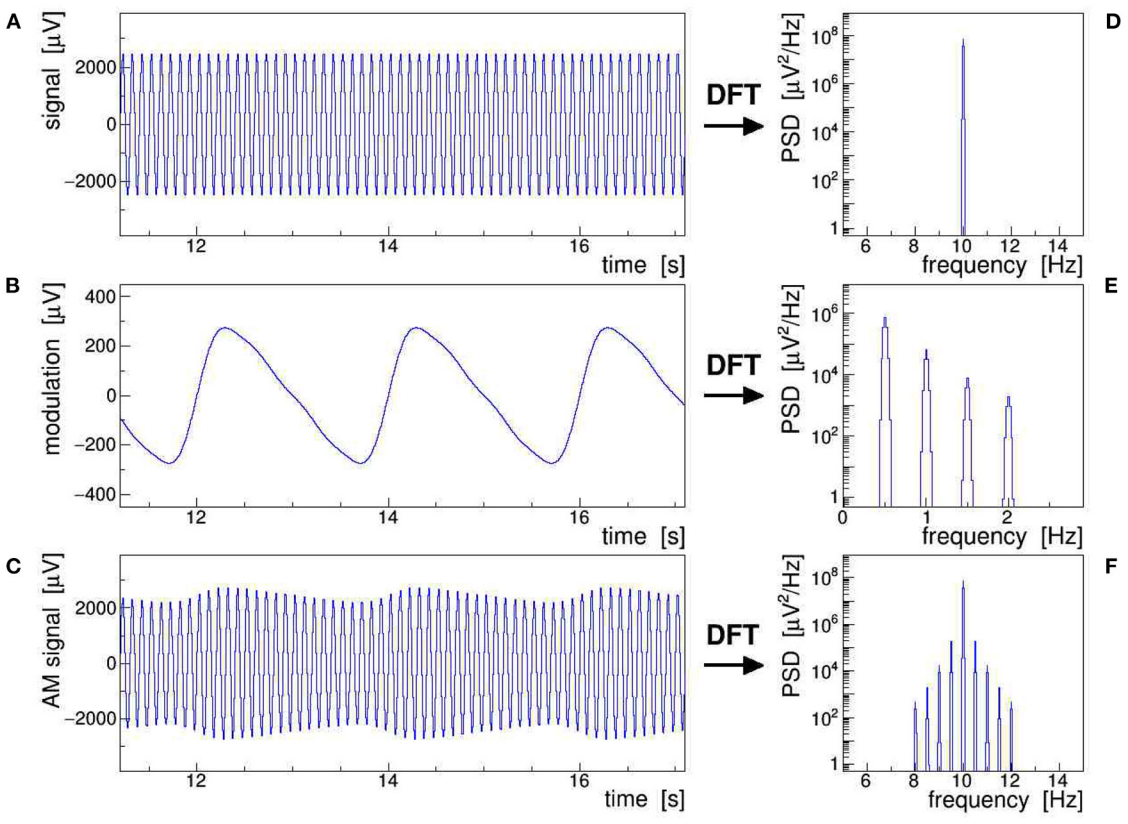

FIGURE 1 | Schematic representation of an amplitude-modulated sinusoidal signal: a 10-Hz sine wave **(A)** is modulated with a 0.5 Hz saw tooth **(B)** resulting in the amplitude modulation (AM) signal **(C)**. The power spectral density (PSD) of the corresponding discrete Fourier transforms are shown in frames **(D)**–**(F)**. This figure also exemplifies Equation (6), which states that the multiplication of **(A)** with **(B)**, giving **(C)** in the time domain, corresponds to a convolution of **(D)** with **(E)**, giving **(F)** in the frequency domain.

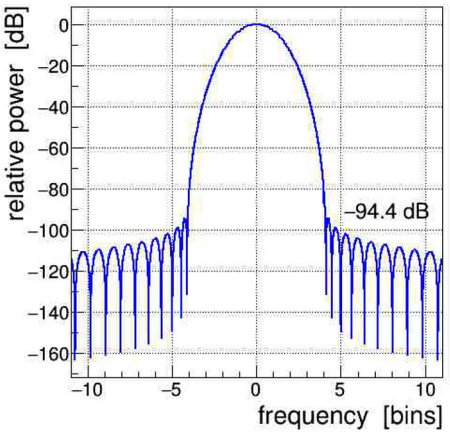

FIGURE 2 | Frequency spectrum of the Kaiser–Bessel windowing function, with parameter $\alpha = 4$, applied in the discrete Fourier transform (DFT); frequency is expressed in bins of width $1/T$, with T being the time span of the Fourier-transformed signal. The power leakage of this window is very low, all side lobes are at < -94 dB, i.e., a factor of nearly 10 orders of magnitude below the central lobe.

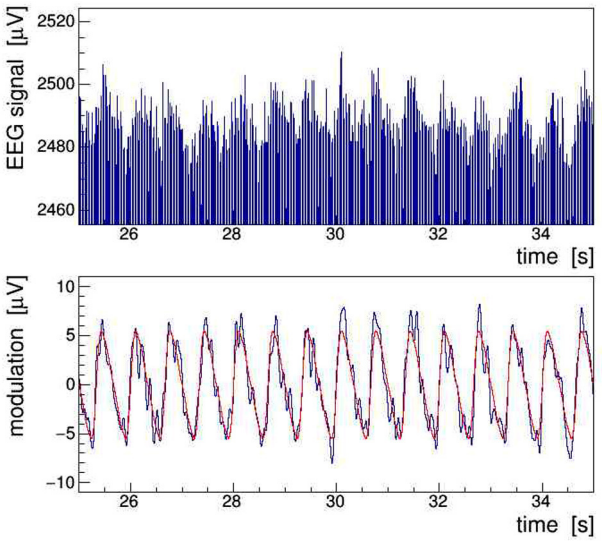

FIGURE 3 | Simulation of an amplitude-modulated 40-Hz sinusoidal signal of 5 mV_{pp} added on top of a random baseline of pink noise. (Top) Upper edge of the full signal visualizing the 1.5 Hz saw-tooth modulation at 10 μV_{pp} depth. (Bottom) Envelope of the signal recovered by demodulation (black) shown with the overlaid true modulation signal (red).

distributions of the respective discrete Fourier transform (DFT), presented in frames **(D)**–**(F)**, show that **(F)** results indeed from folding **(D)** with **(E)**, as expressed by Equation (6). The original saw tooth can be retrieved from the modulated signal by applying either of Equations (7)–(9), combined with proper low-pass filtering. Here, we have posited that the modulation of the signal is stationary, i.e., that its ensemble-averaged moments (mean, variance, etc.) remain constant over the Fourier-transformed signal segment, while ergodicity is not explicitly required (Bendat and Piersol, 2010). This assumption is justified when analyzing epochs of EEG signals shorter than the typical time scales of slow impedance changes caused by sweating or drying conductive paste, as well as of sporadic shifts due to, e.g., posture changes.

All signals shown in **Figure 1** were Fourier transformed into the frequency domain using a Kaiser–Bessel windowing function with parameter $\alpha = 4$; its frequency response is shown in **Figure 2** and its detailed characteristics are given in Heinzel et al. (2002). It is indeed very important to control the side-lobe power leakage and keep it well below the expected level of the side-band artifacts induced in the EEG data. We selected this particular window type because it offers a large side-lobe suppression of −94.4 dB together with a reasonably good frequency resolution corresponding to a width of the main lobe at its base of $\Delta f = \pm 4.1$ frequency bins.[2]

2.3. Simulation of EEG Signals With Concurrent tACS

In order to achieve a more realistic demonstration of the artifacts induced in EEG by concurrent tACS, we have run a computer simulation in which the intrinsic brainwave signal was mimicked by sampling pink noise, i.e., a random distribution with its power falling off at −10 dB/frequency decade, and the tACS signal was added as a 40-Hz sinusoidal signal amplitude-modulated with a 1.5 Hz saw-tooth beat.[3] In addition, a closer to reality (see section 4), that is, a much weaker modulation index of 0.002 was chosen. As shown in **Figure 3**, the characteristic fluctuations of the signal AM envelope remain visible, but only barely so, because of the random nature of the underlying pink noise. In the frequency domain, however, the modulation artifacts appear very prominently. The PSD spectrum resulting from a DFT of the simulated signal, presented in **Figure 4**, shows that the modulation-induced side-band power is substantial when compared with the underlying brainwave power. Consequently, in a quantitative analysis of tACS-induced changes of the EEG, not only the stimulation artifact itself will have to be removed with very high precision, but also its side bands will eventually have to be cleaned. Notice that in this simulation, the leakage of the Kaiser–Bessel window function is negligible as it stays more than two orders of magnitude below the pink noise spectrum.

3. HARDWARE DEMONSTRATOR OF STIMULATION ARTIFACTS

3.1. Setup and Data Recording

When moving from simulations to real EEG data, in a first step, we aimed at investigating the stimulation artifacts in a realistic, yet fully controlled laboratory setting. To do so, we have assembled a hardware demonstrator with the following components:

[2]With a frequency binning of 0.05 Hz, this results in 0.4 Hz.

[3]We preferred generating pink noise over using pre-recorded EEG data in order to achieve a well-defined, reproducible drop of the noise power with frequency.

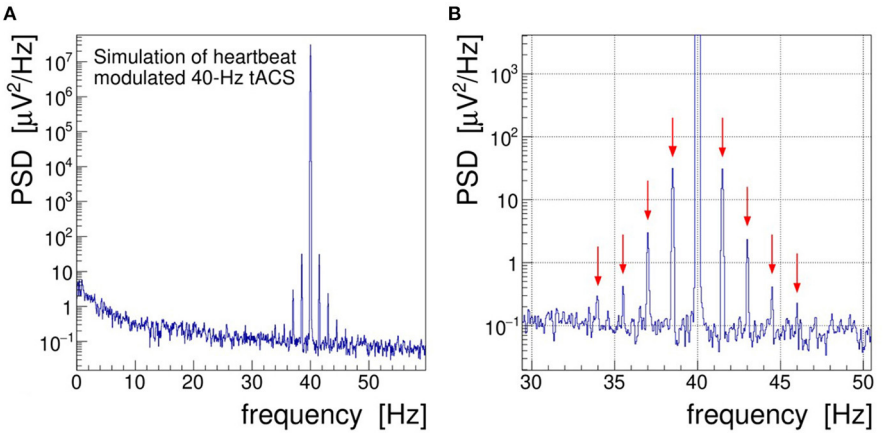

FIGURE 4 | (A) Power spectral density (PSD) distribution obtained by Fourier transforming the simulated signal shown in **Figure 3**. In this simulation, the electroencephalogram (EEG) signal is realized by sampling a pink noise distribution and the transcranial alternating current stimulation (tACS) signal is represented by a 40-Hz sine wave modulated at the level of $m = 0.2\%$ with a 1.5 Hz saw tooth. **(B)** Zoom into the gamma frequency band; red arrows mark the side peaks arising at $f = 40 \pm n \times 1.5$ Hz through the amplitude modulation of the tACS voltage.

- a scalp phantom, realized as coarse-grained finite-element 4.7 kΩ resistor network;
- a variable impedance—to mimic periodic effects, e.g., heartbeat and respiration—implemented as a light-dependent resistor (LDR) rhythmically illuminated by a light-emitting diode (LED);
- a digital signal generator, model FY6800 (FeelTech, China)—to drive the LED;
- a tACS device, the DC Stimulator Plus (neuroConn GmbH, Germany)—to inject a sinusoidal current into the phantom;
- a 64 EEG channel + 8 AUX channel 24-bit recorder, actiCHamp (Brain Products GmbH, Germany)—to acquire multichannel data;
- a 4-channel digital storage oscilloscope, DS1104Z (Rigol Technologies, China)—used for testing purposes only, but not on a human subject.

In this setup, shown schematically in **Figure 5**, the data acquisition (DAQ) system used to digitize EEG signals was either a state-of-the-art 72-channel EEG recorder or, for some basic tests, a digital storage oscilloscope. The main rationale behind realizing a hardware demonstrator was that it allowed to acquire data with the full instrumental chain—stimulator, electrode leads, and EEG recorder—in the actual laboratory environment, i.e., including the real power-line interferences (50 Hz and harmonics), amplifier noise and non-linearities, as well as stimulator noise and harmonics. We refrained from using a 3d multi-layer head phantom, like the ones discussed by Owda and Casson (2020) and Vosskuhl et al. (2020), as our aim was to obtain sample EEG data for our testing purposes only. Furthermore, we were also not concerned with volume vs. scalp conduction or capacitive electrode impedance effects. Our resistive-net phantom provided the means to record in a controlled and reproducible, yet sufficiently realistic way the data required to design and validate adequate artifact removal procedures.

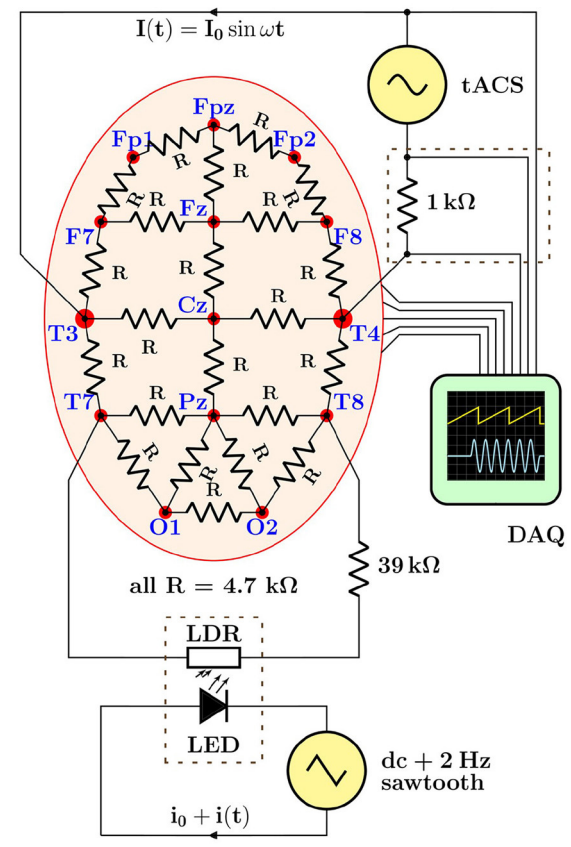

FIGURE 5 | Schematic overview of the hardware demonstrator designed to generate electroencephalogram (EEG) data with typical transcranial alternating current stimulation (tACS) artifacts in a realistic but fully controllable laboratory setting. The lower dashed rectangle stands for the light-tight enclosure holding the light-emitting diode (LED)/light-dependent resistor (LDR) setup used to induce rhythmic impedance changes; the upper dashed rectangle represents the breakout box from which tACS voltage and current signals are derived, see text for details.

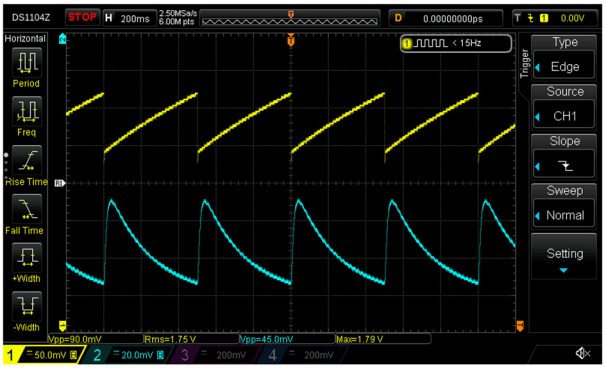

FIGURE 6 | Scope traces of the saw tooth (here 2-Hz, $\Delta U = 0.1$ V) light-emitting diode (LED) driving voltage (yellow) and the beat-induced impedance changes in the scalp phantom of the demonstrator (blue).

Demonstrator data were recorded with a basic montage consisting of four EEG leads connected to the phantom (Fp1, Fp2, Fpz as ground, and Cz as reference) as well as derivations of the tACS voltage and current signals (see section 4 and upper dashed box in **Figure 5**) fed into two of the bipolar AUX channels of the recorder; all signals were sampled at a rate of 1 kHz. The stimulator was set to deliver a 40-Hz sinusoidal stabilized current of 0.5 mA_{pp} through a total impedance of 4.2 kΩ across sites T3 and T4. The modulation of the scalp impedance was achieved by connecting the LDR/LED pair across sites T7 and T8, and driving the LED with the programmable signal generator that provided 0.2 V saw-tooth pulses at 2 Hz repetition rate on top of a 2 V DC pedestal; the modulation intensity could be easily set by adjusting the amplitude of the saw tooth. The driving voltage of the LED and the resulting impedance changes, visualized as voltage drop across the LDR, are visible in the scope traces shown in **Figure 6**. Notice, in particular, that the characteristic response of the LED/LDR couple leads to slightly non-linear variations of the mock scalp impedance.

In the following text and pictures, we designate the induced 2-Hz modulation as "heartbeat" or, in brief, "HB." A 10-s long segment of demonstrator data is presented in **Figure 7** showing the demodulated, filtered, and detrended signal envelope—called modulation kernel by Noury et al. (2016)—both in the time **(A)** and frequency **(B)** domains. The frequency spectrum was obtained by low-pass filtering (25 Hz, 32nd-order, zero-delay Butterworth) and Fourier-transforming ($\alpha = 4$ Kaiser–Bessel window) the kernel. As discussed in section 2.2, this filter is needed to suppress the harmonics of the stimulation signal; it also removes operational noise picked up in the laboratory environment (mostly 50 Hz power line interferences).

3.2. Artifact-Removal Procedures

Here, we propose a two-step procedure to remove the tACS artifacts from the recorded EEG data. In a first step, we remove the AM-induced side-band power by reversing[4] the amplitude-modulation process described in section 2.1. In a second step, we delete the main and by far dominant stimulation artifact by subtracting a properly scaled and phase-shifted segment of the concurrently recorded tACS current signal. These cleaning steps are applied one by one to each EEG channel of interest and to each data episode of interest, meaning that all EEG channels are processed individually and independently. The advantage of such a procedure is that it can be applied universally—in particular, to few-channel montages—with the sole condition that the tACS current signal is also available in the recorded data sets.

In order to achieve our first goal, i.e., the removal of AM-induced side-band power, we rewrite the amplitude $A(t)$ of the tACS-induced potential in a given EEG signal as

$$A(t) = A_\circ + K(t) = A_\circ \left[1 + m\,\hat{K}(t)\right],$$

where $A_\circ$ is the constant amplitude of the unmodulated signal and $K(t) = mA_\circ\hat{K}(t)$ represents the modulation of the amplitude. In this expression, the normalized kernel $\hat{K}(t)$ encodes the time dependence of the signal envelope and, as already introduced in Equation (2), m expresses the relative depth of the modulation. From the measured EEG signal, $K(t)$ is obtained by (1) AM demodulation (see section 2.2), (2) detrending of the retrieved envelope to remove the constant term, and (3) low-pass filtering to suppress the harmonics of the stimulation signal. With $K(t)$ available individually for each EEG channel and episode of interest, we can apply a multiplicative correction to the measured signal. The basic idea is to divide out the kernel under the assumption that the modulation is a small perturbation only, i.e., $m \ll 1$; this is indeed justified as data reveal typically values of $m \approx 10^{-4} - 10^{-2}$ (see Noury et al., 2016 and section 4). To expand on this, let us write the total EEG signal $V_{\rm sig}$ observed at a given scalp site as a superposition of intrinsic and induced signals

$$V_{\rm sig}(t) = V_{\rm eeg}(t) + V_{\rm tacs}(t) = V_{\rm eeg}(t) + A(t)\,\hat{I}_{\rm tacs}(t),$$

where $V_{\rm eeg}(t)$ is the intrinsic EEG signal of interest (including environmental and instrumental noise) and $V_{\rm tacs}(t)$ is the modulated voltage induced at this site by the applied stimulation current $I_{\rm tacs}(t)$; here, the artifactual signal is expressed as a function of the normalized stimulation current $\hat{I}_{\rm tacs}(t)$. Both signals, $V_{\rm sig}(t)$ and $I_{\rm tacs}(t)$, are measured and an estimate of $A(t)$, and hence $m\hat{K}(t)$, is obtained by demodulation of $V_{\rm sig}(t)$. We proceed to remove the modulation artifact from the recorded EEG signal by applying sample by sample the following operation:

$$\begin{aligned} V_{\rm sig}(t) \;\Rightarrow\; V^{(1)}_{\rm sig}(t) &= \frac{V_{\rm sig}(t)}{\left[1 + (m + \Delta m)\,\hat{K}(t + \Delta t)\right]} \\ &= \frac{V_{\rm eeg}(t) + A(t)\,\hat{I}_{\rm tacs}(t)}{\left[1 + (m + \Delta m)\,\hat{K}(t + \Delta t)\right]} \\ &\simeq V_{\rm eeg}(t) + \frac{A(t)\,\hat{I}_{\rm tacs}(t)}{\left[1 + (m + \Delta m)\,\hat{K}(t + \Delta t)\right]} \\ &\simeq V_{\rm eeg}(t) + A_\circ\,\hat{I}_{\rm tacs}(t), \end{aligned} \tag{10}$$

[4]A cleaning scheme following this line of thought has already been suggested in Noury et al. (2016).

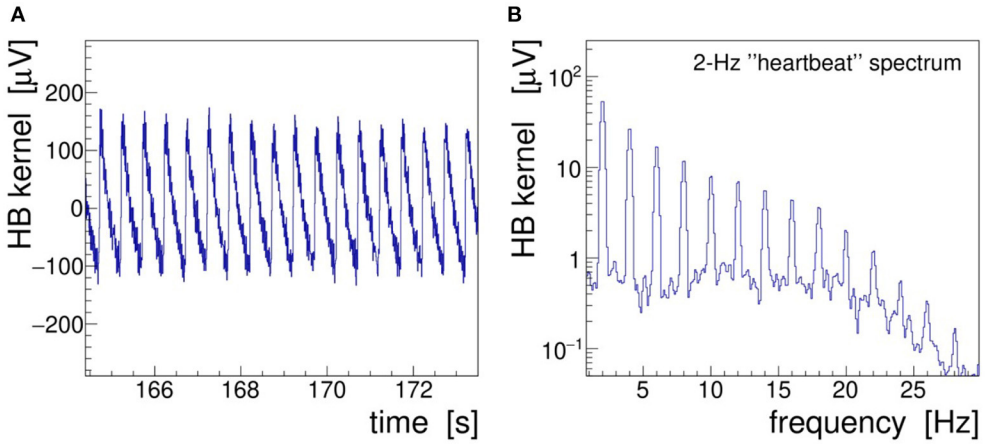

FIGURE 7 | Heartbeat modulation kernel retrieved by demodulation of the demonstrator electroencephalogram (EEG) signal Fp1 recorded during 40-Hz transcranial alternating-current stimulation (tACS) application and 2-Hz saw-tooth impedance modulation. **(A)** Demodulated signal in the time domain and **(B)** r.m.s. spectrum of the modulation kernel in the frequency domain.

where $V_{\mathrm{sig}}^{(1)}(t)$ stands now for the AM-corrected signal after cleaning step one. The approximation is valid in most practical cases, as the division only marginally affects the intrinsic EEG signal itself when $m \ll 1$. The parameters Δt and Δm represent small adjustments of t and m, respectively ($\Delta t/t, \Delta m/m \ll 1$). They are needed to achieve an optimal subtraction of the artifact: the time adjustment Δt corrects for possible small phase differences between $V_{\mathrm{sig}}(t)$ and $V_{\mathrm{tacs}}(t)$, caused by the hardware or the analysis (e.g., different filters applied), whereas adjustments of the modulation index Δm correct for slow drifts of the modulation depth during averaging over a number of time spans. Best values of both Δt and Δm are determined in a regression procedure[5] set up, such as to optimally remove the AM-induced side-band power in the data segment of interest. This requires computing the Fourier transform repeatedly within the regression loop, as the optimization is controlled by the ratio of integrated power in the side-bands to the power in the main peak. To minimize this ratio, we have used a robust simplex algorithm (Nelder and Mead, 1965), which does not require the gradients of the functional to be minimized. The efficacy of this procedure is demonstrated on our Fourier-transformed (20-s data segments, $\alpha = 4$ Kaiser–Bessel window) phantom data in **Figure 8** where the PSD distributions are compared before and after applying the first cleaning step. One clearly sees that the side-band artifacts are reduced by up to four orders of magnitude (i.e., $\leq$40 dB) in the vicinity of the main peak. The efficacy decreases slowly when moving further away from the stimulation frequency, say by $\pm$20 Hz, although in these regions the side-peak power is fading out anyway. This particular behavior is not surprising, however, as the regressed parameters in Equation (10) are, by construction of the minimized functional, most sensitive

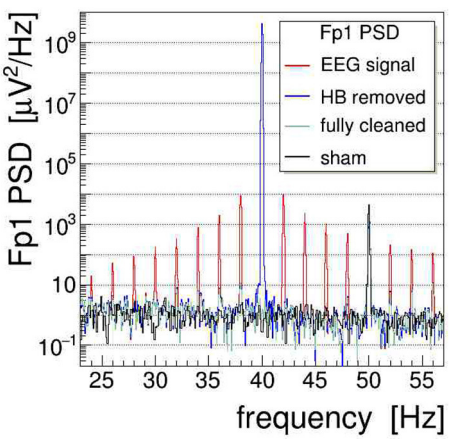

FIGURE 8 | Power spectral density (shown in red, 0.05 Hz bins) of the demonstrator electroencephalogram (EEG) signal Fp1 during 40-Hz transcranial alternating current stimulation (tACS) application and amplitude modulation with a 2-Hz saw-tooth "heartbeat" (HB). The modulation causes substantial and far-reaching spread of power to both sides of the stimulation frequency. By applying the two-step cleaning procedure outlined in the text, first, the amplitude modulation (AM)-induced artifact is strongly suppressed (blue spectrum) and, second, the main artifact at 40 Hz is removed, resulting in a fully cleaned power spectral density (PSD) spectrum (overlaid in green). For comparison, the cleaned PSD obtained without stimulation, i.e., under sham condition, is also shown (black). See text for a discussion of the persisting power in the 50-Hz peak.

to the lower harmonics of the AM kernel. It remains to be explored whether a more sophisticated filtering of the kernel can help to further improve the cleaning. In **Figure 8**, we also show the PSD obtained under a "sham" condition, i.e., for data recorded while the stimulator was switched off. Comparing sham with the clean-signal PSD, we conclude that the cleaning procedure introduces no bias in the power spectrum. A further

[5]In the regression, the two parameters Δm and Δt were adjusted once per analyzed EEG signal and epoch, i.e., in total $N_{\mathrm{sig}} \times N_{\mathrm{epo}}$ times.

point to notice is that the PSD at 50-Hz remains largely unaltered due to power-line noise interfering at this particular frequency; full removal can only be achieved by applying a dedicated notch filter.

The second step, i.e., the removal of the main tACS artifact, is achieved on the AM-cleaned signal $V^{(1)}_{\rm sig}(t)$ by subtracting sample by sample a properly scaled and phase-shifted copy of the normalized stimulation signal $\hat{I}_{\rm tacs}(t)$, resulting in the fully cleaned signal $V^{(2)}_{\rm sig}(t)$, as follows:

$$V^{(1)}_{\rm sig}(t) \;\Rightarrow\; V^{(2)}_{\rm sig}(t) = V^{(1)}_{\rm sig}(t) - n_\circ\, I_{\rm tacs}(t + \Delta t). \qquad (11)$$

The optimal scaling factor $n_\circ$ and time shift Δt are again determined with the help of a simplex regression by minimizing the residual stimulation power summed over the data segment of interest. **Figure 8** shows that the second cleaning step completely removes the huge stimulation artifact from the PSD distribution. This is quite remarkable considering that to cleanly subtract an artifact more than nine orders of magnitude (i.e., $\geq$90 dB) bigger than the intrinsic EEG baseline requires very high precision on the parameters of Equation (11). In fact, a more detailed investigation revealed that the length of the signal segment on which these parameters are optimized impacts the efficacy of the second cleaning step: using a too large segment results in not subtracting the artifact completely, while using a very short one entails local over-subtraction, possibly producing a dip at 40 Hz. A certain degree of oversubtraction is to be expected as, in the present case, the method targets one specific frequency, just like a digital notch filter would do.

The full, two-step cleaning procedure is eventually applied to the recorded EEG data in a signal-by-signal and epoch-by-epoch manner. As the regression coefficients are recomputed for each epoch, slow trends in impedance change, caused by drying electrode paste, sweating, etc., will not impair the correction. Furthermore, the described procedure has the advantage of also being applicable to few-electrode EEG montages.

4. APPLICATION TO HUMAN SUBJECT DATA

We now turn to our investigation of AM effects on multichannel EEG data recorded from a healthy subject during application of tACS. We first describe the experiment, then we assess the size of stimulation-induced artifacts in the EEG power spectra, and finally we evaluate the efficacy of the cleaning procedures introduced in the previous section.

4.1. Experimental Techniques

A multichannel EEG was recorded from a healthy subject (age range 20–25) using an electrode cap instrumented with 61 active scalp electrodes according to the 10–10 positioning system; the ground electrode was placed on the forehead at position Fpz and all signals were referenced to electrode Cz. An electrooculogram (EOG) was taken with passive electrodes from the outer canthi of both eyes and supraorbitally to the left eye; likewise, passive electromyogram (EMG) electrodes were fixed at the chin. Both, EOG and EMG leads were connected to bipolar AUX inputs of the EEG recording device (actiCHamp, Brain Products, Germany). Electrocardiogram (ECG) electrodes were fixed below the left clavicle and left costal arch of the subject, and a pressure sensor belt was put on, delivering ECG and respiration signals, respectively, to further bipolar AUX inputs. Data of all EEG and AUX channels were filtered (0.16 Hz high-pass and 1,000 Hz low-pass at 12-dB/octave) and digitized at a sampling rate of 10 kHz.

Stimulation current was applied to the subject through four 3.5×4 cm^2 conducting silicone-rubber electrodes placed across frontal and temporal sites F5/F7 and TP9, respectively, F6/F8 and TP10, and connected pair-wise to the output jacks of a tACS stimulator (DC Stimulator Plus, neuroConn, Germany). The current leads were thereby routed through a custom-built breakout box, allowing to derive voltage and current signals that were both fed into additional AUX inputs of the EEG recorder. The current derivation was taken as the voltage drop over a 1 kΩ resistor (see upper dashed box in **Figure 5**) while still warranting full galvanic isolation of the subject during the experiment.

The experiment consisted of recording a number of few-minute episodes of EEG and AUX data while applying a sinusoidal tACS current of 0.6 mA peak-to-peak (electrode impedance of 6.8–7.6 kΩ) at frequencies of either 40, 70, or 100 Hz for 3 min at a time. Recording started and stopped about 20–30 s before and after stimulation, respectively. Care was taken to avoid driving the EEG amplifiers into saturation, which would otherwise have resulted in distorted or even clipped signals. From the hardware side, currents up to about 1.5 mA would have been tolerable but, as they provoked excessive skin irritations on the subject, we refrained from using them. The implied current limitation is also typical for sleep studies employing concurrent tACS–EEG where one wants to avoid induced awakenings (Voss et al., 2014). For all recordings, the subject was seated in an upright position, immobile, awake, and with eyes closed.

For the offline analysis, the data were low-pass filtered at 333 Hz, notch-filtered at the power-line frequency and at its odd harmonics ($f = 50$, 150, 250, and 350 Hz, $\Delta f = 0.5$ Hz), and then decimated by a factor 10 to a sampling rate of 1 kHz. The EOG, EMG, and ECG signals were furthermore low-pass filtered at 25 Hz to block the stimulation frequency; filtering was not required, however, for the RESP signal derived from the respiration belt piezo sensor which had no electrical contact with the subject's skin.

To localize individual heartbeat and breathing events in time, we have applied a QRS-complex detector (Pan and Tompkins, 1985; Kohler et al., 2002) to the ECG signal and a feature search to the RESP signal. The event times were furthermore synced with the nearest zero-crossing of the recorded tACS signal, shifting each event by an appropriate amount of samples.[6] This syncing is necessary to preserve the phase relation of the stimulation current when averaging EEG segments over a sequence of heartbeats or breathing events.

[6]One sample corresponds to 1 ms at the 1 kHz sampling rate used in the analysis.

4.2. Assessing the Stimulation Artifacts

The characteristic frequency dependence of a subject's natural EEG spectrum is thought to follow roughly the one of pink noise, with the consequence that any modulation artifacts are more easily visible for stimulation frequencies in the gamma band or above where the intrinsic EEG power is lowest. Therefore, we focus our discussion on the EEG data recorded with 40, 70, or 100 Hz tACS.

A sample of EEG data recorded during stimulation from channels Fz, ECG, and RESP is presented in **Figure 9**. The onset of stimulation with 100 Hz tACS is clearly visible in the EEG around time $t = 18$ s, with the electrophysiological signal becoming completely overpowered by the tACS-induced potential. Obviously, any quantitative analysis of EEG signals recorded during tACS application requires this nuisance effect to be removed with great care and precision. In particular, in cases where the EEG frequency band of interest is directly contaminated by artifactual power, application of digital filters, as done here on the ECG signal, is generally not a viable solution. We found, however, that the subtraction of the concurrently recorded stimulation current $I_{\text{tacs}}(t)$, applying Equation (11), provides a reliable and satisfactory means to remove the main tACS artifact. The result of this procedure is displayed in **Figure 10** where the restored Fz signal is confronted with its original, contaminated instance. This direct comparison in the time domain offers already a good appreciation of the applied method; a more quantitative discussion in the frequency domain is given in the following subsection.

4.3. Performance of the Artifact Removal Procedures

The efficacy of the applied tACS removal procedure can be better assessed in the frequency domain because there also weak contributions induced by the stimulation current can be easily recognized. The topographic map displayed in **Figure 14A** exemplifies the overwhelming electric signal produced by the

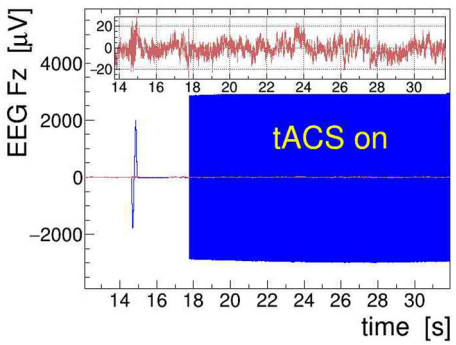

FIGURE 10 | Removal of the main transcranial alternating-current stimulation (tACS) artifact from the electroencephalogram (EEG) signal. The signal recorded at site Fz is shown (in blue); at $t = 18$ s, a stimulation with 100 Hz is started producing a more than 100-fold increase of the signal amplitude. The clean signal obtained with the removal procedure introduced in section 3 is overlaid (in red) and also shown enlarged on the inset.

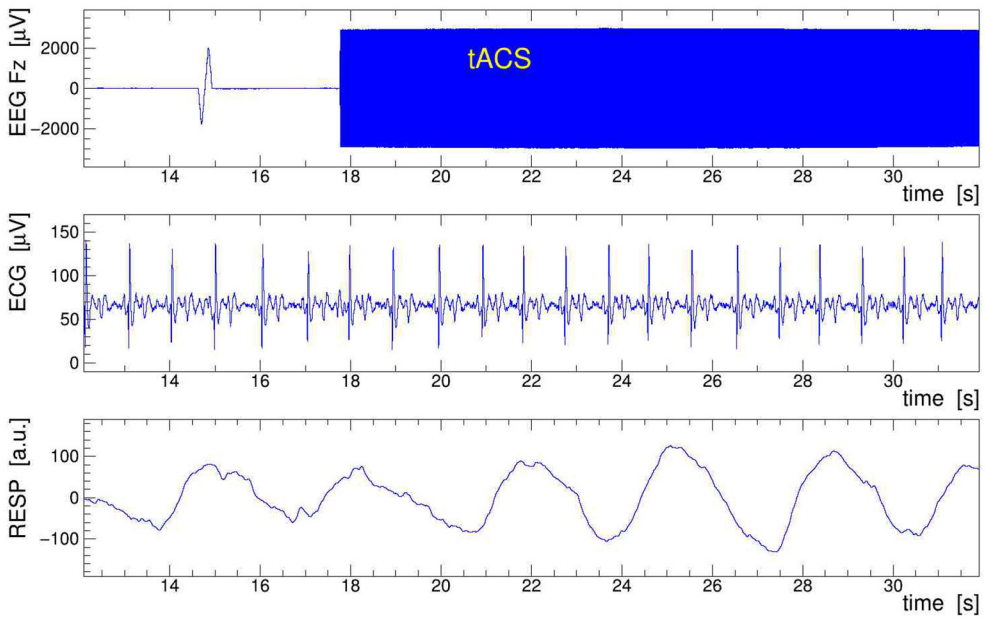

FIGURE 9 | Sample of electroencephalogram (EEG) data taken on human subject while 100-Hz transcranial alternating current stimulation (tACS) was applied. Shown are 20 s of the EEG signal Fz (top frame), the electrocardiogram (ECG) signal (middle frame), and the respiration belt signal (bottom frame). In Fz, note the switch-on spike at $t = 15$ s and the onset of stimulation at $t = 18$ s, resulting in a larger than 100-fold increase of the signal amplitude. The low-pass filtered ECG and RESP signals show the subject's heartbeat and respiration events, respectively; they serve to extract the event-averaged amplitude modulation (AM) kernels that are used to remove the modulation from the EEG signal.

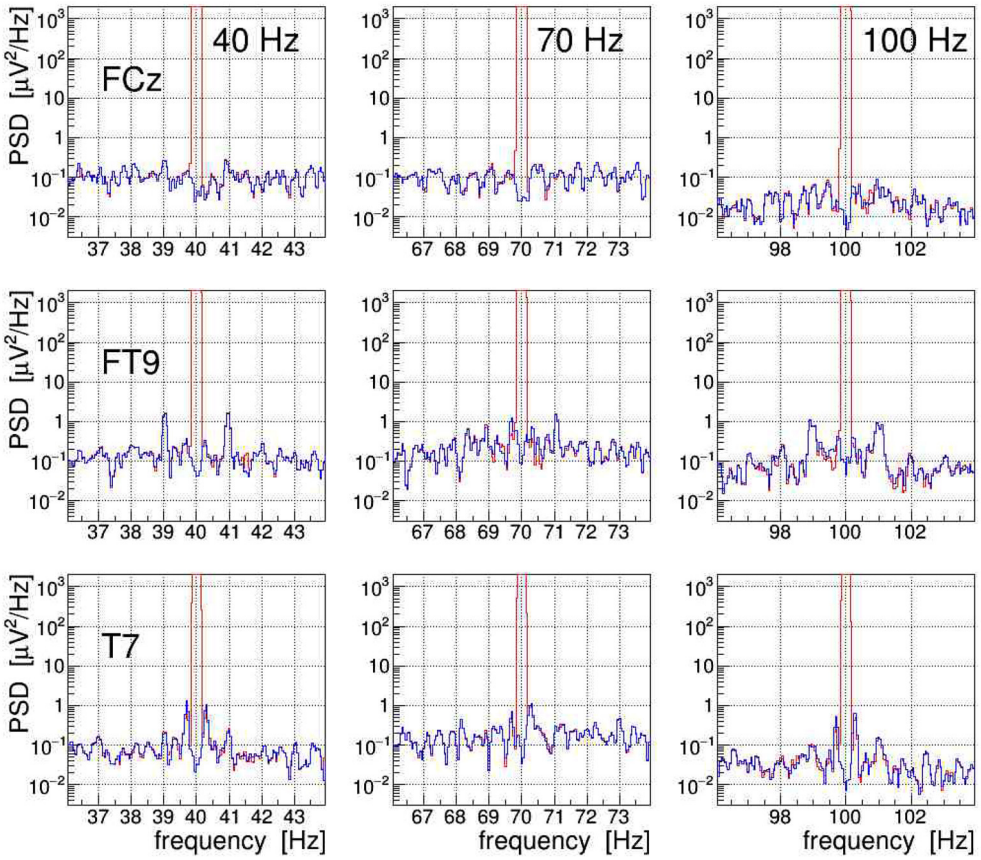

FIGURE 11 | On-subject electroencephalogram (EEG) power spectra at the three electrode sites FCz, FT9, and T7 (from top to bottom) recorded during transcranial alternating current stimulation (tACS) application at one of the three frequencies 40, 70, or 100 Hz (from left to right). The power spectral density (PSD) obtained from 20-s episodes (0.05 Hz frequency bins) are shown for the uncorrected signal (in red) and for the signal with only the main tACS artifact removed (in blue). For at least two of these electrodes, one can clearly see amplitude modulation (AM)-induced side-band power, caused either by the heartbeat of the subject (FT9) or by his respiration (T7). For site FCz, the AM effects are also present but they are much weaker.

stimulation current on all EEG electrode sites, particularly in close proximity to the tACS rubber pads.[7] More specifically, **Figure 11** shows a set of PSD distributions obtained by DFT (0.05 Hz bins, $\alpha = 4$ Kaiser–Bessel window) of 20-s long episodes of the three signals FCz, FT9, and T7, which are recorded while stimulation current was applied at frequencies of either 40, 70, or 100 Hz. These three signals were chosen to exemplify the typical characteristics of the stimulation artifacts observed in the data and to also illustrate the performance of our removal algorithms. The PSD are shown for the uncorrected EEG (in red) as well as after removal of the main tACS artifact by applying Equation (11) to the signals (in blue). From this set of power spectra, one can see that for all stimulations applied, the cleaned FCz signal is basically artifact free while on electrodes FT9 and T7 prominent side-band peaks remain visible at about ± 1 and ± 0.3 Hz of the central frequency. The peaks corresponding to higher beat harmonics are expected to be very weak and, in our data, they are just barely visible above the intrinsic EEG baseline.

The $\Delta f \simeq \pm 1$ Hz frequency separation matches the heartbeat rate of the subject recorded at about 60–70 beats/min, and the $\Delta f \approx \pm 0.3$ Hz intervals agree with the recorded respiration rate of about 20 breaths/min. Our observations corroborate that, depending on the electrode site on the scalp, the EEG can be amplitude modulated by the heartbeat and the respiration at varying degrees of intensity. From the ratio of the side-band power to the main peak power, one can compute the modulation index m which characterizes the effect size. For heartbeat-induced modulation, we find values of m up to $\simeq 1.0 \times 10^{-3}$ and likewise, for respiration-induced modulation, up to $\simeq 1.2 \times 10^{-3}$. These values are compatible with the modulation effects reported by Noury et al. (2016), although the observed absolute side-band power differs between both experiments. Note, however, that differences in experimental conditions, in particular in the respective EEG montage used, in the placement of the tACS electrodes, in the intensity of the stimulation currents applied, but also (uncontrollable) inter-subject differences may explain these dissimilarities. Ultimately, all results concur in showing that the subtraction of the main tACS artifact is not sufficient to also remove the AM-induced side-band artifact.

[7]The corresponding power topographies for 70- and 100-Hz tACS look very similar to the presented 40-Hz map.

Another, more direct way to quantify modulation effects is to demodulate the EEG signal at the given stimulation frequency (see section 2.2). To achieve this, we have computed the norm of its analytic signal by applying Equation (9) to the EEG. After detrending the result of this operation, needed to remove the constant term of the signal envelope, the AM kernel $K(t)$ is obtained. As the modulation index is found to be of order $\leq 10^{-3}$ only, resulting in a very noisy single-event kernel, we have averaged $K(t)$ over all heartbeats or respiratory events located within a given 30-s interval, and then low-pass filtered (32nd order Butterworth) the heartbeat-averaged and respiration-averaged kernels $\bar{K}(\Delta t)$ at 3.5 and 1 Hz, respectively; in this, Δt stands for the relative time in the interval with respect to the heartbeat or breathing event. Here, it is important to realize that the event-averaging produces a kernel for either the heartbeat or the respiration, i.e., we end up with two separate kernels for each EEG signal. The $\bar{K}(\Delta t)$ extracted by demodulating and event-averaging the FCz, FT9, and T7 signals, recorded during a 100-Hz stimulation, are shown in **Figure 12** as a function of Δt. The amplitudes of the displayed kernels are a direct measure of the modulation effect size m and they confirm that the tACS signal on site FT9 is mostly modulated by the heartbeats while, on site T7, it is mostly affected by respiration.

With the event-averaged kernels available, we can finally proceed to remove the amplitude-modulation artifacts from the measured EEG signals. Following the procedures outlined in section 3, we apply the corrections to each recorded EEG signal in three steps: first, we use the heartbeat-averaged AM kernel to remove, using Equation (10), the corresponding modulation from the EEG signal; second, we repeat this operation with the respiration-averaged AM kernel; and third, we suppress with Equation (11) the by far dominant artifact at the main stimulation frequency (by 85 dB for signal FCz, 83 dB for FT9, and 70 dB for T7). This cascaded cleaning procedure is exemplified in **Figure 13** with the EEG signals recorded from electrodes FCz, FT9, and T7. Shown are the PSD distributions of the signals at different stages of the procedure: the PSD of the uncorrected signal is plotted in red, the PSD of the signal with heartbeat AM removed is shown in blue, and the final result, after removal of the respiration AM and the main artifact, is shown as green line. The figure also superimposes the respective PSD obtained during 20-s long off-stimulation episodes, i.e., under a "sham" condition (shown in black). Comparing with the artifact-corrected PSD, we find that the cleaning method is free of bias, comparable to our observations on the demonstrator.

To summarize our results, **Figure 14** presents topographic maps of the fully cleaned PSD obtained for a stimulation frequency of 40 Hz in **(B)**, 70 Hz in **(C)**, and 100 Hz in **(D)**. In generating these maps, the PSD has been integrated over a narrow frequency band, centered on the stimulation frequency, and normalized to a corresponding artifact-free frequency interval. This normalization intends to remove channel-by-channel gain and effect variations, resulting ideally in a clean PSD ratio of one. As **Figure 14** shows, the ratio stays indeed close to unity (within 10–20%) on most of the scalp, demonstrating that the artifact removal works reliably over more than eight decimal orders of magnitude. However, in the fronto-temporal regions, a slight tendency to rise above one is visible and may point to

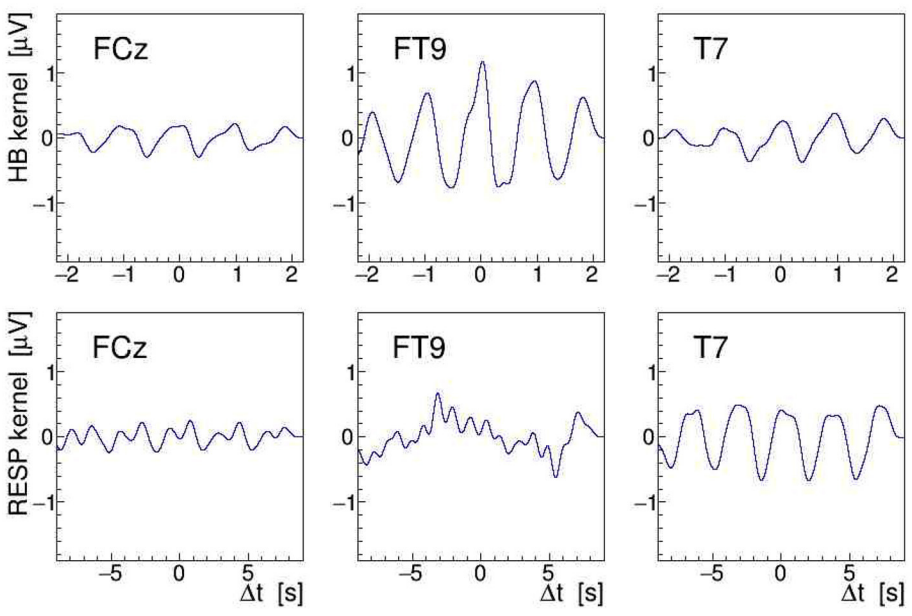

FIGURE 12 | On-subject average amplitude modulation (AM) kernels $\bar{K}(\Delta t)$ obtained by demodulation of the electroencephalogram (EEG) signals recorded during 30 s of 100 Hz transcranial alternating current stimulation (tACS) application from electrodes FCz, FT9, and T7 (left to right). These kernels were obtained by averaging short segments of the signal envelope, time-locked either to individual heartbeats (upper row) or to individual breathing events (lower row). The $\bar{K}(\Delta t)$ are displayed as a function of relative time within the segments centered on the given electrocardiogram (ECG) or RESP events (see **Figure 9**).

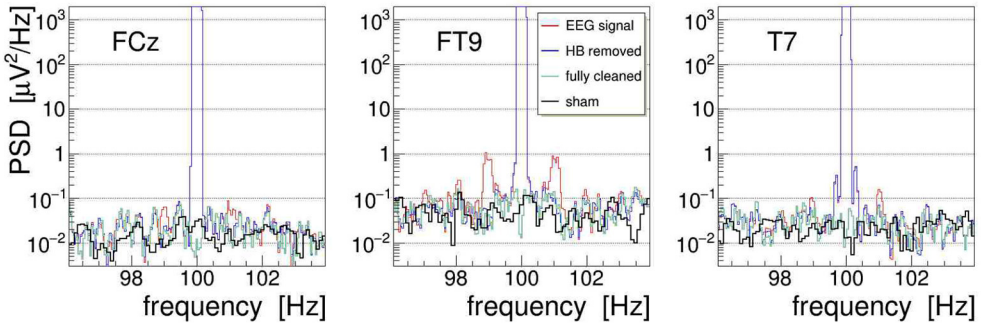

FIGURE 13 | On-subject power spectral density (PSD) of the electroencephalogram (EEG) signals FCz, FT9, and T7 recorded during 100-Hz transcranial alternating-current stimulation (tACS) application (shown in red). The three artifact-removal steps discussed in the text have been applied, namely (1) removal of the heartbeat modulation (blue), (2) removal of the respiration modulation (not shown), and (3) removal of the main artifact at the stimulation frequency, yielding finally the fully cleaned PSD (green). For comparison, the fully cleaned PSD obtained after the end of stimulation, i.e., under sham condition, is also shown (black).

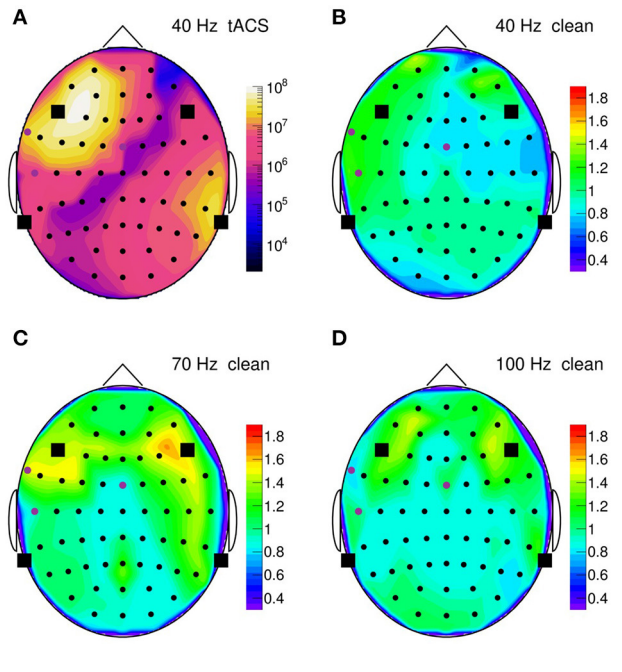

FIGURE 14 | (A) Topographic map of the on-subject power spectral density (PSD) observed in the 35–45 Hz frequency band during 40-Hz stimulation, normalized channel-by-channel to the respective 50–70 Hz power; PSD is computed over a 30 s time span. Round symbols indicate the electroencephalogram (EEG) electrodes, squares represent the transcranial alternating current stimulation (tACS) electrodes. **(B)** Topographic map of the normalized PSD after artifact removal; **(C)** same for 70-Hz stimulation (normalized to the 80–100 Hz power); **(D)** same for 100-Hz stimulation (normalized to the 110–150 Hz power).

a genuine increase of EEG activity induced by the stimulation. More studies are certainly required to clarify this point.

Note finally that, although we present all results in the frequency domain, the cleaning procedure itself is completely applied in the time domain. The fully cleaned EEG signal is hence also obtained in the time domain (see as well **Figure 10**), meaning that it can be subjected at will to any further analysis in either domain, time or frequency.

4.4. Limitations

In this paper, we have provided proof-of-principle results for a few stimulation frequencies only, 40, 70 and 100 Hz, all lying in the low and high gamma bands. This choice resulted from our observation that the side-band artifacts were very weak or even not observable for much lower frequencies, e.g., 10 Hz, in line with the overall rising trend of the intrinsic EEG power toward low frequencies. We see, however, no obvious reason why our cleaning procedures should not remain valid for stimulation frequencies situated in the lower bands. On the other hand, for very low frequencies ($f_s \ll 10$ Hz), the small spacing between the overtones of the main artifact will eventually lead those harmonics to intermingle with the side-band frequencies. In other words, in cases where the artifacts would nonetheless remain visible, their spectrum would tend to develop a very complex structure, which then may become difficult to fully remove.

As already stated in section 4, we have kept the stimulation current at 0.6 mA_{pp}. This was mainly motivated by our interest in applying combined tACS–EEG in sleep studies. In studies of sleep, the tolerance level for skin irritations, like tingling and burning sensations, as well as for induced visual effects (phosphenes) is usually quite low. However, these limitations may apply to a much lesser degree in many other investigations involving awake subjects. In that respect, the validation of our method would indeed have to be extended with higher stimulation currents. Still, all transformations involved in the cleaning procedure being linear, we do not expect the latter to fail when applied to larger currents, at least insofar as the EEG amplifier dynamic range can also accommodate the larger signals.

Another limitation of our experiment was that the subject kept largely immobile with eyes closed, again a setting typical for sleep studies. In investigations on awake subjects, in particular studies targeting cognitive and motor tasks (see, e.g., Santarnecchi et al., 2013; Guerra et al., 2018; Bologna et al., 2019), additional movement artifacts caused by eye saccades and blinking, head

movements, body shifts, etc., can distort the recorded EEG. Unfortunately, because of their largely non-periodic nature, these artifacts are not directly amenable to a treatment with the cleaning algorithms discussed here. We believe, however, that our procedures can be combined with other cleaning methods, e.g., a modified eye blink detection and removal algorithm that synchronizes with the periodic stimulation current.

5. SUMMARY

In this paper, we have discussed the nuisance effects induced in the EEG during application of transcranial alternating current stimulation confirming, in particular, the recent observation of amplitude-modulation effects by Noury et al. (2016). Assuming that *ad hoc* physiological mechanisms, involving the heartbeat or respiration, lead to rhythmic changes of the body impedance, these must in turn induce an amplitude modulation of the tACS artifact in the measured EEG signals. We have demonstrated how such modulation effects can be produced in phantom data recorded with a demonstrator setup. We have further described a multi-step artifact-removal procedure and validated its implementation on these recordings as well as on human subject data, while focusing on stimulation frequencies in the low and high gamma bands. In line with former observations, we were thus able to implement modulation effects artificially (phantom data) and confirm their existence in our human-subject recordings. However, the observed effect sizes turned out to be of lesser magnitude than those reported originally in Noury et al. (2016). We hypothesize that these differences are caused by dissimilarities of the used experimental protocols (e.g., distances between tACS electrode placement and EEG recording sites) as well as by inter-subject differences. It would be interesting to follow up on this line of thought with more systematic investigations, as this could lead to specific recommendations how to best minimize such artifacts in future studies. Our cleaning approach has, furthermore, the potential to lend itself to adaptive parametric filtering techniques, e.g., along the lines discussed by Kohli and Casson (2019). This will, however, require more dedicated investigations. The ability to monitor the actual impact of the stimulation on targeted neuronal circuits would be of great value, not only for basic science but also in the applied medical fields. In the clinical context, there is an emerging interest in tACS as a supportive treatment of various mental (Klimke et al., 2016; Elyamany et al., 2020; Kayarian et al., 2020) and movement (Krause et al., 2014; Castiglia et al., 2018; Felice et al., 2019; Guerra et al., 2020) disorders. While general guidelines for the application of electrical stimulations have been proposed (Antal et al., 2017; Lefaucheur et al., 2017), one should keep in mind that, in clinical settings, simple EEG protocols and robust analysis procedures, such as the one presented in this paper are to be preferred. To conclude, we believe that the results of the present study can help making progress into that direction.

DATA AVAILABILITY STATEMENT

The raw data supporting the conclusions of this article will be made available by the authors, without undue reservation.

ETHICS STATEMENT

Ethical review and approval was not required for the study on human participants in accordance with the local legislation and institutional requirements. The patients/participants provided their written informed consent to participate in this study.

AUTHOR CONTRIBUTIONS

RH designed, implemented, and applied the analysis algorithms, and prepared the manuscript. JK-G supervised the EEG data collection. UV and AK contributed to the study design and critically reviewed the manuscript. All authors contributed to the article and approved the submitted version.

ACKNOWLEDGMENTS

We thank Maria Ruse for her help in data acquisition.

REFERENCES

Antal, A., Alekseichuk, I., Bikson, M., Brockmöller, J., Brunoni, A., Chen, R., et al. (2017). Low intensity transcranial electric stimulation: safety, ethical, legal regulatory and application guidelines. *Clin. Neurophysiol.* 128, 1774–1809. doi: 10.1016/j.clinph.2017.06.001

Bendat, J. S., and Piersol, A. G. (2010). *Random Data–Analysis and Measurement Procedures*. New York, NY: John Wiley & Sons.

Bologna, M., Guerra, A., Paparella, G., Colella, D., Borrelli, A., Suppa, A., et al. (2019). Transcranial alternating current stimulation has frequency-dependent effects on motor learning in healthy humans. *Neuroscience* 411, 130–139. doi: 10.1016/j.neuroscience.2019.05.041

Caldwell, D. J., Cronin, J. A., Rao, R. P. N., Collins, K. L., Weaver, K. E., Ko, A. L., et al. (2020). Signal recovery from stimulation artifacts in intracranial recordings with dictionary learning. *J. Neural Eng.* 17:026023. doi: 10.1088/1741-2552/ab7a4f

Castiglia, L., Formaggio, E., Tenconi, E., Gallo, L., Tonellato, M., Masiero, S., et al. (2018). Effects of personalized transcranial alternating current stimulation associated with physical therapy on motor and cognitive functions in people with Parkinson's disease. *Ann. Phys. Rehabil. Med.* 61:e255. doi: 10.1016/j.rehab.2018.05.592

Elyamany, O., Leicht, G., Herrmann, C. S., and Mulert, C. (2020). Transcranial alternating current stimulation (tACS): from basic mechanisms towards first applications in psychiatry. *Eur. Arch. Psychiatry Clin. Neurosci.* 271, 135–156. doi: 10.1007/s00406-020-01209-9

Fehér, K. D., Nakataki, M., and Morishima, Y. (2017). Phase-dependent modulation of signal transmission in cortical networks through tACS-induced neural oscillations. *Front. Hum. Neurosci.* 11:471. doi: 10.3389/fnhum.2017.00471

Felice, A. D., Castiglia, L., Formaggio, E., Cattelan, M., Scarpa, B., Manganotti, P., et al. (2019). P73-s TACS and physical therapy for motor and cognitive symptoms in Parkinson's disease: randomized cross-over trial. *Clin. Neurophysiol.* 130:e114. doi: 10.1016/j.clinph.2019.04.601

Guarnieri, R., Brancucci, A., D'Anselmo, A., Manippa, V., Swinnen, S. P., Tecchio, F., et al. (2020). A computationally efficient method for the attenuation of alternating current stimulation artifacts in electroencephalographic recordings. *J. Neural Eng.* 17:046038. doi: 10.1088/1741-2552/aba99d

Guerra, A., Asci, F., D'Onofrio, V., Sveva, V., Bologna, M., Fabbrini, G., et al. (2020). Enhancing gamma oscillations restores primary motor cortex plasticity in Parkinson's disease. *J. Neurosci*. 40, 4788–4796. doi: 10.1523/JNEUROSCI.0357-20.2020

Guerra, A., Bologna, M., Paparella, G., Suppa, A., Colella, D., Lazzaro, V. D., et al. (2018). Effects of transcranial alternating current stimulation on repetitive finger movements in healthy humans. *Neural Plast*. 2018, 1–10. doi: 10.1155/2018/4593095

Haslacher, D., Nasr, K., Robinson, S. E., Braun, C., and Soekadar, S. R. (2020). Stimulation artifact source separation (SASS) for assessing electric brain oscillations during transcranial alternating current stimulation (tACS). *Neuroimage* 228:11751. doi: 10.1016/j.neuroimage.2020.117571

Heinzel, G., Rüdiger, A., and Schilling, R. (2002). *Spectrum and Spectral Density Estimation by the Discrete Fourier Transform (DFT), Including a Comprehensive List of Window Functions and Some New Flat-Top Windows*. Technical report, Max Planck Gesellschaft. Available online at: http://hdl.handle.net/11858/00-001M-0000-0013-557A-5

Helfrich, R. F., Knepper, H., Nolte, G., Strüber, D., Rach, S., Herrmann, C. S., et al. (2014a). Selective modulation of interhemispheric functional connectivity by HD-tACS shapes perception. *PLoS Biol*. 12:e1002031. doi: 10.1371/journal.pbio.1002031

Helfrich, R. F., Schneider, T. R., Rach, S., Trautmann-Lengsfeld, S. A., Engel, A. K., and Herrmann, C. S. (2014b). Entrainment of brain oscillations by transcranial alternating current stimulation. *Curr. Biol*. 24, 333–339. doi: 10.1016/j.cub.2013.12.041

Herrmann, C. S., Rach, S., Neuling, T., and Strüber, D. (2013). Transcranial alternating current stimulation: a review of the underlying mechanisms and modulation of cognitive processes. *Front. Hum. Neurosci*. 7:279. doi: 10.3389/fnhum.2013.00279

Kayarian, F. B., Jannati, A., Rotenberg, A., and Santarnecchi, E. (2020). Targeting gamma-related pathophysiology in autism spectrum disorder using transcranial electrical stimulation: opportunities and challenges. *Autism Res*. 13, 1051–1071. doi: 10.1002/aur.2312

Klimke, A., Nitsche, M. A., Maurer, K., and Voss, U. (2016). Case report: successful treatment of therapy-resistant OCD with application of transcranial alternating current stimulation (tACS). *Brain Stimul*. 9, 463–465. doi: 10.1016/j.brs.2016.03.005

Kohler, B. U., Hennig, C., and Orglmeister, R. (2002). The principles of software QRS detection. *IEEE Eng. Med. Biol. Mag*. 21, 42–57. doi: 10.1109/51.993193

Kohli, S., and Casson, A. J. (2019). Removal of gross artifacts of transcranial alternating current stimulation in simultaneous EEG monitoring. *Sensors* 19:190. doi: 10.3390/s19010190

Krause, V., Wach, C., Südmeyer, M., Ferrea, S., Schnitzler, A., and Pollok, B. (2014). Cortico-muscular coupling and motor performance are modulated by 20 Hz transcranial alternating current stimulation (tACS) in Parkinson's disease. *Front. Hum. Neurosci*. 7:928. doi: 10.3389/fnhum.2013.00928

Lefaucheur, J. P., Antal, A., Ayache, S. S., Benninger, D. H., Brunelin, J., Cogiamanian, F., et al. (2017). Evidence-based guidelines on the therapeutic use of transcranial direct current stimulation (tDCS). *Clin. Neurophysiol*. 128, 56–92. doi: 10.1016/j.clinph.2016.10.087

Nelder, J. A., and Mead, R. (1965). A simplex method for function minimization. *Comput. J*. 7, 308–313. doi: 10.1093/comjnl/7.4.308

Neuling, T., Ruhnau, P., Weisz, N., Herrmann, C. S., and Demarchi, G. (2017). Faith and oscillations recovered: on analyzing EEG/MEG signals during tACS. *Neuroimage* 147, 960–963. doi: 10.1016/j.neuroimage.2016.11.022

Noury, N., Hipp, J. F., and Siegel, M. (2016). Physiological processes non-linearly affect electrophysiological recordings during transcranial electric stimulation. *Neuroimage* 140, 99–109. doi: 10.1016/j.neuroimage.2016.03.065

Noury, N., and Siegel, M. (2017). Phase properties of transcranial electrical stimulation artifacts in electrophysiological recordings. *Neuroimage* 158, 406–416. doi: 10.1016/j.neuroimage.2017.07.010

Owda, A. Y., and Casson, A. J. (2020). Electrical properties, accuracy, and multi-day performance of gelatine phantoms for electrophysiology. *bioRxiv*. doi: 10.1101/2020.05.30.125070

Pan, J., and Tompkins, W. J. (1985). A real-time QRS detection algorithm. *IEEE Trans. Biomed. Eng*. 32, 230–236. doi: 10.1109/TBME.1985.325532

Paulus, W., Peterchev, A. V., and Ridding, M. (2013). "Transcranial electric and magnetic stimulation," in *Handbook of Clinical Neurology*, eds A. M. Lozano and M. Hallett (Amsterdam: Elsevier), 329–342. doi: 10.1016/B978-0-444-53497-2.00027-9

Santarnecchi, E., Polizzotto, N. R., Godone, M., Giovannelli, F., Feurra, M., Matzen, L., et al. (2013). Frequency-dependent enhancement of fluid intelligence induced by transcranial oscillatory potentials. *Curr. Biol*. 23, 1449–1453. doi: 10.1016/j.cub.2013.06.022

Voss, U., Holzmann, R., Hobson, A., Paulus, W., Koppehele-Gossel, J., Klimke, A., et al. (2014). Induction of self awareness in dreams through frontal low current stimulation of gamma activity. *Nat. Neurosci*. 17, 810–812. doi: 10.1038/nn.3719

Vosskuhl, J., Mutanen, T. P., Neuling, T., Ilmoniemi, R. J., and Herrmann, C. S. (2020). Signal-space projection suppresses the tACS artifact in EEG recordings. *Front. Hum. Neurosci*. 14:536070. doi: 10.3389/fnhum.2020.536070

Witkowski, M., Garcia-Cossio, E., Chander, B. S., Braun, C., Birbaumer, N., Robinson, S. E., et al. (2016). Mapping entrained brain oscillations during transcranial alternating current stimulation (tACS). *Neuroimage* 140, 89–98. doi: 10.1016/j.neuroimage.2015.10.024

Zaehle, T., Rach, S., and Herrmann, C. S. (2010). Transcranial alternating current stimulation enhances individual alpha activity in human EEG. *PLoS ONE* 5:e13766. doi: 10.1371/journal.pone.0013766

Conflict of Interest: The authors declare that the research was conducted in the absence of any commercial or financial relationships that could be construed as a potential conflict of interest.

frontiers in Human Neuroscience

PERSPECTIVE
published: 14 June 2021
doi: 10.3389/fnhum.2021.699473

Transcranial Auricular Vagus Nerve Stimulation (taVNS) and Ear-EEG: Potential for Closed-Loop Portable Non-invasive Brain Stimulation

Philipp Ruhnau[1,2]* *and Tino Zaehle*[1,2]*

[1] Department of Neurology, Otto von Guericke University, Magdeburg, Germany, [2] Center for Behavioral Brain Sciences, Otto von Guericke University, Magdeburg, Germany

No matter how hard we concentrate, our attention fluctuates – a fact that greatly affects our success in completing a current task. Here, we review work from two methods that, in a closed-loop manner, have the potential to ameliorate these fluctuations. Ear-EEG can measure electric brain activity from areas in or around the ear, using small and thus portable hardware. It has been shown to capture the state of attention with high temporal resolution. Transcutaneous auricular vagus nerve stimulation (taVNS) comes with the same advantages (small and light) and critically current research suggests that it is possible to influence ongoing brain activity that has been linked to attention. Following the review of current work on ear-EEG and taVNS we suggest that a combination of the two methods in a closed-loop system could serve as a potential application to modulate attention.

Keywords: attention, ear-EEG, mobile EEG, non-invasive brain stimulation, taVNS

OPEN ACCESS

Edited by:
Florian H. Kasten,
University of Oldenburg, Germany

Reviewed by:
Martin Georg Bleichner,
University of Oldenburg, Germany
Bashar W. Badran,
Medical University of South Carolina, United States
Peijing Rong,
China Academy of Chinese Medical Sciences, China

***Correspondence:**
Philipp Ruhnau
mail@philipp-ruhnau.de
Tino Zaehle
tino.zaehle@ovgu.de

Specialty section:
This article was submitted to Brain Imaging and Stimulation, a section of the journal Frontiers in Human Neuroscience

Received: *23 April 2021*
Accepted: *21 May 2021*
Published: *14 June 2021*

Citation:
Ruhnau P and Zaehle T (2021) Transcranial Auricular Vagus Nerve Stimulation (taVNS) and Ear-EEG: Potential for Closed-Loop Portable Non-invasive Brain Stimulation. Front. Hum. Neurosci. 15:699473. doi: 10.3389/fnhum.2021.699473

INTRODUCTION

We experience natural lapses of attention in everyday life. These fluctuations are common, and yet they can have drastic consequences if they occur in situations that require constant high attention. For instance, a major part of traffic accidents caused by human error are linked to attention lapses.

Imagine, then, if one could make use of a device that is not only capable of detecting changes in this system, but could also prevent them from occurring altogether. Such a device would have incredible potential to enhance attention in various demographics – from students learning for a test, to air-traffic control officers directing pilots safely to the airport – but also offer a variety of applications for clinical populations with attention deficits.

Current systems can detect early physiological markers of drowsiness (e.g., heart rate, respiratory activity, and eye movement) and send out warning signals to alert an individual to a lapse of attention. The fact that many vehicle companies now implement such "drowsiness detectors" or "attention assist" systems emphasizes how promising this feedback approach is. However, these approaches are still *reactive* – acting when the attention system is already fluctuating. Here, we suggest an approach that has the potential to proactively prevent such fluctuations.

This system needs to be (I) portable, to allow use in everyday life; (II) adaptable to the individual's brain state in real time; and (III), able to stimulate the brain's attention system non-invasively.

A system with this potential would need to comprise two parts: first, a method to read out attentive states in real time and second, a system that is capable of modulating cortical states in or close to real time. We suggest the use of the electroencephalogramm (EEG), specifically ear-EEG as a read-out and transcutaneous auricular vagus nerve stimulation (taVNS) to modulate brain activity. Combining these two into a closed-loop, would allow the three points from above to be addressed.

In the following we will provide a brief overview of work on ear-EEG and taVNS. As marker of attention, we will focus on cortical alpha oscillations. We think a closed-loop system based on ear-EEG and taVNS would provide us with a flexible, efficient, and individually tailored system that could be used to actively influence participants' attention in real time.

MOBILE EEG AND RECORDINGS FROM THE EAR

The first mobile EEG systems where already envisioned in the first half of the 20th century by a pioneer of EEG research, Herbert Jasper (see De Vos and Debener, 2014). Today these visions have become reality and mobile EEG systems allow for the recordings of brain activity in everyday life situations, with much greater potential to treat a variety of disorders compared to lab-based research (Debener et al., 2012). Mobile systems have been used in highly different settings, such as during physical activity (Scanlon et al., 2019), in the work space (Wascher et al., 2016), during driving (Wang et al., 2018), and even while walking a tightrope (Leroy and Cheron, 2020).

One great potential in using mobile EEG systems lies in the chance to report brain activity to the wearer and allowing for quick adjustments in behavior. This method, termed biofeedback, has used EEG to allow subjects to change their own state of mind to, for instance to alleviate stress, since the 1960s (e.g., Brown, 1974, 1977). However, this type of research, which quickly developed into treatment types, was always limited to the laboratory or clinical setting. Given that our environment is much more complex than the typical lab setting and what we can show on computer screens and present via headphones, the advantage of taking biofeedback out "for a walk" is obvious (Debener et al., 2012). The mobility of today's EEG systems gives us the option to bring them in situations that biofeedback might be most beneficial, for instance, in anxiety inducing situations or during work where attention fluctuations can have the most impact.

A relatively novel type of mobile EEG measures electrophysiologic brain signals via electrodes connected to the ear. This can be done by either placing electrodes in the ear canal or the zymba concha (in-ear-EEG; Kidmose et al., 2012; Looney et al., 2012; Lee et al., 2014) or the area behind the ear (around-the-ear EEG/cEEGrid; Debener et al., 2015; Bleichner and Debener, 2017; Kaongoen and Jo, 2020). Major advantages of the method are its portability and unobtrusiveness – even more so than mobile EEG caps – and thereby chance to study brain activity for extended times. Ear-EEG has been suggested as a clinical tool, for instance, to diagnose epilepsy (Zibrandtsen et al., 2017; Gu et al., 2018) or to monitor sleep quality (Mikkelsen et al., 2017; Tabar et al., 2020). There are also initial results showing that levels of concentration could be monitored using ear-EEG (Kaongoen and Jo, 2020). Finally, ear-EEG has also shown to be able to track the focus of attention (Mirkovic et al., 2016) even in everyday life situations (Hölle et al., 2021).

Studies comparing ear-EEG with conventional EEG have evaluated well-known electrophysiological parameters. It has been shown that event-related potentials – such as the N1, an index of auditory sensory processing, and the P300, indexing the processing of task relevant stimuli – can be measured reliably (Looney et al., 2012; Debener et al., 2015; Mirkovic et al., 2016; Krigolson et al., 2017). Many recent developments improve the data quality that can be captured at the ear by improving the sensors or data acquisition (Kappel et al., 2019a,b; Sintotskiy and Hinrichs, 2020). Ear-EEG is most sensitive to temporal cortex activity (Meiser et al., 2020), which is great to monitor auditory system activity, such as attention to a specific sound stream (Fiedler et al., 2017). However, also dominant parietal activity, particularly neural oscillations in the alpha frequency range (around 10 Hz) can be detected well using ear-EEG (Looney et al., 2011; Debener et al., 2015; Mikkelsen et al., 2015).

Alpha brain activity is particularly interesting because it has been linked to a number of attention mechanisms and active inhibition (Jensen and Mazaheri, 2010; Klimesch, 2012; Frey et al., 2015). Most notably, attended locations are accompanied by a reduction in oscillatory alpha activity in the contralateral (compared to the ipsilateral) hemisphere that processes the location. For instance, focusing on our left hand will reduce alpha activity in the right somatosensory cortex, compared to the left, and vice versa (Haegens et al., 2011). Consequently, when alpha activity increases attention drops and subjects are more likely to miss information. Thus, an unobtrusive system that can, in real-time, measure attention drops via alpha activity reduction would open the gate to its modulation.

TRANSCUTANEOUS AURICULAR VAGUS NERVE STIMULATION

Transcutaneous auricular vagus nerve stimulation (taVNS) is a new, non-invasive neuromodulation method. TAVNS is based on electrical stimulation of cutaneously distributed vagal afferents. Unlike more established non-invasive brain stimulation methods such as transcranial direct current stimulation (tDCS) and transcranial alternating current stimulation (tACS), taVNS does not directly modulate the reactivity of neurons within specific cortical target areas. Instead, taVNS aims to promote increased noradrenergic neurotransmission through indirect stimulation of the locus coeruleus (LC), which in turn causes systemic modulation of brain function.

Transcranial auricular vagus nerve stimulation was derived from invasive vagus nerve stimulation (iVNS) that is used to treat a number of neuropsychiatric disorders (Broncel et al., 2020). IVNS is based on a neurosurgical implantation of electrodes

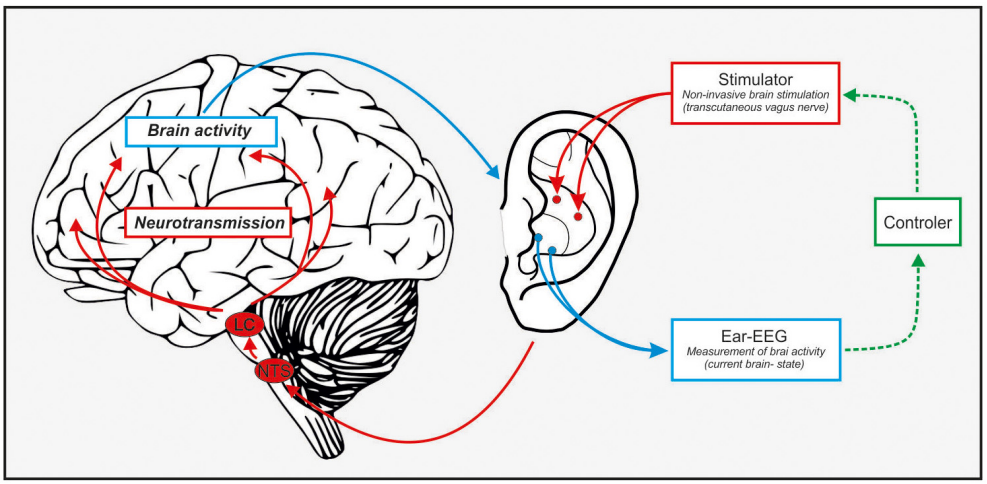

FIGURE 1 | Schematic illustration of a closed-loop in-ear stimulator/recorder. Ear-EEG can pick up on attention markers (alpha oscillations, event-related P300), this information gets fed to a controller that – given a decrease in attention – can start the taVNS which stimulates the NTS-LC system and elevate NE levels. This in turn should result in an increase of attention (or a reduction of the decrease).

around the left cervical vagus nerve and comes with all typical side effects associated with an invasive intervention (Fahy, 2010). The obvious benefit of taVNS over iVNS is that it is non-invasive, reducing costs and risk, and therefore having a much broader application field. It is safe and well tolerated (Redgrave et al., 2018) and has the great potential to both reduce clinical symptoms in patient populations as well as to serve basic science gain. Precisely because cost is typically a major factor that both limits access to medicine and constrains basic science, taVNS has the ultimate potential to significantly improve fairness in medical care and use in basic science.

In the last decade, there is growing evidence for a successful application of taVNS to reduce symptoms in a wide range of medical conditions including drug-resistant epilepsy and depression (Hein et al., 2013; Bauer et al., 2016), but also tinnitus (De Ridder et al., 2014), schizophrenia (Hasan et al., 2015), Alzheimer's dementia (Kaczmarczyk et al., 2018), or chronic pain (Napadow et al., 2012). Furthermore, taVNS together with neurorehabilitation has successfully improved motor disorder symptoms in adults and children (Badran et al., 2020; Cook et al., 2020). Moreover, in healthy participants, taVNS has been proven efficient in modulating attention and cognition (Sun et al., 2017; Fischer et al., 2018; Sellaro et al., 2018). These cognitive effects of taVNS in healthy subjects and patients are assumed to be related to concentration shifts of the neurotransmitter norepinephrine (NE) and gamma-aminobutyric acid (GABA) (Van Leusden et al., 2015) caused by a stimulation of the locus coeruleus (LC) via afferent vagal fibers. For that purpose, taVNS is usually applied via electrodes attached to the cymba concha of the auricle and intends to stimulate the afferent vagal fibers of the auricular branch. TaVNS activates Aß-fibers signaling impulses ascending from the periphery to the brainstem nuclei and hereinafter to the cortex (Broncel et al., 2020; Butt et al., 2020). In particular, these vagal fibers terminate in the nucleus of the solitary tract (NTS) (Knowles and Aziz, 2009), which has widespread projections to several forebrain, limbic and brainstem sites, including the LC, the main source of noradrenaline in the human brain (Aston-Jones et al., 1991). In accordance to this anatomical connection, the core mechanism of action for taVNS relies on an activation of the locus coeruleus-norepinephrine (LC-NE) system (Frangos et al., 2015; Yakunina et al., 2017). Accordingly, in animal models and patient data, the direct link between electrical stimulation of the afferent vagal fibers and increased NE release via LC activation has been demonstrated (Dorr and Debonnel, 2006; Manta et al., 2013; Hulsey et al., 2017). Strong evidence for comparable mechanisms underlying the effects of non-invasive application of VNS in healthy participants stems from functional neuroimaging studies that consistently demonstrated taVNS induced activations in brain stem regions, including the NTS, and the LC (see Badran et al., 2018a for a recent review). Furthermore, electrophysiological marker of the LC-NE system such as the P300 component of the event-related potential (Nieuwenhuis et al., 2005; Chmielewski et al., 2017) can support the hypothesis that taVNS enhances central NE levels. Accordingly, the amplitude of the P300 is enhanced during invasive VNS (Brázdil et al., 2001; Schevernels et al., 2016) as well as during the application of taVNS (Rufener et al., 2018; Ventura-Bort et al., 2018; Lewine et al., 2019). A recent comprehensive study showed that taVNS in healthy participants systematically affected the LC-NE system indicated by a robust pupil dilation effect, accompanied by an attenuation of occipital alpha activity (Sharon et al., 2021). This study demonstrated that taVNS in healthy participants might well be able to increase attention by an elevation of noradrenaline.

Finally, animal and human studies have linked stimulation of the vagal afferent fibers to Gamma-aminobutyric acid (GABA) transmission due to activation of the NTS as well. Thus, an increase in GABA transmission can be assumed as a secondary

mechanism of action of taVNS (Keute et al., 2018; Broncel et al., 2019). Alternatively, it has been assumed that taVNS always has a combined effect on both, NE and GABA (Beste et al., 2016).

Although attention is regulated by several neurotransmitter systems, noradrenaline is one of the most important. Accordingly, central noradrenaline is involved in the control of attention (Woodward et al., 1979), and further plays an important modulatory role in cognitive processes such as vigilance, arousal, learning, and memory (Aston-Jones et al., 1991). It has been consistently shown that reducing central NE had deleterious effects on attention (Smith and Nutt, 1996), while elevating central NE improved performance in attention tasks (Sirviö et al., 1993; Bunsey and Strupp, 1995), indicating that an increased NE activity facilitates cortical circuit function that promote alertness and attention (Aston-Jones and Cohen, 2005).

Animal and human data further show that NE maintains an active role in regulating sustained and flexible attention (Aston-Jones et al., 1997; Aston-Jones and Cohen, 2005). Analogously, in healthy humans noradrenergic manipulation impairs sustained attention (Coull et al., 1995; Smith and Nutt, 1996), as well as focused and divided attention during dichotic listening experiments (Clark et al., 1986).

GABA is the main inhibitory neurotransmitter in the adult mammalian brain, but its role in the regulation of arousal and attention is less clearly defined. However, several data point to the notion that GABA plays an important role in the regulation of attention as well (Paine et al., 2015; Leonte et al., 2018). Animal data demonstrate a direct link between GABA levels in the brain and visual attention (Petersen et al., 1987) and relate the activity of GABAergic neurons to the regulation of attention (Paine et al., 2011; McGarrity et al., 2017). Consequently, decreasing GABA functioning impairs visual attention (Paine et al., 2011) while sub-optimally increasing it impairs attentional processing as well (Pezze et al., 2014).

Thus, attentional functions are strongly dependent on noradrenergic and GABAergic transmission. TaVNS has been demonstrated to be efficient in modulating these neurotransmitters and, accordingly directly affecting attentional processes.

COMBINING taVNS AND IN-EAR EEG

We suggest that combining the two mentioned methods offers a great opportunity for a portable, closed-loop, monitoring, and non-invasive stimulation device to stabilize fluctuations of sustained attention in a brain-state dependent manner (see **Figure 1** for a schematic illustration). Here, in-ear EEG will provide the biomarker-feedback signals that, in turn, modify stimulation parameters based on the adaptive feedback signal (closed-loop).

The EEG signal provides reliable markers of attention states; such as fluctuations in the cortical alpha rhythm that mirror attentional fluctuations (Fiedler et al., 2017; Jeong and Jeong, 2020). The ear-EEG system gives subjects the opportunity to move freely and wear the device for long periods of time. At the same time brain activity can be recorded at high temporal precision with the opportunity to transmit these data wirelessly (Bleichner and Debener, 2017; Kaveh et al., 2020). This would allow for constant monitoring of the participant's attention state. The ear-EEG readout can be easily processed by small controllers which could in turn provide information to the wearer.

Electroencephalogramm brain signals have been used directly as informative biofeedback in closed-loop systems, for instance, to reduce an imbalance of brain rhythms in tinnitus (Hartmann et al., 2014), as a treatment for epilepsy (Tan et al., 2009), or to improve symptoms in attention deficit disorder (Monastra et al., 2002). Sending feedback to the participant based on brain activity is powerful and fast, yet it is only slightly faster than measuring and reporting peripheral physiology (e.g., drowsiness detectors in cars, García et al., 2010; Leonhardt et al., 2018). The substantial improvement needed is a fast track to brain activity underlying attention lapses. This fast track could be provided by non-invasive transcranial brain stimulation, such as taVNS, which as reviewed above can successfully modulate brain activity via the LC-NE route. This non-invasive stimulation technique directly influences the attention network in the brain (Fang et al., 2016) and is therefore an ideal partner of ear-EEG. Furthermore, it has been shown that alpha oscillations can be modulated via taVNS (Sharon et al., 2021). Therefore, a closed-loop ear system focusing on alpha activity seems very promising.

A major advantage of the closed-loop system is that it respects state-dependent efficacy of non-invasive brain stimulation (Bergmann, 2018). It has been shown that transcranial electric stimulation of a specific neuronal population is more effective when applied when the region is active. For instance, stimulation is much more successful when targeting a region engaged in a task (Alagapan et al., 2016; Li et al., 2018) while stimulation efficacy of highly active regions is limited (Ruhnau et al., 2016). So far this has not been evaluated for taVNS and further the mechanism of action is rather global, instead of region specific for tACS or tDCS, therefore future research is essential to uncover state-dependent efficacy of taVNS.

There are a number of attention trainings that improve attention function and generalize to other cognitive functions (for a review see Tang and Posner, 2009; for a meta-analysis see Peng and Miller, 2016). It is important to compare effects of a closed-loop system to those of training programs to evaluate the benefit of such a system. Furthermore, a combination of taVNS and ear-EEG with attention trainings could be a fruitful avenue that might improve the benefit from the training. As mentioned before, brain stimulation depends on the brain state, thus applying stimulation during a training of attention might be even more beneficial.

In our view, alpha activity fluctuations are the best candidate at the moment to read out attentional states, they can be extracted in real time, and can be directly modulated non-invasively via taVNS. Consequently, groups that are affected by reduced alpha activity are ideal targets for the proposed closed-loop system. There are a number of disorders that can be linked to dysfunctional alpha activity compared to healthy control groups (for a review see Başar, 2013), such as depression (Jiang et al., 2016; Alexander et al., 2019), attention deficit

disorder (Hasler et al., 2016), Alzheimer's (Jafari et al., 2020), and Parkinson's disease (Zhu et al., 2019).

Furthermore, closed-loop EEG-VNS system can be of use in healthy populations in situations where a high and constant level of attention is required, for instance during aviating or driving. The great potential of this closed-loop system is the ongoing and extremely fast measurement of the brain state and immediate intervention when an attention lapse is approaching.

It is important to mention that research on brain stimulation has shown long-term plasticity effects due to stimulation. That means a permanent application of the closed-loop system is neither necessary nor intended, because stimulation-based functional and anatomical changes will improve attention abilities and reduce symptoms in patients following short-term application.

A NEED FOR PARAMETRIZATION OF taVNS SETTINGS

We want to take this opportunity to point out that taVNS results have recently shown variable efficacy of the method. There have been a number of studies providing inconsistent results of efficacy of taVNS, either absent effects or even inverted effects (e.g., Keute et al., 2018, 2019; Borges et al., 2021). One reason for this might be the variability of taVNS stimulation parameters in use. There have been a number of different stimulation frequencies (between 0.5 and 30 Hz), pulse width (50–500 μs), intensities (0.5–50 mA) and stimulation locations (see Burger et al., 2020 for a list of parameters). Very few studies aim to evaluate the role of taVNS parameters on efficacy. For instance, recently a study (Sharon et al., 2021) showed that taVNS when applied for a short time (3 s) can influence the pupil size – an index of LC driven NE level modulation – which has not been found for a more typical long-interval (30 s on/off) taVNS protocol (Keute et al., 2019). Unfortunately, there are no studies as of yet that evaluate which parameters influence taVNS efficacy systematically. Thus, at the moment we have no knowledge whether it is the duration of taVNS as suggested by Sharon et al. (2021) or any other of the parameters such as intensity, pulse width, or electrode size, which were all different in the two studies.

A promising approach might be to relate other physiological parameters that have been connected to vagal stimulation to neurostimulation efficacy. As such, the taVNS efficacy in modulating the heart rate (Badran et al., 2018b) and coupling of cardiac to neural activity seem promising (Keute et al., 2021) but warrant further investigation as well.

As with any new approaches in neuromodulation there is an urgent need to evaluate how to set the stimulations to yield maximal effects. This is not just an issue for taVNS but for the whole field of transcranial brain stimulation (Parkin et al., 2015; Frohlich and Townsend, 2021). One way to evaluate the effects of different parameters is to study efficacy of taVNS in a closed-loop as we proposed here. It would allow us to monitor effects in real time and adjust the stimulator accordingly, homing in to maximal efficacy.

LIMITATIONS AND CHALLENGES

An obvious challenge for a combination of taVNS and ear-EEG are their close proximity in the (most likely same) ear. For the EEG this means that there is unlikely a recordable signal, while the stimulation is running. Thus, the impact on the stimulation on brain activity can only be measured with a delay. Designs similar to Sharon et al. (2021) that use short taVNS trains followed by no-stimulation intervals will help investigate the stimulation effects in the closed-loop system.

Another challenge is posed by the size of the ear, which limits space for electrodes. It remains to be tested whether similar locations can be used for stimulation and recording (in the ear canal, for instance) or which placements of recording and stimulating electrodes is the most feasible, following space constraints, and the most effective. A combination of taVNS and cEEGrids (Bleichner and Debener, 2017; Meiser et al., 2020) seems promising because sensors and stimulator electrodes would be apart by design.

It is, furthermore, critical that the link between the measured alpha activity with ear-EEG and a potential attention drop is further investigated. Previous research showed that alpha power preceding weak visual stimuli can predict detection performance (e.g., Hanslmayr et al., 2007; van Dijk et al., 2008; for a review see Ruhnau et al., 2014). The causal involvement of alpha power in visual attentive states has been further confirmed using transcranial magnetic stimulation (Romei et al., 2011). However, how well ear-EEG can pick up these alpha fluctuations linked to (dominantly visual) attention, remains an open question. Thus, before a closed-loop system can leave the lab, an evaluation *in the lab* is essential. For instance, future studies should evaluate if ear-EEG signals in the alpha range can predict visual perception in near-threshold cases (such as in Hanslmayr et al., 2007; van Dijk et al., 2008). Given that alpha power lateralization is often a good predictor (Thut et al., 2006), ear-EEGs on the left and right ear might be essential to test this lateralization properly.

Moreover, it is important to emphasize that keeping attention at a high level for an extended time is not beneficial, nor intended with the system we propose. There are time limits how long people in different professions are allowed to work before they are required to take a break. For instance, in the EU professional drivers are not allowed to drive a vehicle longer than 9 h per day (with few exceptions), or interpreters working for the United Nations are required to take at least one and a half hour breaks between maximally 2.5–3 h work sessions. Maintaining high levels of focus is tiring and requires rest. Hence, an application that we suggest, should not aim to increase the duration on a task but rather normalize attention fluctuations while on the task.

Typical mobile stimulators contain constraints as to the specific settings of the stimulation (tailored to the individual user) and the daily dose. These factors also need to be investigated and kept in mind when using taVNS and ear-EEG together. Given that taVNS is still a relatively novel non-invasive brain stimulation tool, it is important to properly record and monitor short term as well as long term side effects and adjust protocols to avoid them as well as possible. Similar standards as suggested for other transcranial stimulation techniques might be chosen as

a baseline (for comprehensive guidelines see Rossi et al., 2009; Antal et al., 2017) but data on unwanted effects needs to be carefully collected and monitored.

CONCLUSION

In summary, the use of a closed-loop system consisting of ear-EEG and taVNS holds the promise of a potential therapeutic option in neuropsychiatric patients as well as a supportive device in healthy populations. Therefore, we highly encourage to explore the usability of such a closed-loop system.

Further research is needed to determine the exact parameters of optimal taVNS to fully exploit its potential. Research efforts will need to focus on the systematic investigation of suitable parameter settings, especially stimulation duration, to maximize efficacy as well as long-term effectiveness.

AUTHOR CONTRIBUTIONS

PR and TZ wrote the manuscript and prepared the artwork. Both authors contributed to the article and approved the submitted version.

FUNDING

This study was supported by the Federal State of Saxony-Anhalt and the European Regional Development Fund (ERDF) in the Center for Behavioral Brain Sciences (CBBS, ZS/2016/04/78113).

REFERENCES

Alagapan, S., Schmidt, S. L., Lefebvre, J., Hadar, E., Shin, H. W., and Fröhlich, F. (2016). Modulation of cortical oscillations by low-frequency direct cortical stimulation is state-dependent. *PLoS Biol.* 14:e1002424. doi: 10.1371/journal.pbio.1002424

Alexander, M. L., Alagapan, S., Lugo, C. E., Mellin, J. M., Lustenberger, C., Rubinow, D. R., et al. (2019). Double-blind, randomized pilot clinical trial targeting alpha oscillations with transcranial alternating current stimulation (tACS) for the treatment of major depressive disorder (MDD). *Transl. Psychiatry* 9:106. doi: 10.1038/s41398-019-0439-0

Antal, A., Alekseichuk, I., Bikson, M., Brockmöller, J., Brunoni, A. R., Chen, R., et al. (2017). Low intensity transcranial electric stimulation: safety, ethical, legal regulatory and application guidelines. *Clin. Neurophysiol.* 128, 1774–1809. doi: 10.1016/j.clinph.2017.06.001

Aston-Jones, G., Rajkowski, J., and Kubiak, P. (1997). Conditioned responses of monkey locus coeruleus neurons anticipate acquisition of discriminative behavior in a vigilance task. *Neuroscience* 80, 697–715. doi: 10.1016/S0306-4522(97)00060-2

Aston-Jones, G., Shipley, M. T., Chouvet, G., Ennis, M., van Bockstaele, E., Pieribone, V., et al. (1991). "Afferent regulation of locus coeruleus neurons: anatomy, physiology and pharmacology," in *Progress in Brain Research Neurobiology of the Locus Coeruleus*, eds C. D. Barnes and O. Pompeiano (New York, NY: Elsevier), 47–75. doi: 10.1016/S0079-6123(08)63799-1

Aston-Jones, G., and Cohen, J. D. (2005). Adaptive gain and the role of the locus coeruleus–norepinephrine system in optimal performance. *J. Comp. Neurol.* 493, 99–110. doi: 10.1002/cne.20723

Badran, B. W., Dowdle, L. T., Mithoefer, O. J., LaBate, N. T., Coatsworth, J., Brown, J. C., et al. (2018a). Neurophysiologic effects of transcutaneous auricular vagus nerve stimulation (taVNS) via electrical stimulation of the tragus: a concurrent taVNS/fMRI study and review. *Brain Stimulat.* 11, 492–500. doi: 10.1016/j.brs.2017.12.009

Badran, B. W., Jenkins, D. D., Cook, D., Thompson, S., Dancy, M., DeVries, W. H., et al. (2020). Transcutaneous auricular vagus nerve stimulation-paired rehabilitation for oromotor feeding problems in newborns: an open-label pilot study. *Front. Hum. Neurosci.* 14:77. doi: 10.3389/fnhum.2020.00077

Badran, B. W., Mithoefer, O. J., Summer, C. E., LaBate, N. T., Glusman, C. E., Badran, A. W., et al. (2018b). Short trains of transcutaneous auricular vagus nerve stimulation (taVNS) have parameter-specific effects on heart rate. *Brain Stimulat.* 11, 699–708. doi: 10.1016/j.brs.2018.04.004

Başar, E. (2013). Brain oscillations in neuropsychiatric disease. *Dialogues Clin. Neurosci.* 15, 291–300.

Bauer, S., Baier, H., Baumgartner, C., Bohlmann, K., Fauser, S., Graf, W., et al. (2016). Transcutaneous vagus nerve stimulation (tVNS) for treatment of drug-resistant epilepsy: a randomized, double-blind clinical trial (cMPsE02). *Brain Stimulat.* 9, 356–363. doi: 10.1016/j.brs.2015.11.003

Bergmann, T. O. (2018). Brain state-dependent brain stimulation. *Front. Psychol.* 9:2108. doi: 10.3389/fpsyg.2018.02108

Beste, C., Steenbergen, L., Sellaro, R., Grigoriadou, S., Zhang, R., Chmielewski, W., et al. (2016). Effects of concomitant stimulation of the GABAergic and norepinephrine system on inhibitory control–a study using transcutaneous vagus nerve stimulation. *Brain Stimulat.* 9, 811–818. doi: 10.1016/j.brs.2016.07.004

Bleichner, M. G., and Debener, S. (2017). Concealed, unobtrusive ear-centered EEG acquisition: cEEGrids for transparent EEG. *Front. Hum. Neurosci.* 11:163. doi: 10.3389/fnhum.2017.00163

Borges, U., Pfannenstiel, M., Tsukahara, J., Laborde, S., Klatt, S., and Raab, M. (2021). Transcutaneous vagus nerve stimulation via tragus or cymba conchae: are its psychophysiological effects dependent on the stimulation area? *Int. J. Psychophysiol.* 161, 64–75. doi: 10.1016/j.ijpsycho.2021.01.003

Brázdil, M., Chadim, P., Daniel, P., Kuba, R., Rektor, I., Novák, Z., et al. (2001). Effect of vagal nerve stimulation on auditory and visual event-related potentials. *Eur. J. Neurol.* 8, 457–461. doi: 10.1046/j.1468-1331.2001.00262.x

Broncel, A., Bocian, R., Kłos-Wojtczak, P., and Konopacki, J. (2019). GABAergic mediation of hippocampal theta rhythm induced by stimulation of the vagal nerve. *Brain Res. Bull.* 147, 110–123. doi: 10.1016/j.brainresbull.2019.02.010

Broncel, A., Bocian, R., Kłos-Wojtczak, P., Kulbat-Warycha, K., and Konopacki, J. (2020). Vagal nerve stimulation as a promising tool in the improvement of cognitive disorders. *Brain Res. Bull.* 155, 37–47. doi: 10.1016/j.brainresbull.2019.11.011

Brown, B. B. (1974). *New Mind, New Body: Bio-Feedback: New Directions for the Mind*. Oxford: Harper & Row.

Brown, B. B. (1977). *Stress and the Art of Biofeedback*. Oxford: Harper & Row.

Bunsey, M. D., and Strupp, B. J. (1995). Specific effects of idazoxan in a distraction task: evidence that endogenous norepinephrine plays a role in selective attention in rats. *Behav. Neurosci.* 109, 903–911. doi: 10.1037/0735-7044.109.5.903

Burger, A. M., D'Agostini, M., Verkuil, B., and Diest, I. V. (2020). Moving beyond belief: a narrative review of potential biomarkers for transcutaneous vagus nerve stimulation. *Psychophysiology* 57:e13571. doi: 10.1111/psyp.13571

Butt, M. F., Albusoda, A., Farmer, A. D., and Aziz, Q. (2020). The anatomical basis for transcutaneous auricular vagus nerve stimulation. *J. Anat.* 236, 588–611. doi: 10.1111/joa.13122

Chmielewski, W. X., Mückschel, M., Ziemssen, T., and Beste, C. (2017). The norepinephrine system affects specific neurophysiological subprocesses in the modulation of inhibitory control by working memory demands. *Hum. Brain Mapp.* 38, 68–81. doi: 10.1002/hbm.23344

Clark, C. R., Geffen, G. M., and Geffen, L. B. (1986). Role of monoamine pathways in attention and effort: effects of clonidine and methylphenidate in normal adult humans. *Psychopharmacology (Berl.)* 90, 35–39. doi: 10.1007/BF00172868

Cook, D. N., Thompson, S., Stomberg-Firestein, S., Bikson, M., George, M. S., Jenkins, D. D., et al. (2020). Design and validation of a closed-loop,

motor-activated auricular vagus nerve stimulation (MAAVNS) system for neurorehabilitation. *Brain Stimulat.* 13, 800–803. doi: 10.1016/j.brs.2020.02.028

Coull, J. T., Middleton, H. C., Robbins, T. W., and Sahakian, B. J. (1995). Contrasting effects of clonidine and diazepam on tests of working memory and planning. *Psychopharmacology (Berl.)* 120, 311–321. doi: 10.1007/BF02311179

De Ridder, D., Vanneste, S., Engineer, N. D., and Kilgard, M. P. (2014). Safety and efficacy of vagus nerve stimulation paired with tones for the treatment of tinnitus: a case series. *Neuromodulation* 17, 170–179. doi: 10.1111/ner.12127

De Vos, M., and Debener, S. (2014). Mobile EEG: towards brain activity monitoring during natural action and cognition. *Int. J. Psychophysiol.* 91, 1–2. doi: 10.1016/j.ijpsycho.2013.08.010

Debener, S., Emkes, R., De Vos, M., and Bleichner, M. (2015). Unobtrusive ambulatory EEG using a smartphone and flexible printed electrodes around the ear. *Sci. Rep.* 5:16743. doi: 10.1038/srep16743

Debener, S., Minow, F., Emkes, R., Gandras, K., and De Vos, M. (2012). How about taking a low-cost, small, and wireless EEG for a walk? *Psychophysiology* 49, 1617–1621. doi: 10.1111/j.1469-8986.2012.01471.x

Dorr, A. E., and Debonnel, G. (2006). Effect of vagus nerve stimulation on serotonergic and noradrenergic transmission. *J. Pharmacol. Exp. Ther.* 318, 890–898. doi: 10.1124/jpet.106.104166

Fahy, B. G. (2010). Intraoperative and perioperative complications with a vagus nerve stimulation device. *J. Clin. Anesth.* 22, 213–222. doi: 10.1016/j.jclinane.2009.10.002

Fang, J., Rong, P., Hong, Y., Fan, Y., Liu, J., Wang, H., et al. (2016). Transcutaneous vagus nerve stimulation modulates default mode network in major depressive disorder. *Biol. Psychiatry* 79, 266–273. doi: 10.1016/j.biopsych.2015.03.025

Fiedler, L., Wöstmann, M., Graversen, C., Brandmeyer, A., Lunner, T., and Obleser, J. (2017). Single-channel in-ear-EEG detects the focus of auditory attention to concurrent tone streams and mixed speech. *J. Neural Eng.* 14:036020. doi: 10.1088/1741-2552/aa66dd

Fischer, R., Ventura-Bort, C., Hamm, A., and Weymar, M. (2018). Transcutaneous vagus nerve stimulation (tVNS) enhances conflict-triggered adjustment of cognitive control. *Cogn. Affect. Behav. Neurosci.* 18, 680–693. doi: 10.3758/s13415-018-0596-2

Frangos, E., Ellrich, J., and Komisaruk, B. R. (2015). Non-invasive access to the vagus nerve central projections via electrical stimulation of the external ear: fMRI evidence in humans. *Brain Stimulat.* 8, 624–636. doi: 10.1016/j.brs.2014.11.018

Frey, J. N., Ruhnau, P., and Weisz, N. (2015). Not so different after all: the same oscillatory processes support different types of attention. *Brain Res.* 1626, 183–197. doi: 10.1016/j.brainres.2015.02.017

Frohlich, F., and Townsend, L. (2021). Closed-loop transcranial alternating current stimulation: towards personalized non-invasive brain stimulation for the treatment of psychiatric illnesses. *Curr. Behav. Neurosci. Rep.* 8, 51–57. doi: 10.1007/s40473-021-00227-8

García, I., Bronte, S., Bergasa, L. M., Hernandez, N., Delgado, B., and Sevillano, M. (2010). "Vision-based drowsiness detector for a realistic driving simulator," in *Proceedings of the 13th International IEEE Conference on Intelligent Transportation Systems* (Funchal: IEEE), 887–894. doi: 10.1109/ITSC.2010.5625097

Gu, Y., Cleeren, E., Dan, J., Claes, K., Van Paesschen, W., Van Huffel, S., et al. (2018). Comparison between scalp EEG and behind-the-ear EEG for development of a wearable seizure detection system for patients with focal epilepsy. *Sensors* 18:29. doi: 10.3390/s18010029

Haegens, S., Händel, B. F., and Jensen, O. (2011). Top-down controlled alpha band activity in somatosensory areas determines behavioral performance in a discrimination task. *J. Neurosci.* 31, 5197–5204. doi: 10.1523/JNEUROSCI.5199-10.2011

Hanslmayr, S., Aslan, A., Staudigl, T., Klimesch, W., Herrmann, C. S., and Bäuml, K.-H. (2007). Prestimulus oscillations predict visual perception performance between and within subjects. *Neuroimage* 37, 1465–1473. doi: 10.1016/j.neuroimage.2007.07.011

Hartmann, T., Lorenz, I., Müller, N., Langguth, B., and Weisz, N. (2014). The effects of neurofeedback on oscillatory processes related to tinnitus. *Brain Topogr.* 27, 149–157. doi: 10.1007/s10548-013-0295-9

Hasan, A., Wolff-Menzler, C., Pfeiffer, S., Falkai, P., Weidinger, E., Jobst, A., et al. (2015). Transcutaneous noninvasive vagus nerve stimulation (tVNS) in the treatment of schizophrenia: a bicentric randomized controlled pilot study. *Eur. Arch. Psychiatry Clin. Neurosci.* 265, 589–600. doi: 10.1007/s00406-015-0618-9

Hasler, R., Perroud, N., Meziane, H. B., Herrmann, F., Prada, P., Giannakopoulos, P., et al. (2016). Attention-related EEG markers in adult ADHD. *Neuropsychologia* 87, 120–133. doi: 10.1016/j.neuropsychologia.2016.05.008

Hein, E., Nowak, M., Kiess, O., Biermann, T., Bayerlein, K., Kornhuber, J., et al. (2013). Auricular transcutaneous electrical nerve stimulation in depressed patients: a randomized controlled pilot study. *J. Neural Transm.* 120, 821–827. doi: 10.1007/s00702-012-0908-6

Hölle, D., Meekes, J., and Bleichner, M. G. (2021). Mobile ear-EEG to study auditory attention in everyday life. *Behav. Res. Methods* doi: 10.3758/s13428-021-01538-0 Available online at: https://link.springer.com/article/10.3758%2Fs13428-021-01538-0#citeas.

Hulsey, D. R., Riley, J. R., Loerwald, K. W., Rennaker, R. L., Kilgard, M. P., and Hays, S. A. (2017). Parametric characterization of neural activity in the locus coeruleus in response to vagus nerve stimulation. *Exp. Neurol.* 289, 21–30. doi: 10.1016/j.expneurol.2016.12.005

Jafari, Z., Kolb, B. E., and Mohajerani, M. H. (2020). Neural oscillations and brain stimulation in Alzheimer's disease. *Prog. Neurobiol.* 194:101878. doi: 10.1016/j.pneurobio.2020.101878

Jensen, O., and Mazaheri, A. (2010). Shaping functional architecture by oscillatory alpha activity: gating by inhibition. *Front. Hum. Neurosci.* 4:186. doi: 10.3389/fnhum.2010.00186

Jeong, D.-H., and Jeong, J. (2020). In-ear EEG based attention state classification using echo state network. *Brain Sci.* 10:321. doi: 10.3390/brainsci10060321

Jiang, H., Popov, T., Jylänki, P., Bi, K., Yao, Z., Lu, Q., et al. (2016). Predictability of depression severity based on posterior alpha oscillations. *Clin. Neurophysiol.* 127, 2108–2114. doi: 10.1016/j.clinph.2015.12.018

Kaczmarczyk, R., Tejera, D., Simon, B. J., and Heneka, M. T. (2018). Microglia modulation through external vagus nerve stimulation in a murine model of Alzheimer's disease. *J. Neurochem.* 146, 76–85. doi: 10.1111/jnc.14284

Kaongoen, N., and Jo, S. (2020). "An ear-EEG-based brain-computer interface using concentration level for control," in *Proceedings of the 2020 8th International Winter Conference on Brain-Computer Interface (BCI)*, Gangwon.

Kappel, S. L., Makeig, S., and Kidmose, P. (2019a). Ear-EEG forward models: improved head-models for ear-EEG. *Front. Neurosci.* 13:943. doi: 10.3389/fnins.2019.00943

Kappel, S. L., Rank, M. L., Toft, H. O., Andersen, M., and Kidmose, P. (2019b). Dry-contact electrode ear-EEG. *IEEE Trans. Biomed. Eng.* 66, 150–158. doi: 10.1109/TBME.2018.2835778

Kaveh, R., Doong, J., Zhou, A., Schwendeman, C., Gopalan, K., Burghardt, F. L., et al. (2020). wireless user-generic ear EEG. *IEEE Trans. Biomed. Circuits Syst.* 14, 727–737. doi: 10.1109/TBCAS.2020.3001265

Keute, M., Demirezen, M., Graf, A., Mueller, N. G., and Zaehle, T. (2019). No modulation of pupil size and event-related pupil response by transcutaneous auricular vagus nerve stimulation (taVNS). *Sci. Rep.* 9:11452. doi: 10.1038/s41598-019-47961-4

Keute, M., Machetanz, K., Berelidze, L., Guggenberger, R., and Gharabaghi, A. (2021). Neuro-cardiac coupling predicts transcutaneous auricular vagus nerve stimulation effects. *Brain Stimulat.* 14, 209–216. doi: 10.1016/j.brs.2021.01.001

Keute, M., Ruhnau, P., Heinze, H.-J., and Zaehle, T. (2018). Behavioral and electrophysiological evidence for GABAergic modulation through transcutaneous vagus nerve stimulation. *Clin. Neurophysiol.* 129, 1789–1795. doi: 10.1016/j.clinph.2018.05.026

Kidmose, P., Looney, D., and Mandic, D. P. (2012). "Auditory evoked responses from ear-EEG recordings," in *Proceedings of the 2012 Annual International Conference of the IEEE Engineering in Medicine and Biology Society*, (San Diego, CA: IEEE), 586–589. doi: 10.1109/EMBC.2012.6345999

Klimesch, W. (2012). Alpha-band oscillations, attention, and controlled access to stored information. *Trends Cogn. Sci.* 16, 606–617. doi: 10.1016/j.tics.2012.10.007

Knowles, C. H., and Aziz, Q. (2009). Basic and clinical aspects of gastrointestinal pain. *PAIN* 141, 191–209. doi: 10.1016/j.pain.2008.12.011

Krigolson, O. E., Williams, C. C., Norton, A., Hassall, C. D., and Colino, F. L. (2017). Choosing MUSE: validation of a low-cost, portable EEG system for ERP research. *Front. Neurosci.* 11:109. doi: 10.3389/fnins.2017.00109

Lee, J. H., Lee, S. M., Byeon, H. J., Hong, J. S., Park, K. S., and Lee, S.-H. (2014). CNT/PDMS-based canal-typed ear electrodes for inconspicuous EEG recording. *J. Neural Eng.* 11:046014. doi: 10.1088/1741-2560/11/4/046014

Leonhardt, S., Leicht, L., and Teichmann, D. (2018). Unobtrusive vital sign monitoring in automotive environments—a review. *Sensors* 18:3080. doi: 10.3390/s18093080

Leonte, A., Colzato, L. S., Steenbergen, L., Hommel, B., and Akyürek, E. G. (2018). Supplementation of gamma-aminobutyric acid (GABA) affects temporal, but not spatial visual attention. *Brain Cogn.* 120, 8–16. doi: 10.1016/j.bandc.2017.11.004

Leroy, A., and Cheron, G. (2020). EEG dynamics and neural generators of psychological flow during one tightrope performance. *Sci. Rep.* 10:12449. doi: 10.1038/s41598-020-69448-3

Lewine, J. D., Paulson, K., Bangera, N., and Simon, B. J. (2019). Exploration of the impact of brief noninvasive vagal nerve stimulation on EEG and event−related potentials. *Neuromodulation* 22, 564–572. doi: 10.1111/ner.12864

Li, L. M., Violante, I. R., Leech, R., Ross, E., Hampshire, A., Opitz, A., et al. (2018). Brain state and polarity dependent modulation of brain networks by transcranial direct current stimulation. *Hum. Brain Mapp.* 40, 904–915. doi: 10.1002/hbm.24420

Looney, D., Kidmose, P., Park, C., Ungstrup, M., Rank, M., Rosenkranz, K., et al. (2012). The in-the-ear recording concept: user-centered and wearable brain monitoring. *IEEE Pulse* 3, 32–42. doi: 10.1109/MPUL.2012.2216717

Looney, D., Park, C., Kidmose, P., Rank, M. L., Ungstrup, M., Rosenkranz, K., et al. (2011). "An in-the-ear platform for recording electroencephalogram," in *Proceedings of the 2011 Annual International Conference of the IEEE Engineering in Medicine and Biology Society*, Boston, MA, 6882–6885.

Manta, S., El Mansari, M., Debonnel, G., and Blier, P. (2013). Electrophysiological and neurochemical effects of long-term vagus nerve stimulation on the rat monoaminergic systems. *Int. J. Neuropsychopharmacol.* 16, 459–470. doi: 10.1017/S1461145712000387

McGarrity, S., Mason, R., Fone, K. C., Pezze, M., and Bast, T. (2017). Hippocampal neural disinhibition causes attentional and memory deficits. *Cereb. Cortex* 27, 4447–4462. doi: 10.1093/cercor/bhw247

Meiser, A., Tadel, F., Debener, S., and Bleichner, M. G. (2020). The sensitivity of ear-EEG: evaluating the source-sensor relationship using forward modeling. *Brain Topogr.* 33, 665–676. doi: 10.1007/s10548-020-00793-2

Mikkelsen, K. B., Kappel, S. L., Mandic, D. P., and Kidmose, P. (2015). EEG recorded from the ear: characterizing the ear-EEG method. *Front. Neurosci.* 9:438. doi: 10.3389/fnins.2015.00438

Mikkelsen, K. B., Villadsen, D. B., Otto, M., and Kidmose, P. (2017). Automatic sleep staging using ear-EEG. *Biomed. Eng. OnLine* 16:111. doi: 10.1186/s12938-017-0400-5

Mirkovic, B., Bleichner, M. G., De Vos, M., and Debener, S. (2016). Target speaker detection with concealed EEG around the ear. *Front. Neurosci.* 10:349. doi: 10.3389/fnins.2016.00349

Monastra, V. J., Monastra, D. M., and George, S. (2002). The effects of stimulant therapy, EEG biofeedback, and parenting style on the primary symptoms of attention-deficit/hyperactivity disorder. *Appl. Psychophysiol. Biofeedback* 27, 231–249. doi: 10.1023/A:1021018700609

Napadow, V., Edwards, R. R., Cahalan, C. M., Mensing, G., Greenbaum, S., Valovska, A., et al. (2012). Evoked pain analgesia in chronic pelvic pain patients using respiratory-gated auricular vagal afferent nerve stimulation. *Pain Med.* 13, 777–789. doi: 10.1111/j.1526-4637.2012.01385.x

Nieuwenhuis, S., Aston-Jones, G., and Cohen, J. D. (2005). Decision making, the P3, and the locus coeruleus–norepinephrine system. *Psychol. Bull.* 131, 510–532. doi: 10.1037/0033-2909.131.4.510

Paine, T. A., Cooke, E. K., and Lowes, D. C. (2015). Effects of chronic inhibition of GABA synthesis on attention and impulse control. *Pharmacol. Biochem. Behav.* 135, 97–104. doi: 10.1016/j.pbb.2015.05.019

Paine, T. A., Slipp, L. E., and Carlezon, W. A. (2011). Schizophrenia-like attentional deficits following blockade of prefrontal cortex GABA a receptors. *Neuropsychopharmacology* 36, 1703–1713. doi: 10.1038/npp.2011.51

Parkin, B. L., Ekhtiari, H., and Walsh, V. F. (2015). Non-invasive human brain stimulation in cognitive neuroscience: a primer. *Neuron* 87, 932–945. doi: 10.1016/j.neuron.2015.07.032

Peng, P., and Miller, A. C. (2016). Does attention training work? A selective meta-analysis to explore the effects of attention training and moderators. *Learn. Individ. Differ.* 45, 77–87. doi: 10.1016/j.lindif.2015.11.012

Petersen, S. E., Robinson, D. L., and Morris, J. D. (1987). Contributions of the pulvinar to visual spatial attention. *Neuropsychologia* 25, 97–105. doi: 10.1016/0028-3932(87)90046-7

Pezze, M., McGarrity, S., Mason, R., Fone, K. C., and Bast, T. (2014). Too little and too much: hypoactivation and disinhibition of medial prefrontal cortex cause attentional deficits. *J. Neurosci.* 34, 7931–7946. doi: 10.1523/JNEUROSCI.3450-13.2014

Redgrave, J., Day, D., Leung, H., Laud, P. J., Ali, A., Lindert, R., et al. (2018). Safety and tolerability of transcutaneous vagus nerve stimulation in humans; a systematic review. *Brain Stimulat.* 11, 1225–1238. doi: 10.1016/j.brs.2018.08.010

Romei, V., Driver, J., Schyns, P. G., and Thut, G. (2011). Rhythmic TMS over parietal cortex links distinct brain frequencies to global versus local visual processing. *Curr. Biol.* 21, 334–337. doi: 10.1016/j.cub.2011.01.035

Rossi, S., Hallett, M., Rossini, P. M., Pascual-Leone, A., and Safety of Tms Consensus Group. (2009). Safety, ethical considerations, and application guidelines for the use of transcranial magnetic stimulation in clinical practice and research. *Clin. Neurophysiol.* 120, 2008–2039. doi: 10.1016/j.clinph.2009.08.016

Rufener, K. S., Geyer, U., Janitzky, K., Heinze, H.-J., and Zaehle, T. (2018). Modulating auditory selective attention by non-invasive brain stimulation: differential effects of transcutaneous vagal nerve stimulation and transcranial random noise stimulation. *Eur. J. Neurosci.* 48, 2301–2309. doi: 10.1111/ejn.14128

Ruhnau, P., Hauswald, A., and Weisz, N. (2014). Investigating ongoing brain oscillations and their influence on conscious perception–network states and the window to consciousness. *Front. Psychol* 5:1230. doi: 10.3389/fpsyg.2014.01230

Ruhnau, P., Neuling, T., Fuscà, M., Herrmann, C. S., Demarchi, G., and Weisz, N. (2016). Eyes wide shut: transcranial alternating current stimulation drives alpha rhythm in a state dependent manner. *Sci. Rep.* 6:27138. doi: 10.1038/srep27138

Scanlon, J. E. M., Townsend, K. A., Cormier, D. L., Kuziek, J. W. P., and Mathewson, K. E. (2019). Taking off the training wheels: measuring auditory P3 during outdoor cycling using an active wet EEG system. *Brain Res.* 1716, 50–61. doi: 10.1016/j.brainres.2017.12.010

Schevernels, H., van Bochove, M. E., De Taeye, L., Bombeke, K., Vonck, K., Van Roost, D., et al. (2016). The effect of vagus nerve stimulation on response inhibition. *Epilepsy Behav.* 64, 171–179. doi: 10.1016/j.yebeh.2016.09.014

Sellaro, R., de Gelder, B., Finisguerra, A., and Colzato, L. S. (2018). Transcutaneous vagus nerve stimulation (tVNS) enhances recognition of emotions in faces but not bodies. *Cortex* 99, 213–223. doi: 10.1016/j.cortex.2017.11.007

Sharon, O., Fahoum, F., and Nir, Y. (2021). Transcutaneous vagus nerve stimulation in humans induces pupil dilation and attenuates alpha oscillations. *J. Neurosci.* 41, 320–330. doi: 10.1523/JNEUROSCI.1361-20.2020

Sintotskiy, G., and Hinrichs, H. (2020). In-ear-EEG–a portable platform for home monitoring. *J. Med. Eng. Technol.* 44, 26–37. doi: 10.1080/03091902.2020.1713238

Sirviö, J., Jäkälä, P., Mazurkiewicz, M., Haapalinna, A., Riekkinen, P., and Riekkinen, P. J. (1993). Dose- and parameter-dependent effects of atipamezole, an α2-antagonist, on the performance of rats in a five-choice serial reaction time task. *Pharmacol. Biochem. Behav.* 45, 123–129. doi: 10.1016/0091-3057(93)90095-B

Smith, A., and Nutt, D. (1996). Noradrenaline and attention lapses. *Nature* 380, 291–291. doi: 10.1038/380291a0

Sun, L., Peräkylä, J., Holm, K., Haapasalo, J., Lehtimäki, K., Ogawa, K. H., et al. (2017). Vagus nerve stimulation improves working memory performance. *J. Clin. Exp. Neuropsychol.* 39, 954–964. doi: 10.1080/13803395.2017.1285869

Tabar, Y. R., Mikkelsen, K. B., Rank, M. L., Hemmsen, M. C., Otto, M., and Kidmose, P. (2020). Ear-EEG for sleep assessment: a comparison with actigraphy and PSG. *Sleep Breath* doi: 10.1007/s11325-020-02248-1 Available online at: https://link.springer.com/article/10.1007%2Fs11325-020-02248-1#citeas.

Tan, G., Thornby, J., Hammond, D. C., Strehl, U., Canady, B., Arnemann, K., et al. (2009). Meta-analysis of EEG biofeedback in treating epilepsy. *Clin. EEG Neurosci.* 40, 173–179. doi: 10.1177/155005940904000310

Tang, Y.-Y., and Posner, M. I. (2009). Attention training and attention state training. *Trends Cogn. Sci.* 13, 222–227. doi: 10.1016/j.tics.2009.01.009

Thut, G., Nietzel, A., Brandt, S. A., and Pascual-Leone, A. (2006). Alpha-band electroencephalographic activity over occipital cortex indexes visuospatial attention bias and predicts visual target detection. *J. Neurosci.* 26, 9494–9502. doi: 10.1523/JNEUROSCI.0875-06.2006

van Dijk, H., Schoffelen, J.-M., Oostenveld, R., and Jensen, O. (2008). Prestimulus oscillatory activity in the alpha band predicts visual discrimination ability. *J. Neurosci.* 28, 1816–1823. doi: 10.1523/JNEUROSCI.1853-07.2008

Van Leusden, J. W. R., Sellaro, R., and Colzato, L. S. (2015). Transcutaneous vagal nerve stimulation (tVNS): a new neuromodulation tool in healthy humans? *Front. Psychol.* 6:102. doi: 10.3389/fpsyg.2015.00102

Ventura-Bort, C., Wirkner, J., Genheimer, H., Wendt, J., Hamm, A. O., and Weymar, M. (2018). Effects of transcutaneous vagus nerve stimulation (tVNS) on the P300 and alpha-amylase level: a pilot study. *Front. Hum. Neurosci.* 12:202. doi: 10.3389/fnhum.2018.00202

Wang, H., Dragomir, A., Abbasi, N. I., Li, J., Thakor, N. V., and Bezerianos, A. (2018). A novel real-time driving fatigue detection system based on wireless dry EEG. *Cogn. Neurodyn.* 12, 365–376. doi: 10.1007/s11571-018-9481-5

Wascher, E., Heppner, H., Kobald, S. O., Arnau, S., Getzmann, S., and Möckel, T. (2016). Age-sensitive effects of enduring work with alternating cognitive and physical load. A study applying mobile EEG in a real life working scenario. *Front. Hum. Neurosci.* 9:711. doi: 10.3389/fnhum.2015.00711

Woodward, D. J., Moises, H. C., Waterhouse, B. D., Hoffer, B. J., and Freedman, R. (1979). Modulatory actions of norepinephrine in the central nervous system. *Fed. Proc.* 38, 2109–2116.

Yakunina, N., Kim, S. S., and Nam, E.-C. (2017). Optimization of transcutaneous vagus nerve stimulation using functional MRI. *Neuromodulation* 20, 290–300. doi: 10.1111/ner.12541

Zhu, M., HajiHosseini, A., Baumeister, T. R., Garg, S., Appel-Cresswell, S., and McKeown, M. J. (2019). Altered EEG alpha and theta oscillations characterize apathy in Parkinson's disease during incentivized movement. *NeuroImage Clin.* 23:101922. doi: 10.1016/j.nicl.2019.101922

Zibrandtsen, I. C., Kidmose, P., Christensen, C. B., and Kjaer, T. W. (2017). Ear-EEG detects ictal and interictal abnormalities in focal and generalized epilepsy–a comparison with scalp EEG monitoring. *Clin. Neurophysiol.* 128, 2454–2461. doi: 10.1016/j.clinph.2017.09.115

Conflict of Interest: The authors declare that the research was conducted in the absence of any commercial or financial relationships that could be construed as a potential conflict of interest.

frontiers in Human Neuroscience

ORIGINAL RESEARCH
published: 23 June 2021
doi: 10.3389/fnhum.2021.661432

A Comparison of Closed Loop vs. Fixed Frequency tACS on Modulating Brain Oscillations and Visual Detection

Heiko I. Stecher[1†], Annika Notbohm[2†], Florian H. Kasten[1] and Christoph S. Herrmann[1,3]*

[1] Experimental Psychology Lab, Department of Psychology, European Medical School, Cluster of Excellence "Hearing4all", Carl von Ossietzky University, Oldenburg, Germany, [2] Department of Neurological Rehabilitation, Municipal Hospital of Bremen, Bremen, Germany, [3] Research Center Neurosensory Science, Carl von Ossietzky University, Oldenburg, Germany

Transcranial alternating current stimulation has emerged as an effective tool for the exploration of brain oscillations. By applying a weak alternating current between electrodes placed on the scalp matched to the endogenous frequency, tACS enables the specific modulation of targeted brain oscillations This results in alterations in cognitive functions or persistent physiological changes. Most studies that utilize tACS determine a fixed stimulation frequency prior to the stimulation that is kept constant throughout the experiment. Yet it is known that brain rhythms can encounter shifts in their endogenous frequency. This could potentially move the ongoing brain oscillations into a frequency region where it is no longer affected by the stimulation, thereby decreasing or negating the effect of tACS. Such an effect of a mismatch between stimulation frequency and endogenous frequency on the outcome of stimulation has been shown before for the parietal alpha-activity. In this study, we employed an intermittent closed loop stimulation protocol, where the stimulation is divided into short epochs, between which an EEG is recorded and rapidly analyzed to determine a new stimulation frequency for the next stimulation epoch. This stimulation protocol was tested in a three-group study against a classical fixed stimulation protocol and a sham-treatment. We targeted the parietal alpha rhythm and hypothesized that this setup will ensure a constant close match between the frequencies of tACS and alpha activity. This closer match should lead to an increased modulation of detection of visual luminance changes depending on the phase of the tACS and an increased rise in alpha peak power post stimulation when compared to a protocol with fixed pre-determined stimulation frequency. Contrary to our hypothesis, our results show that only a fixed stimulation protocol leads to a persistent increase in post-stimulation alpha power as compared to sham. Furthermore, in none of the stimulated groups significant modulation of detection performance occurred. While the lack of behavioral effects is inconclusive due to the short selection of different phase bins and trials, the physiological results suggest that a constant stimulation with a fixed frequency is actually beneficial, when the goal is to produce persistent synaptic changes.

Keywords: transcranial alternating current stimulation, alpha, EEG, closed loop, visual perception

OPEN ACCESS

Edited by:
Tamer Demiralp, Istanbul University, Turkey

Reviewed by:
Sacit Karamürsel, Koç University, Turkey
Surjo R. Soekadar, Charité – Universitätsmedizin Berlin, Germany

***Correspondence:**
Christoph S. Herrmann
christoph.herrmann@uni-oldenburg.de

[†]These authors share first authorship

Specialty section:
This article was submitted to Brain Imaging and Stimulation, a section of the journal Frontiers in Human Neuroscience

Received: *30 January 2021*
Accepted: *03 May 2021*
Published: *23 June 2021*

Citation:
Stecher HI, Notbohm A, Kasten FH and Herrmann CS (2021) A Comparison of Closed Loop vs. Fixed Frequency tACS on Modulating Brain Oscillations and Visual Detection. Front. Hum. Neurosci. 15:661432. doi: 10.3389/fnhum.2021.661432

INTRODUCTION

Non-invasive methods of brain stimulations like transcranial alternating current stimulation (tACS) find increasing use in neuroscience (Antal et al., 2017; Veniero et al., 2019). tACS is assumed to modulate endogenous brain oscillations in a frequency specific manner. It is frequently used as a tool in intervention studies, with the aim of exploring the functional role of brain oscillations for cognitive processes (Thut et al., 2012; Bergmann et al., 2016; Herrmann et al., 2016). In the past, tACS was successfully used to modulate cognitive functions like visual and auditory perception (Neuling et al., 2012; Brignani et al., 2013; Kasten et al., 2018a), memory (Vosskuhl et al., 2015; Alekseichuk et al., 2016), motor functions (Feurra et al., 2011b), and attention (Kasten et al., 2020). There is also growing research in clinical applications (Clancy et al., 2018; Mellin et al., 2018; Ahn et al., 2019; Alexander et al., 2019). There are currently two presumptions about how tACS achieves its effect. The first is entrainment of ongoing brain oscillations to the driving frequency during stimulation (Thut et al., 2011; Herrmann et al., 2016; Liu et al., 2018). According to the laws of entrainment an oscillator (like a brain rhythm) will synchronize to another coupled oscillator (like tACS), if their frequencies have a close match, or if the driving force of the external oscillator is very high (Pikovsky et al., 2002). The second presumed mechanism is a lasting change of synaptic plasticity of the stimulated networks (Zaehle et al., 2010; Vossen et al., 2015; Liu et al., 2018; Wischnewski et al., 2018). While most effects of tACS occur during the application of the stimulation (online) (Feurra et al., 2011a; Polanía et al., 2012; Brignani et al., 2013), there are also offline-effects that show that functional changes (Marshall et al., 2006; Garside et al., 2014; Kasten and Herrmann, 2017) as well as physiological changes (Reato et al., 2013; Kasten et al., 2016) persist for some time after the end of the stimulation as measured in the electroencephalography (EEG) and magnetic encephalography (MEG).

Recent work has pointed out that the effects of tACS can be quite inconsistent (Veniero et al., 2017; Clayton et al., 2018; Fekete et al., 2018; Sliva et al., 2018), and it has been proposed that the transferability of tACS-findings may be limited by a variety of factors: the dependency of the effects on brain states (Feurra et al., 2013; Herrmann et al., 2013; Neuling et al., 2013; Alagapan et al., 2016), the challenges that come with individual differences in brain anatomy (Krause and Cohen Kadosh, 2014), and the close match between stimulation frequency and brain rhythm that is required according to the laws of entrainment (Fröhlich, 2015; Notbohm et al., 2016). The expected decrease of the stimulation effect by a growing deviation between tACS-frequency and endogenous rhythm was already shown in *in-vitro* and animal studies (Schmidt et al., 2014; Negahbani et al., 2019) and a growing amount of studies suggest a similar role of mismatching frequencies in humans (Vossen et al., 2015; Stecher et al., 2017; Kasten et al., 2019).

A promising approach to address many of the challenges of tACS are so-called "closed-loop" setups. Instead of pre-determining stimulation parameters, from experience and models alone, the parameters are dynamically tuned to the current brain activity in near real time (Boyle and Frohlich, 2013; Wilde et al., 2015; Bergmann et al., 2016; Karabanov et al., 2016; Thut et al., 2017). Respective novel approaches of applying frequency and phase specific tACS corresponding to current brain activity have shown promising results in memory consolidation during sleep (Jones et al., 2018; Ketz et al., 2018) and phase-dependent modulation of the α-rhythm via closed-loop tACS are currently studied (Zarubin et al., 2020).

In this study, we aim to address the problem of frequency specific tACS in the α-range. We employed a closed loop stimulation protocol with adaptive tACS-frequency and tested it against established, fixed tACS-protocols using a single, pre-determined frequency. Previous tACS research in α-band modulation relied on (rapid) preliminary estimation of the individual alpha frequency (IAF) before stimulation (e.g., Zaehle et al., 2010) or even stimulation at a prefixed frequency (Helfrich et al., 2014). The rapid estimation of the IAF before stimulation is usually limited by the scarce amount of data and the quick analysis. Moreover, recent research suggested that the alpha-activity is not as frequency-stable as previously expected (Haegens et al., 2014; Mierau et al., 2017; Benwell et al., 2019). Therefore, a growing amount of studies found a mismatch between the predetermined individual stimulation frequency and the prevalent IAF as established post stimulation by the thorough analysis of more abundant EEG-data (Vossen et al., 2015; Stecher et al., 2017; Stecher and Herrmann, 2018; Kasten et al., 2019). While these studies were not perfectly balanced to explore the effects of the occurring mismatches, their results suggest that a portion of effects of tACS in the α-band are caused by deviation between IAF and ISF. Under the assumption, that entrainment is a necessary perquisite for tACS-effects, such a deviation between driving and endogenous frequency could decrease or prohibit a synchronization of brain rhythms to the tACS. In order to explore whether the effects of tACS can be increased by accounting for shifts in the ongoing α-activity, we designed an experiment where the stimulation frequency was continuously matched to the current prevalent peak-frequency of the α-activity, by adapting a new ISF (individual stimulation frequency) every 8 s from a posterior EEG-recording and stimulating in intermittent epochs of 8 s. This intermediate design is necessary, as the stimulation introduces a substantial artifact into the recording, rendering the analysis of data obtained during tACS extremely difficult (Noury et al., 2016; Herrmann and Strüber, 2017; Kasten et al., 2018b). tACS-protocols employing intermittent 8 s epochs with a cumulative length of 11–15 min were previously shown to be the shortest possible duration to produce physiological aftereffects of increased band-power (Vossen et al., 2015), while shorter epochs such as 1 and 3 s showed no effect (Strüber et al., 2015; Vossen et al., 2015). To compare the effect of the adaptive stimulation to the conventional fixed stimulation, we contrasted the results to a sham-stimulation and a fixed-frequency condition. To maintain a consistent state of mental alertness, we coupled the stimulation to a visual detection task, where changes in luminance, phase-locked to specific cycles of the stimulation, had to be detected.

We hypothesized that both verum tACS-groups would show an increased α-power after stimulation when compared to the sham group. Furthermore, we expected a larger increase of power

following the adaptive tACS (closed-loop) when compared to the stimulation at a predetermined fixed frequency, as a closer match of the stimulation frequency to the endogenous alpha activity should result in a higher proportion of entrainment during the stimulation. This higher proportion of entrainment should be accompanied by a stronger effect of synaptic plasticity in the underlying neuronal networks. We further expect a larger modulation of the detection performance within the stimulated epochs in the closed-loop condition as the applied tACS-waveform will better coincide with peaks and troughs of the ongoing α-activity, thereby increasing and decreasing the chance of visual detection in the respective phases (Mathewson et al., 2009).

MATERIALS AND METHODS

Participants

Sixty students of the University of Oldenburg aged between 18 and 35 (mean: 24.4 ± 3 years) participated in the study. Each gave written informed consent to participate and have their results anonymously published and received monetary compensation. The participants were subdivided into three groups: sham, fixed stimulation frequency (fIAF), and closed-loop stimulation (cIAF). The groups were counterbalanced for gender. Group assignment was done randomly by a computer after subject preparation and information. Due to equipment failure six participants were omitted from further analysis. Additionally, two participants of the sham-group showed an abnormal increase in α-activity (5 σ outside of the population mean) and were discarded from the statistics. The resulting group sizes were sham $N = 17$ (7 ♀), cIAF $N = 17$ (9 ♀), and fIAF $N = 18$ (8 ♀).

The participants were informed about the general goal and the procedure of the experiment and filled out a short questionnaire regarding the exclusion criteria. All participants reported to be free of psychiatric medication at the time of the experiment. Subjects stated no history of epilepsy, no neurological or psychiatric disorders, no cognitive impairments, no intracranial metal or cochlear implants, and normal or corrected to normal eyesight. After finishing the experiment participants were asked whether they thought they were stimulated and to complete a short questionnaire assessing possible adverse effects of tACS (Brunoni et al., 2011). All participants were naïve regarding the aim of the study. The study was approved by the Commission for Research Impact Assessment and Ethics at the University of Oldenburg.

Experimental Setup

Participants were seated in a dimly lit room in front of a light emitting diode (LED) in 50 cm distance centered between their eyes. The experimental setup is depicted in **Figure 1**: Following the preparation of the electrodes, participants performed a staircase procedure to determine the individual brightness threshold for the detection task. The one up/one-down staircase started at a photodiode voltage of 2.365 V and decreased/increased by 0.001 V for every correct/incorrect response, until 15 reversals were reached. The individual detection threshold was then calculated as the mean voltage of the reversals 5–10. During a 1-min EEG recording, an individual eye-blink threshold was determined. The subsequent experimental session started with a 10 min pre-stimulation EEG, followed by a 40 min part during which intermittent tACS was administered. The stimulation part was followed by another 10 min EEG recording. During the whole session, participants performed a visual detection task. The stimulation block was subdivided into 150 epochs containing 8 s of stimulation and 8 s of interleaved EEG recording. In the closed-loop and the fix-frequency groups, tACS was applied for 8 s in each sequence (including 1 s of linear fade in). The sham stimulation consisted of a 1 s fade in followed by a 1 s fade out at a fixed frequency. This application of a current every 8 s in all three conditions should ensure a better blinding than established methods of only comparatively very short placebo-conditions, which have been recently criticized (Turner et al., 2021).

The participants were tasked to detect changes in the LED's brightness and react by pressing a button with their right index finger. The changes in brightness lasted 10 ms and were a reduction in LED-voltage by the previously determined individual threshold. The changes in brightness are referred to as targets in the following. Targets occurred at four phase positions relative to the applied sinusoidal tACS: at 0°, 90°, 180°, or 270°. Two targets were presented per stimulation sequence (8 s) and then likewise presented at the same positions of the subsequent interleaved EEG-sequence. Targets appeared after the stimulation fade-in of 1 s and were jittered by ±1.75 s in the first and second half of the stimulation sequence. The order of the tACS phase angle at the time of the target presentation was randomized between subjects.

EEG and Individual Alpha Frequency Estimation

The EEG was measured with 25 sintered Ag-AgCl electrodes fitted in an elastic cap (EasyCap, Falk Minow, Munich, Germany). A standard 10–20 layout was applied with a vertical EOG-electrode, referenced to the tip of the nose. The ground electrode was positioned at FPz. Impedances were kept under 10 kΩ. The signals were recorded via BrainVision Recorder (BrainProducts GmbH, Gilching, Germany) with a resolution of 16.35 nV and at a sampling rate of 250 Hz, to favor faster processing in the closed loop stimulation. A high cutoff filter of 250 Hz and a low cutoff filter at 0.1 Hz were applied during the recording.

In order to determine the initial individual peak alpha frequency for the stimulation, the 10 min pre-stimulation EEG recording was used. For the fixed-frequency and the sham group, the estimated peak frequency was used as the ISF for the remainder of the experiment. For the closed-loop group, a new ISF was determined from 7 s of each interleaved EEG-sequence (see **Figure 2**). For the estimation of the frequency, the data of electrode Pz was subdivided into 1 s sequences, zero padded to 1250 sampling points to offer a resolution of 0.2 Hz and multiplied with a Hanning-window. Data-seconds containing values above the individual eye blink threshold were discarded. To correct for the 1/f characteristic of the power spectrum,

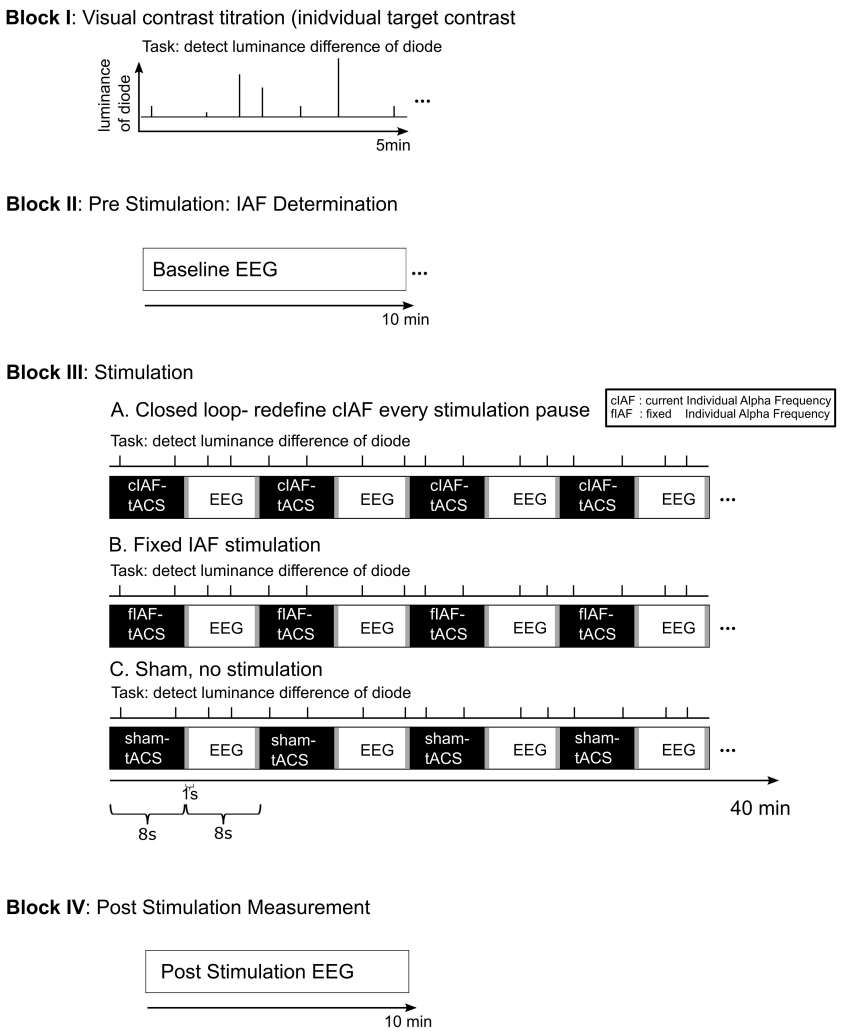

FIGURE 1 | Experimental Procedure. The experiment was divided into four blocks: 1. The participants performed a 5 min titration procedure to establish an individual luminance threshold for the detection task. 2. A 10 min EEG recording was conducted pre-stimulation. From this data, the individual stimulation frequency for the fixed stimulation and the sham group was established. 3. The stimulation part consisted of 150 epochs of 8 s of stimulation interleaved with 8 s stimulation free EEG-recording. For the fixed stimulation and the sham group, the predetermined ISF was used. For the closed loop group, the stimulation frequency for each epoch of stimulation was determined from the preceding stimulation-free epoch. During the whole stimulation block, the participants performed a visual luminance detection task. 4. The session concluded with a further 10 min of stimulation free EEG.

the power at each frequency was multiplied with the respective frequency. The IAF was determined as the maximum value in the power spectrum between 7.2 and 12.8 Hz. In order to ensure that the value reflected an actual peak in the spectrum rather than noise, an additional constraint was applied, requiring that the power at the identified maximum was larger than the average power in the whole band (the mean of 7.2 and 12.8 Hz) plus one standard error. If no IAF could be found, a stimulation of 10 Hz was applied.

Electrical Stimulation

For tACS, two surface conductive-rubber electrodes (5 × 7 cm) were centered at Cz and Oz underneath the EEG recording cap. The electrode's positions were chosen in order to stimulate the parieto-occipital cortex, in accordance to previous studies (Neuling et al., 2013). The rubber electrodes were fixed to the head using Neurodiagnostic Electrode Paste (Ten20; weaver and company) and impedance was kept below 10 kΩ. A stimulation current of 1 mA (peak to peak) was applied according to the group at the individual stimulation frequency with a battery-operated NeuroConn Stimulator DC (Neurocare, Illmenau, Germany). The stimulation was only exerted during the 40 min stimulation part in 8 s sequences, resulting in a total of 20 min of stimulation. The stimulation signal was continuously controlled within a MATLAB loop, by accessing the BrainVision-Recorders remote data access port, establishing the ISF by the procedure as described above and generating a sinusoidal signal with the respective parameters at 1,000 Hz sampling frequency. The generated signal was streamed via a digital-to-analog converter (DAQ NI USB 6229, National Instruments,

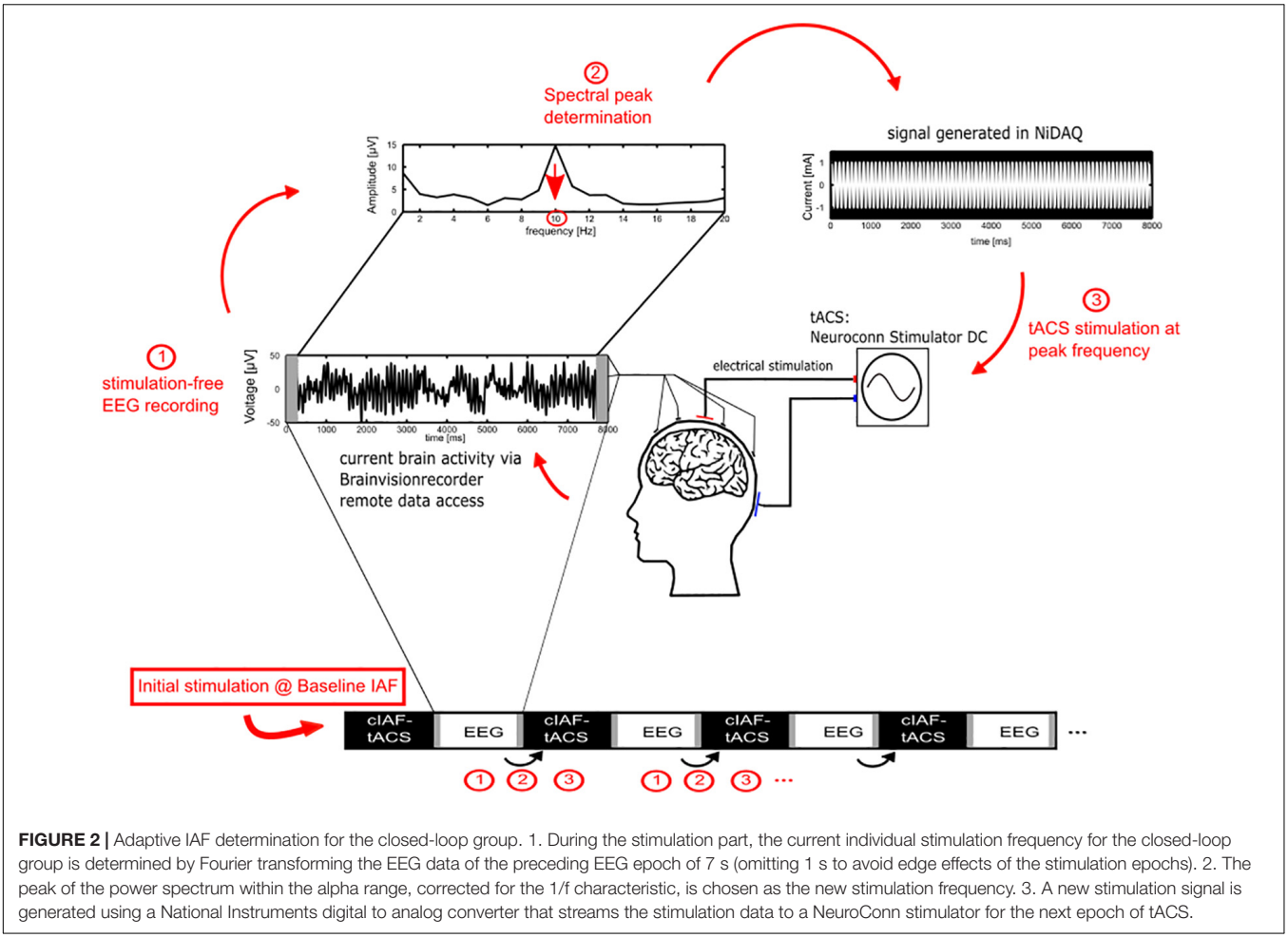

FIGURE 2 | Adaptive IAF determination for the closed-loop group. 1. During the stimulation part, the current individual stimulation frequency for the closed-loop group is determined by Fourier transforming the EEG data of the preceding EEG epoch of 7 s (omitting 1 s to avoid edge effects of the stimulation epochs). 2. The peak of the power spectrum within the alpha range, corrected for the 1/f characteristic, is chosen as the new stimulation frequency. 3. A new stimulation signal is generated using a National Instruments digital to analog converter that streams the stimulation data to a NeuroConn stimulator for the next epoch of tACS.

Austin, TX, United States) to the remote port of the stimulator [**Figure 2**(3)].

Post-measurement EEG Data Analysis

The EEG data were analyzed using MATLAB 2018a and the fieldtrip toolbox (Oostenveld et al., 2011). The stimulation epochs were cut from the data, and linear trends and the mean were subtracted from each channel. The data were then filtered using a 1 Hz high pass filter and a 100 Hz low pass filter, using a two-pass Butterworth filter of sixth order. In order to clear the data from raw muscle and movement artifacts, trials containing voltage deflections exceeding $> 150\mu V$ were discarded. The remaining trials were fed into an Independent Component Analysis (ICA) and eye-movement components manually selected and rejected. The data was then rearranged into a 10 min pre-stimulation block, 149 intermittent 7 s epochs between stimulation epochs (the last block was omitted due to a strong electrical artifact caused by the NiDAQ-shutdown), and a 10 min post-stimulation block. Blocks were subsequently divided into 1 s trials and Fourier transformed, using a 5 s zero padding and a Hanning-taper. Alpha peak power in each block was determined by identifying the peak α-power (maximum between 6.5 and 13 Hz) at electrode Pz in the averaged spectrum of each block.

Statistical Analysis

Statistical analysis was performed using R 4.0.2 (R Foundation for statistical Computing, Vienna, Austria). The behavioral analysis was conducted on the detection performance data during the stimulation measurement. In order to explore phase-dependent modulatory effects on the visual detection task, we calculated the detection performance for the four phase bins during tACS and the four bins in between stimulation epochs for every participant. As we assumed any behavioral modulation to be sinusoidal, we subsequently performed a sine-fit through the four points of performance values for every participant and condition (during tACS, during break) with a fixed frequency of 1 cycle and free values for intercept and amplitude. As the individual latency between visual processing of the stimuli and the tACS field was unknown, we also allowed a random value for phase. For every participant we took the values of the fitted sine during stimulation and the fitted sine during the break and calculated relative values for amplitude and ordinary R^2 of the fits. We then used a Kruskal Wallis test to check if the behavioral modulation between both conditions differed by group. The hypothesized effect of tACS on post-stimulation alpha power was tested by employing a Kruskal Wallis test on the relative increase in peak power between the groups. This test was chosen as peak power

was not normally distributed and did not fulfill the criteria for an ANOVA. As there is no alternative for a non-parametric repeated measures ANOVA, the percent change on peak-power relative to the pre-stimulation measurement was calculated. We also tested the average α-power during the non-stimulated epochs within the stimulation-measurement relative to the pre-stimulation power with a Kruskal Wallis test, to determine if physiological differences were already present during the stimulation part.

RESULTS

Adverse Effects

A Kruskal-Wallis test on the reported adverse effects of the stimulation did not reveal any difference in responses between the three groups (all $p > 0.05$). The most frequent reported effects (scores of three or higher) were "trouble concentrating" ($N = 16$) and "tiredness" ($N = 6$). There was also no difference in the believe to have received stimulation ($p = 0.547$), indicating that the blinding worked successfully.

Behavioral Results

The detection performance for the targets distributed over the four different phase bins and the fitted sine-waves show no striking differences between groups and conditions (see **Figures 3A–C**). We tested the relative differences between the amplitudes of the fitted sines during break-trials and stimulation-trials for every group by using a Kruskal Wallis test (see **Figure 3D**), with the between factor group (sham, cIAF, fIAF). There were no significant differences ($X^2 = 4.45$, $df = 2$, $p < 0.108$). The same analysis was repeated for the ordinary R^2 of the fitted sinusoidal (**Figure 3E**) to explore if the groups differed in how well the modulation of detection was explained by a sine-function. The analysis again revealed no significant differences between the groups ($X^2 = 1.98$, $df = 2$, $p < 0.372$).

In a recent article, Zoefel et al. (2019) compared different methods for the exploration of phase-dependent modulations of perception. They could show that simple sinus-fit method as we employed it here is not optimal for datasets with a limited number of phase bins and a small number of trials. The most optimal method they tested was a logistical regression with circular predictors. By employing their provided scripts for our dataset, we repeated the behavioral analysis with the described LOG REGRESS FISHER and LOG REGRESS PERM methods. For the LOG REGRESS FISHER-method, the phase of each trial was sine and cosine transformed to obtain a linear predictor. The dichotomous responses of each trial were then included in a regression model. For every participant, two regression models were created: one from trials during stimulation breaks and the second from trials during stimulation. Each regression model was then compared to an intercept-only model by using an *F*-Test. The resulting *p*-values for every participant and condition were then combined according to group using Fisher's method. For no group or condition the regression model provided a better fit than the intercept only model (all $p > 0.1$). For the LOG REGRESS PERM-method the trials and circular predictors were used to fit a multinomial logistic regression and the resulting root-mean square of the regression coefficients (sine and cosine) was stored for every participant and condition. This process was then repeated 100 times for every participant and condition with randomly permutated phases for all trials, resulting in 100 randomized surrogate datasets for every participant and condition. The average root-mean square of every condition was then compared against the average respective surrogate distributions for every group. The *z*-test was not significant for any group or condition (all $p > 0.01$).

Physiological Results

We first wanted to explore how much the IAF shifted over time and explore whether the shifts differed between the three different groups. As can be seen in **Figure 4**, all groups showed a variance in peak frequency over all intermediate windows between the stimulation epochs. We tested the number of shifts in frequency by testing the variance in peak frequencies per participant between groups. An ANOVA revealed no significant differences between the frequency-variance between groups [$F_{(1,49)} = 0.4$, $p = 0.645$]. As can be seen in **Figure 5**, the stimulation frequency in both stimulated groups did not always match perfectly with the prevalent IAF as determined from the post-stimulation block. During 19 (σ 11.1) epochs on average per participant in the closed-loop stimulation group, the closed loop system failed to detect an IAF-peak and a stimulation of 10 Hz was applied.

For the physiological results in the post-stimulation block, a Shapiro Wilk test showed that the relative α-power values were not normally distributed in all groups. Therefore, a Kruskal Wallis test was chosen as a non-parametric alternative to an ANOVA. The Kruskal Wallis test showed a significant difference of α-power changes between the groups ($X^2 = 6.8979$, $p < 0.032$), and a pairwise Wilcoxon rank sum test (Bonferroni-Holm corrected) revealed that the fixed-stimulation group showed significantly increased power as compared to the sham group ($p < 0.025$) (see **Figure 6**), whereas the comparison between closed loop- group and sham group was not significant ($p < 0.474$). The Kruskal Wallis test on the α-power (averaged over all stimulation-free epochs) during the stimulation part revealed no such differences between the groups ($X^2 = 3.5283$, $p = 0.171$).

As the aftereffect of α-tACS is known to depend on match between stimulation frequency and the current IAF, we explored if the observed power-increase correlated with the variance that the IAF showed during the unstimulated epochs (**Figure 7**). While both stimulated groups showed a negative correlation between individual variance in IAF over time, this correlation was only significant for the fIAF-group.

Furthermore, as the adaptive frequency estimation was based on a quick and rough method, we explored the resulting accuracy of both stimulated conditions as defined by the difference between ISF and IAF per epoch as established with *post-hoc*. We did so in order to establish that the difference in post-stimulation α-power between both groups was not based on a lack of stimulations accuracy within the closed-loop group. Both stimulated groups did not show a significant difference mean deviation between ISF and IAF (see **Figure 8A**), as tested by a Wilcoxon rank sum test ($Z = -0.59$, $p = 0.56$), maintaining that

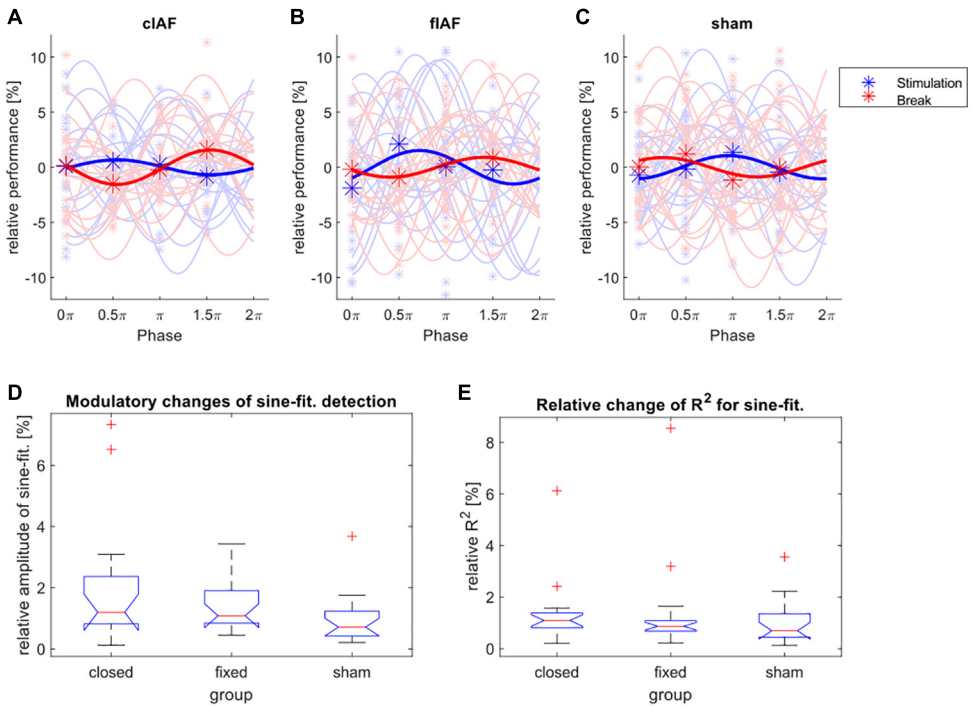

FIGURE 3 | Modulation of detection performance. **(A–C)** Detection performance during the four phase bins (asterisks) and fitted individual sine waves for every participant (light colors) and the average over all participants (dark colors), during stimulation epochs (blue) and between the stimulation epochs (red). The performance is shown relative to the mean over all four phases. **(D)** Boxplot of relative change in amplitude (performance during stimulation divided by performance during break) of the sine-wave fitted on the detection performances of the four phase bins. **(E)** Boxplot of relative changes (stimulation divided by break) of the ordinary R^2-values of the fitted sine-waves for all three groups.

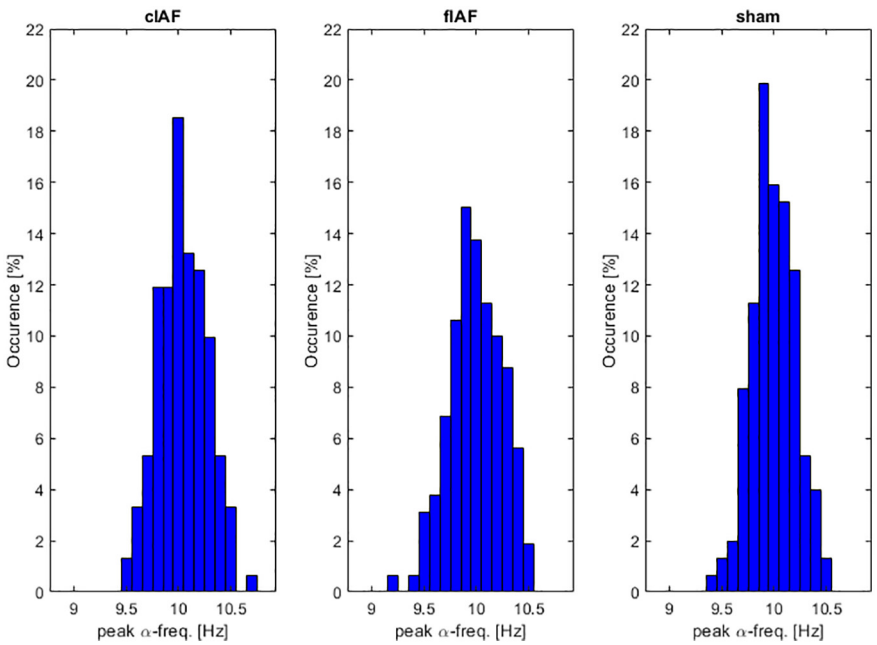

FIGURE 4 | α-frequency distribution. Occurrences of peak α-frequency between stimulation epochs. Histograms show the prevalence of peak-frequencies within the alpha range, averaged over participants.

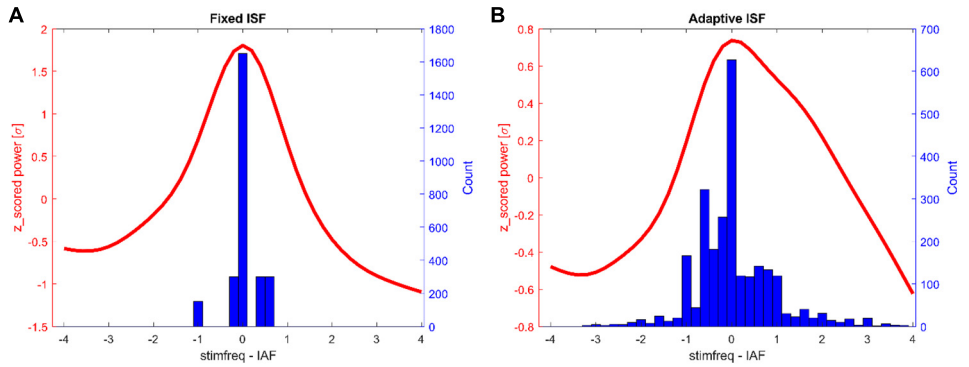

FIGURE 5 | Histograms of tACS-frequencies during stimulation epochs (blue) and the average normalized α-spectrum post stimulation (red, all frequencies centered on post-stimulation α-peak). Shown are the counts for all participants (150 trials each). **(A)** Fixed stimulation group. **(B)** Closed-loop stimulation group.

our results were not caused by a lack of stimulation accuracy in the closed-loop condition. Additionally, we tested whether the post-stimulation power was dependent on the accuracy of stimulation but we could not find significant correlation for any group (see **Figure 8B**).

DISCUSSION

Our aim in this study was to study the effectiveness of a closed loop α-tACS system where the stimulation frequency is continuously adapted to the current endogenous alpha-frequency. We found that stimulation with a fixed frequency led to an increase of post-stimulation α-power when compared to sham. This increase was not significant during the stimulation-measurement when we analyzed the unstimulated epochs. The post-stimulation increase is comparable to previous findings (Neuling et al., 2013; Vossen et al., 2015; Kasten et al., 2016). Surprisingly, we could not find evidence for the hypothesized stronger increase in post stimulation α-power when we constantly adapted the stimulation frequency to the current individual α-frequency.

Additionally, the tACS did not led to difference in phase-dependent modulation of visual detection between the stimulated and the unstimulated epochs. This effect was also absent when we employed a more sensitive method suggested by Zoefel et al. (2019). Previous attempts to modulate visual perception in a phase-specific way by brain stimulation have shown mixed results (Kasten and Herrmann, 2020). Evidence for phasic modulation has been shown in a visual-oddball task using tACS (Helfrich et al., 2014) and in a discrimination task using rTMS (Jaegle and Ro, 2014). However, more recent studies with similar detection tasks as employed here failed to find phase-specific effects for tACS (de Graaf et al., 2020) and oscillating transcranial current stimulation (otCS) (Sheldon and Mathewson, 2018). The differences in the parameters of task, stimulation, and analysis makes a direct comparison quite difficult. Different approaches have been used to uncover effects of phasic modulation in the past. Only recently, a comprehensive comparison of different approaches and a recommendation for a common procedure has been proposed by Zoefel et al. (2019). Their results suggest that a number of trials exceeding those used in our and others' studies are necessary to robustly uncover effects of phasic modulation on behavior.

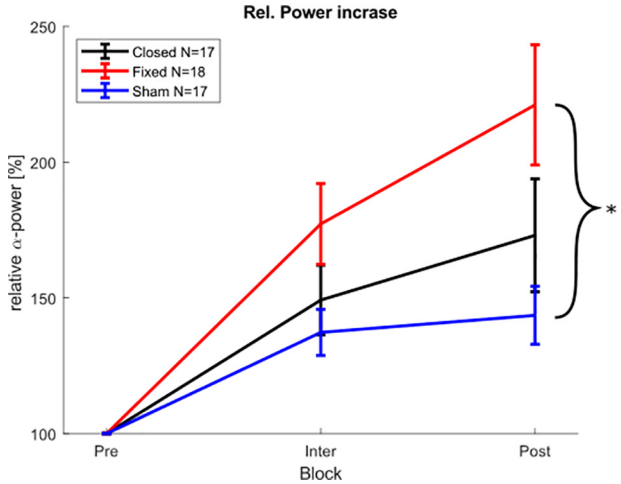

FIGURE 6 | Physiological aftereffect. Average posterior α-peak power during and after stimulation block, relative to pre-stimulation power. Error bars depict the standard error of the mean. The asterisk marks significant differences. The power during the stimulation block was calculated from the 150 stimulation free epochs between the stimulation epochs.

This suggests that perhaps the choice of our behavioral task itself was suboptimal for the exploration of the question whether an adaptive stimulation frequency is beneficial in functional modulation over a fixed frequency approach. The physiological outcomes of our study, however, suggest that adherence to a fixed stimulation frequency can be beneficial if the goal of the stimulation is to produce a robust aftereffect.

Previous studies found a dependence of the post-stimulation power on the mismatch between ISF and IAF (Stecher et al., 2017; Stecher and Herrmann, 2018; Kasten et al., 2019), while some work even suggests that a stimulation frequency slightly below the IAF yields stronger plasticity effects (Herrmann et al., 2013;

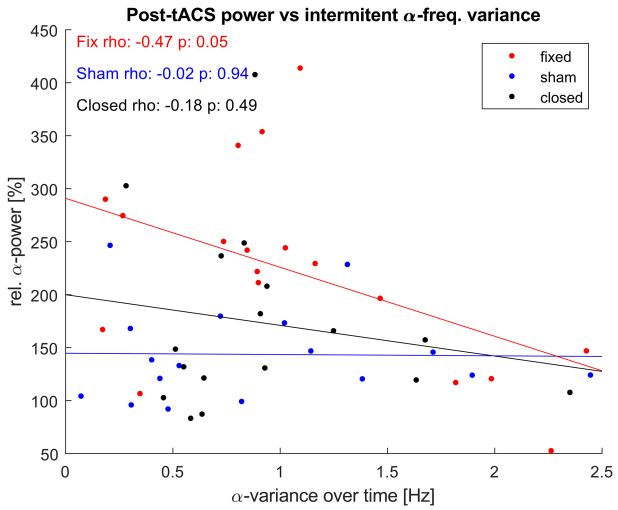

FIGURE 7 | α-power vs. α-frequency variance. Correlation between relative posterior α-power post stimulation and the variance of the IAF displayed during the intermediate unstimulated-epochs. One dot represents power and α-variance values of a single participant. Lines show the least-square error lines per group.

Vossen et al., 2015). The prevalent notion suggested that a closer fit between stimulation frequency and endogenous frequency would lead to an increased amount of entrainment during which the synapses of the underlying oscillatory networks are strengthened. This notion is supported by findings that link the aftereffects of tACS to NMDA-receptors (Wischnewski et al., 2018). One possible explanation as to why this aftereffect only occurs for fixed ISFs and not for adaptive ISFs is that during a fixed-ISF stimulation, those networks with a fitting resonant frequency experience synaptic strengthening according to the rules of spike timing dependent plasticity (STDP) (Song et al., 2000; Feldman, 2012) while an ever-shifting ISF will cause conflicting effects in networks of neighboring frequencies. Previous modelling studies suggest that tACS shifts the probability of spikes occurring within a network in a phase-dependent way (Ozen et al., 2010; Reato et al., 2010). Within a recurrent network of fitting eigenfrequency pre-synaptic spikes occur more likely within a time-window, that is "causal" for post-synaptic spikes (Herrmann et al., 2013), thereby leading to long term potentiation (LTP) over the course of multiple tACS-cycles due to NMDA-receptor mediated plasticity. If the tACS-frequency shifts into a region where spikes are occurring outside of this time-window, either no plasticity effects may occur or the probability of spikes occurring may even be shifted to time-windows where the spikes occur after post-synaptic activity, now causing synaptic depression in networks that were strengthened in the previous stimulation epoch. This would suggest that within our closed-loop stimulation group, the size of the tACS-aftereffect should depend on the stability of the ISF. While the results of the fixed stimulation group hint into this direction (c.f. **Figure 5**), the wide array of parameters on which such a stability depends (positive and negative frequency shifts, sequence of frequencies, number of failed IAF-estimations and prevalence of different frequencies) make it hard to find a single suitable testable predictor for the closed-loop stimulation.

The universality of our results is mainly limited by three design-choices: First, the setting of 8 s epochs of stimulation was motivated by previous results, showing that intermittent tACS of 8 s show comparable effect to continuous stimulation and the offered opportunity to perform rough artifact-correction methods. The method, however, neglects any variance of the peak

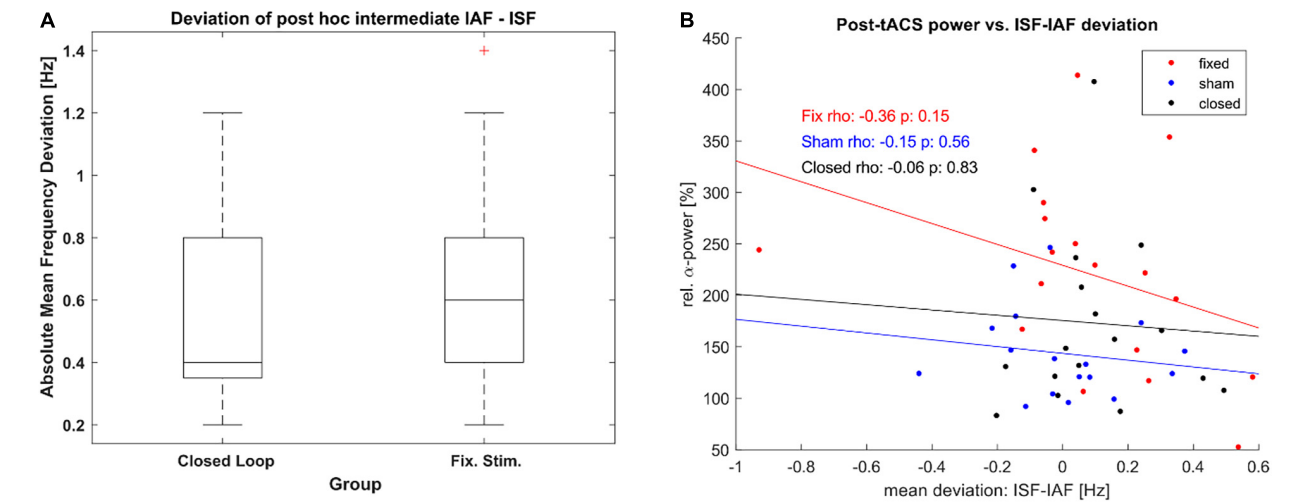

FIGURE 8 | Stimulation accuracy. **(A)** Boxplot of Frequency Deviation [mean absolute difference between estimated stimulation frequency (ISF) of each epoch and the determined α-frequency (IAF) as per *post-hoc* analysis] for both the closed loop tACS and the fixed frequency tACS group. Boxes mark the ends of the 25th and the 75th percentile of the samples' distributions, the horizontal lines mark the median of each group. The whiskers correspond to +/–2.7σ of the data. **(B)** Correlation between relative posterior α-power post stimulation and the mean deviation between ISF and IAF during the intermediate unstimulated-epochs. One dot represents power and frequency-deviation values of a single participant. Lines show the least-square error lines per group.

IAF over the respective time. It is possible that the prevalent α-frequency encountered a shift within 8 s, resulting in an unfitting stimulation frequency for the following epoch and offering only a slow adaptation to changes. Intermittent tACS-protocols that employ substantially shorter or longer stimulation epochs might yield different physiological and functional results, with very-short stimulation epochs or even a true "online" approach offering the opportunity of instant-frequency adaption, omitting larger jumps in stimulation frequency. Second, the fast procedure we employed to quickly estimate the IAF during the stimulation block could result in an insufficient stimulation accuracy due to lacking robustness against stronger artifacts and the reliance on zero padded 1 s chunks. This seems evident in the fact that the deviation between stimulation frequency and *post-hoc* established IAF, while smaller, was not significantly better in the adaptive condition compared to the fixed-frequency condition. Future closed-loop designs could improve the frequency-estimation by relying on online artifact techniques developed for Brain Computer Interfaces (Schlögl et al., 2007) and methods to compute the instantaneous frequency (Cohen, 2014). On a minor point, the choice to stimulate at a fixed frequency of 10 Hz in our adaptive design instead of reusing the last estimated IAF might have been less than ideal. Such sudden shift could cause a ISF that is too far from the endogenous frequency to have any effect. Given that the IAF will probably not change as drastically within this time-window, it might have been better to just repeat the last employed ISF. Third, our behavioral detection task consisted of visual stimuli presented at only four different phase bins with only 75 trials per phase. This number is rather low and would require a large effect size to statistically uncover phasic modulations as could be shown by Zoefel et al. (2019). Their findings suggest that a maximization of the number of trials per phase bin should be sought for in future studies in order to uncover effects of phase-dependent modulation.

In this study we successfully employed an intermittent closed loop stimulation setup. While we found no evidence for our originally hypothesized advantages of such a system over a fixed stimulation setup for the evocation of physiological changes and functional modulation of brain rhythms, we could demonstrate that a fixed stimulation setup produces more robust physiological aftereffects. We could, however, not show that the physiological aftereffects were in any way associated with perceptual changes. The absence of any behavioral effects in the fixed-frequency stimulation group compared to sham likely means that our paradigm was not satisfactorily designed to show any advantages of an adaptive closed loop stimulation protocol. Futures studies should employ behavioral tasks where phasic modulation by tACS has been successfully shown before in order to properly address this research question.

DATA AVAILABILITY STATEMENT

The raw data supporting the conclusions of this article will be made available by the authors, without undue reservation.

ETHICS STATEMENT

The studies involving human participants were reviewed and approved by the Commission for Research Impact Assessment and Ethics at the University of Oldenburg. The patients/participants provided their written informed consent to participate in this study.

AUTHOR CONTRIBUTIONS

AN, FK, and CH: designed the study. AN and FK: acquired the data. HS, AN, and FK: analyzed the data. HS, AN, FK, and CH: wrote the manuscript. All authors contributed to the article and approved the submitted version.

FUNDING

This work was supported by DFG (Deutsche Forschungsgemeinschaft) Priority Program 1665 to CH (SPP1665 HE 3353/8-2).

REFERENCES

Ahn, S., Mellin, J. M., Alagapan, S., Alexander, M. L., Gilmore, J. H., Jarskog, L. F., et al. (2019). Targeting reduced neural oscillations in patients with schizophrenia by transcranial alternating current stimulation. *Neuroimage* 186, 126–136. doi: 10.1016/j.neuroimage.2018.10.056

Alagapan, S., Schmidt, S. L., Lefebvre, J., Hadar, E., Shin, H. W., Fröhlich, F., et al. (2016). Modulation of cortical oscillations by low-frequency direct cortical stimulation is state-dependent. *PLoS Biol.* 14:e1002424. doi: 10.1371/journal.pbio.1002424

Alekseichuk, I., Turi, Z., Amador de Lara, G., Antal, A., and Paulus, W. (2016). Spatial working memory in humans depends on theta and high gamma synchronization in the prefrontal cortex. *Curr. Biol.* 26, 1513–1521. doi: 10.1016/j.cub.2016.04.035

Alexander, M. L., Alagapan, S., Lugo, C. E., Mellin, J. M., Lustenberger, C., Rubinow, D. R., et al. (2019). Double-blind, randomized pilot clinical trial targeting alpha oscillations with transcranial alternating current stimulation (tACS) for the treatment of major depressive disorder (MDD). *Transl. Psychiatry* 9:106.

Antal, A., Alekseichuk, I., Bikson, M., Brockmöller, J., Brunoni, A. R., Chen, R., et al. (2017). Low intensity transcranial electric stimulation: safety, ethical, legal regulatory and application guidelines. *Clin. Neurophysiol.* 128, 1774–1809. doi: 10.1016/j.clinph.2017.06.001

Benwell, C. S. Y. Y., London, R. E., Tagliabue, C. F., Veniero, D., Gross, J., Keitel, C., et al. (2019). Frequency and power of human alpha oscillations drift systematically with time-on-task. *Neuroimage* 192, 101–114. doi: 10.1016/j.neuroimage.2019.02.067

Bergmann, T. O., Karabanov, A., Hartwigsen, G., Thielscher, A., Siebner, H. R., Ole, T., et al. (2016). Combining non-invasive transcranial brain stimulation with neuroimaging and electrophysiology: current approaches and future perspectives. *Neuroimage* 140, 4–19. doi: 10.1016/j.neuroimage.2016.02.012

Boyle, M. R., and Frohlich, F. (2013). "EEG feedback-controlled transcranial alternating current stimulation," in *Proceeding of the 2013 6th International IEEE/EMBS Conference on Neural Engineering (NER)*, (IEEE), 140–143.

Brignani, D., Ruzzoli, M., Mauri, P., and Miniussi, C. (2013). Is transcranial alternating current stimulation effective in modulating brain oscillations? *PLoS One* 8:e56589. doi: 10.1371/journal.pone.0056589

Brunoni, A. R., Amadera, J., Berbel, B., Volz, M. S., Rizzerio, B. G., and Fregni, F. (2011). A systematic review on reporting and assessment of adverse effects associated with transcranial direct current stimulation. *Int. J. Neuropsychopharmacol.* 14, 1133–1145. doi: 10.1017/s1461145710001690

Clancy, K. J., Baisley, S. K., Albizu, A., Kartvelishvili, N., Ding, M., and Li, W. (2018). Lasting connectivity increase and anxiety reduction via transcranial alternating current stimulation. *Soc. Cogn. Affect. Neurosci.* 13, 1305–1316. doi: 10.1093/scan/nsy096

Clayton, M. S., Yeung, N., and Cohen Kadosh, R. (2018). Electrical stimulation of alpha oscillations stabilises performance on visual attention tasks. *J. Exp. Psychol. Gen* 148, 203–220. doi: 10.1037/xge0000502

Cohen, M. X. (2014). Fluctuations in oscillation frequency control spike timing and coordinate neural networks. *J. Neurosci.* 34, 8988–8998. doi: 10.1523/jneurosci.0261-14.2014

de Graaf, T. A., Thomson, A., Oever, S., Sack, A. T., and Van Bree, S. (2020). Does alpha phase modulate visual target detection? Three experiments with tACS-phase-based stimulus presentation. *Eur. J. Neurosci.* 51, 2299–2313. doi: 10.1111/ejn.14677

Fekete, T., Nikolaev, A. R., Knijf, F., De Zharikova, A., and van Leeuwen, C. (2018). Multi-electrode alpha tACS during varying background tasks fails to modulate subsequent alpha power. *Front. Neurosci.* 12:428. doi: 10.3389/fnins.2018.00428

Feldman, D. E. (2012). The spike timing dependence of plasticity. *Neuron* 75, 556–571. doi: 10.1016/j.neuron.2012.08.001

Feurra, M., Bianco, G., Santarnecchi, E., Del Testa, M., Rossi, A., and Rossi, S. (2011a). Frequency-dependent tuning of the human motor system induced by transcranial oscillatory potentials. *J. Neurosci.* 31, 12165–12170. doi: 10.1523/jneurosci.0978-11.2011

Feurra, M., Pasqualetti, P., Bianco, G., Santarnecchi, E., Rossi, A., and Rossi, S. (2013). State-dependent effects of transcranial oscillatory currents on the motor system: what you think matters. *J. Neurosci.* 33, 17483–17489. doi: 10.1523/jneurosci.1414-13.2013

Feurra, M., Paulus, W., Walsh, V., and Kanai, R. (2011b). Frequency specific modulation of human somatosensory cortex. *Front. Psychol.* 2:1–6. doi: 10.3389/fpsyg.2011.00013

Fröhlich, F. (2015). Experiments and models of cortical oscillations as a target for noninvasive brain stimulation. *Prog. Brain Res.* 222, 41–73. doi: 10.1016/bs.pbr.2015.07.025

Garside, P., Arizpe, J., Lau, C.-I. I., Goh, C., and Walsh, V. (2014). Cross-hemispheric alternating current stimulation during a nap disrupts slow wave activity and associated memory consolidation. *Brain Stimul.* 8, 520–527. doi: 10.1016/j.brs.2014.12.010

Haegens, S., Cousijn, H., Wallis, G., Harrison, P. J., and Nobre, A. C. (2014). Inter- and intra-individual variability in alpha peak frequency. *Neuroimage* 92, 46–55. doi: 10.1016/j.neuroimage.2014.01.049

Helfrich, R. F., Schneider, T. R., Rach, S., Trautmann-Lengsfeld, S. A., Engel, A. K., and Herrmann, C. S. (2014). Entrainment of brain oscillations by transcranial alternating current stimulation. *Curr. Biol.* 24, 333–339. doi: 10.1016/j.cub.2013.12.041

Herrmann, C. S., and Strüber, D. (2017). What can transcranial alternating current stimulation tell us about brain oscillations? *Curr. Behav. Neurosci. Reports* 4, 128–137. doi: 10.1007/s40473-017-0114-9

Herrmann, C. S., Rach, S., Neuling, T., and Strüber, D. (2013). Transcranial alternating current stimulation: a review of the underlying mechanisms and modulation of cognitive processes. *Front. Hum. Neurosci.* 7:279. doi: 10.3389/fnhum.2013.00279

Herrmann, C. S., Strüber, D., Helfrich, R. F., and Engel, A. K. (2016). EEG oscillations: from correlation to causality. *Int. J. Psychophysiol.* 103, 12–21. doi: 10.1016/j.ijpsycho.2015.02.003

Jaegle, A., and Ro, T. (2014). Direct control of visual perception with phase-specific modulation of posterior parietal cortex. *J. Cogn. Neurosci.* 26, 422–432. doi: 10.1162/jocn_a_00494

Jones, A. P., Choe, J., Bryant, N. B., Robinson, C. S. H. H., Ketz, N. A., Skorheim, S. W., et al. (2018). Dose-dependent effects of closed-loop tACS delivered during slow-wave oscillations on memory consolidation. *Front. Neurosci.* 12:867. doi: 10.3389/fnins.2018.00867

Karabanov, A., Thielscher, A., and Roman, H. (2016). Transcranial brain stimulation: closing the loop between brain and stimulation. *Curr. Opin. Neurol.* 29, 397–404. doi: 10.1097/wco.0000000000000342

Kasten, F. H., and Herrmann, C. S. (2017). Transcranial alternating current stimulation (tACS) enhances mental rotation performance during and after stimulation. *Front. Hum. Neurosci.* 11:2. doi: 10.3389/fnhum.2017.00002

Kasten, F. H., and Herrmann, C. S. (2020). Discrete sampling in perception via neuronal oscillations—evidence from rhythmic, non-invasive brain stimulation. *Eur. J. Neurosci.* doi: 10.1111/ejn.15006 [Epub ahead of print].

Kasten, F. H., Dowsett, J., and Herrmann, C. S. (2016). Sustained aftereffect of α-tACS lasts up to 70 min after stimulation. *Front. Hum. Neurosci.* 10:245.

Kasten, F. H., Duecker, K., Maack, M. C., Meiser, A., and Herrmann, C. S. (2019). Integrating electric field modeling and neuroimaging to explain inter-individual variability of tACS effects. *Nat. Commun.* 10, 1–11.

Kasten, F. H., Maess, B., and Herrmann, C. S. (2018a). Facilitated event-related power modulations during transcranial alternating current stimulation (tACS) revealed by concurrent tACS-MEG. *eNeuro* 5:ENEURO.0069-18.2018.

Kasten, F. H., Negahbani, E., Fröhlich, F., Herrmann, C. S., Kasten, F. H., Negahbani, E., et al. (2018b). Non-linear transfer characteristics of stimulation and recording hardware account for spurious low-frequency artifacts during amplitude modulated transcranial alternating current stimulation (AM-tACS). *Neuroimage* 179, 134–143. doi: 10.1016/j.neuroimage.2018.05.068

Kasten, F. H., Wendeln, T., Stecher, H. I., and Herrmann, C. S. (2020). Hemisphere-specific, differential effects of lateralized, occipital–parietal α- versus γ-tACS on endogenous but not exogenous visual-spatial attention. *Sci. Rep.* 10, 1–11. doi: 10.1167/10.2.26

Ketz, N., Jones, A. P., Bryant, N. B., Clark, V. P., and Pilly, P. K. (2018). Closed-loop slow-wave tACS improves sleep-dependent long-term memory generalization by modulating endogenous oscillations. *J. Neurosci.* 38, 7314–7326. doi: 10.1523/jneurosci.0273-18.2018

Krause, B., and Cohen Kadosh, R. (2014). Not all brains are created equal: the relevance of individual differences in responsiveness to transcranial electrical stimulation. *Front. Syst. Neurosci.* 8:25. doi: 10.3389/fnsys.2014.00025

Liu, A., Vöröslakos, M., Kronberg, G., Henin, S., Krause, M. R., Huang, Y., et al. (2018). Immediate neurophysiological effects of transcranial electrical stimulation. *Nat. Commun.* 9:5092.

Marshall, L., Helgadóttir, H., Mölle, M., and Born, J. (2006). Boosting slow oscillations during sleep potentiates memory. *Nature* 444, 610–613. doi: 10.1038/nature05278

Mathewson, K. E., Gratton, G., Fabiani, M., Beck, D. M., and Ro, T. (2009). To see or not to see: prestimulus phase predicts visual awareness. *J. Neurosci.* 29, 2725–2732. doi: 10.1523/jneurosci.3963-08.2009

Mellin, J. M., Alagapan, S., Lustenberger, C., Lugo, C. E., Alexander, M. L., Gilmore, J. H., et al. (2018). Randomized trial of transcranial alternating current stimulation for treatment of auditory hallucinations in schizophrenia. *Eur. Psychiatry* 51, 25–33. doi: 10.1016/j.eurpsy.2018.01.004

Mierau, A., Klimesch, W., and Lefebvre, J. (2017). State-dependent alpha peak frequency shifts: experimental evidence, potential mechanisms and functional implications. *Neuroscience* 360, 146–154. doi: 10.1016/j.neuroscience.2017.07.037

Negahbani, E., Stitt, I. M., Davey, M., Doan, T. T., Dannhauer, M., Hoover, A. C., et al. (2019). Transcranial alternating current stimulation (tACS) entrains alpha oscillations by preferential phase synchronization of fast-spiking cortical neurons to stimulation waveform. *bioRxiv* [preprint]. *bioRxiv 563163,

Neuling, T., Rach, S., and Herrmann, C. S. (2013). Orchestrating neuronal networks: sustained after-effects of transcranial alternating current stimulation depend upon brain states. *Front. Hum. Neurosci.* 7:161. doi: 10.3389/fnhum.2013.00161

Neuling, T., Rach, S., Wagner, S., Wolters, C. H., and Herrmann, C. S. (2012). Good vibrations: oscillatory phase shapes perception. *Neuroimage* 63, 771–778. doi: 10.1016/j.neuroimage.2012.07.024

Notbohm, A., Kurths, J., and Herrmann, C. S. (2016). Modification of brain oscillations via rhythmic light stimulation provides evidence for entrainment but not for superposition of event-related responses. *Front. Hum. Neurosci.* 10:10. doi: 10.3389/fnhum.2016.00010

Noury, N., Hipp, J. F., and Siegel, M. (2016). Physiological processes non-linearly affect electrophysiological recordings during transcranial electric stimulation. *Neuroimage* 140, 99–109. doi: 10.1016/j.neuroimage.2016.03.065

Oostenveld, R., Fries, P., Maris, E., and Schoffelen, J. M. (2011). FieldTrip: open source software for advanced analysis of MEG, EEG, and invasive electrophysiological data. *Comput. Intell. Neurosci.* 2011:156869.

Ozen, S., Sirota, A., Belluscio, M. A., Anastassiou, C. A., Stark, E., Koch, C., et al. (2010). Transcranial electric stimulation entrains cortical neuronal populations in rats. *J. Neurosci.* 30, 11476–11485. doi: 10.1523/jneurosci.5252-09.2010

Pikovsky, A., Rosenblum, M., Kurths, J., and Hilborn, R. C. (2002). Synchronization: a universal concept in nonlinear science. *Am. J. Phys.* 70, 655–655.

Polanía, R., Nitsche, M. A., Korman, C., Batsikadze, G., Paulus, W., Polanía, R., et al. (2012). The importance of timing in segregated theta phase-coupling for cognitive performance. *Curr. Biol.* 22, 1314–1318.

Reato, D., Gasca, F., Datta, A., Bikson, M., Marshall, L., and Parra, L. C. (2013). Transcranial electrical stimulation accelerates human sleep homeostasis. *PLoS Comput. Biol.* 9:e1002898. doi: 10.1371/journal.pcbi.1002898

Reato, D., Rahman, A., Bikson, M., and Parra, L. C. (2010). Low-intensity electrical stimulation affects network dynamics by modulating population rate and spike timing. *J. Neurosci.* 30, 15067–15079.

Schlögl, A., Keinrath, C., Zimmermann, D., Scherer, R., Leeb, R., and Pfurtscheller, G. (2007). A fully automated correction method of EOG artifacts in EEG recordings. *Clin. Neurophysiol.* 118, 98–104.

Schmidt, S. L., Iyengar, A. K., Foulser, A. A., Boyle, M. R., and Fröhlich, F. (2014). Endogenous cortical oscillations constrain neuromodulation by weak electric fields. *Brain Stimul.* 7, 878–889.

Sheldon, S. S., and Mathewson, K. E. (2018). Does 10-Hz cathodal oscillating current of the parieto-occipital lobe modulate target detection? *Front. Neurosci.* 12:83. doi: 10.3389/fnins.2018.00083

Sliva, D. D., Black, C. J., Bowary, P., Agrawal, U., Santoyo, J. F., Philip, N. S., et al. (2018). A prospective study of the impact of transcranial alternating current stimulation on EEG correlates of somatosensory perception. *Front. Psychol.* 9:2117. doi: 10.3389/fpsyg.2018.02117

Song, S., Miller, K. D., and Abbott, L. F. (2000). Competitive hebbian learning through spike-timing-dependent synaptic plasticity. *Nat. Neurosci.* 3, 919–926.

Stecher, H. I., and Herrmann, C. S. (2018). Absence of alpha-tACS aftereffects in darkness reveals importance of taking derivations of stimulation frequency and individual alpha variability into account. *Front. Psychol.* 9:984. doi: 10.3389/fpsyg.2018.00984

Stecher, H. I., Pollok, T. M., Strüber, D., Sobotka, F., Herrmann, C. S., Christoph, S., et al. (2017). Ten minutes of α-tACS and ambient illumination independently modulate EEG α-power. *Front. Hum. Neurosci.* 11:257. doi: 10.3389/fnhum.2017.00257

Strüber, D., Rach, S., Neuling, T., and Herrmann, C. S. (2015). On the possible role of stimulation duration for after-effects of transcranial alternating current stimulation. *Front. Cell. Neurosci.* 9:1–7. doi: 10.3389/fnsys.2015.00148

Thut, G., Bergmann, T. O., Fröhlich, F., Soekadar, S. R., Brittain, J.-S., Valero-Cabré, A., et al. (2017). Guiding transcranial brain stimulation by EEG/MEG to interact with ongoing brain activity and associated functions: a position paper. *Clin. Neurophysiol.* 128, 843–857.

Thut, G., Miniussi, C., Gross, J., Miniussi, C., and Gross, J. (2012). The functional importance of rhythmic activity in the brain. *Curr. Biol.* 22, R658–R663.

Thut, G., Schyns, P. G., and Gross, J. (2011). Entrainment of perceptually relevant brain oscillations by non-invasive rhythmic stimulation of the human brain. *Front. Psychol.* 2:170. doi: 10.3389/fpsyg.2011.00170

Turner, C., Jackson, C., and Learmonth, G. (2021). Is the "end-of-study guess" a valid measure of sham blinding during transcranial direct current stimulation? *Eur. J. Neurosci.* 53, 1592–1604.

Veniero, D., Benwell, C. S. Y., Ahrens, M. M., and Thut, G. (2017). Inconsistent effects of parietal α-tACS on Pseudoneglect across two experiments: a failed internal replication. *Front. Psychol.* 8:952. doi: 10.3389/fpsyg.2017.00952

Veniero, D., Strüber, D., Thut, G., and Herrmann, C. S. (2019). Noninvasive brain stimulation techniques can modulate cognitive processing. *Organ. Res. Methods* 22, 116–147.

Vossen, A., Gross, J., and Thut, G. (2015). Alpha power increase after transcranial alternating current stimulation at alpha frequency (α-tACS) reflects plastic changes rather than entrainment. *Brain Stimul.* 8, 499–508.

Vosskuhl, J., Huster, R. J., and Herrmann, C. S. (2015). Increase in short-term memory capacity induced by down-regulating individual theta frequency via transcranial alternating current stimulation. *Front. Hum. Neurosci.* 9:257. doi: 10.3389/fnhum.2015.00257

Wilde, C., Bruder, R., Binder, S., Marshall, L., and Schweikard, A. (2015). Closed-loop transcranial alternating current stimulation of slow oscillations. *Curr. Dir. Biomed. Eng.* 1, 85–88.

Wischnewski, M., Engelhardt, M., Salehinejad, M. A., Kuo, M.-F.-F., Nitsche, M. A., Schutter, D. J. L. G., et al. (2018). NMDA receptor-mediated motor cortex plasticity after 20 Hz transcranial alternating current stimulation. *Cereb. cortex* 29, 1–8.

Zaehle, T., Rach, S., and Herrmann, C. S. (2010). Transcranial alternating current stimulation enhances individual alpha activity in human EEG. *PLoS One* 5:13766.

Zarubin, G., Gundlach, C., Nikulin, V., Villringer, A., and Bogdan, M. (2020). Transient amplitude modulation of alpha-band oscillations by short-time intermittent closed-loop tACS. *Front. Hum. Neurosci.* 14:366. doi: 10.3389/fnhum.2020.00366

Zoefel, B., Davis, M. H., Valente, G., and Riecke, L. (2019). How to test for phasic modulation of neural and behavioural responses. *Neuroimage* 202:116175.

Conflict of Interest: CH has filed a patent application on brain stimulation and received honoraria as editor from Elsevier Publishers, Amsterdam.

The remaining authors declare that the research was conducted in the absence of any commercial or financial relationships that could be construed as a potential conflict of interest.

frontiers in Human Neuroscience

REVIEW
published: 02 August 2021
doi: 10.3389/fnhum.2021.662976

A Review of Studies Leveraging Multimodal TMS-fMRI Applications in the Pathophysiology and Treatment of Schizophrenia

*Sachin Pradeep Baliga[1] and Urvakhsh Meherwan Mehta[2]**

[1] Department of Psychiatry, TN Medical College and BYL Nair Charitable Hospital, Mumbai, India, [2] Department of Psychiatry, National Institute of Mental Health and Neurosciences, Bengaluru, India

The current review provides an overview of the existing literature on multimodal transcranial magnetic stimulation, and functional magnetic resonance imaging (TMS/fMRI) studies in individuals with schizophrenia and discusses potential future avenues related to the same. Multimodal studies investigating pathophysiology have explored the role of abnormal thalamic reactivity and have provided further evidence supporting the hypothesis of schizophrenia as a disorder of aberrant connectivity and cortical plasticity. Among studies examining treatment, low-frequency rTMS for the management of persistent auditory verbal hallucinations (AVH) was the most studied. While multimodal TMS/fMRI studies have provided evidence of involvement of local speech-related and distal networks on stimulation of the left temporoparietal cortex, current evidence does not suggest the superiority of fMRI based neuronavigation over conventional methods or of active rTMS over sham for treatment of AVH. Apart from these, preliminary findings suggest a role of rTMS in treating deficits in neurocognition, social cognition, and self-agency. However, most of these studies have only examined medication-resistant symptoms and have methodological concerns arising from small sample sizes and short treatment protocols. That being said, combining TMS with fMRI appears to be a promising approach toward elucidating the pathophysiology of schizophrenia and could also open up a possibility toward developing personalized treatment for its persistent and debilitating symptoms.

Keywords: brain connectivity, concurrent TMS/fMRI, simultaneous TMS-fMRI, psychosis, neuroplasticity, treatment resistance, causal inferences

OPEN ACCESS

Edited by:
Nivethida Thirugnanasambandam, National Brain Research Centre (NBRC), India

Reviewed by:
Andrea Guerra, Sapienza University of Rome, Italy
Hyuntaek Oh, Baylor College of Medicine, United States

****Correspondence:***
Urvakhsh Meherwan Mehta
urvakhsh@gmail.com

Specialty section:
This article was submitted to Brain Imaging and Stimulation, a section of the journal Frontiers in Human Neuroscience

Received: *02 February 2021*
Accepted: *21 June 2021*
Published: *02 August 2021*

Citation:
Baliga SP and Mehta UM (2021) A Review of Studies Leveraging Multimodal TMS-fMRI Applications in the Pathophysiology and Treatment of Schizophrenia. Front. Hum. Neurosci. 15:662976. doi: 10.3389/fnhum.2021.662976

INTRODUCTION

Schizophrenia is a severe mental illness characterized by positive (such as delusions, hallucinations), negative (anhedonia, asociality), cognitive (such as working memory deficits) symptom clusters. It has a life-time prevalence of around 1% and typically begins in late adolescence or early adulthood, leading to substantial disability, morbidity and mortality. While the exact pathophysiology of the illness remains elusive, schizophrenia is generally considered to be caused by a combination of genetic liability and environmental influences.

Current pharmacological strategies primarily focus on improving positive symptoms, with little or no effect on the negative and cognitive symptoms. Furthermore, the medications are effective in

only 50% of the cases, thus creating a need for newer strategies to target not only resistant positive symptoms, but also the other symptom clusters (de Araújo et al., 2012). Transcranial magnetic stimulation (TMS) is a neuromodulatory technique that acts via electromagnetic induction to generate an electric current in the superficial layers of the cortex. Single or paired-pulse TMS can be used as a neurophysiological probe to understand brain functions (Polanía et al., 2018). With these paradigms, TMS can have an excellent temporal resolution to the order of milliseconds (Bolognini and Ro, 2010). Further, when given repetitively in trains, rTMS can have differential effects by causing excitatory or inhibitory changes depending on the stimulation pattern and the cortical state (Wagner et al., 2007). These perturbation effects can cause plastic changes lasting 30–45 min and can be used to enhance or disrupt the underlying cortical networks. TMS over a target area causes effects in the underlying target areas and remote anatomically and functionally interconnected regions. Hence, TMS has limited spatial resolution when used on its own unless combined with an imaging modality (Wagner et al., 2007).

In contrast, functional magnetic resonance imaging (fMRI) offers the advantage of having a high spatial resolution. When combined with TMS as a neurophysiological probe, fMRI can be used to confirm the findings of 'virtual lesions' created using TMS (Pascual-Leone et al., 2000). Similarly, we can measure TMS-induced disruption of one node in a brain network on other distant nodes to yield brain connectivity metrics (Wagner et al., 2007). While fMRI has a weaker temporal resolution than EEG, it has an added advantage due to its ability to detect and monitor activity changes across larger and deeper areas such as subcortical structures (Siebner et al., 2009).

Electrophysiological and neurobiological research in the last two decades has demonstrated schizophrenia to be a disconnection syndrome involving widespread neuronal networks (Maran et al., 2016; Li et al., 2019; Mehta et al., 2019). However, these studies were based on individual applications of investigational techniques and were primarily correlational. Combining existing investigational techniques allows us to overcome their individual shortcomings and pave way for better understanding of pathophysiology of psychiatric illnesses. For example, combining TMS with EEG (TMS/EEG) can allow for simultaneous perturbation and measurement of neurophysiological correlates of cortical functioning in schizophrenia (Vittala et al., 2020). Using this technique, studies have demonstrated evidence of dysfunction in the frontal thalamocortical circuits in general and impaired cortical connectivity in the dorsolateral prefrontal cortex (DLPFC) in particular as compared to healthy controls using the single pulse paradigm (Li et al., 2021). Similarly, it is now possible to perform concurrent TMS/fMRI to interfere with specifically targeted networks and examining the cortical- and behavioral-level after-effects. fMRI exploits neurovascular coupling and can easily map TMS-evoked neuronal activity with high spatial resolution while providing a whole-brain coverage. However, owing to significant technical challenges, the concurrent TMS/fMRI setup currently exists in only a few specialized labs worldwide. The TMS coil has to be devoid of ferromagnetic material like other equipment in the MR environment. The TMS stimulator either has to be kept inside a shielded metal cabinet or outside the MR room, to which the coil then has to be connected using a waveguide. Additionally, a low-pass filter is necessary to filter out external high-frequency noise (Bungert et al., 2012a). Conventional MR radiofrequency (RF) coils pose obvious constraints on the positioning of the TMS coil. To surmount this issue, single-channel transmit/receive (Tx/Rx) volume 'bird-cage' coils can be used, which provide an adequate opening for optimal positioning of the TMS coil (Bestmann et al., 2003). However, these are single-channel RF coils which are insufficient for performing modern parallel multiband imaging sequences. Hence, some labs now use commercially available or custom-made flexible multichannel surface RF coil arrays (Wang et al., 2017; Oh et al., 2019) which can easily accommodate MR compatible TMS coils and also provide high-quality images for a concurrent TMS/fMRI study. To stabilize the TMS coil in a fixed position for the entire duration of the fMRI recording, customized MR compatible coil holders are required (Bestmann et al., 2003; Moisa et al., 2009).

The presence of a TMS coil between the subject's head and the RF coil leads to local field inhomogeneities causing significant limitations in the signal-to-noise ratio (SNR). To overcome this, thinner MR compatible 7-channel surface RF-coil arrays have been developed, which can be mounted directly below the TMS coil. These novel arrays have been shown to achieve a five-fold rise in SNR at 3 cm depth underneath the TMS coil as compared to the bird-cage coils (Navarro de Lara et al., 2015, 2017). However, this arrangement can cause a reduction in the effective stimulation intensity and pose difficulties in reaching suprathreshold intensities in subjects with high motor threshold.

Use of concurrent TMS/fMRI can lead to static artifacts due to the presence of TMS coil on the magnetic field of the scanner, or cause dynamic artifacts during the actual discharging of the TMS coil. The field inhomogeneities caused by the TMS coil itself can be reduced using shimming techniques before image acquisition (Bungert et al., 2012b). Apart from these, eddy currents created by the changing MR fields in the copper windings of the TMS coil can be prevented using MR compatible TMS coils. Tiny leakage currents generated in the capacitors inside the TMS device can transmit through the coil, causing image artifacts (Weiskopf et al., 2009). These can be minimized using actively controlled high-voltage relay-diode systems to electrically insulate the TMS coil from the stimulator until immediately before and after each TMS pulse or by using built-in leakage filters (Weiskopf et al., 2009). Dynamic artifacts caused by the TMS pulse on the RF pulse can be prevented by setting precise time intervals between the two techniques (Bestmann et al., 2003; Navarro de Lara et al., 2017).

Clearly, setting up and running an adequately accurate system of acquiring concurrent TMS/fMRI data is contingent upon strong multidisciplinary technological expertise, timely quality control evaluations and a liberal financial support to acquire and maintain such state-of-the-art equipment. Once these aforementioned challenges have

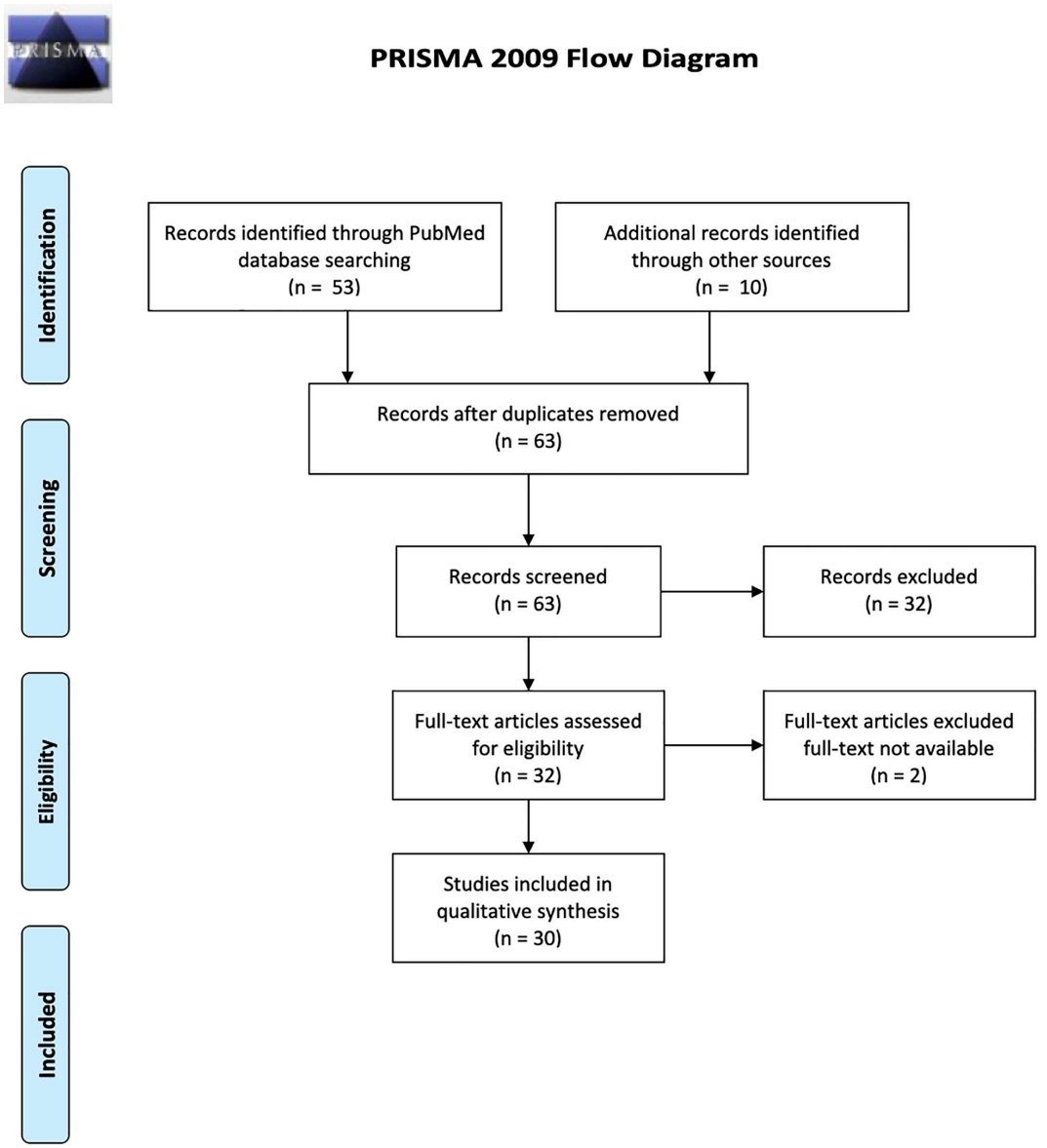

FIGURE 1 | PRISMA diagram describing selection of studies for the review.

been met, TMS/fMRI can be used to effectively to make causal inferences based on a specific hypothesis. For example, based on the evidence of abnormal activity in the subgenual anterior cingulate cortex (sgACC) in individuals with depression, a study by Vink et al. (2018) assessed for the propagation of TMS-induced activity to sgACC after stimulation of left dorsolateral prefrontal cortex (DLPFC). Combined TMS/fMRI approaches facilitate a better understanding of brain physiology in general and psychiatric illnesses like schizophrenia in particular by overcoming the shortcomings of either technique alone. The following review provides an overview of the existing literature on multimodal TMS/fMRI in individuals with schizophrenia and potential future avenues.

MATERIALS AND METHODS

We conducted a systematic review was based on the recommended PRISMA guidelines[1] using the PubMed electronic database. We searched for all publications whose titles or abstracts contained the following terms: magnetic resonance imaging OR functional MRI OR FMRI AND Transcranial magnetic stimulation OR TMS AND schizophrenia OR psychosis. We established the following inclusion criteria: (a) Experiments recruiting individuals with a diagnosis of schizophrenia, (b) use of single-/paired-pulse/repetitive TMS, and (c) use of resting-state or task-based fMRI. We included

[1]http://www.prisma-statement.org/

all kinds of publications such as case-control and open-label studies, case reports, and conference abstracts. Review articles and experiments which explored physiological processes in otherwise healthy subjects using TMS/fMRI were excluded. Both the authors conducted the searches and the selection process independently.

For the selected titles, full-text articles were retrieved, and reference lists of each were searched for additional publications. In case of incomplete or missing information, the corresponding author of the included studies were contacted. The initial search strategy yielded 53 results; after applying the selection criteria, 30 studies were included in the review based on both authors' consensus. These were then categorized as those exploring schizophrenia pathophysiology (n = 6 studies) and those exploring treatment of schizophrenia (n = 24 studies). **Figure 1** describes the flow diagram of the selection/inclusion process followed in this review.

RESULTS

Multimodal TMS/fMRI Studies Exploring the Pathophysiology of Schizophrenia

A summary of all the 6 studies investigating the pathophysiology of schizophrenia has been presented in **Table 1**. These can be understood as those exploring cortical connectivity and those exploring cortical reactivity. Three of these experiments have utilized interleaved (concurrent) TMS/fMRI, while the rest have used it in a sequential or offline fashion by obtaining independent measurements and then correlating the two.

Cortical Connectivity

Single-pulse TMS (spTMS) to the precentral gyrus has been utilized with concurrent fMRI to measure response in synaptically connected regions (thalamus, medial superior frontal cortex, insula) in a case-control study (Guller et al., 2012a). Schizophrenia patients showed reduced activation in the thalamus, medial superior frontal cortex, and insula response to spTMS to the precentral gyrus. Functional connectivity analyses revealed weaker thalamus-medial superior frontal cortex and thalamus-insula connectivity in patients, thereby demonstrating aberrant thalamic connectivity in schizophrenia (Guller et al., 2012a). In an extension of the experiment, resting state functional connectivity (rsFC), white matter (WM) structural connectivity, and gray matter (GM) integrity were assessed in the same subjects using DTI (Guller et al., 2012b). The study found impaired effective connectivity (measured using spTMS/fMRI) but normal functional connectivity (measured using resting state fMRI or rsfMRI) in schizophrenia patients and failed to find any WM or GM abnormalities that could explain the aberrant functional thalamic connectivity.

Cortical Reactivity

Short Interval Intracortical Inhibition (SICI) is a paired-pulse TMS paradigm that is known to be mediated by $GABA_A$ receptors (Kujirai et al., 1993). Previous literature has consistently demonstrated SICI to be deficient in individuals with schizophrenia, implying a reduction in intracortical GABAergic neurotransmission (Radhu et al., 2013). A case-control study was conducted by Lindberg et al. to assess neural correlates of motor inhibition using concurrent fMRI/TMS. The study utilized a Stop Signal Task (SST) as a measure of volitional motor inhibition and the rapidity of inhibition process was estimated for each subject (labeled Stop Signal Reaction Time, SSRT). Simultaneously, motor evoked potentials (measure of cortical excitability) and SICI (measure of motor inhibition) were recorded during the stop-go task of the SST. Following this, fMRI data during motor inhibition was recorded using a modified version of the SST. The study demonstrated that despite having an equal motor inhibition performance on the SST, fMRI showed greater prefrontal and premotor activation in schizophrenia during the inhibition task than controls (Lindberg et al., 2016). This task-related modulation of SICI was notably higher in subjects who showed less inhibition-related activity in pre-SMA and cingulate motor area, providing direct evidence of task-related deficiency of SICI modulation. Another case-control study performed measurements of SICI, followed by seed-based whole-brain functional connectivity (FC) using the SICI stimulation site and diffusion tensor imaging (Du et al., 2019). Higher resting-state left prefrontal-motor cortex functional connectivity, accompanied by a higher functional anisotropy of left corona radiata was found to predict less inhibitory deficits (or higher SICI), implying that a top-down prefrontal influence might partly mediate the inhibitory deficits in the motor cortex in schizophrenia.

A recent case-control study by Webler et al. (2020) assessed for prefrontal excitability and interhemispheric functional connectivity using concurrent TMS/fMRI in schizophrenia patients and compared them with healthy controls. In both groups, resting motor threshold (RMT) was estimated at baseline and the left-sided DLPFC (Brodmann area 9) was then stimulated using 35 triplet TMS pulses at 100 ms apart (10Hz) at 0, 80, 100, and 120% of RMT in a randomized order. Simultaneously, fMRI was performed to assess for activation patterns in bilateral BA 9 and neighboring BA46. The study found that schizophrenia patients showed hyperexcitability in left-sided BA9 and BA46 compared to healthy controls for equal TMS intensity. Also, on stimulating the left BA9, healthy controls showed increased right-sided BA9 activity compared to schizophrenia patients, thereby demonstrating impaired interhemispheric connectivity in the patients (Webler et al., 2020).

Pathophysiology of Auditory Verbal Hallucinations

Apart from these studies, one study has investigated auditory verbal hallucinations (AVH) using TMS/fMRI (Hoffman et al., 2007). The study aimed to identify cortical sites where treatment with rTMS produced significant reduction in AVH and then assess statistical relationship between clinical response and fMRI changes in these regions. For this study, patients of schizophrenia with resistant AVH were divided into continuous or intermittent hallucinators. For intermittent hallucinators, BOLD activation maps comparing hallucination and non-hallucination periods were generated by using a behavioral task to demarcate onset and offset of each hallucination event. In continuous hallucinators,

TABLE 1 | Technical aspects and principal findings of TMS/fMRI studies exploring pathophysiology of schizophrenia.

Authors	Subjects	Concurrent pharmacotherapy	Investigation	What was being studied	How TMS and fMRI were combined	TMS target	Findings
Webler et al. (2020)	19 SZ 11 HC recruited. Final sample had 8 SZ and 11 HC	unmedicated	Cortical excitability and interhemispheric connectivity	L BA9 activation and FC between L and R BA9 compared to HC.	Concurrent TMS/fMRI	L DLPFC (BA9)	At equal TMS intensity, hyperexcitability in L BA9 and BA46 in SZ group HC showed ↑ activation in R BA9 implying better FC between L and R BA9.
Du et al. (2019)	24 SZ 30 HC	20 patients on antipsychotics, rest unmedicated. Those on BZDs excluded.	Middle Prefrontal-Motor Cortex connectivity	rsFC between M1 and PFC and its association with SICI	Motor cortex seed based whole brain rsfMRI and DTI done at baseline followed by ppTMS for measuring SICI	M1	↑rsFC between L PFC-M1 associated with ↑SICI and lesser symptoms ↓ FA at left CR in SZ group. SICI derived rsFC between L PFC-M1 had positive correlation with FA of left CR in SZ group.
Lindberg et al. (2016)	28 SZ or SZA 21 HS 31 HC	22 patients on antipsychotics, rest unmedicated. Those on AEDs, BZDs and antidepressants excluded.	Neural correlates of motor inhibition	SICI during a motor inhibition task (Stop Signal Task) and its relation to activity in Cortical inhibition network	TMS for obtaining SICI fMRI during Stop Signal Task	M1	↓ SICI during motor inhibition in SZ group despite equivalent motor inhibition performance as compared to HS and HC ↑ activation in B/l IFG, L MeFG during motor inhibition in SZ group compared to HC and ↑ activation in prefrontal, cingulate and pre-SMA compared to HS.
Guller et al. (2012a)	14 SZ 14 HC	All patients on antipsychotics	Aberrant thalamic functioning	Peak amplitude of thalamic response to cortical perturbation using spTMS	Concurrent spTMS/fMRI	L PCG	No difference in BOLD response of cortical tissue underlying site of stimulation ↓ response to spTMS in thalamus, mSFG and insula in SZ group. ↓ thalamus-mSFG and thalamus-insula effective FC in SZ group
Guller et al. (2012b)	14 SZ 14 HC	All patients on antipsychotics	Resting state functional connectivity, WM structural connectivity (FA) and GM integrity (VBM)	rsfMRI and structural (WM and GM) data using DTI	Concurrent spTMS/fMRI	L PCG	No rsFC differences between thalamus and PCG, thalamus and SFG, thalamus and insula, SFG and PCG, insula and PCG. No group differences in FA of tracts connecting spTMS-responsive voxels of thalamus and PCG, thalamus and SFG, thalamus and insula, PCG and SFG, PCG and insula ↓VBM measures in thalamus in SZ group compared to HC, but disappeared after correction for multiple comparisons. ↓VBM measures in R posterior insula in SZ group compared to HC. However, no difference in spTMS induced insular response between groups.

(continued)

TABLE 1 | continued

Authors	Subjects	Concurrent pharmacotherapy	Investigation	What was being studied	How TMS and fMRI were combined	TMS target	Findings
Hoffman et al., 2007	16 SZ divided into continuous hallucinators (n = 8) and intermittent hallucinators (n = 8)	All patients on psychotropics, details not provided.	Pathophysiology of AVH	Identifying cortical areas where TMS produces significant improvement in AVH	For intermittent AVH – BOLD maps of hallucination and non-hallucination periods were compared, while for continuous AVH, maps of BOLD signal correlations relative to functionally defined Wernicke's area created to obtain 3–6 cortical sites; then probed using 1 Hz TMS in a crossover design. Clinical response correlated with fMRI findings.	Active – variable, based on AVH related activation patterns. Sham – TP area with coil angled with coil angled 45^0 off scalp.	In intermittent hallucinators, low levels of hallucination related activity in Broca's area predicted greater L TPJ TMS rate of response. In continuous hallucinators, ↓ coupling between Wernicke's area and right homologue of Broca's area predicted greater L TPJ TMS rate of response.

SZ = schizophrenia; SZA = schizoaffective disorder; HS = Healthy siblings; HC = healthy controls; a = active; s = sham; d = days; w = week; L = left; R = right; b/l = bilateral; spTMS = single pulse TMS; SICI = Short Interval Intracortical Inhibition; AVH = auditory verbal hallucinations; BA = Brodmann Area; DLPFC = Dorsolateral prefrontal cortex; PCG = precentral gyrus; SFG = Superior frontal gyrus; mSFG = medial superior frontal gyrus; IFG = inferior frontal gyrus; MeFG = medial frontal gyrus; M1 = Primary motor cortex; SMA = supplementary motor area; TP = temporoparietal; TPJ = temporoparietal junction; CR = corona radiata; ↑ = increases; ↓ = decreases; FC = functional connectivity; rsFC = resting state functional connectivity; rCBF = regional cerebral blood flow; BOLD = blood oxygen level dependent; DTI = diffusion tensor imaging; WM = white matter; GM = gray matter; FA = functional anisotropy; VBM = voxel based morphometry.

functionally defined Wernicke's area was delineated in each case using the activation patterns generated while listening to external speech. Correlations between BOLD signal time course in Wernicke's area, and other regions were used to map functional coupling to the former. In both groups, activation maps for AVH were then created around Wernicke's area and 3–6 cortical sites for each case were identified. These were then probed using 1-Hz (16 min, once daily for 3 days) and sham rTMS using a crossover design. To the site producing greatest clinical benefit, 3 more days of active rTMS was administered after unmasking. The study demonstrated that temporoparietal areas of the dominant hemisphere were involved in experience of AVH and rTMS to these areas produced greater rates of improvement as compared to anterior temporal sites and sham stimulation. The study also demonstrated involvement of inferior frontal regions in the pathophysiology of AVH as suggested by higher levels of coactivation involving inferior frontal and temporoparietal areas during hallucination periods and a robust negative correlation between temporoparietal rTMS response and hallucination-related activation/coupling involving inferior frontal regions.

Multimodal TMS/fMRI Studies Exploring the Treatment of Schizophrenia

A summary of all the studies exploring the treatment of schizophrenia has been presented in **Supplementary Table 1**. Additional details of the rTMS treatment-related parameters and outcome measures used in the studies have been provided in **Table 2**. Among positive symptoms of schizophrenia, the management of treatment-resistant AVH has been explored the most. These multimodal studies have either utilized fMRI for target localization (neuronavigation) or the comparison of pre- and post-treatment functional connectivity changes or both.

Hallucinations

Most studies have utilized block design fMRI for target localization using language tasks to create individualized cortical targets of auditory processing areas for treatment using rTMS. This is based on the hypothesis that abnormalities in the speech/language network underlie the pathophysiology of AVH in schizophrenia (Hoffman et al., 1999; Gavrilescu et al., 2010; Oertel-Knöchel et al., 2014). Others have utilized the event-related/symptom capture fMRI paradigm to create individualized activation maps for target localization (Sommer et al., 2007; Slotema et al., 2011; de Weijer et al., 2014). The second group of multimodal studies has utilized fMRI to assess whether rTMS leads to functional connectivity changes in the areas implicated in AVH and whether these changes correlate with clinical improvement. Based on the existing literature, the efficacy of fMRI-guided rTMS over sham for AVH has not clearly been established (Schönfeldt-Lecuona et al., 2004; Slotema et al., 2011; de Weijer et al., 2014; Paillère-Martinot et al., 2017).

Similarly, studies directly comparing fMRI guided and non-guided (10/20 EEG system based) treatment of AVH has also not found any superiority of the former over the latter (Sommer et al., 2007; Slotema et al., 2011). However, there has been evidence from some sham-controlled studies that active rTMS to the

TABLE 2 | TMS/fMRI studies on treatment of schizophrenia: rTMS parameters and outcome measures.

Authors	rTMS parameters	Number of sessions	Outcome measure/assessment
Hallucinations			
Slotema et al. (2011)	1 Hz, 90% RMT, 15 min	15 (3w)	AHRS, Positive subscale of PANSS, PSYRATS at baseline, weekly for 3w and monthly follow-up for 3m
Paillère-Martinot et al. (2017)	1 Hz, 100% RMT, 20 min	10	SAPS, AHRS at baseline and last day of treatment.
Vercammen et al. (2010)	1 Hz, 90% RMT, 20 min	12 (twice daily)	P3 item of PANSS before and after treatment. Brain activity in B/L TPJ, IFG, ACC, amygdala and insula.
Bais et al. (2017)	1 Hz, 90% RMT, 20 min (for B/l group, 10 min on each side)	12 (twice daily)	P3 item of PANSS and AHRS before and after treatment. Effect of treatment on network connectivity within and between components of DMN, ASM, SAL, LFP, RFP and BFT during a word evaluation task.
de Weijer et al. (2014)	1 Hz, 90% RMT, 20 min and 20 Hz, 80% RMT, 13 trains, 10 s on, 50 s off	Daily for 5 days, then weekly maintenance for 3w (total 8 sessions)	AHRS at baseline, after 5d and after 3w of maintenance treatment.
Schönfeldt-Lecuona et al. (2004)	1 Hz, 90% RMT, 16 min	5	Haddock self-rating scale at baseline and after treatment
Kindler et al. (2013)	1Hz Group (n = 8): 1 Hz, 90% RMT, Day 1: 8 min Day 2: 12 min Day 3–10: 16 min TBS Group (n = 7): cTBS 30Hz Day 1–3:4 × 801 pulses (total 3,204 pulses); Day 4–10:2 × 801 pulses (total 1,602 pulses)	10	PANSS, PSYRATS at baseline and after treatment
Maïza et al. (2013)	20 Hz, 80% RMT, 13 trains, 10s on, 50s off (only to SZ group)	4 (twice daily)	AHRS Correlation between L pSTS activity and AHRS Correlation between mean GM volume and activation in L pSTS
Briend et al. (2017)	20 Hz, 80% RMT, 13 trains, 10 s on, 50 s off (only SZ group)	4 (twice daily)	AHRS at baseline and d12 Comparison of baseline FC in L pSTS between SZ and HC Correlation between FC and AHRS
Fitzgerald et al. (2007)	1 Hz, 90% RMT, 15 min	10	PANSS, auditory hallucinations subscale of PSYRATS, HCS weekly.
Homan et al. (2012)	1Hz Group: 1 Hz, 90% RMT Day 1: 8 min Day 2: 12 min Day 3–10: 16 min TBS Group: cTBS 30Hz Day 1–3:4 × 801 pulses (total 3,204 pulses); Day 4–10:2 × 801 pulses (total 1,602 pulses)	10	Comparison of resting rCBF in L STG between responder (AHRS reduction $\geq$ 50%) and non-responders
Sommer et al. (2007)	1 Hz, 90% RMT, 20 min	15 (3w)	AHRS, positive scale of PANSS at baseline, end of each treatment week and follow-up at 6 and 13w from baseline
Montagne-Larmurier et al. (2009)	20 Hz, 80% RMT, 13 trains, 10 s on, 50 s off	4 (twice daily)	AHRS at baseline and d12

(continued)

TABLE 2 | continued

Authors	rTMS parameters	Number of sessions	Outcome measure/assessment
Zöllner et al. (2020)	cTBS 30Hz Day 1–3:4 × 801 pulses (total 3,204 pulses); Day 4–10:2 × 801 pulses (total 1,602 pulses)	10	Comparison of brain activation (PAC) at baseline vs. remission of AVH using an auditory stimulation paradigm
Giesel et al. (2012)	1 Hz Week 1: 80% RMT, 10 min Week 2: 100% RMT, 10 min Week 3: 100% RMT, 20 min Week 4: 100% RMT, 20 min along with external verbal stimulation during ITI.	20 (4w)	AHRS at baseline and weekly. Brain activity during AVH and during external verbal stimulation.
Jardri et al. (2008)	1 Hz, 100% RMT, 1000 pulses/session	10	VAS, SF-36 at baseline and after treatment
Jardri et al. (2007)	1 Hz	10 (sessions repeated every 5w)	AHRS, CGAS at baseline and after treatment.
Negative symptoms			
Brady et al. (2019)	iTBS 50Hz, 100% AMT, 2s on, 8s off, total 600 pulses	10 (twice per day)	Baseline rsfMRI and SANS in network discovery cohort. rsfMRI and PANSS at baseline and after treatment (in network validation cohort)
Basavaraju et al. (2019)	iTBS 50Hz, 80% AMT, 2s on, 8s off, total 600 pulses	10 (twice per day)	Seed based rsfMRI and SANS at baseline and after treatment.
Dlabac-de Lange et al. (2015)	10 Hz, 90% RMT, 20 trains, 10s on, 50s off	30 (twice per day)	SANS, PANSS Negative subscale at baseline and after treatment. Performance in ToL task i/f/o reaction time and accuracy pre- and post-treatment. Effect of treatment on brain activation during ToL task
Neurocognition			
Prikryl et al. (2012)	10 Hz, 110% RMT, 15 trains, 10s on, 30s off	15 (3w)	PANSS and neuronal activation during VFT task at baseline and after treatment.
Guse et al. (2013)	10 Hz, 110% RMT, 10 trains, 10s on, 30s off	15 (3w)	Activation patterns during letter 2-back task at baseline and after treatment
Social cognition			
Liemburg et al. (2018)	10 Hz, 90% RMT, 20 trains, 10s on, 50s off	15 (3w)	Activation patterns during Wall of Faces (social-emotional evaluation) task before and after treatment.
Agency			
Jardri et al. (2009)	1 Hz, 100% RMT, total 1000 pulses	10	Self-other discrimination tasks (Motor agency, source monitoring and speech awareness) and activation patterns in agency network during them. AHRS, CGAS

S = second; d = days; w = week; m = month; L = left; R = right; b/l = bilateral; RMT = resting motor threshold; AVH = auditory verbal hallucinations; TP3 – midpoint of the line joining T3 to P3 as per EEG 10–20 system; TP4 – midpoint of the line joining T4 to P4 as per EEG 10–20 system; TPJ – temporoparietal junction; TPC – temporoparietal cortex; STG = superior temporal gyrus; MTG = middle temporal gyrus; AG = angular gyrus; HG = Heschl's gyrus; SMG = supramarginal gyrus; PAC = primary auditory cortex; Spt = Sylvian parietotemporal; pSTS = posterior superior temporal sulcus; SSC = somatosensory cortex; PFC = prefrontal cortex; DLPFC = dorsolateral prefrontal cortex; ACC = anterior cingulate cortex; PCC = posterior cingulate cortex; MFG = middle frontal gyrus; IFG = inferior frontal gyrus; MeFG = medial frontal gyrus; FP = frontoparietal; IPL = inferior parietal lobule; DMN = default mode network; ASM = auditory sensorimotor network; SAN = salience network; LFP = left frontoparietal network; RFP = right frontoparietal network; BFT = bilateral frontotemporal network; ↑ = increases; ↓ = decreases; AHRS = Auditory Hallucinations Rating Scale; PANSS = Positive And Negative Syndromes Scale; PSYRATS = Psychotic Symptom Rating Scales; SAPS = Scale For The Assessment of Positive Symptoms; SANS = Scale For The Assessment of Negative Symptoms; HCS = Hallucination Change Score; VAS = Visual Analog Scale; SF36 = 36 item Short Form survey; CGAS = Childrens Global Assessment Scale; ToL = Tower of London; VFT = verbal fluency task; ASL = arterial spin labeling; GM = gray matter; FC = functional connectivity; rCBF = regional cerebral blood flow.

temporoparietal junction affects local speech-related network as well as its connections to distal networks (Vercammen et al., 2010; Bais et al., 2017). The first study demonstrated increased connectivity between left temporoparietal junction (TPJ) and right insula secondary to active treatment (Vercammen et al., 2010). The second study compared the effects of left TPJ, bilateral TPJ, and sham stimulation on inner speech-related brain networks (Bais et al., 2017). It showed that active rTMS to the left or bilateral TPJ areas resulted in a weaker network contribution of the left supramarginal gyrus to the bilateral frontotemporal network, which was hypothesized to a reduced likelihood of speech intrusions. However, only left TPJ stimulation led to stronger network contributions of right superior temporal gyrus to functional areas involved in attention and cognitive control, hinting toward the possible superiority of left TPJ stimulation to bilateral TPJ stimulation.

Apart from AVH, management of treatment resistant coenesthetic hallucinations has also been explored in a single case study. Based on activity in bilateral somatosensory cortices (SSC) during active hallucinations using data-driven analyses, the patient was administered 10 days of neuronavigated 1Hz rTMS over SSC, with which the frequency and intensity of coenesthetic hallucinations decreased (Jardri et al., 2008). However, sham stimulation of the same site was not tried prior to the active stimulation.

Negative Symptoms

Only three studies have specifically examined efficacy of rTMS for treating negative symptoms using multimodal TMS/fMRI approach (Dlabac-de Lange et al., 2015; Basavaraju et al., 2019; Brady et al., 2019). The earliest of these, a double-blind randomized sham controlled trial (RCT), examined the effect of 3 weeks of 10 Hz rTMS to bilateral DLPFC (located using EEG 10–20 system) on frontal brain activation in patients with negative symptoms of schizophrenia, as measured by fMRI during the Tower of London (ToL) task (Dlabac-de Lange et al., 2015). The study demonstrated an increased activity in the right DLPFC and right medial frontal gyrus in the active arm, which was accompanied by significant improvement in negative symptoms as compared to the sham arm. The second RCT employed a different approach by using rsfMRI to identify functional connectivity correlates of negative symptoms (Brady et al., 2019). The study found the functional connectivity breakdown between the right DLPFC and the midline cerebellar node in the default network as the most significant predictor of negative symptom severity in a network discovery cohort. Five days of twice daily cerebellar intermittent theta burst stimulation (iTBS) led to improvement in negative symptoms and this was associated with the reversal of functional dysconnectivity in an independent cohort. However, a subsequent sham controlled RCT of 5 days of twice daily iTBS to cerebellar vermis demonstrated a significant but equal improvement in negative symptoms in both active and sham groups at the end of treatment and at 6-week follow-up (Basavaraju et al., 2019). Nevertheless, only the active TMS group showed a significant engagement of the cerebellar-prefrontal resting-state functional connectivity.

Cognitive Symptoms

Two studies have examined the effect of rTMS on cognition in schizophrenia using task-based fMRI (Prikryl et al., 2012; Guse et al., 2013). Both of these have assessed for improvement in performance of working memory (WM) tasks (verbal fluency and letter 2-back) along with changes in neuronal activation during task-based fMRI using a double-blind sham-controlled design. The first trial found equal improvement in WM task performance in both arms and failed to show any differences in task-based activation in either groups (Prikryl et al., 2012). The second trial also utilized an additional healthy control arm to compare baseline and post-treatment scores with schizophrenia patients. The study did not find any differences in WM task-based activation between schizophrenia patients and healthy controls after 3 weeks of 10Hz rTMS (110% RMT, ITI 30 s, 1000 stimuli per session) or surprisingly, even at baseline (Guse et al., 2013).

Social Cognition

Only one sham controlled study has indirectly assessed the role of rTMS in social cognition in schizophrenia using multimodal approach (Liemburg et al., 2018). The RCT primarily assessed for activity changes in the prefrontal cortex during an ambiguous socio-emotional processing (Wall of Faces) task at baseline and compared with those after 3 weeks of 10Hz rTMS to bilateral DLPFC. It demonstrated a reduction in task-based activation in frontal, parietal and striatal regions, which they hypothesized to be possibly secondary to more effective processing in the prefrontal brain networks secondary to active treatment.

Agency

The role of rTMS in self-agency has been examined in a case study of childhood-onset schizophrenia who had persistent self-awareness impairments along with resistant AVH (Jardri et al., 2009). Based on abnormal activation in the right inferior parietal lobule (IPL) and related self-awareness network during self-agency related tasks (collision paradigm for motor-agency, block design experiment for speech awareness, and two scales for source monitoring), the patient was administered 10 days of 1Hz rTMS to the right TPJ. There was an improvement in the performance of self-other discrimination tasks associated with increased activity in the right IPL. However, there was no improvement in AVH until the patient was also administered a course of 1Hz rTMS to left TPJ, suggesting a functional dissociation between self-agency and hallucinations related networks.

DISCUSSION

The studies reviewed here illustrate the variety of concurrent TMS/fMRI experiments that have been conducted in patients with schizophrenia. These include isolated case reports, open-label and randomized control trials. The studies exploring treatment have assessed for effects of rTMS on hallucinations, negative symptoms, neurocognition, social cognition, and agency, while the studies exploring pathophysiology have in general looked at altered cortical

excitability or connectivity in schizophrenia as compared to healthy controls.

Studies Exploring Pathophysiology

The findings of multimodal studies evaluating cortical reactivity are different from that of prior research. While the study by Lindberg et al. (2016) did demonstrate a task-related deficiency in SICI during motor inhibition, this was associated with increased motor inhibition-related processing in the prefrontal and premotor areas. Previous studies have, in general, shown decreased prefrontal activation response inhibition tasks in schizophrenia patients (Kaladjian et al., 2007; Hughes et al., 2012).

The experiments on cortical connectivity demonstrated impaired effective connectivity between the thalamus and insula and thalamus and superior frontal gyrus, thereby implicating thalamic abnormalities in the pathogenesis of schizophrenia (Guller et al., 2012a,b). This is in line with previous neuropathological and neuroimaging research that has demonstrated thalamic dysfunction in schizophrenia (Clinton and Meador-Woodruff, 2004; Harms et al., 2007). An important point worth mentioning here is that while functional connectivity primarily provides an index of coactivation of two or more brain regions, it does not give any information as to the causal or primary contribution of one area over the other. In contrast, TMS-fMRI can help to infer causal influences of one brain region over the other via effective connectivity (Friston, 2011). This could help understand the heterogeneity from rs-fMRI studies by creating a better characterization of intra and inter-individual variability, thus paving the way for a more tailor-made or personalized approach toward treatment using rTMS. Findings of altered prefrontal interhemispheric connectivity in the study by Weber et al. (Webler et al., 2020) parallel those in previous TMS studies on motor cortex, which have demonstrated transcallosal inhibition abnormalities in patients of schizophrenia (Boroojerdi et al., 1999; Fitzgerald et al., 2002). Previous structural neuroimaging studies have also pointed toward corpus callosum impairments in schizophrenia (Foong et al., 2000; Keshavan et al., 2002).

Left TPJ is probably the commonest targeted area in treating persistent AVH using various non-invasive brain stimulation modalities. While other areas such as the inferior frontal gyrus (IFG; Broca's area or its right homologous region) might be considered as potential targets for treating AVH based on the activation patterns during AVH, the exploratory study by Hoffman et al. (2007) demonstrated no improvement in delivering rTMS to these areas and also underscored the importance of left-sided TPJ stimulation for treatment of AVH.

An important point worth mentioning here is that a variety of psychotropics, including antidepressants, antipsychotics, mood stabilizers and benzodiazepines can have an effect on TMS measures of cortical excitability (Ziemann et al., 2015). Antiepileptic mood stabilizers are known cause an increase in values in RMT while BZDs are known to increase SICI. Antipsychotics such as haloperidol have also been noted to decrease SICI. Similarly, concurrent administration of psychotropics can also have effects on TMS measures of cortical plasticity. Antipsychotics like Haloperidol and Sulpiride have been shown to suppress plasticity induced by various NIBS methods. Mood stabilizers such as lamotrigine can reduce LTP-like plasticity. Whereas, SSRIs such as citalopram have also been shown to promote LTP-like plasticity and abolish LTD-like plasticity. These effects have in general been shown to persist and normalize only after withdrawal of the drug. While conducting studies that explore pathophysiology of schizophrenia, there are obvious difficulties in recruiting patients who are unmedicated and in acute phase of psychosis. It is not surprising that subjects in all studies in the current review barring one (Webler et al., 2020) were on antipsychotics at the time of assessment. Some of these studies excluded those on mood stabilizers and benzodiazepines at the time of assessment, while others had subjects who were on stable doses of benzodiazepines, mood stabilizers and antidepressants at the time of assessment. When compared to health controls who are essentially drug free, it is expected that the findings related to cortical excitability and plasticity will be altered to an extent by concurrent administration of psychotropics.

Studies Exploring Treatment

Functional magnetic resonance imaging-based target localization for rTMS offers a promising approach toward providing personalized therapy for various symptom domains of schizophrenia. However, current research has not proved unequivocally whether this approach is superior to the conventional 10/20 EEG based system. Most studies have been conducted on patients with medication-resistant symptoms and are plagued by methodological concerns stemming from small sample sizes and shorter duration of treatment/number of pulses. Moreover, the cost-effectiveness of such a treatment in clinical settings in terms of time, money, and workforce also needs to be considered.

There are also particular concerns with regards to fMRI-based neuronavigated rTMS, which merit a mention. Target localization for AVH in current multimodal studies has been performed using event related fMRI or block design fMRI, both of which are types of task-based fMRI. The main caveat with task-based fMRI is that the demonstration of functional connectivity between two regions does not imply a causal relationship or even a direct connection between the said regions. Furthermore, block design paradigm of fMRI for AVH is based on the concept that areas related to language processing are the same ones involved in the pathogenesis of AVH, which need not be necessary. Similarly, targets determined using both block-based and event-related fMRI can include structures that are deeper and even inaccessible to TMS. Target localization for negative symptoms has been performed using seed based rsfMRI, which at best can provide only indirect measurements of neural activity. In comparison to this, using concurrent TMS/fMRI might help in a more efficient localization of target by allowing to observe immediate response to local perturbation and also provide direct proof of target engagement (Windischberger, 2019; Bergmann et al., 2021).

Furthermore, considering that psychiatric illnesses involve abnormalities in complex neural networks, it seems too simplistic and reductionistic to expect that stimulation or inhibition

of a single area will improve symptoms. Recent research in obsessive-compulsive disorder and depression has shown that a deeper and broader area of stimulation targeting subcortical regions using deep TMS may be a better alternative to the focal cortical stimulation using the F8 coil (Tendler et al., 2016; Lusicic et al., 2018). It has been suggested that deep-TMS might be more helpful due to targeting more widespread networks, thus questioning the need for functional imaging (Tendler et al., 2016).

The utility of rTMS is limited by its depth of penetration, making it possible to target only superficial cortical structures. However, combining fMRI with TMS also enables us to examine the effects of stimulating superficial cortical structures on deeper connections. This has been utilized in studies in healthy subjects to understand various aspects of brain physiology. For example, Zito et al. (2020) found the network-related sense of agency in healthy subjects to be amenable to inhibition by low-frequency rTMS. Another study by Hermiller et al. (2020) attempted theta burst stimulation to the hippocampal network targeted location in the parietal cortex during concurrent fMRI while performing a memory task and demonstrated increased activity of the targeted hippocampus during scene encoding and subsequently increased recollection. Such insights obtained from studies in healthy subjects could help understand physiological mechanisms and plan future experiments in patients with schizophrenia.

The current review has certain limitations. The main objective of this review was to discuss concurrent TMS/fMRI studies in schizophrenia. Hence, studies in normal healthy individuals that have investigated physiological mechanisms that might be aberrant in schizophrenia (for example, potential pathways for AVH, sense of agency) were excluded from this study. Also, this review has only examined studies published in the English language and may have missed out studies published in non-English languages. Most studies that have been reviewed here have not utilized interleaved TMS/fMRI, possibly due to the aforementioned technical and methodological challenges. Future studies using TMS/fMRI will require further optimization of these challenges while also using proper sham conditions to improve the quality of the studies. Correspondingly, further technical refinements in the entire process of concurrent TMS/fMRI are necessary so that these can be easily replicated across different centers. In conclusion, there is a definitive role of experiments combining TMS and fMRI in schizophrenia. Larger and adequately powered multicentric trials employing combined TMS/fMRI are needed to get consistent and reliable results. Such multimodal techniques appear to be a promising approach in elucidating the pathophysiology of schizophrenia and could also open up a possibility toward the development of a personalized approach toward treatment of its debilitating symptoms.

AUTHOR CONTRIBUTIONS

SB and UM performed the literature review. SB prepared the first draft. UM supervised and SB edited the manuscript. Both authors contributed to the article and approved the submitted version.

SUPPLEMENTARY MATERIAL

The Supplementary Material for this article can be found online at: https://www.frontiersin.org/articles/10.3389/fnhum.2021.662976/full#supplementary-material

REFERENCES

Bais, L., Liemburg, E., Vercammen, A., Bruggeman, R., Knegtering, H., and Aleman, A. (2017). Effects of low frequency rTMS treatment on brain networks for inner speech in patients with schizophrenia and auditory verbal hallucinations. *Prog. Neuro-Psychopharmacol. Biol. Psychiatry* 78, 105–113. doi: 10.1016/j.pnpbp.2017.04.017

Basavaraju, R., Ithal, D., Thanki, M., Hr, A., Thirthalli, J., Pascual-Leone, A., et al. (2019). T79. INTERMITTENT THETA BURST STIMULATION OF CEREBELLAR VERMIS IN SCHIZOPHRENIA: IMPACT ON NEGATIVE SYMPTOMS AND BRAIN CONNECTIVITY. *Schizophr. Bull.* 45:S234. doi: 10.1093/schbul/sbz019.359

Bergmann, T. O., Varatheeswaran, R., Hanlon, C. A., Madsen, K. H., Thielscher, A., and Siebner, H. R. (2021). Concurrent TMS-fMRI for causal network perturbation and proof of target engagement. *NeuroImage* 237:118093. doi: 10.1016/j.neuroimage.2021.118093

Bestmann, S., Baudewig, J., Siebner, H. R., Rothwell, J. C., and Frahm, J. (2003). Subthreshold high-frequency TMS of human primary motor cortex modulates interconnected frontal motor areas as detected by interleaved fMRI-TMS. *NeuroImage* 20, 1685–1696. doi: 10.1016/j.neuroimage.2003.07.028

Bolognini, N., and Ro, T. (2010). Transcranial Magnetic Stimulation: Disrupting Neural Activity to Alter and Assess Brain Function. *J. Neurosci.* 30, 9647–9650. doi: 10.1523/JNEUROSCI.1990-10.2010

Boroojerdi, B., Töpper, R., Foltys, H., and Meincke, U. (1999). Transcallosal inhibition and motor conduction studies in patients with schizophrenia using transcranial magnetic stimulation. *Br. J. Psychiatry* 175, 375–379. doi: 10.1192/bjp.175.4.375

Brady, R. O., Gonsalvez, I., Lee, I., Öngür, D., Seidman, L. J., Schmahmann, J. D., et al. (2019). Cerebellar-Prefrontal Network Connectivity and Negative Symptoms in Schizophrenia. *Am. J. Psychiat.* 176, 512–520. doi: 10.1176/appi.ajp.2018.18040429

Briend, F., Leroux, E., Delcroix, N., Razafimandimby, A., Etard, O., and Dollfus, S. (2017). Impact of rTMS on functional connectivity within the language network in schizophrenia patients with auditory hallucinations. *Schizoph. Res.* 189, 142–145. doi: 10.1016/j.schres.2017.01.049

Bungert, A., Chambers, C. D., Long, E., and Evans, C. J. (2012a). On the importance of specialized radiofrequency filtering for concurrent TMS/MRI. *J. Neurosci. Methods* 210, 202–205. doi: 10.1016/j.jneumeth.2012.07.023

Bungert, A., Chambers, C. D., Phillips, M., and Evans, C. J. (2012b). Reducing image artefacts in concurrent TMS/fMRI by passive shimming. *NeuroImage* 59, 2167–2174. doi: 10.1016/j.neuroimage.2011.10.013

Clinton, S. M., and Meador-Woodruff, J. H. (2004). Thalamic dysfunction in schizophrenia: neurochemical, neuropathological, and in vivo imaging abnormalities. *Schizophrenia Res.* 69, 237–253. doi: 10.1016/j.schres.2003.09.017

de Araújo, A. N., de Sena, E. P., de Oliveira, I. R., and Juruena, M. F. (2012). Antipsychotic agents: efficacy and safety in schizophrenia. *Drug Healthc. Patient Saf.* 4, 173–180. doi: 10.2147/DHPS.S37429

de Weijer, A. D., Sommer, I. E. C., Lotte Meijering, A., Bloemendaal, M., Neggers, S. F. W., Daalman, K., et al. (2014). High frequency rTMS; a more effective treatment for auditory verbal hallucinations? *Psychiat. Res.* 224, 204–210. doi: 10.1016/j.pscychresns.2014.10.007

Dlabac-de Lange, J. J., Liemburg, E. J., Bais, L., Renken, R. J., Knegtering, H., and Aleman, A. (2015). Effect of rTMS on brain activation in schizophrenia

with negative symptoms: A proof-of-principle study. *Schizophrenia Res.* 168, 475–482. doi: 10.1016/j.schres.2015.06.018

Du, X., Choa, F.-S., Chiappelli, J., Wisner, K. M., Wittenberg, G., Adhikari, B., et al. (2019). Aberrant Middle Prefrontal-Motor Cortex Connectivity Mediates Motor Inhibitory Biomarker in Schizophrenia. *Biol. Psychiatry* 85, 49–59. doi: 10.1016/j.biopsych.2018.06.007

Fitzgerald, P. B., Brown, T. L., Daskalakis, Z. J., deCastella, A., and Kulkarni, J. A. (2002). study of transcallosal inhibition in schizophrenia using transcranial magnetic stimulation. *Schizophrenia Res.* 56, 199–209. doi: 10.1016/S0920-9964(01)00222-5

Fitzgerald, P. B., Sritharan, A., Benitez, J., Daskalakis, Z. J., Jackson, G., Kulkarni, J., et al. (2007). preliminary fMRI study of the effects on cortical activation of the treatment of refractory auditory hallucinations with rTMS. *Psychiatry Res.* 155, 83–88. doi: 10.1016/j.pscychresns.2006.12.011

Foong, J., Maier, M., Clark, C. A., Barker, G. J., Miller, D. H., and Ron, M. A. (2000). Neuropathological abnormalities of the corpus callosum in schizophrenia: a diffusion tensor imaging study. *J. Neurol. Neurosurg. Psychiatry* 68, 242–244. doi: 10.1136/jnnp.68.2.242

Friston, K. J. (2011). Functional and Effective Connectivity: A Review. *Brain Connectiv.* 1, 13–36. doi: 10.1089/brain.2011.0008

Gavrilescu, M., Rossell, S., Stuart, G. W., Shea, T. L., Innes-Brown, H., Henshall, K., et al. (2010). Reduced connectivity of the auditory cortex in patients with auditory hallucinations: a resting state functional magnetic resonance imaging study. *Psychol. Med.* 40, 1149–1158. doi: 10.1017/S0033291709991632

Giesel, F. L., Mehndiratta, A., Hempel, A., Hempel, E., Kress, K. R., Essig, M., et al. (2012). Improvement of auditory hallucinations and reduction of primary auditory area's activation following TMS. *Eur. J. Radiol.* 81, 1273–1275. doi: 10.1016/j.ejrad.2011.03.002

Guller, Y., Ferrarelli, F., Shackman, A. J., Sarasso, S., Peterson, M. J., Langheim, F. J., et al. (2012a). Probing thalamic integrity in schizophrenia using concurrent transcranial magnetic stimulation and functional magnetic resonance imaging. *Archi. Gener. Psychiatry* 69, 662–671. doi: 10.1001/archgenpsychiatry.2012.23

Guller, Y., Tononi, G., and Postle, B. R. (2012b). Conserved functional connectivity but impaired effective connectivity of thalamocortical circuitry in schizophrenia. *Brain Connectiv.* 2, 311–319. doi: 10.1089/brain.2012.0100

Guse, B., Falkai, P., Gruber, O., Whalley, H., Gibson, L., Hasan, A., et al. (2013). The effect of long-term high frequency repetitive transcranial magnetic stimulation on working memory in schizophrenia and healthy controls—A randomized placebo-controlled, double-blind fMRI study. *Behav. Brain Res.* 237, 300–307. doi: 10.1016/j.bbr.2012.09.034

Harms, M. P., Wang, L., Mamah, D., Barch, D. M., Thompson, P. A., and Csernansky, J. G. (2007). Thalamic Shape Abnormalities in Individuals with Schizophrenia and Their Nonpsychotic Siblings. *J. Neurosci.* 27, 13835–13842. doi: 10.1523/JNEUROSCI.2571-07.2007

Hermiller, M. S., Chen, Y. F., Parrish, T. B., and Voss, J. L. (2020). Evidence for Immediate Enhancement of Hippocampal Memory Encoding by Network-Targeted Theta-Burst Stimulation during Concurrent fMRI. *J. Neurosci.* 40, 7155–7168. doi: 10.1523/JNEUROSCI.0486-20.2020

Hoffman, R. E., Hampson, M., Wu, K., Anderson, A. W., Gore, J. C., Buchanan, R. J., et al. (2007). Probing the Pathophysiology of Auditory/Verbal Hallucinations by Combining Functional Magnetic Resonance Imaging and Transcranial Magnetic Stimulation. *Cereb. Cortex* 17, 2733–2743. doi: 10.1093/cercor/bhl183

Hoffman, R. E., Rapaport, J., Mazure, C. M., and Quinlan, D. M. (1999). Selective speech perception alterations in schizophrenic patients reporting hallucinated "voices.". *Am. J. Psychiatry* 156, 393–399. doi: 10.1176/ajp.156.3.393

Homan, P., Kindler, J., Hauf, M., Hubl, D., and Dierks, T. (2012). Cerebral blood flow identifies responders to transcranial magnetic stimulation in auditory verbal hallucinations. *Transl. Psychiatry* 2:e189. doi: 10.1038/tp.2012.114

Hughes, M. E., Fulham, W. R., Johnston, P. J., and Michie, P. T. (2012). Stop-signal response inhibition in schizophrenia: Behavioural, event-related potential and functional neuroimaging data. *Biol. Psychol.* 89, 220–231. doi: 10.1016/j.biopsycho.2011.10.013

Jardri, R., Delevoye-Turrell, Y., Lucas, B., Pins, D., Bulot, V., Delmaire, C., et al. (2009). Clinical practice of rTMS reveals a functional dissociation between agency and hallucinations in schizophrenia. *Neuropsychologia* 47, 132–138. doi: 10.1016/j.neuropsychologia.2008.08.006

Jardri, R., Lucas, B., Delevoye-Turrell, Y., Delmaire, C., Delion, P., Thomas, P., et al. (2007). An 11-year-old boy with drug-resistant schizophrenia treated with temporo-parietal rTMS. *Mol. Psychiatry* 12:320. doi: 10.1038/sj.mp.4001968

Jardri, R., Pins, D., and Thomas, P. A. (2008). case of fMRI-guided rTMS treatment of coenesthetic hallucinations. *Am. J. Psychiatry* 165, 1490–1491. doi: 10.1176/appi.ajp.2008.08040504

Kaladjian, A., Jeanningros, R., Azorin, J.-M., Grimault, S., Anton, J.-L., and Mazzola-Pomietto, P. (2007). Blunted activation in right ventrolateral prefrontal cortex during motor response inhibition in schizophrenia. *Schizophrenia Res.* 97, 184–193. doi: 10.1016/j.schres.2007.07.033

Keshavan, M. S., Diwadkar, V. A., Harenski, K., Rosenberg, D. R., Sweeney, J. A., and Pettegrew, J. W. (2002). Abnormalities of the corpus callosum in first episode, treatment naive schizophrenia. *J. Neurol. Neurosurg. Psychiatry* 72, 757–760. doi: 10.1136/jnnp.72.6.757

Kindler, J., Homan, P., Jann, K., Federspiel, A., Flury, R., Hauf, M., et al. (2013). Reduced neuronal activity in language-related regions after transcranial magnetic stimulation therapy for auditory verbal hallucinations. *Biol. Psychiatry* 73, 518–524. doi: 10.1016/j.biopsych.2012.06.019

Kujirai, T., Caramia, M. D., Rothwell, J. C., Day, B. L., Thompson, P. D., Ferbert, A., et al. (1993). Corticocortical inhibition in human motor cortex. *J. Physiol.* 471, 501–519. doi: 10.1113/jphysiol.1993.sp019912

Li, S., Hu, N., Zhang, W., Tao, B., Dai, J., Gong, Y., et al. (2019). Dysconnectivity of Multiple Brain Networks in Schizophrenia: A Meta-Analysis of Resting-State Functional Connectivity. *Front. Psychiatry* 10:00482. doi: 10.3389/fpsyt.2019.00482

Li, X., Honda, S., Nakajima, S., Wada, M., Yoshida, K., Daskalakis, Z. J., et al. (2021). Research to Elucidate the Pathophysiological Neural Bases in Patients with Schizophrenia: A Systematic Review. *J. Personalized Med.* 11:388. doi: 10.3390/jpm11050388

Liemburg, E. J., Dlabac-De Lange, J. J., Bais, L., Knegtering, H., and Aleman, A. (2018). Effects of bilateral prefrontal rTMS on brain activation during social-emotional evaluation in schizophrenia: A double-blind, randomized, exploratory study. *Schizophrenia Res.* 202, 210–211. doi: 10.1016/j.schres.2018.06.051

Lindberg, P. G., Térémetz, M., Charron, S., Kebir, O., Saby, A., Bendjemaa, N., et al. (2016). Altered cortical processing of motor inhibition in schizophrenia. *Cortex J. Devoted Study Nerv. Syst. Behav.* 85, 1–12. doi: 10.1016/j.cortex.2016.09.019

Lusicic, A., Schruers, K. R., Pallanti, S., and Castle, D. J. (2018). Transcranial magnetic stimulation in the treatment of obsessive-compulsive disorder: current perspectives. *Neuropsychiatr. Dis. Treat.* 14, 1721–1736. doi: 10.2147/NDT.S121140

Maïza, O., Hervé, P.-Y., Etard, O., Razafimandimby, A., Montagne-Larmurier, A., and Dollfus, S. (2013). Impact of repetitive transcranial magnetic stimulation (rTMS) on brain functional marker of auditory hallucinations in schizophrenia patients. *Brain Sci.* 3, 728–743. doi: 10.3390/brainsci3020728

Maran, M., Grent-'t-Jong, T., and Uhlhaas, P. J. (2016). Electrophysiological insights into connectivity anomalies in schizophrenia: a systematic review. *Neuropsychiatr. Electrophysiol.* 2:6. doi: 10.1186/s40810-016-0020-5

Mehta, U. M., Naik, S. S., Thanki, M. V., and Thirthalli, J. (2019). Investigational and Therapeutic Applications of Transcranial Magnetic Stimulation in Schizophrenia. *Curr. Psychiatry Rep.* 21:89. doi: 10.1007/s11920-019-1076-2

Moisa, M., Pohmann, R., Ewald, L., and Thielscher, A. (2009). New coil positioning method for interleaved transcranial magnetic stimulation (TMS)/functional MRI (fMRI) and its validation in a motor cortex study. *J. Magn. Reson. Imaging* 29, 189–197. doi: 10.1002/jmri.21611

Montagne-Larmurier, A., Etard, O., Razafimandimby, A., Morello, R., and Dollfus, S. (2009). Two-day treatment of auditory hallucinations by high frequency rTMS guided by cerebral imaging: a 6 month follow-up pilot study. *Schizoph. Res.* 113, 77–83. doi: 10.1016/j.schres.2009.05.006

Navarro de Lara, L. I., Tik, M., Woletz, M., Frass-Kriegl, R., Moser, E., Laistler, E., et al. (2017). High-sensitivity TMS/fMRI of the Human Motor Cortex Using a Dedicated Multichannel MR Coil. *NeuroImage* 150, 262–269. doi: 10.1016/j.neuroimage.2017.02.062

Navarro de Lara, L. I., Windischberger, C., Kuehne, A., Woletz, M., Sieg, J., Bestmann, S., et al. (2015). A novel coil array for combined TMS/fMRI experiments at 3 T. *Magn. Reson. Med.* 74, 1492–1501. doi: 10.1002/mrm.25535

Oertel-Knöchel, V., Knöchel, C., Matura, S., Stäblein, M., Prvulovic, D., Maurer, K., et al. (2014). Association between symptoms of psychosis and reduced functional connectivity of auditory cortex. *Schizophrenia Res.* 160, 35–42. doi: 10.1016/j.schres.2014.10.036

Oh, H., Kim, J. H., and Yau, J. M. E. P. I. (2019). distortion correction for concurrent human brain stimulation and imaging at 3T. *J. Neurosci. Methods* 327:108400. doi: 10.1016/j.jneumeth.2019.108400

Paillère-Martinot, M.-L., Galinowski, A., Plaze, M., Andoh, J., Bartrés-Faz, D., Bellivier, F., et al. (2017). Active and placebo transcranial magnetic stimulation effects on external and internal auditory hallucinations of schizophrenia. *Acta Psychiatrica Scand.* 135, 228–238. doi: 10.1111/acps.12680

Pascual-Leone, A., Walsh, V., and Rothwell, J. (2000). Transcranial magnetic stimulation in cognitive neuroscience–virtual lesion, chronometry, and functional connectivity. *Curr. Opin. Neurobiol.* 10, 232–237. doi: 10.1016/s0959-4388(00)00081-7

Polanía, R., Nitsche, M. A., and Ruff, C. C. (2018). Studying and modifying brain function with non-invasive brain stimulation. *Nat. Neurosci.* 21, 174–187. doi: 10.1038/s41593-017-0054-4

Prikryl, R., Mikl, M., Prikrylova Kucerová, H., Ustohal, L., Kasparek, T., Marecek, R., et al. (2012). Does repetitive transcranial magnetic stimulation have a positive effect on working memory and neuronal activation in treatment of negative symptoms of schizophrenia? *Neuro Endocrinol. Lett.* 33, 90–97.

Radhu, N., de Jesus, D. R., Ravindran, L. N., Zanjani, A., Fitzgerald, P. B., and Daskalakis, Z. J. A. (2013). meta-analysis of cortical inhibition and excitability using transcranial magnetic stimulation in psychiatric disorders. *Clin. Neurophysiol.* 124, 1309–1320. doi: 10.1016/j.clinph.2013.01.014

Schönfeldt-Lecuona, C., Grön, G., Walter, H., Büchler, N., Wunderlich, A., Spitzer, M., et al. (2004). Stereotaxic rTMS for the treatment of auditory hallucinations in schizophrenia. *Neuroreport* 15, 1669–1673. doi: 10.1097/01.wnr.0000126504.89983.ec

Siebner, H. R., Bergmann, T. O., Bestmann, S., Massimini, M., Johansen-Berg, H., Mochizuki, H., et al. (2009). Consensus paper: combining transcranial stimulation with neuroimaging. *Brain Stimul.* 2, 58–80. doi: 10.1016/j.brs.2008.11.002

Slotema, C. W., Blom, J. D., de Weijer, A. D., Diederen, K. M., Goekoop, R., Looijestijn, J., et al. (2011). Can low-frequency repetitive transcranial magnetic stimulation really relieve medication-resistant auditory verbal hallucinations? Negative results from a large randomized controlled trial. *Biol. Psychiatry* 69, 450–456. doi: 10.1016/j.biopsych.2010.09.051

Sommer, I. E. C., de Weijer, A. D., Daalman, K., Neggers, S. F., Somers, M., Kahn, R. S., et al. (2007). Can fMRI-guidance improve the efficacy of rTMS treatment for auditory verbal hallucinations? *Schizophrenia Res.* 93, 406–408. doi: 10.1016/j.schres.2007.03.020

Tendler, A., Barnea Ygael, N., Roth, Y., and Zangen, A. (2016). Deep transcranial magnetic stimulation (dTMS) – beyond depression. *Expert Rev. Med. Dev.* 13, 987–1000. doi: 10.1080/17434440.2016.1233812

Vercammen, A., Knegtering, H., Liemburg, E. J., den Boer, J. A., and Aleman, A. (2010). Functional connectivity of the temporo-parietal region in schizophrenia: effects of rTMS treatment of auditory hallucinations. *J. Psychiatric Res.* 44, 725–731. doi: 10.1016/j.jpsychires.2009.12.011

Vink, J. J. T., Mandija, S., Petrov, P. I., van den Berg, C. A. T., Sommer, I. E. C., and Neggers, S. F. W. A. (2018). novel concurrent TMS−fMRI method to reveal propagation patterns of prefrontal magnetic brain stimulation. *Hum. Brain Mapp.* 39, 4580–4592. doi: 10.1002/hbm.24307

Vittala, A., Murphy, N., Maheshwari, A., and Krishnan, V. (2020). Understanding Cortical Dysfunction in Schizophrenia With TMS/EEG. *Front. Neurosci.* 14:00554. doi: 10.3389/fnins.2020.00554

Wagner, T., Valero-Cabre, A., and Pascual-Leone, A. (2007). Noninvasive human brain stimulation. *Annu. Rev. Biomed. Eng.* 9, 527–565. doi: 10.1146/annurev.bioeng.9.061206.133100

Wang, W.-T., Xu, B., and Butman, J. A. (2017). Improved SNR for combined TMS-fMRI: A support device for commercially available body array coil. *J. Neurosci. Methods* 289, 1–7. doi: 10.1016/j.jneumeth.2017.06.020

Webler, R. D., Hamady, C., Molnar, C., Johnson, K., Bonilha, L., Anderson, B. S., et al. (2020). Decreased interhemispheric connectivity and increased cortical excitability in unmedicated schizophrenia: A prefrontal interleaved TMS fMRI study. *Brain Stimulat.* 13, 1467–1475. doi: 10.1016/j.brs.2020.06.017

Weiskopf, N., Josephs, O., Ruff, C. C., Blankenburg, F., Featherstone, E., Thomas, A., et al. (2009). Image artifacts in concurrent transcranial magnetic stimulation (TMS) and fMRI caused by leakage currents: Modeling and compensation. *J. Magn. Reson. Imaging* 29, 1211–1217. doi: 10.1002/jmri.21749

Windischberger, C. (2019). Verifying successful brain stimulation by concurrent TMS/fMRI. *Brain Stimulat. Translat. Clin. Res. Neuromodulat.* 12:502. doi: 10.1016/j.brs.2018.12.643

Ziemann, U., Reis, J., Schwenkreis, P., Rosanova, M., Strafella, A., Badawy, R., et al. (2015). and drugs revisited 2014. *Clin. Neurophysiol.* 126, 1847–1868. doi: 10.1016/j.clinph.2014.08.028

Zito, G. A., Anderegg, L. B., Apazoglou, K., Müri, R. M., Wiest, R., Holtforth, M., et al. (2020). Transcranial magnetic stimulation over the right temporoparietal junction influences the sense of agency in healthy humans. *JPN* 2020, 271–278. doi: 10.1503/jpn.190099

Zöllner, R., Hübener, A.-F., Dannlowski, U., Kircher, T., Sommer, J., and Zavorotnyy, M. (2020). Theta-burst stimulation for auditory-verbal hallucination in very-late-onset schizophrenia-like psychosis-a functional magnetic resonance imaging case study. *Front. Psychiatry* 11:294. doi: 10.3389/fpsyt.2020.00294

Conflict of Interest: The authors declare that the research was conducted in the absence of any commercial or financial relationships that could be construed as a potential conflict of interest.

Publisher's Note: All claims expressed in this article are solely those of the authors and do not necessarily represent those of their affiliated organizations, or those of the publisher, the editors and the reviewers. Any product that may be evaluated in this article, or claim that may be made by its manufacturer, is not guaranteed or endorsed by the publisher.

Advantages of publishing in Frontiers

OPEN ACCESS
Articles are free to read for greatest visibility and readership

FAST PUBLICATION
Around 90 days from submission to decision

HIGH QUALITY PEER-REVIEW
Rigorous, collaborative, and constructive peer-review

TRANSPARENT PEER-REVIEW
Editors and reviewers acknowledged by name on published articles

Frontiers
Avenue du Tribunal-Fédéral 34
1005 Lausanne | Switzerland

Visit us: www.frontiersin.org
Contact us: frontiersin.org/about/contact

REPRODUCIBILITY OF RESEARCH
Support open data and methods to enhance research reproducibility

DIGITAL PUBLISHING
Articles designed for optimal readership across devices

FOLLOW US
@frontiersin

IMPACT METRICS
Advanced article metrics track visibility across digital media

EXTENSIVE PROMOTION
Marketing and promotion of impactful research

LOOP RESEARCH NETWORK
Our network increases your article's readership